NANOCLAY IN FLAME RETARDED GLASS REINFORCED POLYPROPYLENE/POLYAMIDE 6 BLEND

Ahmed Shamas

College of Engineering, Design and Physical Sciences

Wolfson Centre for Materials Processing

Department of Mechanical Engineering

University of Brunel

This dissertation is submitted for the degree of Doctor of Philosophy

June 2019

I would like to dedicate this thesis to my loving parents.

Abstract

Under the new European regulation on the restriction of hazardous substances in electrical and electronic equipment (RoHS 2011), owing to both the toxicity and environmental concerns with halogenated flame retardants (HFRs), some of these substances are banned and others restricted as additives. Hence, research on non-halogenated flame retardants has received great interest. Ammonium polyphosphate (APP) is the best in this category. APP is used as an intumescent flame retardant (IFR) along with synergistic agent and to improve flame retardancy of polymers without compromising the mechanical and thermal stability properties; it is also cost effective, because low loading is required.

This study was conducted with three purposes The first aim was to examine the effects of the type of (1) nanoclay [(SP) or Nanofil5 (N5)] and (2) compatibilisers (SEBS-g-MA or PP-g-MA) used and (3) the loading amounts of the GFs (0, 10, 15, and 20 wt.%) and SP (0, 2, and 5 wt.%) on the flame retardancy, thermal stability, and mechanical properties of the flame-retarded PP/PA6 blend nanocomposites. The second aim was to examine the effect of intumescent flame retardant (IFR) loading (15wt.%, 17%, 18% and 20%APP765) on the flame retardancy, thermal stability, and mechanical properties. The third aim was to study the synergistic effect of SP on IFR with varying GF loading (0, 10, 15, 20%GF) to achieve the best flammability resistance.

In this study, APP 765 was used as IFR and nanocomposites of polypropylene (PP)/polyamide-6(PA6) blends reinforced with glass fibres (GFs) and sepiolite (SP) were compounded using a co-rotating twin-screw extruder. The specimens for mechanical testing and analyses were injection moulded and compression moulded.

The morphologies of the blends were characterized by X-ray diffraction (XRD) analyses and indicated that SP had an intercalated morphology in the PP matrix. The thermal stabilities and crystallinities of the nanocomposites were measured by thermal gravimetric analysis (TGA), and the flammability of the nanocomposites was investigated

by UL-94 vertical burning and limiting oxygen index (LOI) tests and mass loss cone calorimetry. We observed that the use of 2 wt.% nanoclay and 18 wt.% APP 765 had a synergistic effect, resulting in a decrease in many of the flammability parameters of the nanocomposites. The peak heat release rate, mass loss rate, and smoke production rate were reduced by 10%, 20% and 30%, respectively, compared to those of pristine PP. A synergistic effect was also observed when 2wt.% SP and 18wt.% APP 765 were used in combination with the GFs of loading 10wt.%; the lowest PHRR and hence the best flame retardant properties were obtained under this condition.

The LOI was 33%, which was significantly higher than that of pristine PP (19%). Moreover, the classification was V0, in contrast to the case for pristine PP, which has no rating. A classification of V1 was achieved when the SP content was increased to 3 wt.%. Finally, the classification was the highest when the GF content was reduced to 10 wt.% and the nanoclay content to 2 wt.%, as this resulted in a synergistic effect of glass fibre on flame retardant additives.

The thermal stability also improved when the amounts of GF and SP used were increased. It was found that when the GF and SP contents were 20 and 2 wt.%, respectively, the maximum decomposition temperature was 20^{o}C higher than that of pristine PP. Further, the decomposition rate also decreased. The char residue increased when both GF and SP increased; the maximum residue was 37 wt.%, which helped prevent heat transfer from the polymer core as well as spreading of fire, in addition to reducing the amount of combustible gases generated.

Raman spectroscopy was employed to investigate the structure of the char residue after cone calorimetry and to assess the flammability of the nanocomposites. It was observed that the ID/IG ratio decreased when the nanoclay content was decreased from 5 wt. % to 2 wt.% or the IFR loading was increased (total content of IFR and SP was 20 wt.%), meaning that the structure of graphite became finer; this prevented the formation of combustible gases and the spreading of fire.

It was also found that all the mechanical properties were improved (except the ductility, which decreased) when the loading amount of the IFR used was increased and that of the nanoclay was decreased. The tensile modulus was the highest, 4.63 GPa, when the nanoclay loading amount was 2 wt.%. For greater loading amounts, the modulus decreased to 3.99 GPa. The addition of GFs along with the nanoclay had a synergistic effect when the SP loading amount was 2 wt.%. All the mechanical properties increased (except the ductility, which decreased) with an increase in the GF and SP loading amounts, owing to the agglomeration of SP in the polymer blend. XRD analysis showed that the peak of the composite with SP lower than 5 wt.%, shifted from 8˚ to 7˚, with the intensity of the peak decreasing and the peak becoming broader, when the SP loading amount was 2 wt.% and the GF content was 10 wt.%.

The best formulation for glass fibre loading with 2%SP is 10% GF to attain the highest retardancy and improved char strength (swelling occurs in this case). The compatibiliser SEBS-g-MA is better than PP-g-MA in term of flame retardancy and thermal stability. In terms of mechanical properties, PP-g-MA is preferred.

Acknowledgements

First of all, I would like to take this opportunity to express my deepest appreciation to my first supervisor Professor. Karnik Tarverdi and my second supervisor Professor Jack Silver for their patience, guidance and support throughout the different stages of this PhD. I must also thank Professor Tarverdi for his valuable comments in the completion of the thesis.

I would like to thank staff and technicians in the Wolfson Centre for Materials at Brunel University, in particularly Dr. Peter Allan for his technical support in injection moulding.

I would like to thank the support from Professor Jose-Marie director of Centre of Materials Engineering (C2MA), university of Ecole des Mines d'Alès(France)for preforming Cone calorimeter testing at his centre.

Finally, my thanks go every member of my family and friends for their great support and continuous encouragement throughout every stage of this study.

Table of Contents

List of Figures

List of Figures

List of Tables

List of Tables

List of Abbreviations

APP	Ammonium polyphosphate
ATH	Aluminium trihydroxide
ATR	Attenuated total reflection
CEC	Cation exchange capacity
CO	Carbon monoxide
CO_2	Carbon dioxide
DMA	Differential Mobility Analyzer
DSC	Differential scanning calorimeter
DTG	Differential thermal gravimetry
EDS	Energy dispersive spectroscopy
EHC	Effective heat of combustion
FIGR	Fire growth rate
FPI	Fire performance index
FR	Flame retardants
FTIR	Fourier-transform infrared spectroscopy
GF	Glass fibre
H_2O	Water vapour
HBr	Hydrobromic acid
HCl	Hydrochloric acid
HCN	Hydrogen cyanide
HFFR	Halogen free flame retardant
HRR	Heat release rate
IFR	Intumescent flame-retardant
LOI	limiting oxygen index
LRS	Laser Raman Spectroscopy
MA	Maleic anhydride
MDH	Magnesium hydroxide
meq.	Miliequivalent weight
MLC	Mass loss cone
MLR	Mass loss rate
N5	Nanofill®5

NC	Nanoclay
NH_3	Ammonia
NO	Nitrogen monoxide
NO_2	Nitrogen dioxide
O_2	Oxygen
PA6	Polyamide 6
PFI	Performance fire index
pHRR	Peak heat released rate
PP	Polypropylene
PP-g-MA	Polypropylene grafted onto maleic anhydride
R	Residual mass
RPM	Revolutions per minute
Sb_2O_3	Antinomy oxide
SEBS-g-MA	styrene/ethylene-co-butylene/styrene grafted with maleic anhydride
SEM	Scanning electron microscopy
SMLR	Specific mass loss rate
SP	Sepiolite
SPR	Smoke production rate
$T_{10\%}$	Temperature at 10% degradation / weight loss
$T_{5\%}$	Temperature at 5% degradation / weight loss
$T_{50\%}$	Temperature at 50% degradation / weight loss
TEM	Transmission electron microscopy
TGA	Thermogravimetric analysis
THR	Total heat release
Tig	Time of ignition
Tm	Melting temperature
Tonset	Onset temperature
UL94v	Underwriters Laboratories vertical testing
WAXS	Wide angle X-ray diffraction
wt.%	Weight percent
XRD	X-ray diffraction

CHAPTER 1 : INTRODUCTION

This chapter covers the introduction, aim and objectives of the research. In general, it describes the polymer material, nanoclay, glass fibre and flame retardant in addition to the development of hybrid nanocomposites. The thesis outline and methodology are also presented.

PP and PA6 are used widely in many applications, including in electrical, building, transport, and household materials. A major drawback of these polymers is their poor flame retardancy, given that they are organic materials. Thus, a primary issue to overcome in the case of PP is how to increase its flame retardancy without adversely affecting its mechanical properties.

1.1 The Background

A polymer is a high molar mass molecular mixture comprised of many repeating monomeric units, which are bonded with each other by covalent bonds over the polymeric chains (Sperling, 2005). The development of polymeric materials, as an engineering material started due to extensive study throughout the twentieth century. Bakelite is known as the first synthetic resin, which was present in 1907, that is frequently used nowadays in elements for the electrical and electronic industries. In 1926, the work of Staudinger got such a breakthrough for thermoplastic materials. The scientific foundation for the systematic study of plastics was initiated by his revolutionary research towards the long chain molecular structure of plastics. Based on the industrial application, polymeric materials can be divided into the subsequent categories: plastics, rubber, synthetic fibres, polymeric coatings, and polymeric additives. Plastics can be broken into two general classes: commodity plastics (such as polyolefins, polystyrene, polyvinyl chloride etc.) and high-performance engineering plastics (such as polyamides, polycarbonates, etc.). The polymer can be used as an engineering material instead of conventional materials like metal, wood, stone, glass, and ceramic. They are very useful

for many applications such as automotive industry, the electronic sector, the packaging and manufacturing of consumer goods (Ehrenstein, 2001).

In 2016, the global production of plastics reached 335 million metric tons, with 60 million metric tons produced in Europe alone Figure 1-1. China is one of the largest producers of plastics in the world, represented more than 25% of the global production followed by Europe 18.5% of global production (Plastic Europe Association, 2016).

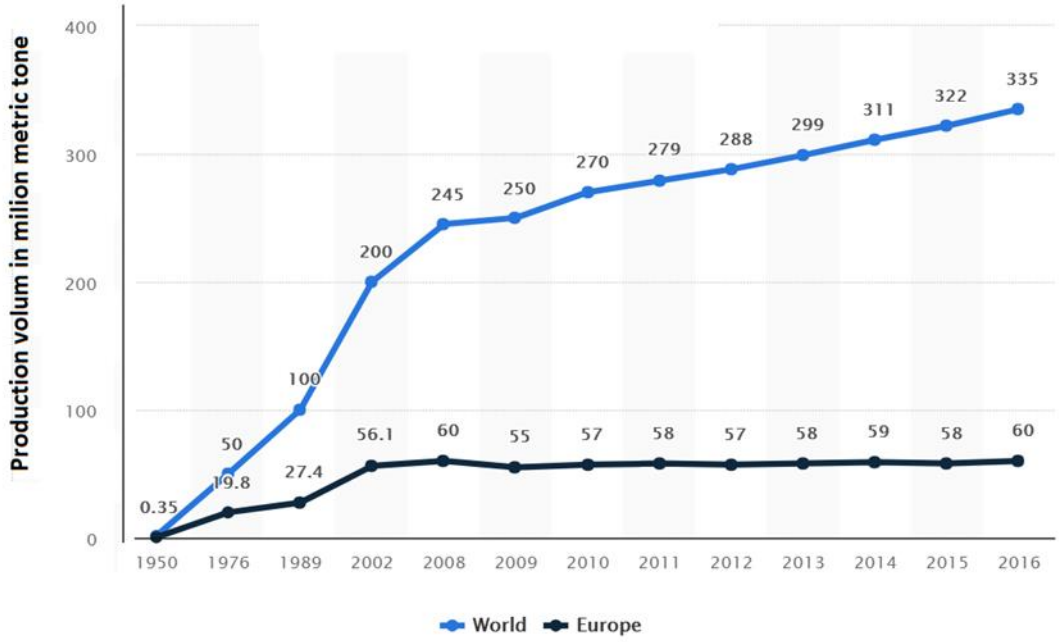

Figure 1-1 : Global plastic production from 1950 to 2016 (in million metric tons)(Statista, 2016)

In Europe 2016, packaging applications are the largest application sector for the plastics industry and represent 39.9% of the overall plastics demand. Building and construction is the second largest application sector with 19.7 % of the total European demand. Automotive is the third sector with a share of 10% of the total demand. Electrical and electronic applications represent 6.2% of the plastics demand and are closely followed by agricultural applications which have a share of 3.3%. Other application sectors such as appliances, household and consumer products, furniture and medical products comprise a total of 20.9% of the European plastics demand(Plastic Europe Association, 2016) as shown in Figure 1-2.

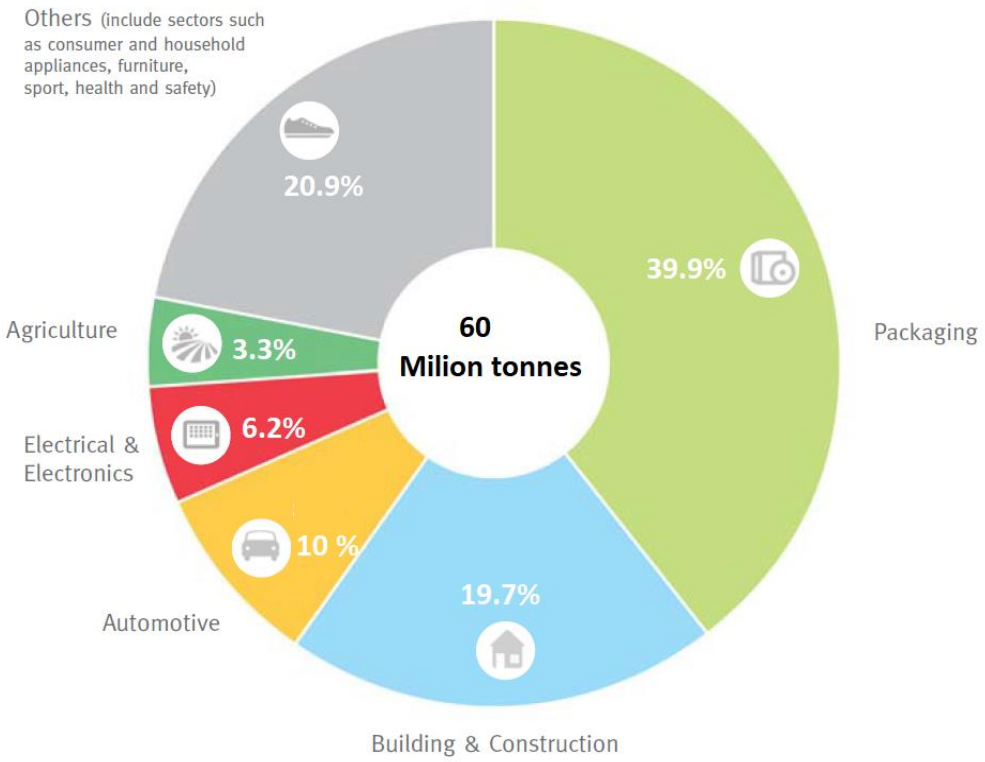

Figure 1-2: European plastics demand by sectors in 2016(Plastic Europe Association, 2016)

Currently, polypropylene (PP) is among the most widely used commodity thermoplastic polymer of propylene monomer produced by G Natta in 1954. PP consists of methyl (CH_3) groups attached to carbon atoms. The polymerization of PP can be seen in the Figure 1-3. PP is in many different industrial applications, suitable for many processing methods. Furthermore, it is known as one of the fastest developing types of commodity thermoplastics, with a market share expansion of 6-7% annually. Its strong growth rate is based on modest cost and favourable properties. PP is a good choice for many applications like fibres, filaments, and injection moulding parts for automobiles, rigid packaging, appliances, medical equipment, food packaging and consumer products. It can be substitute material for glass, metal, and engineering plastics including ABS, polycarbonate, polystyrene, nylon and used large appliances such as ovens, dishwasher, refrigerators, and washing machine. Flame resistance properties of PP need to be improved by means of flame retardants for applications in construction, automobile, home appliances, and electronics (Maier and Calafut, 1998).

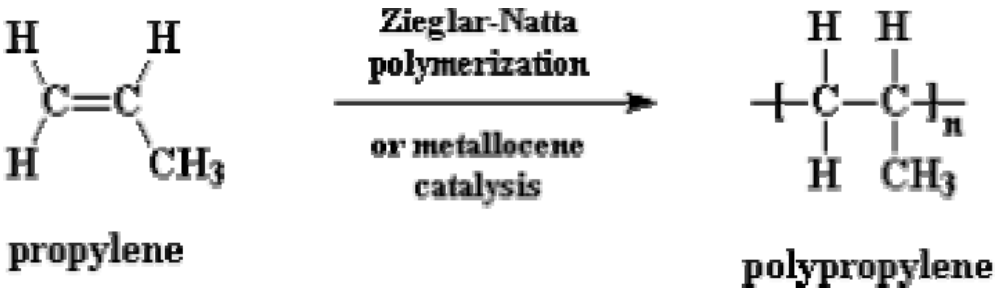

Figure 1-3:Polymerization of Polypropylene

Fire is a unique destructive force of nature and often has physical and chemical components. The reaction between the flame, its fuel, and the surrounding can be strongly nonlinear, and quantitative appraisal of the process involved is often complicated. The burning process and the processes of curiosity in an enclosure fire primarily require mass fluxes and heat fluxes both to and from the fuel and the environment (Troitzsch, 2004).

Every day in Europe there are about twelve fire casualties with 120 people severely injured and the World Health Organisation reports that there are approximately 300,000 deaths per year, globally from fire-related burns. The destruction of Grenfell Tower is considered as one of the UK's worst modern day disaster. The fire accident claimed the lives of 72 people. The accident occurred on 14th June 2017. Aluminium panels known as Reynobond were used as a cladding material with a cheaper version of Polyethylene core as an insulating layer. The Grenfell tower refurbishers compromised on having these Aluminum panels over the use of fire resistant version. The cost of upgrading was estimated to be less than £5,000 according to The Times (Times, 2017).In the USA in 2009, over 1.3 million fires were attended by public fire services, which resulted in 3,010 civilian deaths and 17,050 civilian injuries. [Based on well-known signals of fire Figures in the countries of the world European Flame Retardants Association (2016)].

As mentioned above, PP is an important commodity plastic and is used widely in several areas, including as a building, transportation, and electrical material. However, its applicability is restricted, owing to its high flammability (its limiting oxygen index (LOI) is often lower than 18 wt.%) (Liu *et al.*, 2011b). Therefore, research on flame-retardant

PP has generated significant interest over the past decades. One of the most important methods of enhancing the flame retardancy of PP is to use an IFR.

To minimize flammability, the incorporation of flame retardants (FR) is an efficient method. Also, the use of intumescent flame-retardant (IFR) in polyolefin is a somewhat new technology when compared to the improvement and extensive use of the polyolefins themselves. It is popular that the IFR can be described as an innovative generation of flame retardants for polyolefins: for example polyethylene and polypropylene because of its positive aspects, such as low-smoke, low release of toxic gases during burning, and anti-dripping. Nonetheless, this also has some disadvantages when compared with halogen-containing flame retardants in particular, low flame-retardant performance, and IFR requirements more filler quantity to get the results acquired with the halogenated compound.

Polymer blends have fascinated interest for a few decades like a simple, flexible and economical technique that enables establishing brand new materials with controlled properties from present polymers (Robeson, 2002;Galloway *et al.*, 2004;Jarus *et al.*, 2002;Pernot *et al.*, 2002;Persenaire *et al.*, 2010).

Polymer blending is a new method to enhance the fire properties of polymeric materials. Lizymol and Thomas (1993)examined the thermal stability of three binary blends of poly(vinyl chloride) (PVC), poly(ethylene-co-vinyl acetate) (EVA) and poly(styrene-co-acrylonitrile) (SAN). Results demonstrated that thermal resistance of the blends was observed to become strongly influenced by the miscibility of the homopolymers in the blend. Furthermore, the intrinsic fire behaviour of specific polymer and the blend composition highly modify the fire performances of polymer blends. In an additional research, Lizymol and Thomas (1997)briefly explored the fire behaviour of blends of polymers having different fire behaviours, i.e., PVC (intrinsic fire retardant) and EVA (weak resistance to fire). Results showed that the fire properties of EVA/PVC blends only depend on blend composition and not on blend miscibility. Swoboda *et al.* (2007) demonstrated that both morphology as well as the blend compatibilisation highly impact on the flame retardancy of polycarbonate (PC)/poly(ethylene terephthalate) (PET) blends. The flame retardancy of blends containing under 50 wt% of PC increases linearly

with PC content when blends made up of greater than 50 wt% of PC interact with fire like pure PC because of the development of a continuous PC phase. The chemical connections between polymeric phases in the blends may also modify the fire properties of the finalmaterials. As much as PET/PC blends were concerned, the transesterification reaction between the two polymers was shown to reduce the overall fire performances as a result of reduction in the viscosity of the blends resulting from PET chain scission. Sonnier *et al.* (2012) looked into the relationship between morphology and fire behaviour of a binary polymer blend constituted of a low flammable and charring polymer (PC) and a comparatively flammable and non-charring polymer (PBT). They indicated that the comparable percentage of every polymer is the main parameter which establishes the fire behaviour of the blend and a rise in PBT content lowers the flame retardancy of the blend.

With a perspective to consider advantages of the natural sepiolite properties, the preparation of nanocomposites depending on PP/PA blends has been identified in this study. As a way to enhance the potential of flame retardancy of sepiolite, the incorporation of a charring polymer such as PA6 has been regarded as. It is believed that the usage of PA6 could enhance both the amount and the thermal stability of the char. Truly, Bourbigot *et al.* (1998) confirmed that pristine PA6 might be used successfully as charring agent in intumescent formulations for PP. In this paper, the potential synergistic flame retardant effect of both needle-like clay and charring agent is explored. It is important to note that just natural sepiolite, has been taken into consideration in the study.

Blending of polymers is one of the cost-effective solutions planned to enhance the fire retardancy of these PP/PA6 that contains also compatibilisation agents that can be taken into consideration. The awareness of IFR systems has yet been established for polyolefins and IFR systems that contain PA6 as char promoter have been planned (Almeras *et al.*, 2002).

The incorporation of FRs is an efficient method of minimising the flammability of materials. Further, the use of halogen-free IFRs with polyolefines is a somewhat new technique when compared to the development of polyolefins themselves. IFRs are often described as novel FRs for polyolefins such as polyethylene and PP because of their positive characteristics during burning. For instance, they emit small amounts of smoke,

release fewer toxic gases during burning, and do not drip as much. However, IFRs also have a few disadvantages when compared to halogen-containing FRs. In particular, they show low flame retardancy and require greater amounts of the filler material in order to produce desirable results.

There are some problems associated with the IFR systems, such as their moisture resistance and poor compatibility with the polymer matrix. The blending of the hydrophilic PER and APP with PP leads to considerable decrease in mechanical properties as a consequence. Further drawbacks are the low thermal stability and poor flame retardant efficiency at low FR concentrations. In order to overcome these drawbacks and enhance the flame retardancy, new IFR systems have been developed and synergistic agents have been used in IFR systems (Bourbigot and Duquesne, 2007) .

Many researchers have used MMT nanoclay as filler in hybrid polymeric composites and their laminates due to its well-known exfoliation/intercalation chemistry, surface reactivity, high surface area, cost effectiveness and easy availability (Hossen et al. 2015; Dewan et al. 2013). Some of the important research work on organoclay based polymer composites are given in Table 2. A variety of naturalfibres (from jute to oil palm fibres, either in short fibre, nonwoven mat or in woven fabrics) are modified by the nanoclays.

Despite the fact that the needle-like morphology of sepiolite seems less advantageous than MMT, sepiolite provides processing benefits because of its superior wettability by non-polar polymers. In addition, the fewer contact areas between needles when compared to the contact area between clay layers can give preference to sepiolite dispersion. As a result, the organo-modification of sepiolite is not a prerequisite compared to montmorillonite. Natural sepiolite can hence remain thought of as a cost-effective replacement for organomodified clays (Laoutid *et al.*, 2013).

The term “hybrid” is of Greek-Latin source. Hybridization is a method of adding two reinforcements (either synthetic fibres/nanofillers/natural/ metallic fibres) in one polymeric matrix phase or the incorporation of single reinforcements in polymer blends

in an attempt to produce superior properties that include high mechanical strength, compressive strength, stiffness, thermal stability that cannot be observed in conventional composite materials (Borba *et al.*, 2014;Saba *et al.*, 2014). Hybrid materials are extremely advanced composites materials composed of two or more several constituents at the molecular or nanometre stage. Properties of hybrid composites is considered as the total of the individual elements; as a result it supplies a combo of properties such as tensile modulus, compressive strength and impact strength (Gururaja and Rao, 2012). Hybrid composite materials have considerable engineering applications, where strength to weight ratio, simplicity of fabrication and low cost are expected. The hybrid composite properties with two different fibres are specifically controlled by the individual fibres length, fibres alignment and fibres volume, degree of mixing of fibres, fibres arrangement and fibre-matrix bonding. The incorporation of glass fibre with intumescent flame retardant is to improve both mechanical and thermal stability beside flame retardancy.

Researchers concluded that the incorporation of a very small amount of nanoparticles into a matrix can enhance both thermal and mechanical properties considerably without reducing the weight or process ability of the composite (Hossen *et al.*, 2015). So far many research works have been created on natural fibre hybrid nanocomposite materials by applying nanoparticles like nanotube, metal oxides, nanoclays, carbon nanofiber and other nanoparticles for diverse leading-edge applications.

1.2 Flammability of Polymers

To have a good understanding of the strategic routes to obtain flame retarded PP/PA6 blends it is necessary to first answer some basic questions about flammability of polymers and flame retardancy.

When polymer is subjected to heat or flame, during a fire situation for example, the temperature of a polymer rises, leading to its thermal degradation. Hence, chemical bonds of the polymeric chains are broken to create highly flammable volatiles. These volatile compounds automatically form combustible mixtures with air which ignite easily and burn with a high velocity from the development of radicals (implying $H^{\bullet}$ and $OH^{\bullet}$).

So, a low thermal stability linked to the release of highly flammable volatile molecules is mainly responsible for the flammability of the material.

1.3 Thermal Degradation of Polymers

Knowing polymer degradation is very important for the improvement in current polymer processing techniques. Of specific interest to this thesis is that the first step in start and development of a fire is thermal degradation and decomposition in the solid phase.

Thermal decomposition of a polymer is an endothermic process which requires binding energy of around 200-400 kJ/mol (C-C backbone polymers) supplied to destroy covalent bonds. It is important to differentiate thermal decomposition in the lack of oxygen (pyrolysis) and in the presence of oxygen (thermo-oxidative decomposition). In oxidative decomposition, polymer molecules interact with oxygen and various lower molecular weight decomposition(Laoutid *et al.*, 2009).products are created together with highly reactive $H^{\bullet}$ and $OH^{\bullet}$ radical species undergoing further combustion reactions in the gas phase (Laoutid *et al.*, 2009) .

It is also necessary to combine the energy source (spark, hot spot ...) with oxygen (oxidizer) and a flammable product (fuel) to obtain a fire. The association of these three elements constitutes the "fire triangle" presented in Figure 1-4. The initiation and maintenance of the fire thus obtained requires an interaction between these elements heat transfer and contact between fuel and oxidizer (Price *et al.*, 2001). More precisely, the initiation of a fire passes first by the heating of the material by a source of heat. Beyond a critical temperature, the weakest bonds in the polymer break down and give up radicals which react to form flammable molecules. The ignition then takes place if the rate of release of the volatile products reaches a value sufficiently high for the gaseous-air mixture to be flammable. This step depends on various parameters such as oxygen concentration, temperature, and the nature of the polymer.

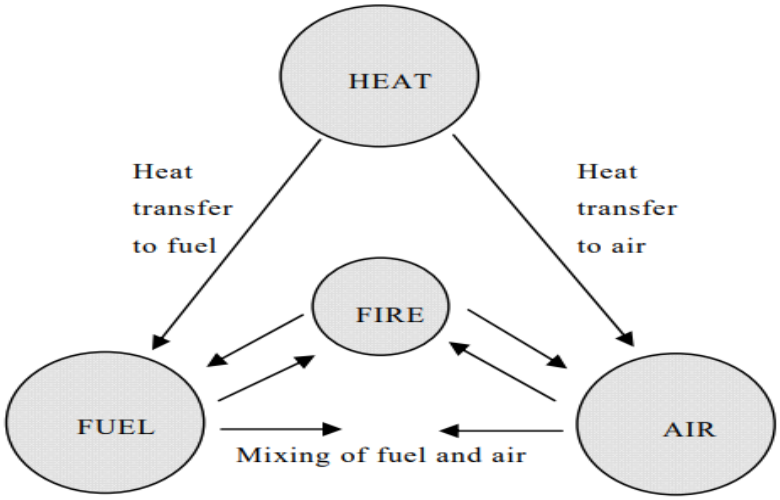

Figure 1-4:Fire triangle (Troitzsch, 2004)

This results in propagation which can be carried out by conduction, convection and / or radiation and which gives rise to a fully developed fire. The main stages of the development of a fire are shown in Figure 1-5 as a function of the temperature of the environment which can reach 1200 ° C. When the contribution of one of the three elements of the fire triangle tends to decrease fire intensity, and then the fire declines and finally goes out.

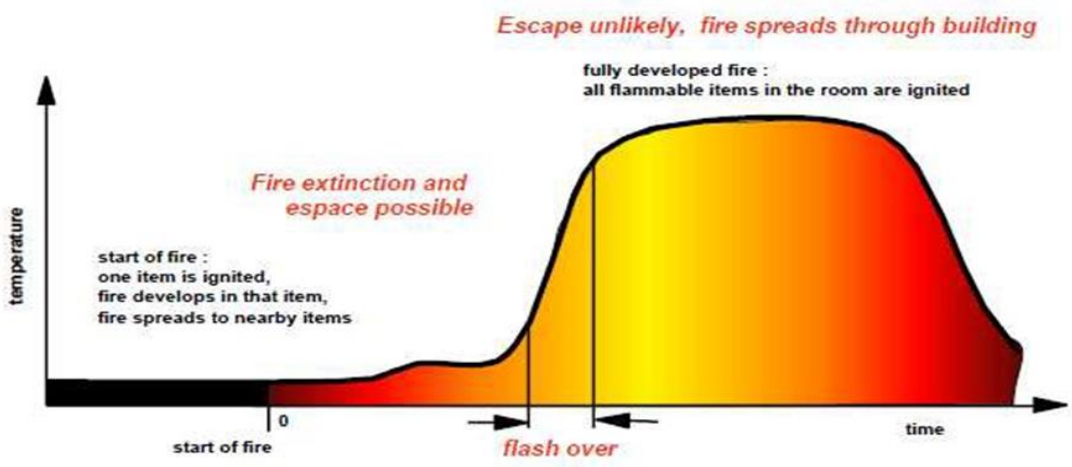

Figure 1-5 : Stages of the development of a fire

1.4 Why Use Flame Rretardants

One of the most dangerous gases released during a fire is carbon monoxide. Due to its characteristics (colourless, odourless and tasteless), it is undetectable and easily intoxicates occupants of a dwelling on fire before they notice the fire. Hydrogen cyanide (HCN) is also a hazardous gas released, as low concentrations in the smoke can cause irreversible health effects after only a few minutes of exposure. It can be generated by certain plastics such as Polypropylene (PP) or polyamides.

The increasing using of polymers in a huge selection of applications leads to a steady desire for enhanced thermal and mechanical properties to endure progressively strict conditions. The decrease in the polymers' tendency to spark and burn efficiently is an essential factor to consider because the polymer materials include a considerable portion of the fire loading in houses, commercial environments and transportation. Hence, it is obvious that fire retardants are an essential part of polymer formulations (Wilkie *et al.*, 2009).

Wakefield (Wakefield, 2010) studied the gas evolved during the combustion; he stated that most polymers generates: carbon monoxide. carbon oxide and hydrogen cyanide (HCN) gas. One of the most dangerous gases released during a fire is carbon monoxide, because of its characteristics (colourless, odourless and tasteless), it is undetectable and easily intoxicated occupants from a burning home before they even notice the fire.

Flame retardants are materials that are incorporated into a variety of materials to reduce the risk of fire injuries and damage by providing increased resistance to ignition or by acting to slow down combustion and thereby delaying the spread of flames. A perfect flame retardant polymer material must possess some special features: significant resistance to ignition and flame propagation, a low rate of combustion and smoke generation, low combustibility and toxicity of combustion gases, acceptability in character and properties and particularly utilizes very little quantity without increasing the cost of the product(Grand and Wilkie, 2000).

The incorporation of FR in the polymer materials also aims to significantly reduce the amount of toxic fumes and gases released during the combustion of plastics, in addition to avoiding the outbreak of fire and its spread if the fire was still able to start.

The use of these additives is carried out wisely, regulations governing their utilisation. The FR is thus added to materials to conform to safety regulations and to provide the required level in terms of fire resistance for the general public. The amount of FR added depends on the application of the material and specifications associated with it (Bourbigot *et al.*, 1993).

1.5 Flame Retardancy

Most polymeric materials ignite easily, burn quickly producing large heat, express flaming drips, and maintain combustion even under oxygen-lacking environments, a feature of fires. Undesirable fires, particularly those coming from plastic products with low resistance to ignition and fast flame spread properties could be prevented by the progression of new flame-retarded polymers targeting application areas such as cable insulation, automotive fuel and ignition systems, printed circuit boards, novel textiles and foams, and housings of electrical equipment. Considerable research work is being exerted both through the academic and the polymer sector on the development of advanced light-weight materials possessing improved flame retardancy along with satisfactory mechanical, thermal, and electrical properties.

1.6 From Micrometre to Nanometre

Nanotechnology is the science to understand and control matter on the order of dimensions of 1 to 100 nm, which appears as unique phenomena enabling new applications (Weiss *et al.*, 2006). Producing structures in the nanometer range, it will become really easy to control fundamental properties of materials: for example, the melting temperature or the mechanical properties without changing the chemical composition of materials. Use of this potential will lead to new high-performance products and technologies when it was not possible to increase properties of the materials.

There are many researches based on that report the enhancement of flammability of nanocomposite materials based on layered silicate nanoclay; however, there are few papers that report the synergistic effect on the intumescent flame-retardant PP with sepiolite reinforced by glass fibre. In the present work, we use sepiolite as a synergistic agent to flame-retard PP, along with intumescent flame retardant (IFR), which is composed of ammonium polyphosphate (APP) and charring agent nylon 6 and reinforced by chopped short glass fibre. The sum of APP to sepiolite is kept at 20 % of total weight.

1.7 Aims and Objectives

Polymer blending offers an effective way of producing new engineering materials and is an interesting alternative for the modification of commodity low-cost polymers. PP and PA6 are two of the most widely used polymers. However, a significant expansion of their field of application depends on improving their flame-retardant properties. Accordingly, the main objective of this study was to produce a flame-retardant PP/PA6 nanocomposite. This nanocomposite contained sepiolite and was reinforced by a short glass fibre using a twin-screw extrusion machine in order to reduce its flammability.

To fulfil the aim of this study, the following objectives were determined:

- Synthesising a glass fibre-reinforced flame-retardant PP/PA6 nanocomposite using the twin screw extruder method;.,
- Studying the effect of compatibiliser on thermal stability, flame retardancy and mechanical properties of PP/PA6/mpp/AP blend with two types of fillers namely sepiolite(SP) and nanofill5(N5).
- Assessing the effect of Intumescent flame retardant (IFR) on thermal stability, flame retardancy and mechanical properties of PP/PA6/mpp/GF/SP blend.

Effect of Glass fibre (GF) on thermal stability, flame retardancy and mechanical properties of PP/PA6/mpp/AP/SP blend.

1.7.1 Research methodology

The work contained within this thesis details the experimental mechanical characterisation of a number of in-house processed flame retarded polypropylene nanocomposite materials. The methodology can be represented by five main steps, as follows:

- Material processing and preparation
- Microstructural and morphological characterisation
- Mechanical characterisation
- Thermal analysis
- Char residue analysis
- Flammability y characterisation

1.7.2 Material processing and preparation

The polypropylene powders were to be combined with pre-treated clay nanoparticles for better distribution. The mixed materials were to be then blended in a twin-screw extruder using two different processing techniques to produce nanocomposite pellets. The pellets were then to be melted under specific temperature and pressure conditions to make a compression moulded plaque. The plaque was to be moulded under pressure using water cooling. Finally, the specimens were to be cut from the plaque into appropriate geometries for a number of tests.

Thermal analysis: DSC, TGA and infrared thermography were to be utilised to examine the consequence of processing and nanoparticle addition on the material crystallinity, degradation temperature and internal heat generation in the material, respectively. The results were to be used to explain the relationship between thermal and mechanical properties of polypropylene -based nanocomposites. Furthermore, the effect of surrounding temperature on the mechanical properties of the material was to be studied and the critical softening temperature was to be determined

1.8 Thesis oOutline

The thesis contains six chapters following the introduction (Chapter 1), a brief description of each chapter is given below:

Chapter 2 presents a review of the literature on the flammability, thermal stability, and mechanical properties of PP and its nanocomposites.

Chapter 3 describes the materials and experimental methods used to prepare the PP/PA6/IFR/SP/GF nanocomposites via the extrusion process as well as the essential characterisation techniques used to evaluate the nanocomposites.

Chapter 4 lists the results of effect of compatibiliser types and nanoclay types on flammability glass fibre reinforced retarded PP/PA6 composites in term of flame resistance, thermal stability and mechanical properties.

Chapter 5 lists the results of effect of intumescent flame retardant and synergistic effects of sepiolite nanofillers composites in term of flame resistance, thermal stability and mechanical properties.

Chapter 6 lists the results of effect of glass fibre loading and synergistic effect of Sepiolite with retarded PP/PA6 nanocomposites composites in term of flame resistance, thermal stability and mechanical properties.

Chapter 7 lists the conclusions of the study as well as recommendations for further work on the subject.

CHAPTER 2 : LITERATURE REVIEW

This chapter deals with the literature review. It will first be devoted to an overview of combustion of polymer and flame retardant (FR) from a historical perspective. Then will present in more detail the different FR use in polymers and for each FR, we will discuss the mechanisms of action associated with it. Finally, it will make a state of the art work on the effect of the FR on the thermal properties, fire retardancy and mechanical properties of plastics in general and on the more specified glass reinforced PP/PA6 composite.

2.1 Burning and Thermal Decomposition of Polymer

In section 2.1 the combustion process was introduced. It is applied to polymer materials. The combustion reaction involves two elements in the presence of an energy source: fuels (reducing reagents) and oxidants (oxidizing reagents). The oxidizer is generally the oxygen contained in the air. The combination of these three elements (fire triangle) is shown in Figure 2-1. Above a critical temperature, heat energy will be sufficient break bonds of the polymer and start free radical reaction which react to decompose of polymer and form flammable molecules. The ignition then takes place if the volatile release rate reaches a sufficiently high value so that the gas-air mixture is a flammable product. This step depends on various parameters such as the oxygen concentration, temperature and nature of the polymer.

There are three stages in the burning process of plastics: heating, degradation and decomposition, volatilisation and oxidation (Troitzsch, 1990). In the heating stage, heat is added and polymer (pyrolysis) leads to a chain scission. In the degradation stage there will be a loss in physical, thermal and electrical properties of a material at higher temperatures(Beyler and Hirschler, 2002). Thermal degradation depends of polymer depends on the environment [air (oxygen) or inert atmosphere]. When a polymer undergoes degradation in an inert atmosphere the heat is endothermic (heat to sample), whereas when in air, the heat is exothermic (release of heat from sample).

The first pyrolysis products contain a complex mixture of combustible and non-combustible gases, liquids, which could consequently volatilize and produce solid carbonaceous chars, along with highly reactive species for example free radicals. The free radicals formed at different stages of the combustion process play a key role in determining the course of this procedure, the speed and magnitude of heat release and the resulting rate of flame spread. Once the initial combustible products in an admixture with atmospheric oxygen achieve the lower ignition limit, they ignite generating the flame. These reactions with oxygen are generally exothermic. The energy released by these processes can start further thermal degradation reactions promulgating the fuel source to support combustion, hence resulting in flame spread. The reactions which occur in the flame are radical chain branching reactions which cause the output of highly energetic hydrogen and hydroxyl radicals (H- and -OH respectively) which propagate the overall combustion process (Troitzsch, 1990).

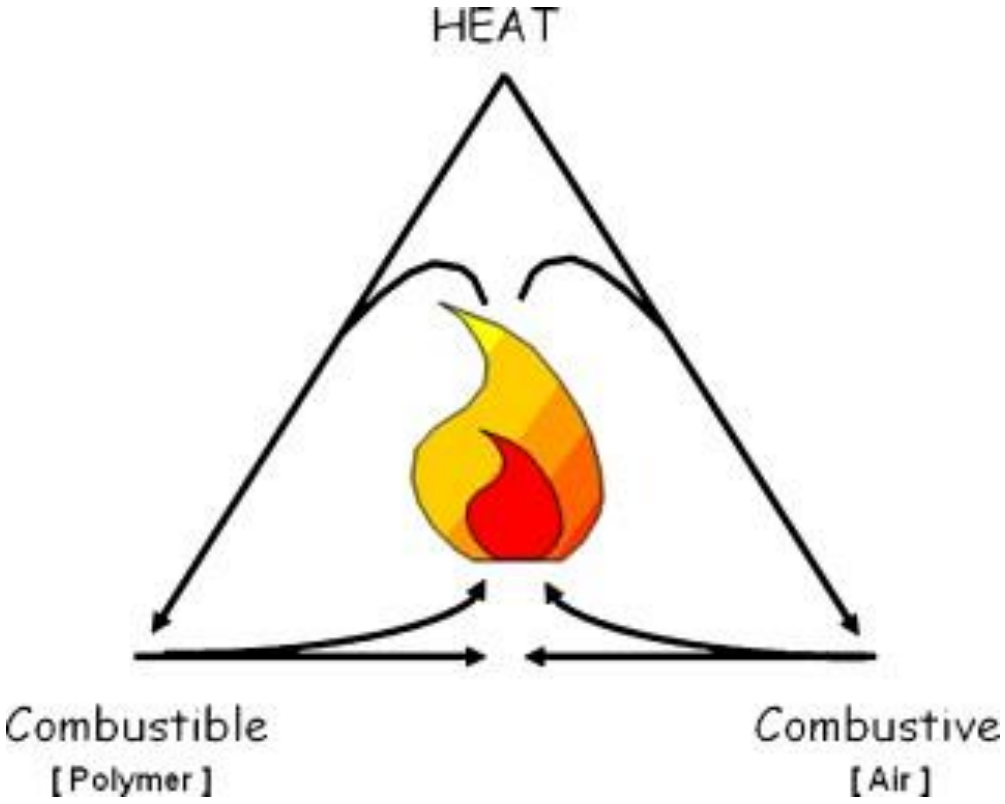

Figure 2-1 : The fire Triangle

2.1.1 Combustion cycle of polymer

Combustion is a highly exothermic chemical reaction, autonomous, capable of accelerating gradually and being accompanied by radiation emission. It is a complex phenomenon involving many parameters and taking place in many steps, the four main ones being: (1) heating, (2) thermal degradation, (3) ignition and (4) propagation. Figure 2-2 summarises the different steps detected during the combustion of polymers and shows where a fire-retardant action can be carried out. When heat is supplied, the material softens, or even melts in the case of thermoplastics. Then, when the source heat to the material is higher than that required for its degradation, decomposition products are

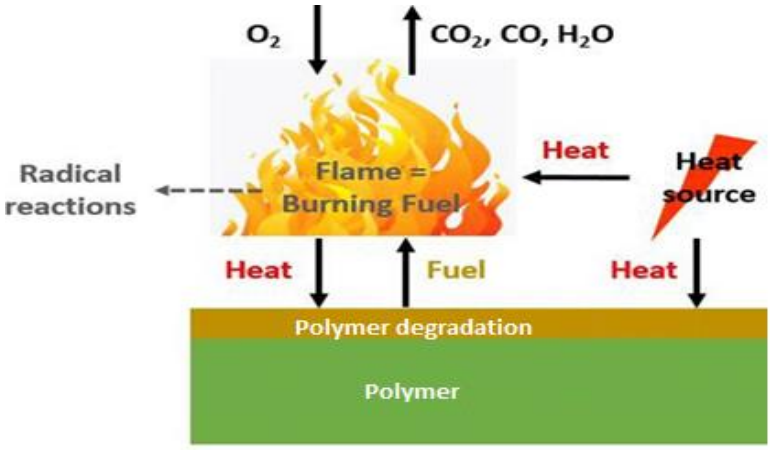

Figure 2-2 Combustion process and reactions occurring in the flame

evolved in the gas phase. These flammable gases are mixed with oxygen from the air and when the system reaches a critical concentration, ignition occurs. A portion of the heat of the flame is returned to the material, Therefore, the combustion process continues without the help of external energy. As long as degradation products are evolved and oxygen continues in adequate amount, there is a self-sustaining flame

which can propagate to its surroundings. (Kiliaris and Papaspyrides, 2010). The flame is formed by the highly exothermic reactions taking place between the radicals formed from the thermal decomposition of polymer and oxygen.]. A fire development depends also on the environment, environmental conditions and heat transfers (Pal and Macskasy, 1991). The combustion of a polymer is the consequence of a combination of the effects of heat, represented by two mechanisms(Laoutid *et al.*, 2009) shown in Figure 2-3.

- **Oxidizing thermal degradation: reaction with oxygen to produce a variety of low molecular weight products.**

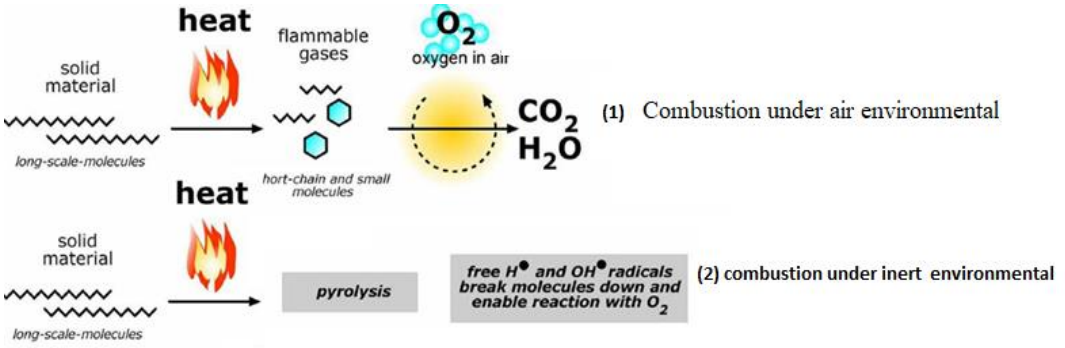

Figure 2-3: Combustion of a polymer under air and under inert environmental (pyrolysis)(European Flame Retardants Association, 2006)

- **Inert thermal degradation (pyrolysis): initiated by chain scission**

In fact, fire retardancy involves in the reduction of heat provided to the polymer, so that the system remains below the critical level that guarantees flame stability. This can be attained by stopping the combustion cycle at different steps:

To improve the fire resistance of a material, the combustion cycle must prevent the flame from forming. An action aimed at obtaining a self-extinguishing material can

also make it possible to achieve the objective and to limit the transfer of heat from the flame to the polymer.

2.1.2 Flammability of Polymers

When polymers are subjected to a satisfactorily large heat energy from a fire, they thermally decompose to produce volatile gases, solid carbonaceous char and smoke (Mouritz and Gibson, 2006) The volatile gases released can either be flammable such as carbon monoxide, methane, low molecular organics, or can be non-flammable such as carbon dioxide and water. When flammable volatile gases diffuse from decomposing polymer into air, they form a gaseous mixture, reacting with oxygen or other oxidizing element leading to ignition and liberating heat. The amount of heat evolved controls the duration of combustion. In presence of sufficient heat feedback to polymer, new decomposition reactions are induced in the solid phase, more combustibles are produced, thus; the process becomes self-sustaining; maintaining combustion of the polymer (Laoutid *et al.*, 2009).

Polymers decompose via a series of chemical reaction mechanisms. The first mechanism is random-chain scission; in which scissions occur randomly throughout the length of the chain. The second mechanism is end-chain scission in which individual monomer units or volatile chain fragments are removed at the chain end. Chain stripping is another mechanism in which atoms or groups that are not part of the main backbone (side/pendant groups) are removed. The last mechanism is cross-linking in which bonds are created between polymer chains, resulting in an increase in molecular weight. In most cases, polymers decompose through the combination of two or more mechanisms.

Polymers that decompose via random chain scission and depolymerization are more flammable than those that decompose via cross-linking and chain stripping. Cross-linking causes creation of char which lowers flammability (Wilkie *et al.*, 2001). In chain stripping, removal of the side/pendant group leads to the formation of double bonds which can give crosslinks. And again, cross-linking results in formation of char, lowering

flammability.Polymers having aromatic or heterocyclic groups in main chain are less combustible than polymers with an aliphatic backbone (Aseeva and Zaikov, 1986). Polymers having short and flexible linkages between aromatic rings tend to crosslink and char. This char formation increases thermal stability and enhances flame retardancy. On the other hand, polymers with relatively long flexible linkages between aromatic rings are relatively more combustible.

Char formation is very important in combustion process. Charring of the polymer can occur via cross-linking, aromatization, fusion of aromatics or graphitization depending on the structure of the polymer(Levchik and Wilkie, 2000). Char is formed only if the cross- linked polymer has aromatic fragments or conjugated double bonds and is prone to aromatization during thermal decomposition (Wilkie *et al.*, 2001). It works as a barrier to heat and mass flow, and stabilizes carbon; preventing its conversion to combustible gases. Char effectiveness depends both on its chemical and physical structure. For an effective barrier; a rigid and crack deficient char structure must be provided to prevent the flow of volatile flammable gases into the flame and to provide sufficient thermal gradient to protect the polymer below its decomposition temperature.

2.1.3 Thermal degradation of polymers

The various degradation mechanisms have been identified in the literature (Beyler and Hirschler, 2002) and Figure 2-4 summarise the main mechanisms of thermal decomposition of polymers : depolymerisation (for example PMMA), random scission (for example : PA6, PE, PP), elimination of groups pending(side group scission) (PVC or PVOH). There are therefore three main mechanisms

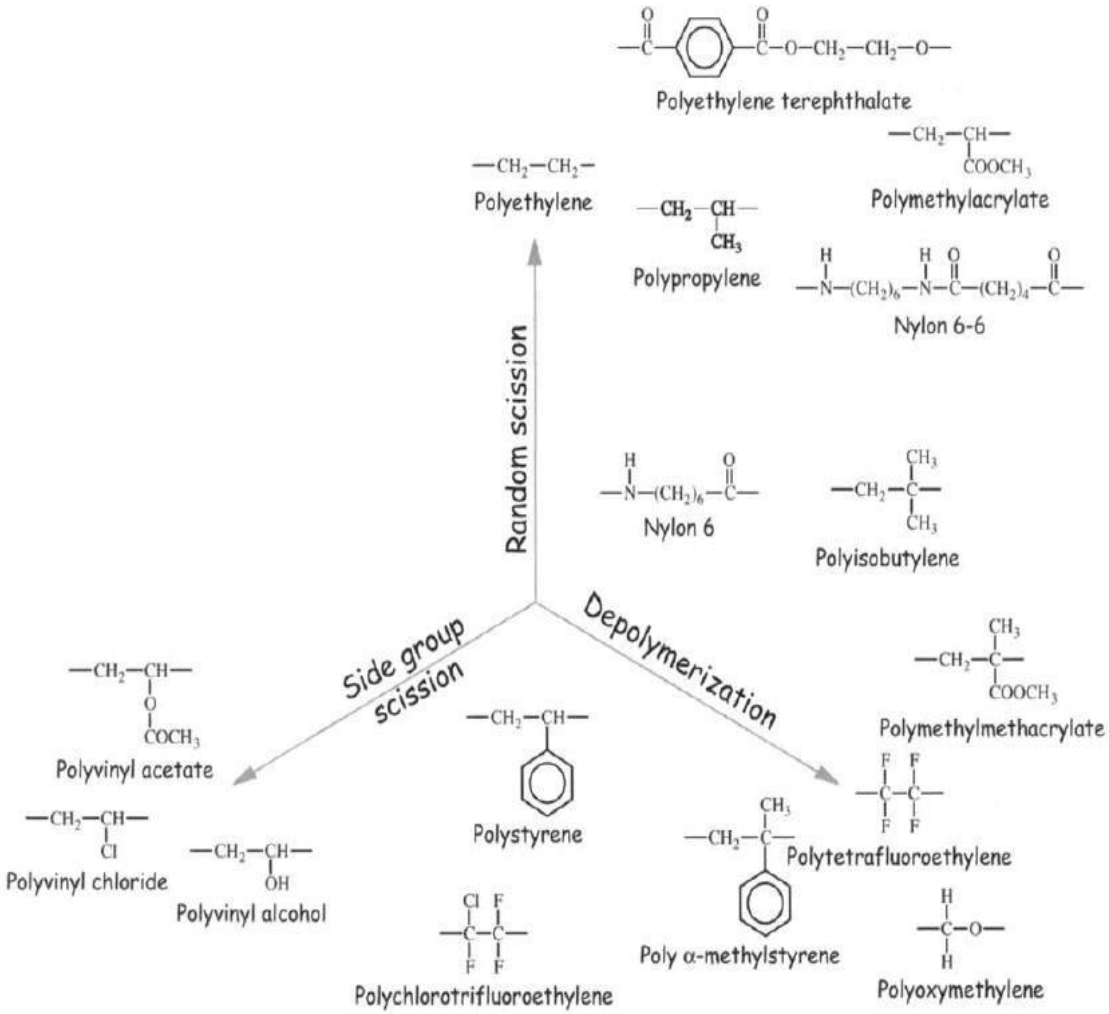

Figure 2-4: Mechanisms of thermal degradation of polymers

- Degradation by random scission. This is the case for polymers whose bonding energies are the same throughout the chain as for example PE or PP.

- Degradation by depolymerisation: This decomposition is in particular linked to the splitting of the chain ends, favouring the formation of monomers. PMMA degrades in this way. The temperature at which the pyrolysis takes place will have a strong influence on the level of monomers formed according to the polymer. For example, while PE produces 0.03% of monomer at 500°C and 5.5% at 800°C, whereas poly-α-

methyl styrene produces 100% monomer at 500°C and 88.5% 800°C (Stauffer, 2003)

.

- Degradation by side group scission (cyclization or crosslinking): It may be due to the splitting of pendant groups present on the chain, as in the case of PVC with the formation of HCl. There may then be elimination and cyclization. This degradation mechanism can also create rearrangement reactions between the chains, thus leading to the formation of a cross-linked network. In both cases, the degradation leads to the formation of a char (charcoal layer composed of products of aromatic structure and of higher molar mass and therefore non-volatile).

2.1.4 Thermal decomposition and burning behaviour of PP

Polypropylene is a polar polyolefin whose structure is recalled in Figure 2-5. Its thermal degradation, notably due to the analysis of degradation products, has been widely studied (Palza *et al.*, 2010). It shows that the decomposition mechanisms of polypropylene are sensitive to the atmosphere (Pal and Macskasy, 1991).

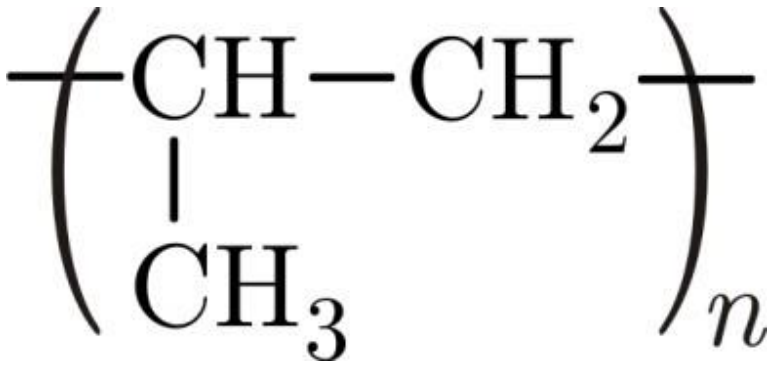

Figure 2-5:Structure of polypropylene

- **Degradation of PP in inert atmosphere**

It is established in the literature (Kiang *et al.*, 1980;Szekely *et al.*, 1987;Salaün *et al.*, 2011) that thermal degradation of PP under an inert atmosphere occurs via a one-step mechanism without leaving any residue as shown in Figure 2-6.

More recently, studies of PP degradation kinetics have shown that the mechanism decomposition mechanism of PP involves multi-step reactions (Tsuchiya and Sumi, 1969;Chrissafis *et al.*, 2007). Chrissafis *et al.* (2007) carried out the modelling of the experimental curves obtained by thermogravimetric analysis under N_2. The kinetic models which allow the best correlation with the experimental results involve a mechanism of degradation of the PP in two autocatalytic steps. The first stage is then associated with a low initial mass loss, and the second stage corresponds to the main decomposition step of the polypropylene. It should be noted that in this study, the authors do not propose a for these two stages of degradation.

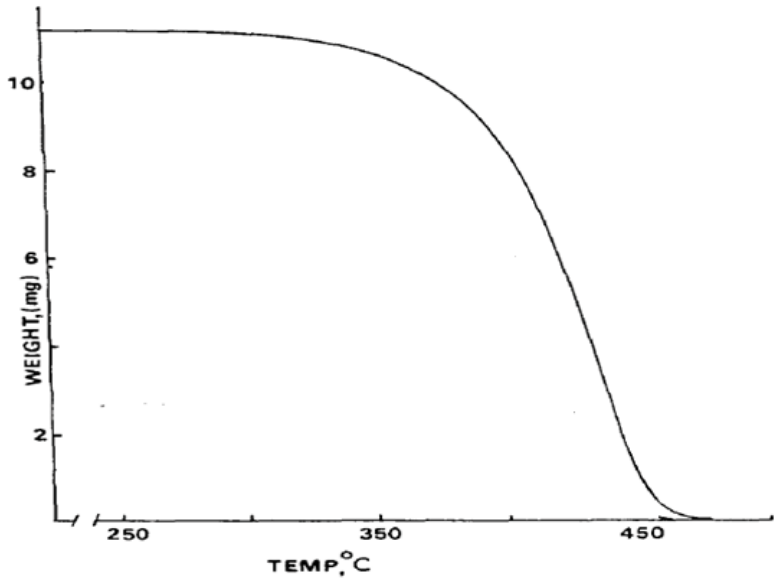

Figure 2-6: Thermogravimetric curves of the degradation of isotactic polypropylene- (Kiang et al., 1980)

- **Thermo-oxidation of PP**

In the same way, as under an inert atmosphere, the mechanism of degradation of polypropylene in the presence of oxygen has been widely studied. Indeed, polypropylene is very sensitive to oxidation since oxygen will cause an early degradation of the matrix, either under the effect of heat or by photo-oxidation (which means that it is formulated with UV stabilizers) (Commereuc et al., 1997; Peterson et al., 2001). The general mechanism of thermo-oxidation of polypropylene is, as for the other polymers, a radical.

chain reaction comprising the initiation, propagation, branching and termination steps. The simplified general scheme of this mechanism has been established and validated by many researchers (Iring and Tüdos, 1990;Gijsman *et al.*, 1993;Gutiérrez *et al.*, 2010) (Figure 2-7).

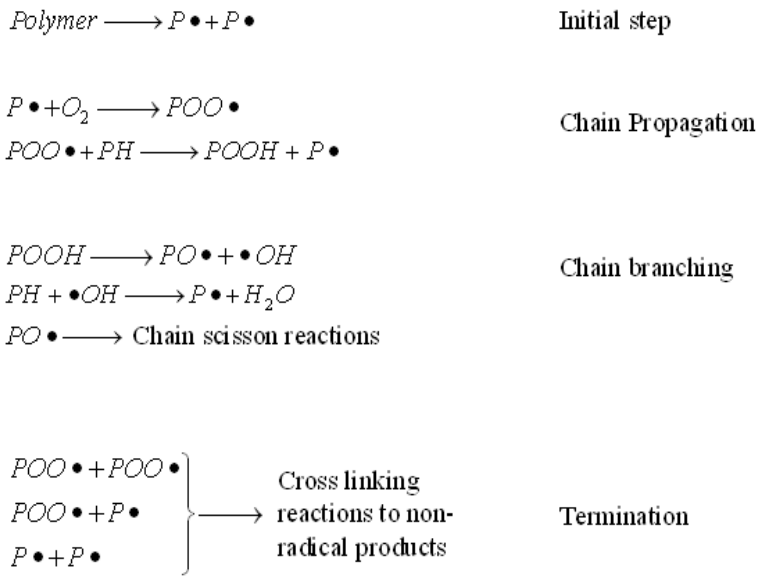

Figure 2-7 : General mechanism of thermo-oxidation of polypropylene (Gutiérrez *et al.*, 2010)

Where PH = Polymer
$P^{\bullet}$ = Polymer alkyl radical
$PO^{\bullet}$ = Polymer oxy radical (Polymer alkoxy radical)
$POO^{\bullet}$ = Polymer peroxy radical (Polymer alkylperoxy radical)

2.1.5 Thermal decomposition and burning behaviour of PA6

Despite a great number of researches in the field of thermal decomposition of polymers, there is not yet a general accepted mechanism for the decomposition of aliphatic nylons. A variety of experimental conditions can be found in the literature which does not lead to a common decomposition pathway of PA6. Levchik *et al.* (1999) however made a review on this topic (Levchik *et al.*, 1999). Some main mechanisms have been identified, involving the release of ε-caprolactam monomer. The depolymerization Figure 2-8 begins at temperatures slightly above 200°C by intramolecular end-group cyclization (end-biting), main chain cyclization (back-biting) or intermolecular aminolysis (Davis *et al.*, 2003).

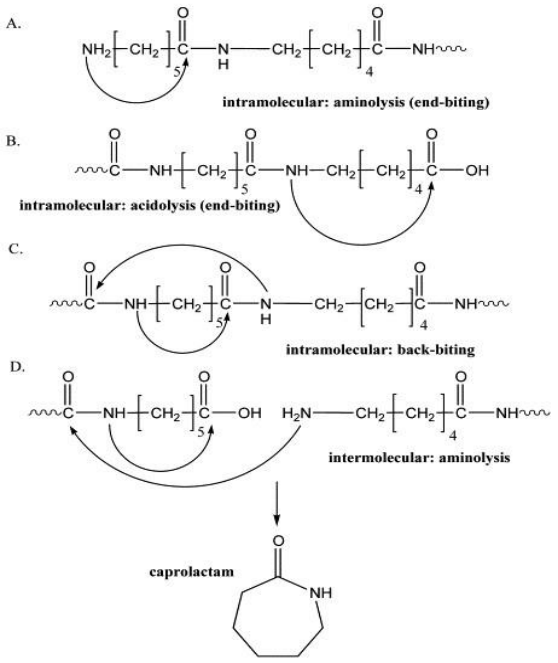

Figure 2-8 : Intra and intermolecular generation of ε-caprolactam during degradation of PA6

The flammability of aliphatic nylons has been investigated by means of many methods, among which the measurement of LOI. A measurement of LOI for various nylon 6 samples was carried out by These researchers supposed the flammability of nylon 6 is connected to the production of fuel. A relation between LOI, molecular weight (viscosity η), concentration of amine (a) and carboxylic (c) chain-ends was proposed Equation (2-1Literature ReviewLiterature Review). (Reimschuessel *et al.*, 1973;Pearce, 1984) Thus, due to their low melt viscosity, aliphatic nylons are considered to have an apparent low flammability.

$$LOI = 13.5\left(1 + \frac{1}{\eta}\right) + \frac{2050}{(13.5\mathrm{a} + \mathrm{ac})} \qquad \text{(2-1Literature ReviewLiterature Review)}$$

Where,

'η' is the viscosity

'a' is the concentration of amine

'c' is the carboxylic

2.2 Polymer Flame Retardancy

Flame retardancy of polymers seems essential to meet safety standards. For this purpose, the fire triangle shown in Figure 2-3 must be interrupted by acting on the combustible polymer. Different methods are possible to make a material flame retardant: either by chemical modification of the polymer, or by the addition of additives such as flame retardants (FR) or by depositing a "Coating" on the surface of the material.

Figure 2-9 summarises the different phenomena observed during the combustion of polymers and shows where a fire-retardant action can be carried out Indeed, fire retardancy consists in the reduction of heat provided to the polymer, so that the system remains below the critical level that ensures flame stability. This can be achieved by stopping the combustion cycle at different steps:

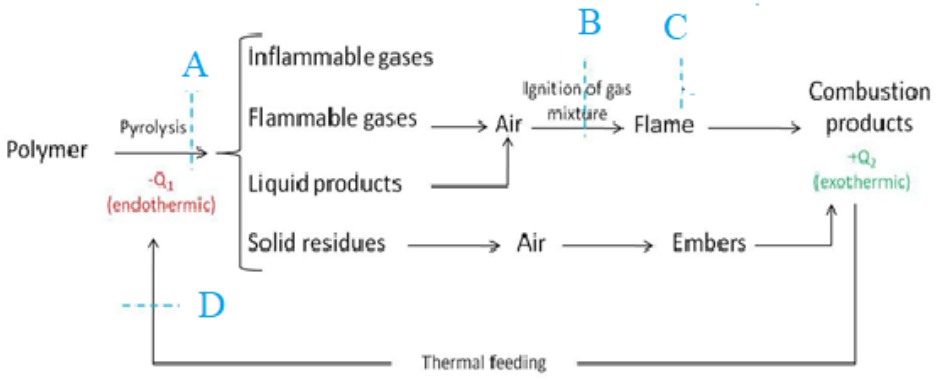

Figure 2-9 :Combustion cycle steps

(i) Modification modifying the pyrolysis process to reduce the amount of flammable volatiles evolved in favour of increasing the formation of less flammable gases or of char (A, Figure 2-9)

(ii) Isolating the flame from the oxygen/air supply (B, Figure 2-9)

- by introducing into the plastic formulations flame inhibitors compounds (C,Figure 2-9)

(iii) Reducing the heat flow back to the polymer to prevent further pyrolysis. This can be achieved by the introduction of a heat sink, e.g. aluminium trihydrate (ATH, Al(OH)3) which decomposes endothermically or by producing a barrier, e.g. char or intumescent coating, formed when the polymer is exposed to fire conditions (D, Figure 2-9)

- In practical terms, the encountered solutions are:

A) use of intrinsically flame-retarded polymers such as poly(tetrafluoroethylene),

- polyoxazoles, polyimides or benzoxazines (Burton, 1993;Bourbigot and Flambard, 2002).
- B) chemical modification of existing polymers: preparation of organic/inorganic epoxy resin prepared from silsesquioxane (Iji and Kiuchi, 2001), synthesis of phosphorus-based epoxy monomers (Levchik and Weil, 2004).
- C) incorporation of flame retardants in the polymer.

The three first solutions are quite interesting, since they permit to produce unique material adapted for each application. However, the main drawback is that this results in higher production costs. The most commonly used solution is therefore the incorporation of flame retardants in the materials.

2.3 Flame Retardants

The primary duty of flame retardant systems is to prevent, minimize, suppress or stop the combustion of a material (Mngomezulu *et al.*, 2014). Flame retardants are known since Roman times (360 BC) when the siege towers timbers were coated with vinegar or Alum to prevent fires. The first patent was recorded by Obadiah Wyld from England in 1735. In the early nineteenth century, Gay-Lussac suggested the use of a phosphate mixture ammonium, ammonium chloride and borax, as a textile flame retardant (Le Bras *et al.*, 2005).

Flame retardants are designed to interfere with the combustion cycle. They are intended to stop or inhibit phenomena occurring in the “fire triangle”, by acting either chemically or physically either in the gas or in the condensed phase. A representation of the four general ways FR act has been proposed Horrocks and Price (2008)and is

presented in Figure 2-9 Flame retardant systems can either work physically (by cooling, the formation of a protective layer or fuel dilution) or chemically (reaction in the condensed or gas phase). They can interrupt with the several processes included in polymer combustion cycle such as heating, pyrolysis, ignition, propagation of thermal degradation. The major modes of action of flame retardant will be presented.

According to a study conducted by Freedonia Group in 2008, the global demand for FR is expected to increase by 4.7% per year, from 1.75 billion tonnes in 2006 to 2.21 billion tonnes in 2011, while the RF market was worth 3.2 billion euros. The Asia-Pacific region is the major consumer with a consumption of 663 million tons in 2006 (Freedonia, 2015). About 90% of global flame retardant production ends up in electronics and plastics, with fabrics and furniture sharing the remaining 10% (Visakh and Yoshihiko, 2015).

A perfect flame retardant polymer material must possess some special features; significant resistance to ignition and flame propagation, a low rate of combustion and smoke generation, low combustibility and toxicity of combustion gases, acceptability in character and properties for particular uses and little increase in cost (Grand and Willkie, 2000).In general, the incorporation of flame retardants into polymers is intended to increase the ignition time, improve the self-extinguishing of the polymer, reduce the amount of heat released, reduce flammable gas, to significantly reduce the amounts of toxic fumes and gases released. Flame retardants are materials which are incorporated into many different materials to minimize the potential risk of fire injuries and damage through increased resistance to ignition or by performing to delay combustion and thereby delaying the spread of flames during their combustion (EFRA, 2007). For the use of these additives to be carried out properly, regulations govern their use.

2.3.1 Types Flame retardant

There are two ways to make a flame retarded polymer matrix composite:

- The reactive flame retardant: the flame retardant reacts chemically with the polymer becoming an integral part of it. The material is homogeneous and the FR no longer exists under its original chemical structure.
- The non-reactive flame retardant (additive flame retardant): the flame retardant is physically mixed with the polymer during the processing step. It is therefore physically introduced into the material.

Table 2-1 Types of flame retardants

	Reactive flame retardant	Non-reactive flame retardant
Advantages	• Basically, immobile in the polymer matrix, therefore, no migration • Very homogeneous material, conservation of physical and	• Low cost • Widely used in industries
Disadvantages	• High cost price, modification of the synthesis process is required, difficult to transpose at the industrial	• Generating more smoke while burning • Required high loading may be

The advantages and disadvantages of the two ways are presented in Table 2-5 Generally, additive flame retardants are preferred because it is easy to process and cost-effective more than reactive flame retardant (Wang and Chow, 2005).

2.3.2 Mode of action of flame retardants

The action of the flame retardants can be carried out at several levels, either in the gas phase or in the condensed phase or both at the same time, by chemical and / or physical mechanisms which interfere with the combustion process of the polymer under the effect of heat (Bourbigot and Duquesne, 2007).

Flame retardants are designed to obstruct the combustion cycle. They are designed to stop or inhibit phenomena manifesting in the "fire triangle", by acting either chemically or physically either in the gas or in the condensed phase. A representation of the four general ways FR act has been suggested by Price *et al.* (2001). This summarised in Table 2-1.The primary duty of flame retardant systems is to prevent, minimize, suppress or stop the combustion of a material (Mngomezulu *et al.*, 2014).

2.3.3 Physical mode of action

In physical action: it occurs by three ways: cooling, fuel dilution and char formation Some flame retardant additives cool the reaction medium by means of decomposing endothermically. This endothermic decomposition causes heat consumption, decreasing temperature below polymer combustion temperature.

Some flame retardants decompose releasing non-flammable gases such as water vapour (H_2O) and carbon dioxide (CO_2). Those gases lead to dilution of combustible gas mixture, decreasing concentration of radicals in flame. Thus; flammability declines.Other flame retardant can lead to formation of protective solid or gaseous layer that can act as a protective barrier. This layer prevents the transfer of heat and oxygen to the polymer and combustible volatile gases to vapour phase. As a result, polymer underlying is protected and volatile gases are separated from oxygen preventing the combustion cycle to be self-sustained.

- Cooling: In cooling mode of action the degradation reactions of the FR additive can play a role in the energy balance of the combustion. The incorporation in the polymer

of additives which decompose endothermically contributes to reducing the calorific balance and delaying combustion. The hydroxides of aluminium ($Al(OH)_3$, Eqn. (2-4)) and hydroxides magnesium ($Mg(OH)_2$, Eqn. (2-5) function according to this principle and their effectiveness is proportional to the quantity of additives introduced into the material.

$$2Al(OH)_3 \rightarrow Al_2O_3 + 3H_2O \quad (1050\ kJ/kg) \tag{2-2}$$

$$Mg(OH)2 \rightarrow 2MgO + 2H2O \quad (1300\ kJ/kg) \tag{2-3}$$

Zinc borates such as $2ZnO.3B2O_3.3.5H_2O$ or $4ZnO.B_2O_3.H_2O$ also decompose endothermically at 290 to 450 °C. They release water, boric acid (H_3BO_3) and boron oxide (B_2O_3).

- Dilution of the gas phase: A release of non-flammable gases (CO_2, NH_3, H_2O, etc.) resulting from the thermal decomposition of the additives contributes to the dilution of the combustible gases below the ignition threshold in the flame zone.

- Formation of a protective layer (char): The combustible zone of the polymer can be protected from the gaseous phase by a solid protective layer. The oxygen required for combustion is limited as well as the heat transfer, which slows the rate of degradation of the polymer. A smaller amount of combustible gas is emitted (Figure 2.8). For example, the phosphorus (or phosphonate) additives act similarly. Their pyrolysis results in the formation of thermally stable pyro- or polyphosphoric derivatives forming a protective vitreous coating. The same applies to additives based on boric acid and inorganic borates. It is the case including boron compounds which form a glassy protecting layer.

2.3.4 Chemical mode action

Main chemical reactions interfering with the combustion process take place in the solid and gaseous phase.

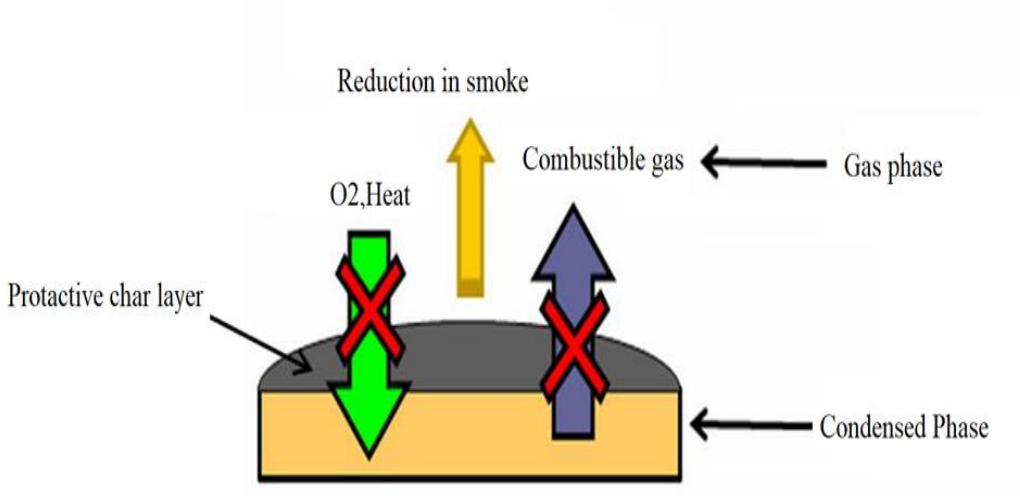

Figure 2-10 : How flame retardant works?

- Gas phase reaction: The flame retardant system or its thermal decomposition products may inhibit free radical reactions by trap-neutralizing the OH° and H° radicals responsible for the propagation of the flame. This is the case of the halogenated compounds which will liberate the radicals (X°). This has the consequence of slowing down the combustion reaction by cutting off the reaction chain.

- Condensed phase: In condensed phase, flame retardants can accelerate the breaking down of polymer causing melting and dripping away from the flame. Melamine cyanurate is one of the most widely used flame retardant additive causing dripping.

Aliphatic bromines are also used to create the same effect in foamed polystyrenes and thin films of polypropylene.

Flame retardants can also cause formation of a carbonaceous char or vitreous layer on the polymer surface. This can occur when a fire retardant removes the side chains and generates double bonds in the polymer. These double bonds give crosslinks, resulting in the formation of char. This char or vitreous layer can act as an insulating barrier in between flame zone and polymer. There are also intumescent systems in which swelling of the surface layer of polymer is sustained via blowing agents. Char produced can provide insulation and slow down heat transfer from the exposed side to the unexposed side of polymer. No FR operates by an exclusively chemical mode of action. Indeed, the modes of chemical actions are always accompanied by one or more physical mechanisms.

Table 2-2: Classes of Flame retardant and their mode of action lame-retardant modes of action

No FR operates by an exclusively chemical mode of action. Indeed, the modes of

Mode of action	Mechanism	Flame retardant
Gas phase		
Flame extinction	Radical inhibition	Halogen- and Phosphorus- based compounds, antimony
Decrease of the flame temperature, flame cooling	Dilution of the combustion gas	Compounds releasing carbon dioxide, water (Mineral fillers)
Condensed phase		
Cooling down the polymer	Endothermic degradation	Metallic hydroxides
Limitation of the fuel supply	Dilution of the polymer	Inert fillers (talc, chalk)
Reducing heat exchanges and fuel supply with the polymer	Creation of a physical (O_2 and fuel) and thermal (heat) protective barrier	Intumescent of vitrifying systems

chemical actions are always accompanied by one or more physical mechanisms.

2.3.5 Classes of Flame Retardants

Flame retardant can be classified into four types: halogenated FR, phosphorus and Nitrogen FR, and, inorganic FR. Table 2-2 summarises the main classes of flame retardants employed and their associated modes of action. resin needs to be substituted with the bromine-containing monomer, resulting in bromine ingredients between 20 to 55 wt.%.

Table 2-3: Modes of action of different class of flame retardants

Flame retardant	Examples	Modes of action
Halogenated	Aromatic (PBDE, TBBA, etc.), aliphatic (brominated phosphate esters,...), cyclic (HBCD, ...)	- Inhibition of radical reactions in the gas phase (capture of energy radicals H° and OH °, replaced by X° of lower energy).
Phosphorus	Ammonium polyphoshate, phosphonates, phosphinates, red phosphorus	- Formation of a char-carbon solid residue. - Formation of radicals (PO°, HPO_2°) to trap active radicals (OH°, H°). - Release of non-combustible gases (H_2O, CO_2, NH_3 ...) which dilute the combustible gases and radicals in the gaseous phase.
Nitrogen	Melamine and its derivatives (melam, melem, melon), and its acid salts (phosphoric, cyanuric,...)	- Dilution of combustible gases by release of NH_3. - Endothermic decomposition. - Crosslinking which promotes the formation of a char. - Endothermic sublimation in the case of salts.
Inorganic	SiO_2, TiO_2, Al_2O_3 $Al(OH)_3$	- Endothermic decomposition: cooling of the polymer. - Dilution of combustible gases: release of water. - Formation of a coated layer consisting of metal oxides (Al_2O_3, MgO) and polyaromatic compounds.

2.3.6 Halogen- based flame retardants

This kind of flame retardant supplies many available compounds through the four halogen atoms, only chlorine and bromine are utilized for the preparation of popular flame retardants. Fluorinated compounds provide an extreme stability, while iodinated ones possess a poor thermal stability that restricts the polymers in which they can be involved.

Brominated and chlorinated flame retardants are usually incorporated in polymers at 20 and 40 wt.% correspondingly (Pitts, 1972). The usage of brominated resins like a copolymer in epoxy systems is likewise popular. In this instance, portion of the standard

Halogen-based compounds work mostly in the gas phase (Yang and Lee, 1986). They are prepared to generate radicals or hydrogen halides throughout their decomposition at temperatures less than that of the polymer. Their operation thus comes from a dilution of the gas phase, which reduces combustibles and oxygen concentrations, linked to reactions with radicals from the flame. In fact, these additives generate halogenated radicals which join together again with hydrogen atoms emitting from the flame retardant itself or from the polymer (Figure 2-11) (Lyons, 1976).

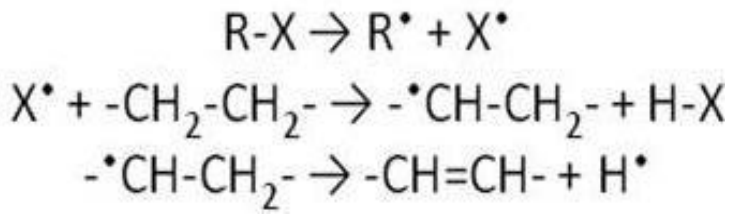

Figure 2-11: Radicals generation by halogen-based flame retardants.

Where,
'R' is the polymer,
'X' may be Br or Cl, and

'HX' halide with halogenated is the active element

When no synergy agent is added in the system, halides volatilize and get in the flame where they react quickly with hydrogen or hydroxyl radicals (Figure 2-11). The capturing of these very dynamic radicals modifies the thermal balance, therefore limiting the progress of combustion (Laoutid *et al.*, 2009)..

As soon as synergists are incorporated into the flame-retarded material, e.g. metallic oxides, metallic salts, compounds containing phosphorus, nitrogen or zinc, the additive loading is reduced. These blends discharge metallic halides once they degrade and these species prevent the flame more effectively than hydrogen halides (Zhang and Horrocks, 2003) as shown in Figure 2-12.

$$H\text{-}X + H^{\bullet} \rightarrow H_2 + X^{\bullet}$$
$$H\text{-}X + OH^{\bullet} \rightarrow H_2O + X^{\bullet}$$

Where,
'R' is the polymer ,
'X' may be Br or Cl, and
'HX' halide with halogenated is the active element.

Figure 2-12: Interactions between halides and radicals from the flame.

Since 2004 the EU have released various restrictions in regards to the use of some halogenated FR [Registration, Evaluation, Authorisation and Restriction of Chemicals (REACH) and restriction of hazardous substances in electrical and electronic equipment (RoHS)] with regards to different studies relating to their harmful effect on the environment and health (Talsness, 2008;Shaw, 2010). lists restrictions of usage for Pentabromodiphenyl-ether (PBDE), Octabromodiphenyl-ether (OBDE), or other substances in specific applications Tris (2,3-dibromopropyl) phosphate, (TRIS), is not

permitted in articles for textiles. As a result, halogenated systems are often prohibited as a result of market need on halogen-free products.

2.3.7 Phosphorous- based flame retardants

Phosphorous- based flame retardants have already been designed to prevent polymers from fire during a long-time period. They are both solid- and gas-phase effective. When burning, a polymer decomposes in volatilized material particles which make up the combustible gases. Making these combustible gases is directly associated with the distribution of the flame: as a result, a method of delaying the fire distribution is to restrict the mechanism of the polymer degradation, attempting to eliminate creation of volatile fuel gases and advantage the decomposition reactions resulting in a carbonaceous char process. Phosphorous based flame retardants are believed to operate using this method. Phosphorus acids are produced through the thermal degradation of the phosphorous flame retardant and after that enhance char formation and reduce flammable-gas generation. Moreover, when decomposed, phosphorous compounds condense and release water, allowing the dilution of the combustible gases and a cooling of the surface of polymer. Phosphorous-based flame retardants such as ammonium polyphosphate, phosphate esters, phosphonates and phosphonates, and red phosphorous, etc.

2.3.1 Organophosphorus flame retardants

Organophosphorus flame retardants are primarily phosphate esters and represent around 20% by volume of the total global production. This category is widely used both in polymers and textile cellulose fibres. Of the halogen-free organophosphorus flame retardants in particular, triaryl phosphates (with three benzene rings attached to a phosphorus-containing group) are used as alternatives to brominated flame retardants. Organophosphorus flame retardants may in some cases also contain bromine or chlorine.

2.3.2 Nitrogen-based flame retardants

The flame-retardant mechanisms of nitrogen-based compounds remain not fully comprehended. The principle mode of action is assumed to be depending on the release during decomposition of nitrogen, diluting the fuel gases. A solid-phase action may also be taken into account: the nitrogen-based additives for instance melamine as well as its derivatives, can lead to cross-linked structures when decomposing, providing the development of a protective protecting layer. Effectiveness needs to occur whether use within mixture with other flame retardants or in high concentrations, but might lead to this situation in a reduction in the mechanical properties of the material (Horacek and Grabner, 1996). Nowadays nitrogen containing flame retardant principal applications are melamine for polyurethane flexible foams, melamine cyanurate in nylons, melamine-phosphates in polyolefin (Horacek and Grabner, 1996). Table 2-2 is a summary of the most frequently-used flame retardants and their primary mode of action.

2.3.3 Metal hydroxides flame retardants (MH)

Flame retardants are metal hydroxides (MH) is commonly used as replacements to brominated flame retardants due to its health and environmental concern and operate as smoke suppressors, an example of MH; aluminium hydroxide and magnesium hydroxide act in physical phase over endothermic dehydration and the formation of a ceramic protective layer. Due to the release of water, the flame is diluted, leading to a delayed ignition. A ceramic protective layer composed of metallic oxides is also obtained, characterized by a high heat capacity (Laoutid *et al.*, 2009) . According international programme on chemical safety (IPCS) the entire category of inorganic flame retardants presents about 50% by amount of the worldwide flame retardant production, primarily as aluminium trihydrate, that is in relation to the largest flame retardant category being used in the marketplace (IPCS, 1994).The major drawback or MH it must be used at higher loading around 60% to be effective as halogenated flame retardant ,which effect the ovral properties of the polymer (Kiuchi *et al.*, 2006).

2.3.4 Ammonium Polyphosphate

Ammonium polyphosphate (APP), an inorganic salt of polyphosphoric acid and ammonia, its chemical formula is [NH4 PO3]n(OH)2 is commonly used as flame retardant in polymers, especially with polyolefins. APP also found an application area to obtain flame retardant textiles (Davies *et al.*, 2005) APP has two main crystal types; crystal phases I and II. Phase I is characterized by a variable linear chain length, showing a lower decomposition temperature and higher water solubility than phase II. Phase II which has a cross-linked and branched structure is more preferred for flame retardant activities (Xanthos, 2005).

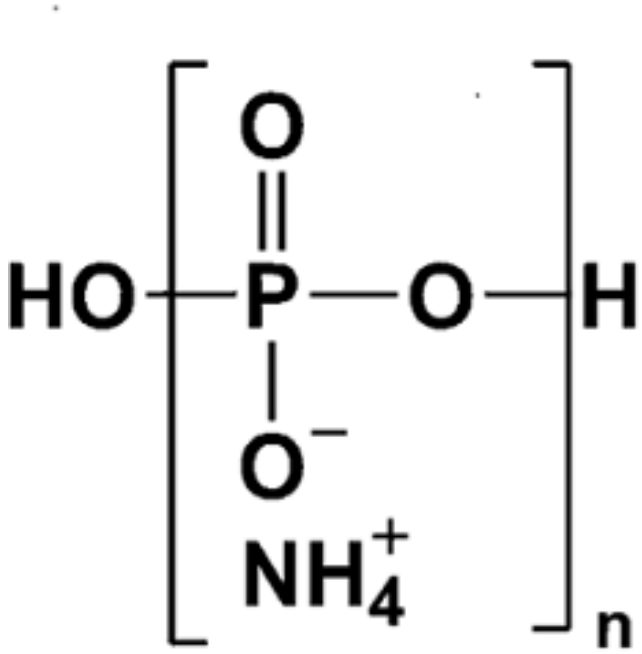

Figure 2-13 :The molecular structure of Ammonium polyphosphate (APP)

The molecular structure of APP is shown in Figure 2-13. APP shows its flame retardant effect in condensed phase by the formation of intumescent char. For better understanding of flame retardant effect of APP, detailed information is given about the intumescent system and how APP forms intumescent char.

Intumescent system was reported in literature in 1938. Intumescent system protects the underlying material by the formation of highly porous, thick and thermally stable char layer (Mouritz and Gibson, 2006) . This layer acts as a physical barrier to reduce the heat and mass (fuel, oxygen) transfer between the gas and condensed phases so it protects the polymer from the effect of flame. The amount and the properties (integrity, stability and foam structure) of the char determine the flame retardant effect of an intumescent system. The major advantage of this system is the decrease in the heat generated during the combustion due to the formation of carbon rather than formation of CO and CO_2 (Li *et al.*, 2005).The flame retardant effect of intumescent char is shown in Figure 2.10 (EFRA, 2007).

In the case of APP, it acts both as an acid source and blowing agent during combustion. The thermal degradation of APP gives polyphosphoric acid, orthophosphates, phosphoric acid, ammonia and water (Xie *et al.*, 2006). The schematic representation of the thermal degradation of APP is shown in Figure 2-14 (Grand and Wilkie, 2000).

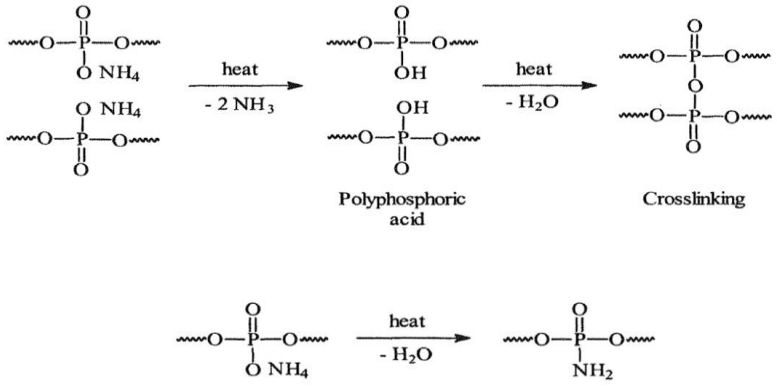

Figure 2-14: The schematic representation of thermal degradation of APP

Polyphosphoric acid, phosphoric acid and orthophosphates acting as an acid source undergo esterification reaction with carbonizing agent. Ammonia and water act as blowing source. In order to increase the barrier effect of intumescent char, different blowing agents can be used with APP. Generally, nitrogen containing compounds such

as; urea, dicyandiamide, melamine and polyamides are used as blowing agent (Camino *et al.*, 1984b). Starch, dextrins, sorbitol, mannitol, pentaerythritol (PER) and char former polymers can be used as carbonizing agent. APP and PER combination is widely used with PP as intumescent flame retardant (Bourbigot *et al.*, 2004b).

Intumescent system was reported in literature in 1938. Intumescent system protects the underlying material by the formation of highly porous, thick and thermally stable char layer (Mouritz and Gibson, 2006) . This layer acts as a physical barrier to reduce the heat and mass (fuel, oxygen) transfer between the gas and condensed phases so it protects the polymer from the effect of flame. The amount and the properties (integrity, stability and foam structure) of the char determine the flame retardant effect of an intumescent system. The major advantage of this system is the decrease in the heat generated during the combustion due to the formation of carbon rather than formation of CO and CO_2 (Li *et al.*, 2005).The flame retardant effect of intumescent char is shown in Figure 2-16 (EFRA, 2007).

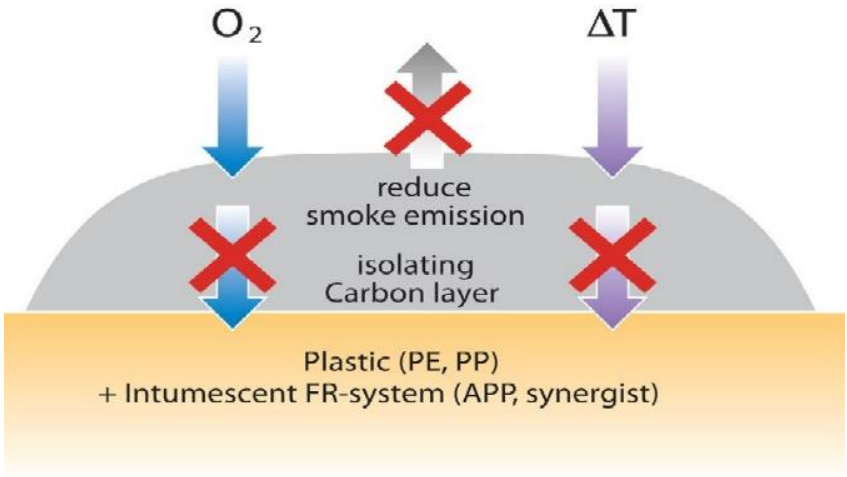

Figure 2-15:Mechanism of intumescent flame retardant

The addition of nitrogen, metal, silicon and boron containing substances shows synergistic effect with intumescent flame retardant (IFR) and increases the limiting oxygen index value of PP composites (Li *et al.*, 2008).

2.3.5 Criteria for selection of a system FR

Before going on to discuss the advantages of the different types of additives used in the fireproofing of the PE, PS and PA 66, let us recall a few requirements that should ideally be satisfied by flame retardant additives (Levchik, 2007;Lewin and Weil, 2001) (Figure 2-17):

- limit changes in polymer processing conditions (ease of processing and stability);
- preserve the physical and mechanical properties of the polymer (compatibility);
- limit the production of smoke and combustion products;
- limit the impact on aging;
- ensure a compromise between cost and performance;
- limit the environmental impact when burning or recycling plastic

It is necessary to recall that the very structure of the polymers leads to changes in the fire behaviour of one polymer to another. A type of flame retardant provides good flame retardancy properties for a given polymer but may often prove ineffective when incorporated into another polymer. Thus, many formulations have been developed for the flame proofing of plastics. They are based on often complex flame-retardant systems with synergistic power and easily incorporated into the polymer matrix.

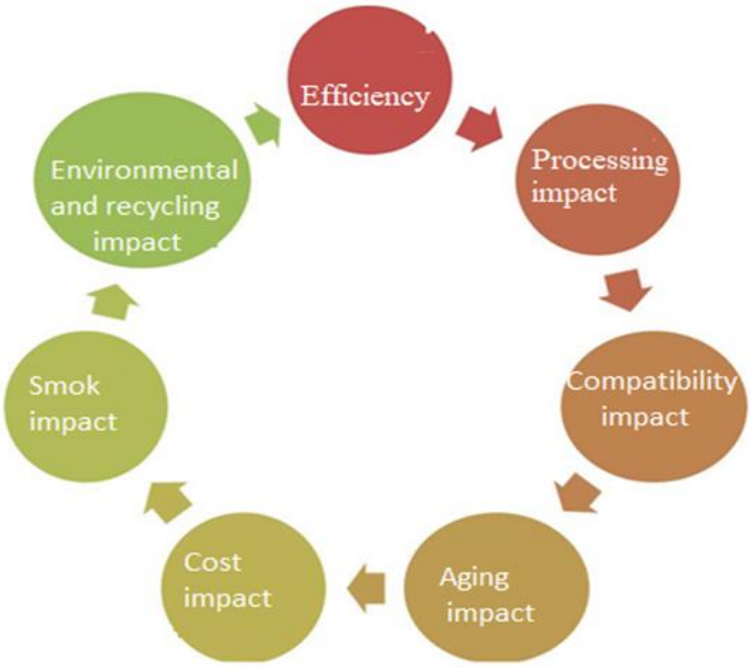

Figure 2-16 :Criteria for selecting a FR system

Obviously, the universal flame retardant additive does not yet exist. However, some additives may satisfy many of these requirements to a greater or lesser extent. For our study, we will focus on the definition of the four main factors that contribute to the improvement of the efficiency of an FR system in the polymer matrix: effect of types of compatibilisers, intumescent flame retardant loading, glass fibre loading rate and effect of synergy of glass fibre with sepiolite.

Ammonium polyphosphate (APP) (one of the components of our FR systems) is particularly useful for oxygen and nitrogen-containing polymers (such as polyurethane and polyamide). It then leads to the carbonization of these polymers. The effectiveness of APP also depends on its rate of incorporation into the matrix. At a relatively low concentration (<5% by weight), APP is not effective in aliphatic polyamides (Levchik *et al.*, 1996). However, it becomes very effective at higher concentrations,> 10 wt.% in

polyamide-6,6,> 20 wt.% in polyamide 11, -12, -6, -10 and> 30 wt.% in polyamide- 6. However, a high level of APP leads to a decrease in the mechanical and fire properties resulting from poor dispersion of APP in the matrix.

2.4 Influence of Intumescent Flame Retardant on Properties

In this section, studies related to flame retardant intumescent systems will be discussed. Its effect on synergy, nanoclay and properties are discussed.

2.4.1 Definition of intumescent

Intumescent systems (Le Bras et al., 1998) are systems that cause the material to expand under thermal irradiation (Figure 2-17). The material is then protected from the heat flux by a generally protective layer with low thermal conductivity. Moreover,this protective layer also limits the transfer of the gases resulting from the pyrolysis of the polymer to the flame as well as the diffusion of oxygen into the material. All this results in a decrease in the degradation rate of the material. In order for this coating to be effective, it must develop sufficiently early in the degradation process, that is to say at a temperature at which the rate of decomposition of the polymer is not too great.

- **Conventional components of intumescent systems are described as comprising in general:**

A source of acid or acid precursor such as sulfuric, phosphoric or boric acid, and their organic derivatives (such as ammonium polyphosphate). This acid is free or formed (during combustion between 100 and 250°C.) initiates the beginning of the first series of reactions (for example the dehydration of the hydrocarbon compound). A polyhydroxylated (carbon-rich) compound such as pentaerythritol, sugars (maltose, etc.),

macromolecular polyholosides (cellulose, starch) which are susceptible to dehydration by acid esterification and lead to crosslinked organic compound.(NH_3, CO_2, H_2O), urea (NH_3, CO_2, H_2O), hydrogen chloride (HCl), and the like, , chlorinated etc. the expanded structure must be provided by a binder (the polymer itself, the degradation products or the like), leading to the formation of a skin covering the foam and preventing the escape of gas during expansion. Certain compounds belonging to intumescent formulations can fulfil several functions. For example, ammonium polyphosphate can both act as an acid source and as a blowing agent with release of ammonia and water.

Figure 2-17: Intumescent char protection layer formation

2.4.2 Mechanism of intumescence

The mechanism of intumescence for polypropylene in the presence of a system composed of ammonium polyphosphate (APP) and pentaerythritol (PER) was studied by Camino *et al.* (1984a). The results were interpreted on the basis of deamination of APP and formation of polyphosphoric acid. They showed that the first steps of the reaction between ammonium polyphosphate and pentaerythritol release water around 210 ° C (formation of ester groups = P (O) OCH_2) (Figure 2-19).

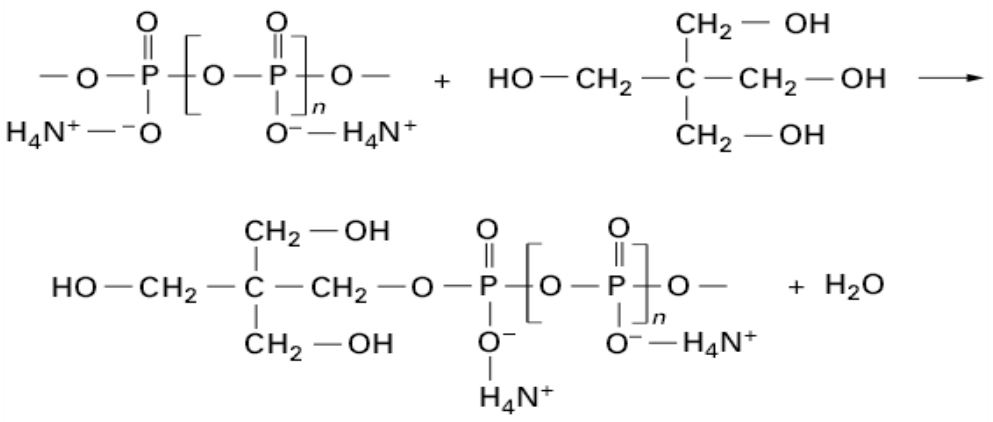

Figure 2-18: The nature of the reaction between APP/PER

The condensation then proceeds to give cyclic structures (cyclic polyphosphate esters) with release of water and ammonia (Figure 2.14). A study was carried out by (Bourbigot *et al.*, 1993) on the APP/PER mixture in order to understand the reactions that occur during the development of the char. They showed the formation of polyaromatic stacks linked by phospho-hydrocarbon bridges by heating the mixture (APP/PER) at different temperatures (280, 350, 430 and 560 °C.). The stacks become larger and organized at higher temperatures, which eventually gives a multicellular residue It is noted in the literature that the organization of the polyaromatic network conditions several physical parameters of the char and consequently its effectiveness Moreover, the performance of the latter depends on the amount of residue formed, its rate of formation, its porosity, the size of the bubbles formed, the presence of cracks on the surface, and the like. It is also important that the thermal stability of the char is high so that it does not degrades at high temperatures so that it continues to protect the undegraded polymer.

2.4.3 Intumescent flame retardants

Intumescence is a useful phenomenon, by which fire is opposed by the creation of an expendable insulating char foam. (Bourbigot et al., 2004) .This char foam layer isolates the oxygen and heat from the polymer exterior and extinguishes the fire

propagate. These types of FRs were originally produced for shielding coatings. The principle elements of the intumescent system are (Camino et al., 1984).

Flame retarding polymers by intumescence is essentially a special case of a condensed phase mechanism. The activity in this case occurs in the condensed phase and radical trap mechanism in the gaseous phase appears to not be involved.

In intumescence, the amount of fuel produced is also greatly diminished and char rather than combustible gases are formed. The intumescent char, however, has a special active role in the process. It constitutes a two-way barrier, both for the hindering of the passage of the combustible gases and molten polymer to the flame as well as the shielding of the polymer from the heat of the flame. Despite the considerable number of intumescent systems developed in the last 15 years, they all seem to be based on the application of three basic ingredients:

- catalyst (acid source),
- charring agent and
- blowing agent (Spumific).

The connection of these elements with each other to produce the char foam is shown in Table 2-4 Figure 2-19. Additives combining the last three ingredients leading to intumescent effect are commercially available. However, intumescent formulations can simply be developed and are more suitable than some commercial grades for some specific applications.

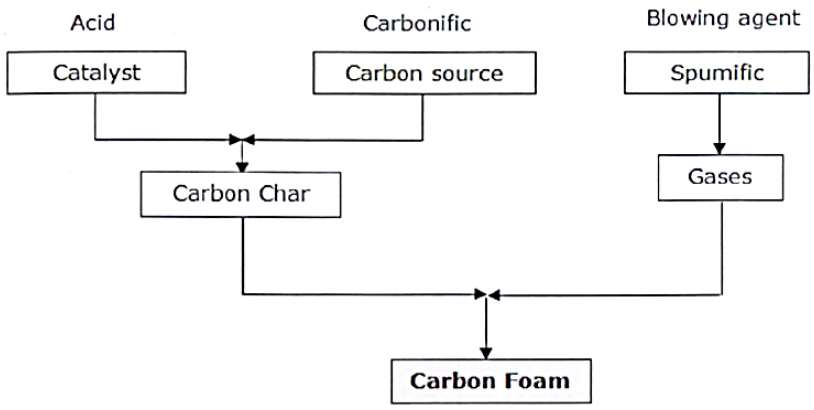

Figure 2-19 : The elements of intumescent flame retardant that form a char

- improvement of the efficiency of an FR system in the polymer matrix: effect of types of compatibilisers, intumescent flame retardant loading, glass fibre loading rate and effect.

Table 2-4: Summary of catalyst, charring and blowing agents for IFR

Acid source	Char former	Blowing agent
Acids	Polyhydric compounds :	Amines /amides :
phosphoric, sulphuric, boric	Starch, Dextrin,	Urea, urea -
Ammonium salts	Sorbitol, pentaerythritol	Formaldehyde
Phosphates, polyphosphates, borates.	Formaldehyde resins –	Resins
Sulphates, halogens.	Phenol	Dicyandiamide
Amines or phosphate amides.	others:	Melamine
Reaction products of urea	Charring polymers (PA6)	Polyamides
Phosphoric acid, melamine phosphate.	PA6-clay nanocomposite,	
Organophosphorous compounds.	Polyurethane,	
Tricresyl phosphate, alkyl phosphate.	Polycarbonate	

2.4.4 Intumescent systems (APP765)

This part will be devoted to a general presentation of the phenomenon of intumescence. Then, we will present in more detail the ammonium polyphosphate (APP) and pentaerythritol (PER) system. This system (APP/PER) has been used alone or in combination with oxides on the three polymer matrices (HDPE, PS and PA 66) as part of our work. Then, we will try to identify the main parameters (overall load rate and ratio of intumescent additives, effect of additives on rheology, effect of additives on mechanical properties and synergy with intumescent systems) of a rational design of a system intumescent.

2.4.5 Balanced design of an intumescent system

First of all, it is obvious that the effectiveness of an intumescent system strongly depends on the polymer matrix into which it is added. For example, the intumescent APP/PER system (30% by mass) is effective in PP (IOL = 30% instead of 17 for virgin(PP). On the other hand, its efficiency is lower in the case of PE (IOL = 24%) instead of 17 for the virgin PE [31]. This behaviour is related to the adequacy between the decomposition / activation temperatures of the three compounds (polymer, APP and PER) as well as the reactivity of the polymer. In this section, we present the important parameters that affect the efficiency of an intumescent system.

2.4.6 Total loading rate and ratio of intumescent additives

When more than one additive participates in the intumescent reaction, the optimum ratio between the ingredients should be sought and the ratio itself may also depend on the overall loading rate. Camino *et al.* (1989)in their study on the intumescent system consisting of APP-PER in polypropylene (PP), showed the dependence of the limiting oxygen index (IOL) on the overall additive content. The LOI increased from 20 %V for pure PP to around 50 %V when intumescent ratio of APP/PER was 3:1when the additive content was increased from 0 to 30% .In another study (Xia *et al.*, 2014) showed

that the use of an intumescent system (APP/PER = 2) in polypropylene exhibits better fire behaviour compared to AP / PER mass ratios equal to 1, 3 or 4. They have suggested that this mass ratio of 2 makes it possible to achieve the optimum ratio of phosphorus / carbon in the char formed during the combustion. The latter ensures a structure and thermophilically properties making it possible to reduce both the heat and mass transfers between the two phases.

2.5 Effect of Additives on Mechanical Properties

Contrary to the viscosity which improves with most of the additives, the mechanical properties of the polymer are modified differently depending on the type of additive incorporated. The mechanical properties of the polymer / additive mixtures are mainly conditioned by the particle size and the shape of the fillers. Indeed, it is established that, in general, the conventional additives of micrometric size have a negative effect on the mechanical properties, whereas in some cases the presence of nanofillers improves them.

As an example, Owen and Harper (1999) showed that the use of antimony trioxide of high particle size (11.8 μm) in an ABS matrix induces a significant reduction in mechanical strength (-30%). (-10%). In another study (Casalini *et al.*, 2012) it was shown that the presence of 1% carbon nanotubes (NTC) increases the viscosity of the polyurea matrix (mixture nanocharges / polydiamine oligomer) unlike to POSS that have no effect. The study also showed that the mechanical properties of all the nanocomposite resins are better than those of the virgin resins with an increase in the strength of the material containing POSS. This effect has been attributed to the three-dimensional form of POSS which does not affect the mobility of oligomers. Moreover, the low interfacial tension of the POSS with the polymer matrix improves the mechanical strength of the polyurea nanocomposite when subjected to mechanical stresses.

Finally, the additive loading can also negatively affect the strength of the material. A high loading rate favors the agglomeration of the particles, creating zones of privileged ruptures (Chang *et al.*, 2003)

2.6 Synergy Efect

In order to achieve better fire behaviour, it is generally necessary to develop a flame retardant system based on a combination of different flame retardants. The concept of synergy makes it possible to optimize the formulations and to improve the performance of the mixtures of two or more additives. The synergistic phenomena can be obtained either by a combination of flame-retardant mechanisms, such as the formation of a charcoal layer) with a phosphorus flame retardant combined with a halogenated flame retardant which is active in the gas phase, or a combination of flame retardants which reinforce the same mechanism. For example, the addition of nanoclays with phosphorous agents which both act in condensed phase and improve the cohesion of the char and thus the barrier effect.

Due to environmental and toxicological problems, halogen-antimony and bromine-phosphorus synergies will not be included in our study. The use of nitrogen additives combined with phosphorus additives can produce interesting synergistic effects (Levchik *et al.*, 1996). The formation of molecules containing N-P bonds can accelerate the production of phosphoric acid and polymer phosphorylation because the N-P bonds are more reactive in the phosphorylation process than the P-O bonds. In addition, the N-P bonds keep the phosphorus in the condensed phase, which generates a reticulated network which promotes the formation of the char layer.

Another well known synergistic system is the combination of metal hydroxides with other FR, such as zinc borate (ZnB). For example, partial substitution of 3% by mass of Mg $(OH)_2$ with ZnB in EVA leads to an increase in the IOL value of 38.5 to 43% and a decrease in the heat peak released (pHRR) of 30%. In this system, the endothermic decomposition of Mg $(OH)_2$ catalyzes the decomposition of ZnB by generating boric

oxide. A vitreous layer is then formed in combination with magnesium oxide (MgO) (Carpentier *et al.*, 2000). Another example is the combination of a small amount of organo-modified montmorillonite and talc with magnesium hydroxide which significantly reduces the pHRR (≈80%) and generates a compact residue (Clerc *et al.*, 2005).

Another example of synergy is the use of a nanoscale silica (8% by mass) in combination with the MDH (52% by mass) in the EVA matrix improves the fire properties (IOL, UL-94, HRR, more coherent char) (Fu and Qu, 2004). Fu and Qu have demonstrated that the silica increases the viscosity and participates with the magnesium oxide (MgO) in formation of char prevents heat and mass transfer.

2.6.1 Synergy with intumescent systems

In order to obtain better fire performance at the same loading rate or to retain the mechanical properties of the material, the APP/PER intumescent system has sometimes been combined with other additives to achieve a synergistic effect. This non-exhaustive part gives some examples from the literature .Gilman and Coll (Gilman *et al.*, 1997) showed that the use of 1.5% Zeolite 4A in combination with APP/PER makes it possible to increase the IOL values of the polymer/APP/PER system by 24 to 26% for PE, 29 to 39% for PS and 29 to 43% for LRAM3.5 (ethylene-acrylate / maleic acid terpolymer.) Also, the use of 1.5% by mass of 13X zeolite with APP/PER in polypropylene makes it possible to obtain an IOL of 45% (+15% relative to the PP/APP/PER composite). (Gilman *et al.*, 1997) The authors explained that the zeolites stabilize the structure by creating silicophosphorus bonds), and decrease the splitting of the P-O-C bonds, leading to an increase in the size of the polyaromatics which contribute to the formation of a more compact and less cracked protective layer.

In another study, titanium α-phosphate (α-TiP) improves the fire properties of the PP/APP/PER composite (Bao *et al.*, 2011). Three hypotheses have been proposed to explain this improvement: a) the α-TiP layers or their dehydrated form reacts as a physical

barrier, b) α-TiP has a catalytic effect which improves the rate of char and c) α-TiP has a high cation exchange capacity as well as an abs capacity.

2.7 Nanocomposites

The incorporation of nanoparticles into polymers has fascinated significantly desire for the last decade. Indeed, aside from providing fire properties to the materials, low loadings obtained do not modify the other properties or even enhance some of them, such as mechanical properties(Morgan and Wilkie, 2007). Survey of the literature with SciFinder® for different keyword combinations helps to get the tendencies in the use of nanoparticles. The incorporation of nanoparticles in polypropylene for enhancing mechanical properties is widely described in polypropylene and nanoparticle. The use of nanoparticles as flame retardants in other polymers is well-known (‘nanoparticle’ and ‘flame retardant’). It is important to note that nanoparticles alone cannot improve the fire resistant property of a polymer. However, when mixed with flame retardant systems like phosphorated compounds, the polymers acquire the required standards. Several recent works have focused on incorporating flame retardants. For example Huang *et al.* (2010) studied the synergy effects of sepiolite on the flame retardancy using the limiting oxygen index, LRS, TGA, UL-94 tests etc on intumescent flame retardant polypropylene (PP/IFR). The IFR system composed of the ammonium polyphosphate modified with γ-aminopropyltriethoxysilane coupling agent, melamine and dipentaerythritol. The results of the study indicated that addition of sepiolite to the PP/IFR and a synergistic flame retardant effect when LOI and UL-94 tests were performed. Also, sepiolite’s addition enhanced the thermal stability. From the mechanical point of view the flexural modulus and Young’s modulus of PP/IFR composites improved.

2.7.1 Types of nanofillers

Nanofillers have, by definition, at least one of their morphological dimensions less than 100 nm and they can be classified into three categories according to their geometry as shown in Figure 2-20(Šupová *et al.*, 2011) nanofillers are incorporated in

polymer at loading from 1% to 10 wt.%(Marquis *et al.*, 2011) .They are combined in addition to conventional fillers and additives, and finally traditional reinforcement fibres such as glass, carbon or aramid fibres.One-dimensional nanofiller (plates/laminas/shells) can be seen in Figure 2-20 (a). The thickness of the nanoplate will be less than 100 nm. In this case of Two-dimensional nanofillers as seen in the Figure 2-20(b.) are available in the form of nanotubes and nanofibers that have diameter lower than 0.1 μm. Two-dimeniosnal nanofillers depicts excellent material properties, particularly in terms of rigidity.

Figure 2-20 (c) shows the three-Dimensional; nanofillers that have dimensions less than 100 nm. isodimensional nanoparticles such as nanometric silica beads are some examples for Three-dimensional nanofillers.

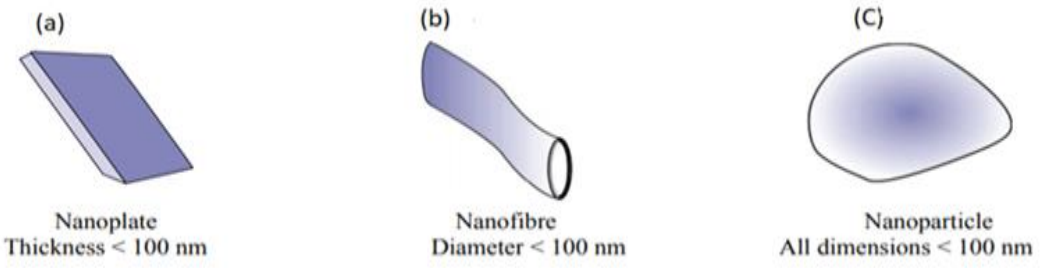

Figure 2-20: Three categories of nanofillers: (a) One-dimensional nanofiller (b), Two-dimensional nanofiller and (c) Three-dimensional nanofiller

Sepiolite can be an additive in a needle-like form and transversal nanometric sizes. This purely natural clay is a crystalline hydrated magnesium silicate of theoretical unit cell formulation $Si_{12}O_{30}Mg_8(OH)_4(OH2)_4.8H_2O$ (Volle *et al.*, 2011) .This structure is made of continuous two-dimensional talc-shape tetrahedral sheets and discontinuous octahedral sheets (Figure 2-21). Owing to these discontinuous octahedral ribbons, periodic nanopores having a rectangular section are produced inside the main structure of the fibre.While these pores are at the top of fibre they form channels. If the pore is included inside the fibre they create a tunnel. Both of them are operating parallel to the mean axis of the fibre. These pores have a cross-section size of 11.5 Å × 3.7 as publicly

stated in the literature (Rautureau and Tchoubar, 1976). The length of the fibres varies between 0.5 and 7 µm along with their cross-section that lies around 20-50 nm. It is especially advantageous to observe that both the tunnels and the channels are naturally filled with zeolitic water in ambient conditions (Figure 2-21) (Ruiz-Hitzky, 2001).

Sepiolite has been popular to strengthen different polymers like polypropylene (Tartaglione *et al.*, 2008), epoxy (Zheng and Zheng, 2006), nylon-6 (Xie *et al.*, 2007), polyurethane (Chen *et al.*, 2007). Furthermore, pristine sepiolite has specific properties of fibrous natural clay, like a high specific surface area (300 m^2 g^{-1}). Efficiently due to the existence of pore of nanometric size, the available interface with another phase increases dramatically. Numerous hydroxyl groups, including silanol (SiOH) and $Mg(OH)_2$, are cladding the clay surface. When dispersed in a polymer matrix, such groups can be included in hydrogen bonding with the hydrophilic polymer matrix through connection to OH, NH and different polar groups (Volle *et al.*, 2011).

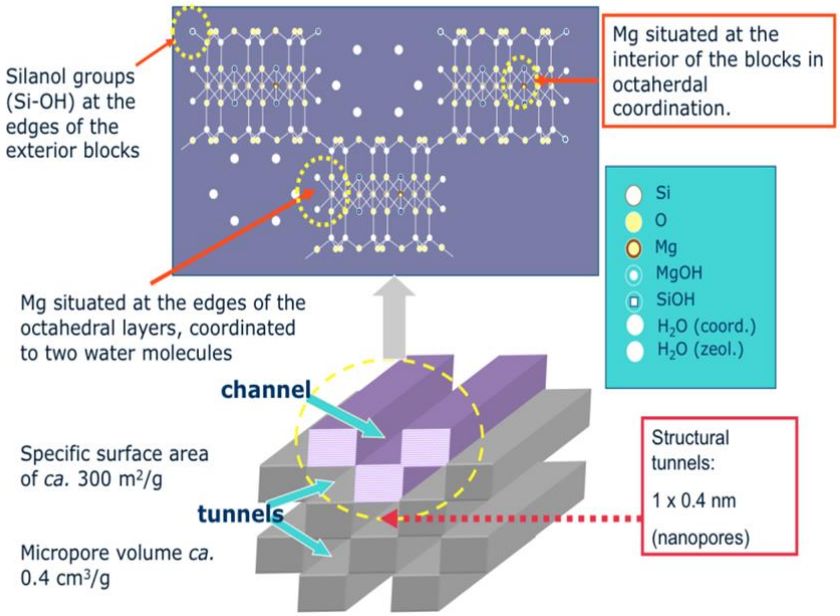

Figure 2-21 : A sepiolite fibre: layer of silica expands as a continuous layer with inversion generating homogeneous size of tunnels and channels (1 × 0.4 Å) over the fibre.

In this section, studies involving effect of nanoclays type on flammability of polymer are discussed. In this study sepiolite and OMMT nanoclays are used for their effect on flame retardancy and synergistic effect is detailed.Marosfoi *et al.* (2008) researched fire retardancy behaviour of polypropylene- magnesium hydroxide-clay composites of various morphologies. They revealed that mixture of montmorillonite and sepiolite clay led to increase time to ignition, and considerably reduced heat release rate. Moreover, they stated that nanofillers-nanofillers connection played crucial role in fire retardant mechanism of polypropylene.

2.7.2 Studies on the influence of nanofiller type

The phosphorus additives pose a compatibility problem when they are incorporated into the PP. The encapsulation of the polyphosphates makes it possible to adjust their polarity and thus improves the compatibility with the polymer. The loading to be used to achieve a satisfactory level of performance is 10 to 15%. Reactive extrusion tests made it possible to synthesize intumescent systems based on melamine phosphate and pentaerythritol. The PP has good compatibility with these water-resistant systems and the mechanical properties are very little modified (Chen et al., 2003). The addition of silicon-based compounds to an intumescent system improves the fire-retardant properties of the system (char formation and radical capture) (Marosi *et al.,* 2002; Wu and Qu, 2001).

More recently, the influence of nanoadditives on the thermal and polymer properties has been the subject of numerous studies by the scientific community. Studies (Bourbigot *et al.*, 2002; Wang *et al.*, 2002; Ye *et al.*, 2002) suggest that the presence of these nanofillers can improve the retarding properties of polymers. As an example, mention may be made of the addition of modified montmorillonites (Zhang *et al.*, 2005), antimony oxide (Ye *et al.*, 2002), or boron siloxanes (Marosi *et al.*, 2002) and carbon nanotubes (Devaux *et al.,* 2004). In particular, clays modified with an organic compound (ammonium or phosphonium (Liu and Wu, 2001) salts) to allow the incorporation of the hydrophilic clay into the polymer matrix, are effective at low loading (5% and less)

(Kandola and Price, 2001). The addition of 2% intercalated silicates to the polypropylene allows a 70% reduction in heat output 1500 kW/m^2 for polypropylene at 450 kW/m^2 for the nanocomposite) (Gilman *et al.,* 2001). Currently, there is no nanocomposite polypropylene sold commercially, but Nanocor Inc. (manufacturer of nano-clay) and Gitto Global Corporation (compounder) have declared themselves interested in the development of polyolefins that are flame retardant by nanotechnology.

An additional aspect can be added to the list of flame retardant strategies: the synergy effect, which will be the subject of part of our study. The synergistic effect consists, when combining two or more flame retardants (FR), in obtaining fire properties higher than those which would be obtained by simple addition of the effects of each of the additives taken separately. In particular, the synergy between ammonium polyphosphate (APP) and zinc borate (ZB) (Samyn *et al.*, 2007, Jimenez *et al.*, 2006) can be .

2.7.3 Nanoclays as flame retardants

Polymer nanocomposite studies on contribution of nanoclays have started in the late 1940s, with much higher clay loadings. It was in 1976 that Unitka Ltd. has first stated that flame retardant properties are enhanced with introduction of layered silicates in PA6 polymers (Fujiwara and Sakamoto, 1976). In 1989 Toyota research group have stated 70% increase in room temperature tensile modulus, an 87°C increase in heat distortion temperature and a significant decrease in water permeability of N6 with nanoclay addition. After that, a comprehensive study on flame retardancy properties of N6/nanoclays has been published by Gilman *et al* in 1997 (Gilman *et al.*, 1997). Following his study, flame retardancy enhancement properties of nanoclays has been investigated with different matrix polymers through various studies and similar reductions in flammability have been achieved.

In the study of Gilman *et al.* (2000) reductions of 50-75% in peak heat release rate is achieved for nylon 6 and polystyrene nanocomposites with nanoclays. They

stated that reductions in heat release rate and mass loss rate were with the general mechanism of the formation of a carbonaceous-silicate structure that builds up on the surface during combustion. This structure insulates the underlying polymer and reduces the speed of mass loss rate of combustible volatiles.

Carbonaceous-silicate structure is developed as a result of removal of polymer by pyrolysis, and leaving clay particles behind. Clay particles gained back their hydrophilic nature after degradation of organic modifier and form stacks. Clay stacks migrate to the surface creating an insulating barrier. Rising bubbles (formed by decomposition of organic modifiers and polymer) enhance accumulation of clays on surface of burning polymer. Also decreased viscosity of the polymer facilitates this migration.

In addition to barrier formation, clay particles also play an important role in char formation. Strong protonic catalytic sites are produced on nanoclay surface upon thermal decomposition of organomodifier. Those sites promote char forming reactions (Jang *et al.*, 2005;Song *et al.*, 2007). The char promotion effect of nanoclay is observed in polymers that do not normally produce char in neat form, such as ethylene vinyl acetate (EVA) (Zanetti *et al.*, 2001b), polystyrene (PS) (Bourbigot *et al.*, 2004a), acrylonitrile butadiene styrene (ABS) (Wang *et al.*, 2003) and polypropylene (PP) (Zanetti *et al.*, 2001a). Organomodifier of the nanoclay is assumed to be responsible in this char promotion. It is observed that nanoclays having larger amount of organomodifier have resulted in higher char content in the system (Song *et al.*, 2007).

Nanoclays can also change degradation pathway of polymers which they are introduced into. Clay layers entrap polymer chains in between and provide a super-heated environment. Polymer chains find chance to go additional, alternative degradation reactions which in turn, leads to a reduction in heat release rate.

Carbon nanotubes were introduced as an alternative to traditional flame retardants and nanoclays by (Kashiwagi *et al.*, 2002) Various studies confirm that CNTs improve

flame retardancy of large range of polymers such as PS (Cipiriano *et al.*, 2007), EVA (Cipiriano *et al.*, 2007), PMMA , PP (Kashiwagi *et al.*, 2004), PA-6 (Schartel *et al.*, 2005), LDPE (Bocchini *et al.*, 2007)even at very low loading rate (<3 wt%). More than 50% reduction in PHRR was detected with incorporation of 0.5 wt% SWCNT in PMMA systems (Kashiwagi *et al.*, 2005).Improved flame properties are attributed to formation of a protective, structured nanotube network layer that acts as a heat shield for the polymer underneath. Network structure can also enhance barrier character, suppressing evolution of combustible volatiles and inhibiting oxygen flow. Consistent with suggested mechanism, flame retardancy is found to be improved with better CNT dispersion that results in more effective network structure (Moniruzzaman and Winey, 2006).

Even though nanoclays and carbon nanotubes have profound contributions on flame properties of polymers, they become inadequate in lowering the total heat evolved (THE) during combustion. THE values remain almost unchanged, suggesting that all polymer burn eventually at the end of fire. Both nanoclays and carbon nanotubes also increase viscosity and inhibit dripping of polymer, which results in insufficient fire test performances like UL-94 and LOI. Time to ignition (TTI) values are also affected unfavourably with introduction of nanoclays into the system since early degradation of the organic modification increase probability of early ignition.

2.7.4 Effect of Sepiolite loading

The mixture of PP-g-MA and sepiolite appeared essential for the development of thermally stable char layer that considerably enhanced the flame retardancy of PP/PA blends. Certainly, when used individually, neither MA-g-PP nor sepiolite nanoparticles resulted in considerable decrease in pHRR values. Furthermore, the reduction in nanoparticles content highly influenced the flame retardancy of the blends and pHRR was found to enhance from 425 kW/m² with 5 wt% of sepiolite to 575 kW/m2 and 845 kW/m2 with 3 wt% and 1 wt% of sepiolite, respectively (Figure 2-22). As confirmed in Figure 2-23, the sepiolite content firmly impacted the quantity of char and its thermal stability. This behaviour is just like what is usually described in fire retardancy of polymer

nanocomposites and is because of the creation of a barrier that limits volatiles mass transport, heat and oxygen diffusion due to the development of char layer at the material surface. So far as PP-g-MA is involved, Bartholmai and Schartel (2004)indicated that the peak of heat release rate reduced considerably with increasing montmorillonite content. Nevertheless, authors identified an absence of significant char formation because the rise in residues recognized related to the quantity of clay incorporated.

2.7.5 Flame retardants used in polyolefins

In this section we are particularly interested in the fire performance of polyolefin-based composites, especially polyethylene and polypropylene. The virgin polyethylene and polypropylene are highly flammable: their IOL is 17-18% and they are not classified in the UL-94 test. The flame proofing of polyolefins can generally be achieved by one of these methods (Coquelle *et al.*, 2015;Jha *et al.*, 1984) as follows:

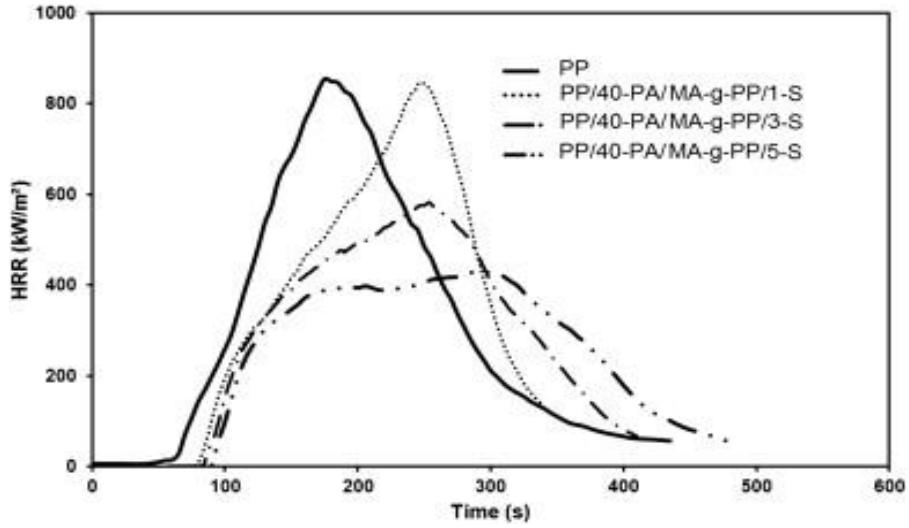

Figure 2-22: HRR of compatibilised with PP-g-MA blend of PP/PA6 comprising different quantities of sepiolite nanoparticles (35 kW/m²)(Laoutid *et al.*, 2013)

.

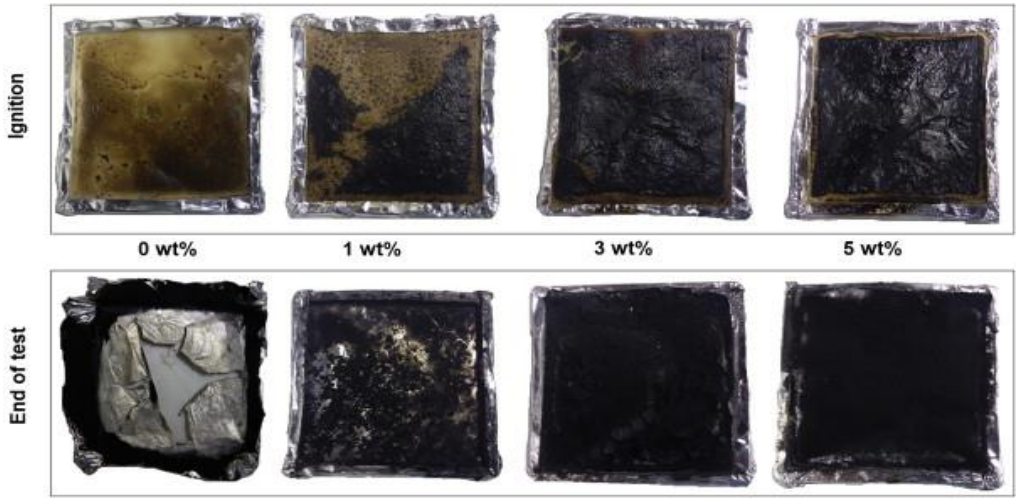

Figure 2-23 : Photograph of char residues of different sepiolite loading after cone calorimeter test(Laoutid *et al.*, 2013)

- By adding loads that produce char (such as an intumescent system). This char makes it possible to partially or totally block the transfers of mass and heat between the condensed phase and the gaseous phase.
- By inhibiting free radicals released to the gas phase (such as halogenated or phosphorus compounds)
- By incorporating inorganic fillers which decompose endothermic ally by releasing water, which will cool the polymer and dilute the volatile fuels.

The literature reports various halogenated compounds (Coquelle *et al.*, 2015), nitrogen (Cullis *et al.*, 1991), phosphorus (Green, 1992) or nanofillers (such as clays (Lepoittevin *et al.*, 2002), oxides (Li *et al.*, 2003), etc.) or polyolefins.In this part, we focus on phosphorus compounds in particular ammonium polyphosphate which is one of the main components used in our work. Flame retardant families containing phosphorus cover a wide range of organic and inorganic components. In general, organic phosphates, phosphinates, red phosphorus, ammonium polyphosphates and phosphonates are the most common compounds used as flame retardants. They act, on the one hand, in the gas phase to trap the free radicals (OH° and H°) and, on the other hand, in the condensed phase, forming acid species which react with the polymer in order to form phosphoric esters]. The decomposition of the esters produces a carbonaceous material which limits the transfer of material to the flame and heat to the polymer.

In polyolefins in general (non-charcoal polymer), the APP alone does not allow to form a char, the corresponding composites are then not classified in the UL-94 test (Anna *et al.*, 2002). It is necessary to combine it with a char promoter (such as pentaerythritol (PER)) in order to obtain an intumescent effect.By way of example, a combination of APP and PER or between diammonium pyrophosphate (PY) and PER in polypropylene makes it possible to increase the IOL values by 17 for the virgin PP to 25% for the PP/APP/PER and 27% for PP/PY/PER, with an overall loading rate of 15% by

weight. The PP / PY / PER mixture results in the formation of a more thermally stable carbonaceous layer than that formed with APP/PER (Bourbigot *et al.*, 2004b). Camino *et al.* (1989) formed decompose by dehydration producing a residue containing carbon and inorganic elements. Then, the residue solidifies at the end of the chemical reactions and the char is thus formed.

Several researchers have tried to combine this intumescent APP/PER system with mineral fillers (metal salts, oxides, borates) or organic (phosphorus compounds) in order to increase their effectiveness. We will present some examples.

2.7.6 Effect of polyamide content on flammability

As a way to explore the effect of PA amount on the fire behaviour of compatibilised PP/PA nanocomposite, a second blend comprising 20 wt.% of PA has been created and tested. Fig. 9a shows HRR curves gathered during mass loss calorimeter test. At constant sepiolite content (5 wt.%), the decrease in PA content from 40 to 20 wt% generated some modifications on HRR curve showing a damaging effect, particularly on the resistance to ignition while the pHRR level stays similar The decrease of PA content, from 40 to 20 wt.%, did not appear to develop a discontinuous PA/sepiolite -rich carbonaceous surface layer upon combustion since pHRR level remains almost like that obtained with 40 wt.% of PA. Thus, this PA amount is kept higher than the critical concentration that enables generating of clear char network. Nevertheless, this reduction influenced the time to ignition (from 90 s to 56 s). The decrease in PA content also induced a reduction of the number of separated domains of carbonaceous char that requires more time for connecting and create constant char.

2.7.7 Influence of glass fibre reinforcement

Research on the usage of nanoclays and short glass fibres jointly as reinforcements in thermoplastic matrix are very limited at that time(Cinausero *et al.*, 2008;Laoutid *et al.*, 2009). However, there has been considerable research interest (Ferry *et al.*, 2001;Liu *et*

al., 2006;Chen and Wang, 2006;Braun *et al.*, 2008;Zhao *et al.*, 2008a;Gunduz *et al.*, 2009;Liu *et al.*, 2011a;Perret *et al.*, 2011;Zhao *et al.*, 2011;Isitman *et al.*, 2009a;Isitman *et al.*, 2009b) in establishing flame-retarded short fibre reinforced thermoplastic composites attributable to their increased mechanical properties, there appears to be few publications focused on the synergistic flame retardancy influence of nanofillers on glass fibre reinforced thermoplastic composites that contains standard flame retardant additives. As a result, one of my aim of this thesis is to examine the flame retardancy effect of using a mixture of nanofillers and short glass fibres in an intumescent flame-retarded polymer.

2.7.8 Relationship between flammability and melt rheological

New reports on a new class of flame retardant (FR) systems that include nanoclay and conventional FR microparticles have revealed that the threshold concentration of FR necessary to achieve satisfactory degrees of flame retardancy can be significantly decreased in the presence of nanoclay Nazare *et al.* (2009). have identified synergistic effects while introducing nanofillers into intumescent formulations. They proposed that the reactivity of nanofillers with the intumescent FR adjusts the physical behaviour of intumescent char during burning.

Bourbigot *et al.* (2004b) have observed synergistic effects while combining nanofillers into intumescent formulations. They suggested that the reactivity of nanofillers with the intumescent FR changes the physical behaviour of intumescent char during burning.

Tung *et al.* (2005) have studied the structural morphology of the dispersed phase in the polymer strongly affects the rheological properties of the polymer system, which can sequentially alter the burning behaviour of the polymer composite. Therefore, he uses two different geometry nanoclay namely: layered structure Cloisite B30 and needle-like nanoclay sepiolite (SP).

2.8 Assessment of Flame Retardancy

The whole set of studied polymer hybrid nanocomposite were tested for their fire behaviour and flammability properties using Cone calorimetry test, limiting oxygen index (LOI), UL94 vertical burning tests, used also micrograph of charred samples and used Raman spectroscopy of charred samples.

2.8.1 Cone calorimeter fire testing

Fire behaviour was assessed by using a Cone calorimeter test (Fire Testing Technology, UK) according to the procedure BS EN ISO 13927(British standard institution, 2015).Temperature of the conical heater was adjusted to produce an external heat flux of 50 kW/m2 on subjected samples. Every time before testing different sample batches, the devices was calibrated to correlate the measured rates of heat release during combustion. In addition to this, the mass of the sample is regularly recorded by the load cell. The sample size is 100 ×100 × 4 mm^3 is positioned in the holder over the load cell in order to measure the estimation of mass loss during the experiment. Conic heaters, set to the related temperature for the preferred external heat flux, continuously radiates the sample from above. The combustion is triggered by an electric spark. Reference measurements on samples indicated that the obtained heat release rates were accurate with error ±10%.

There are many parameters that can be taken from the plot from Cone calorimeter test as shown in Figure 2-24 which give details about flammability of the polymer such as:

- Peak Heat Release Rate (PHRR) (kW/m^2): PHRR regarded as the most important parameter regarding material's capabilities in a fire condition and determines the contribution of the material to the seriousness of flashover of a fire the maximum quantity of heat released from the specimen.

- Total heat released (THE): Area under the heat release rate versus time curve representing the total fire load of a material. Standard unit of THE is MJ/m^2.
- Time to Ignition (TTI) (s): the time between sparking and ignition of a material under external irradiation.
- Time to Peak Heat Release Rate (T_{HRR}) (s): the time elapsed up to peak heat release rate.
- Fire Growth Index (FGI): contribution of a material to fire propagation; ratio of PHRR to TTI.

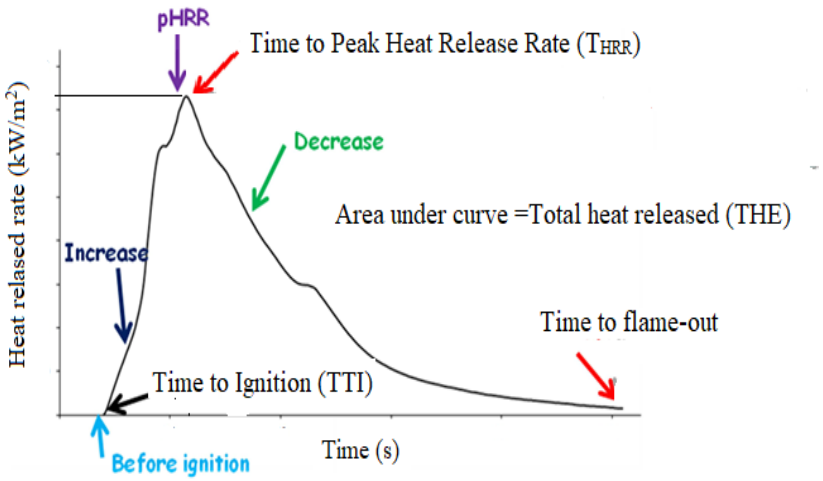

Figure 2-24 :Cone calorimeter test curve screening important fire parameters

- Fire Growth Rate Index (FIGRA): contribution of a material to fire propagation rate; ratio of PHRR to T_{HRR}.

- Char yield (wt.%): weight percent of solid fire residue of a material measured at flame-out.

2.8.2 Limit Oxygen index (LOI) and UL94 Flammability Testing

Limiting oxygen index (LOI) was assessed according to ISO 4589 (British Standards Institution, 2016) on an oxygen index apparatus (Fire Testing Technology, UK) having a oxygen analyser so that precise modifications of the oxygen concentration can be carried out and repeatable results are obtained. Oxygen concentrations were varied based on ISO 4589. The technique entails using a large number of specimens to determine oxygen index with a standard deviation of about 0.2% O_2. Samples were classified based on the standards of Underwriters Laboratories UL94 (Underwriters Laboratories, 2013) because of their flammability using vertical burning tests on a custom flammability meter.

2.8.3 Flammability assessment by Raman spectroscopy

Tuinstra and Koenig (1970) discovered that the intensity ratio of the D peak to the G peak is inversely proportional to an in-plane microcrystalline size and an in-plane phonon correlation length bought from Raman spectroscopy. As a result, the Tuinstra and Koenig relationship has frequently been used to assess in-plane microcrystalline size and to characterize the carbonaceous types. The integration of intensity ratio of the D peak to the G peak is greater the higher will the size of carbonaceous microstructures system could be smaller compared to that from the one without nanoclay (Zhong *et al.*, 2007). These results are in good agreement with those reported from Bourbigot *et al.* (1996a) in which the higher protective shield performance was associated with the smaller size of carbonaceous microstructures. In order to explore the cross-linking and the corresponding flame retardant mechanism, Raman spectroscopy can be used to investigate the structure of char residue after cone tests. Laser Raman spectroscopy (LRS) is often used to characterize the different types of carbonaceous structure formed in the char residue, because Raman signal of graphite crystals, result from lattice vibrations and are very

sensitive to the degree of structural disorder. Normally, Raman spectra of disordered graphite shows quite sharp modes, the G peak will boarhound 1580-1600 cm^{-1} and D peak around 1350 cm^{-1}. The G band is related to the structural organization of char layer and D band only corresponds to amorphous char. Tuinatra and Koenig (T-K) found that the relative intensity ratio R of the D peak to the G peak was inversely proportional to an in-plane microcrystalline size and/or an in-plane phonon correlation length obtained from Raman spectroscopy(Tuinstra and Koenig, 1970;Zhao *et al.*, 2012). As shown in Figure 2-25, each spectrum is subjected to peak fitting using the curve fitting software Origin8.0/ Peak Module to resolve the curve into 2 Gaussian bands.

The intensity ratio of the D peak to the G peak of PP/IFR/1 wt.% SBA-15 is greater than that of PP/IFR as seen from the spectra. Thus, the size of carbonaceous microstructures from PP/IFR/SBA-15 system could be smaller than that from PP/IFR system. These results are in good agreement with those reported from Bourbigot's work (Bourbigot *et al.*, 1996b) in which the higher protective shield efficiency was related to the smaller size of carbonaceous microstructures(Li *et al.*, 2011) .

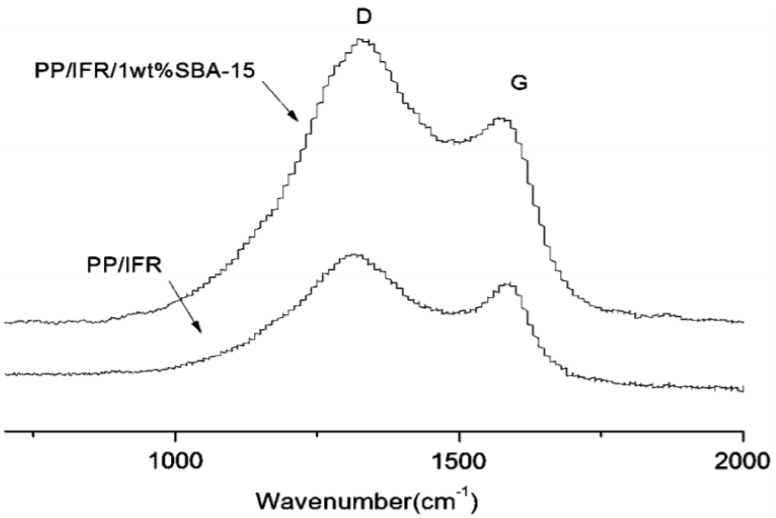

Figure 2-25: Raman spectroscopy of the intumescent char residue obtained from PP/IFR and PP/IFR/1 % SBA-15 blends(Li *et al.*, 2011)

2.9 Conclusion

The chapter reviews the concepts and methods of combustion, thermal decomposition, flammability, flame retardants, synergy effects, intumescence and its mechanism, additives and its effects on nanocomposites. The review, points out that although much of the work based on nanoclays and glass fibres are carried out, yet a very little information on the use of nanoclays and glass fibres in the presence of flame retardants such as Exolit ®AP765, Exolit AP423 and compatibilisers is available. Literatures indicate that glass fibre although improves the mechanical properties and thermal stability but cannot enhance the flame retardancy. Intumescence flame retardancy with sepiolite improves the properties and sepiolite requires no modification Also, it is understood that synergistic effects could be achieved by hybridizing nanoparticles into the matrix of fibre-reinforced composites. Polypropylene (PP), even though one of the most widely used thermoplastic, has certain restrictions with respect to stiffness and strength, and in order to enhance its applications in different areas, inorganic fillers (glass fibre (GF), carbon nanotubes, clays, etc.), are needed while processing the polymer composites. Composites, particularly, glass fibre reinforced PP composite is fairly attractive due to the ease of fabrication, better mechanical properties, good strength and all the above low manufacturing cost(Rahman *et al.*, 2018).

CHAPTER 3 : MATERIALS AND EXPERIMENTAL METHODS

This chapter provides information on the polymer and the additives utilized in this research. Furthermore, the preparation method of the samples is discussed. Then, experiment methods to examine mechanical properties, thermal stability and flame retardancy are presented. Furthermore, experimental techniques used to characterize char residue (condensed phase analysis) such as Raman spectroscopy, SEM and XRD.

3.1 Materials

This part is focused to the materials used in this research, polymers, the compatibilisers, the nanoclay, the flame retardant and glass fibre additives. Processing of the materials is then explained. Inside second section characterization methods are discussed.

3.2 Polymers

The polymer used in this study are polypropylene and polyamide 6

3.2.1 Polypropylene (PP)

PP is a polymer that is obtained by the polymerisation of propylene monomers (CH2=CH-CH3). This semi-crystalline thermoplastic is comparable to high-density polyethylene (HDPE) and is manufactured by an identical process. The PP used was a homopolymer (Icorene® 4014, ICO Polymer, UK; supplied by Schulman Europe) in granular form with melt flow index (MFI) of 44 g/10 min. Table 3-1 lists the main properties of PP. PP is a polymer that is obtained by the polymerisation of propylene monomers (CH2=CH-CH3). This semi-crystalline thermoplastic is comparable to high-density polyethylene (HDPE) and is manufactured by an identical process. The PP used was a homopolymer (Icorene® 4014, ICO Polymer, UK; supplied by Schulman Europe) in granular form with melt flow index (MFI) of 44 g/10 min. Table 3-1 lists the main properties of PP.

3.2.2 Polyamide (PA6)

Polyamide 6 is a polymer containing amide functions - amide function group (N-H- C=O) resulting from a polycondensation reaction between the carboxylic acid functional groups and amine. The aliphatic polyamides are denoted by one or more digits relating to number of carbon atoms contained in the repeat unit. a homopolymerise (zytel®7335F, Du Pont, USA). Table 3-1 lists the main characteristics of Polyamide 6.

Table 3-1 : The main characteristics of polymers used in this study

Material	Density 24°C (g/ cm^3)	Melt Flow(230ºC, 2.16 kg) (g/10min)	Melting Temperature (°C)
Polypropylene (PP)	0.91	15	164
Polyamide (PA6)	1.13	23	221

3.2.3 Nanoclay

As stated earlier, nanocomposites generally display improved performance properties when compared with conventional composites because of their unique phase morphology and improved interfacial properties. For these reasons, nanostructured organic-inorganic composites have attracted significant attention from both primary research and an applications perspective.

In this study, two types of nanosized fillers—layered silicates (Nanofil® 5) and sepiolite (SP) nanofibres—have been used to synthesise polymer nanocomposites.

3.2.4 Nanofil® 5 (N5)

N5 (Süd-Chemie, Germany) is an organically modified, nanodispersible layered silicate based on natural bentonite, and this clay is surface-treated with a dimethyl, di(hydrogenated tallow (HT)) alkyl quaternary ammonium salt. The properties of N5 as provided by the manufacturer are shown in Table 3-2 and Figure 3-1.

Table 3-2: Properties of nanoclay Nanofill ® 5

Property	Unit	Value
Exchange capacity (CEC) in milliequivalent (mEq)	mEq/100g	93
Interlayer spacing	nm	2.8
Moisture content	%	1.3
Weight loss on ignition	%	38
Bulk density	g/cm^3	2.7

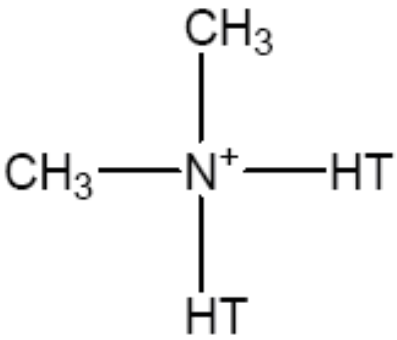

Figure 3-1: Chemical structure of Nanofill5

Where HT stands for the hydrogenated tallow-based compound containing ~65 % C18, ~30 % C16, and ~5 % C14. N^+ ammonium cation, CH_3 stand for methyl group .

3.2.5 Sepiolite Clay (SP)

SP is a family of fibrous hydrated magnesium silicate with the theoretical half unit-cell formula $Si_{12}O_{30}Mg_8(OH)_4$ $(OH_2)_4 \cdot 8H_2O$ characterized by a needle-like morphology. The sepiolite, however, from the other layered silicates because of the lack

of a continuous octahedral sheet. It composed of two tetrahedral silica sheets and a central octahedral sheet containing Mg, but continuous only in one direction in (c-axis). as in Figure 3-2 More blocks are linked together along their longitudinal edges by Si-O-Si bonds, and this creates channels along the c-axis. Because of the discontinuity of the external silica sheets, a significant number of silanol groups (SiOH) are situated at the edges of this mineral. It can have a surface area as high as 200–300 m^2/g(Nehra *et al.*, 2018) , vary between 0.2–4 μm in length, 10–30 nm wide and 5–10 nm thick (Ma *et al.*, 2007) as shown in Figure 3-2.These properties (associated to a modulus of E=180 GPa for a sepiolite fibre), good abundance and to a relative low cost make sepiolite nanofillers attractive nanoparticles blends of thermoplastic, elastomeric or thermoset polymers designer nanocomposites with new properties.

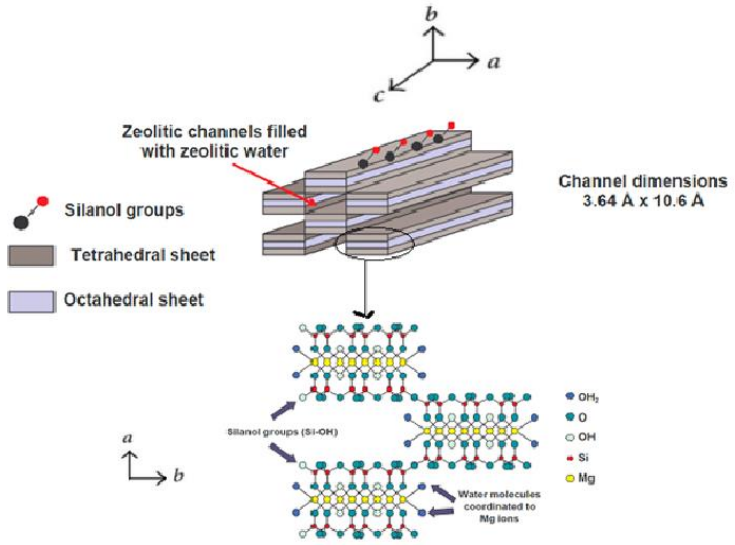

Figure 3-2: Sepiolite Nanoclay structure

3.3 Compatibilisers

Compatibilisers are used to create interactions between the PP matrix and the organoclay. Furthermore, they are necessary to enable the opening of the silicate layers so that the PP matrix can enter between the layers. In this study, maleic-anhydride-grafted polypropylene (PP-g-MA) copolymer (Polybond 3200, Addivant, USA; properties shown in Table 3-3) was used as a compatibiliser and poly[styrene-(ethylene-co-butylene)-styrene]-grafted maleic anhydride (SEBS-g-MA) (Kraton FG 1901; denoted as S), as a blend compatibiliser.

3.3.1 PP-g-MA Compatibilisers

In this study, polypropylene-grafted maleic anhydride modified (PP-g-MA - named as mpp) was used. Polybond 3200 was used as compatibilising agent. It was supplied by (Addivant, USA) to reduce miscibility between blend and increase adhesion force between polar matrix and organic nanoclay. The structure and properties of PP-g-MA in Figure 3-3 and Table 3-3.

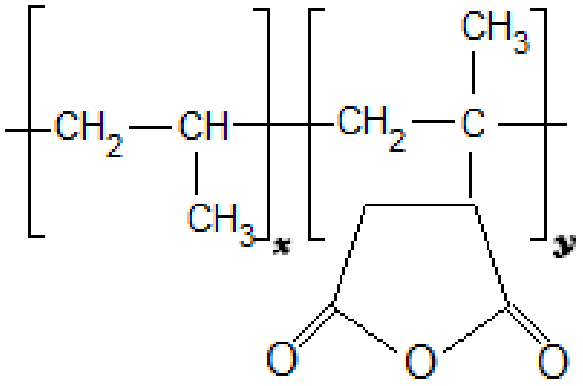

Figure 3-3:The chemical structure of PP-g-MA

Table 3-3: Properties of Polybond 3200

Property	Unit	Value
Melt index @ 190°C, 2.16Kg (ASTM D-1238)	g/10 min	115
Density @ 23°C, ASTM D-792	g/cm^3	0.91
Bulk density, ASTM D-1895B	g/cm^3	0.6
Melting point, DSC	°C	157
Maleic anhydride content	%	0.8 - 1.2

3.3.2 Poly[styrene-(ethylene-co-butylene)-styrene]-grafted maleic anhydride compatibilisers

SEBS-g-MA (Kraton FG 1901; denoted as S) was used as compatibiliser between the incompatible polymers to increase the adhesion force between the matrix and to form a polar polymer such as PP hydrophobic with organic clay. Figure 3-4 shows the chemical structure of SEBS-g-MA and Table 3-4, its properties

Table 3-4: Properties of SEBS-g-MA compatibilisers as received

Property	Unit	Value
Melt index @ 230°C, 5 kg (ASTM D-1238)	g/10 min	22
Density @ 23°C, ASTM D-792	g/cm^3	0.91
Bulk density, ASTM D-1895B	g/cm^3	0.6
Processing temperature	°C	225
Maleic anhydride content	%	1.4–2
Styrene/rubber ratio	%	30/70
Elongation to break	%	500

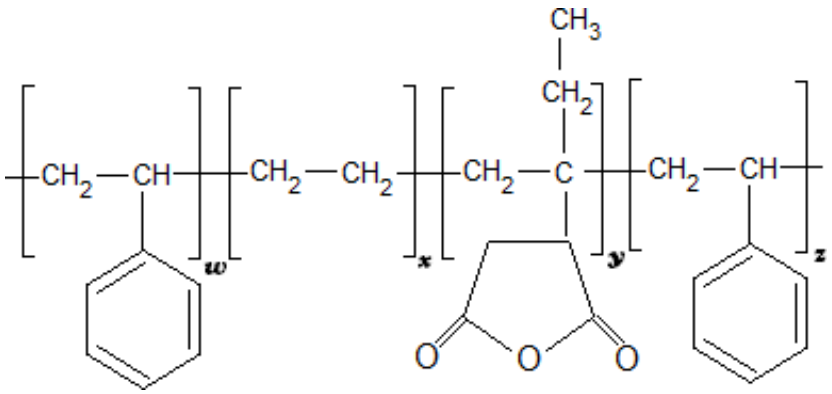

Figure 3-4: Chemical structure of SEBS-g-MA

3.4 Short Glass Fibre (GF)

A large percentage of continuous filament GF is cut into short lengths of few tens of 10 millimetres for use as reinforcement in various applications. The short GFs are usually distributed randomly along two or three principal axes, as shown in Figure 3-5. In this study, chopped GF (P968 grade; Vetrotex, France) with density of 2.6 g/cm3, diameter of around 10–13 µm and length of 4.5 mm is surface-treated by a silane-based coupling agent. Table 3-5 shows a comparison of the properties of E-GFs, obtained from a technical datasheet, and those of S-GFs.

Table 3-5: Characteristics and cost comparison of E & S glass fibres

Fiber type	Tensile strength (MPa)	Compressive strength (MPa)	Density (g/cm^3)	Thermal expansion (µm/m·°C)	Softening T (°C)	Price ($/kg)
E-glass	3400	1080	2.58	5.4	846	~2
S-glass	4800	1600	2.46	2.9	1056	~20

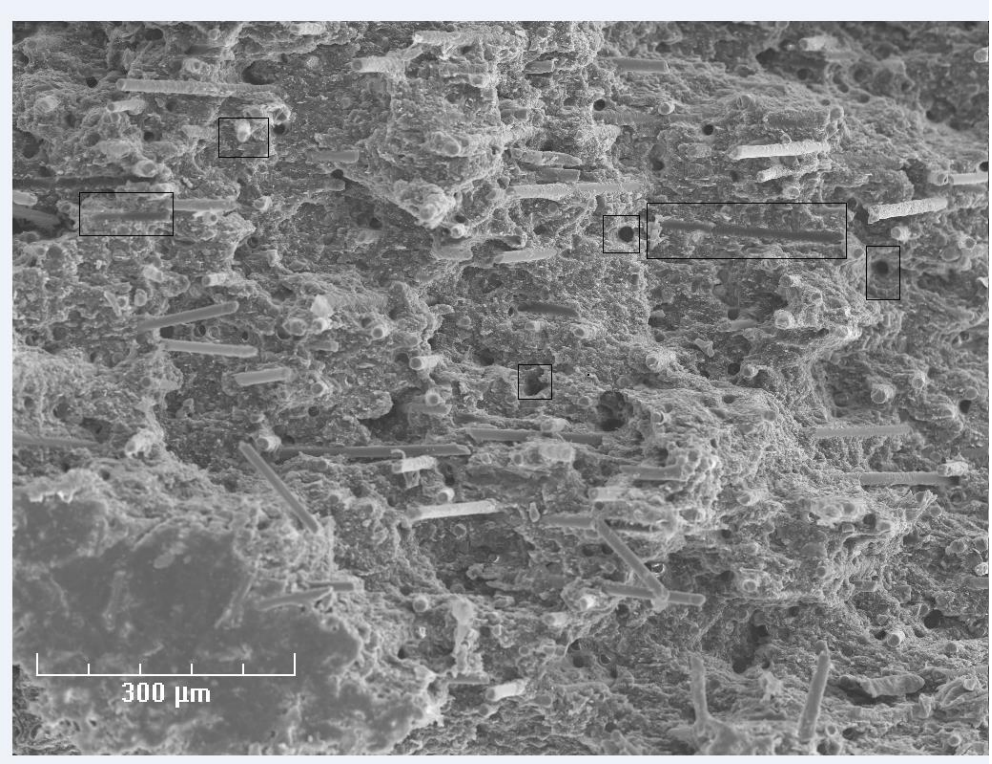

Figure 3-5: SEM picture of chopped glass E-glass fibre randomly oriented with 4.5 mm long and 13 µm wide after impact test

3.5 Flame Retardant Additive (FR)

Ammonium polyphosphate (APP) is an inorganic salt of polyphosphoric acid and ammonia. APP (Exolit, Clariant UK) has the chemical formula (NH4PO3)n, where n > 1000, as shown in Figure 3-6. It is relatively insoluble in water (solubility: <0.1 g/100 ml) (Flame Retardants 2018). APP is thermally stable up to 260°C under air and under nitrogen (Zhang et al., 2013).

3.5.1 FR additive: Exolit® AP 423

Ammonium polyphosphate (Exolit®AP423) is a fine-particle ammonium polyphosphate produced by a special method. It was provided by Clariant, it is made up of 31-32% by mass of phosphorus and 14-15% by mass of nitrogen. The average particle size is 8 µm shown in Figure 3-6 and Table 3-6.

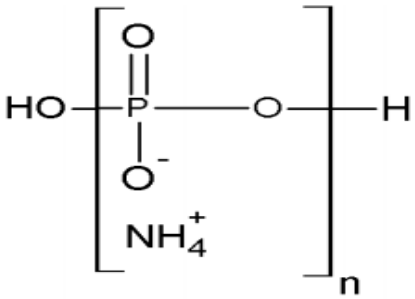

Figure 3-6 : Chemical structure of ammonium polyphosphate (n> 1000

Table 3-6:Specifications of Exolit 423

Material	Commercial Name	Properties
Ammonium polyphosphate (APP)	Exolit® AP 423 (Clariant)	Chemical formula: $[NH_4PO_3]_n$,
		Particle size: 8 µm
		Density: 1.9 g/cm^3
		Bulk density: 0.7g/cm^3
		Phosphorus content: 31–32% [w/w]
		Nitrogen content: 14–15% [w/w]
		Decomposition temperature: >275°C
		Moisture content: <0.5 [wt%]

3.5.2 Flame retardant additive (FR): Exolit®765

Exolit AP 765 is a non-halogenated flame retardant based on phosphorus and nitrogen synergism. The product achieves its flame retardant effect through intumescence. The thermoplastic material foams and crosslinks on exposure to flame

Table 3-7: Specifications of Exolit ®765

Material	Commercial Name	Properties
Ammonium polyphosphate (APP)	Exolit® AP 765 (TP) (Clariant)	Chemical formula: $[NH_4PO_3]_n$, n > 1000
		Particle size: 10 µm
		Appearance: white, free-flowing
		Density: 1.8 g/cm^3
		Bulk density: 0.6 g/cm^3
		Phosphorus content: 23–25% (w/w)
		Nitrogen content: 18–20% (w/w)
		Decomposition temperature: >275°C
		Moisture content: <0.5 [wt.%]

and forms a stable char at the surface acting as a barrier. The protective layer provides a heat-insulation effect, reduces oxygen access and prevents dripping of molten polymer Table 3-7.

3.6 Experimental Methods

This section discusses the techniques used to examine the mechanical properties and thermal stability of the FR materials used in this study. Further, it discusses additional techniques for characterising the materials. Finally, it discusses experimental techniques for condensed phase analysis to characterise the char residue of materials.

3.6.1 Extrusion compounding

Before processing through an extruder, the PP and PA6, SEBS-g-MA and PP-g-MA were dried at 80 °C in a vacuum oven for 24 hours. Sepiolite, Nanofil®5 at 350 °C, 110 °C respectively, in powder form to remove water physically bound. Drying of this polymer is vital as moisture induces a hydrolytic chain scission at the high processing temperature.

The PP/AP6/ SEBS-g-MA blend and its nanocomposites of the blend with Nanofil5, Sepiolite and third components (i.e. chopped glass fibre and ammonium polyphosphate) were melt compounded in a twin-screw extruder Figure 3-7 All the components were premixed in a plastic bag by manually tumbling for 5 minutes and were fed by a calibrated powder twin screw feeder into the extruder. The extruder used was a Betol co-rotating intermeshing twin-screw extruder (40 mm diameter, L/D =21/1) at 200 rpm, the extruder consisted of five barrel sections and each section was equipped with independently controllable electric heating and water cooling system. All of the extrusion variables, including barrel and die temperatures, and the temperature distribution are shown in Table 3-8.

Figure 3-7: Twin screw extruder co-rotating intermeshing

The extruder, in rod form, was cooled quickly by passing through a water bath, drying using a compressed air jet and finally pelletized using a Betol pelletizer. The pellets were further dried in an air oven at 75 °C. overnight Then gunnels were dried at vacuum oven at 75 ° C for 24 hours to remove moisture.

Table 3-8:Temperature profile of the extrusion process

Section	Zone 1	Zone 2	Zone 3	Zone 4	Zone 5	Die
Temperature (° C)	180	190	200	220	220	220

3.6.2 Injection Moulding

The specimens for mechanical properties were obtained by injection moulding in a Demag NC III, 150 Tone was used to mould plates and tensile test bars for the first batch of polypropylene and blends prepared by extrusion with concentrations and material classifications given in Table3-9. Polypropylene blends of prepared composites were injection moulded into plaques according to BS EN ISO 6603 using injection moulding machine.

Table 3-9: Injection moulding processing parameters

Moulding Parameters	Value
Nozzle temperature (°C)	220
Mold temperature (°C)	30
Hold time (Second)	62.5
Injection pressure (bar)	160

3.7 Preparation of Nanocomposites

All the samples were prepared by melt blending PP/PA6 blend with different additives (see Tables below in a co-rotating, twin screw extrude as mention in section 3.6.1). The pellets were injection moulded using a Demag NC III, 150 Tone (T = 180—220 °C, mould temperature = 80 °C) in order to obtain square sheet specimens 100 × 100 × 4 (mm^3). The sample names and compositions are given in Table 1 and Table 2. Prior to the processing, PA 6 and SEBS-*g*-MA (S), PP-g-MA were dried at 80 °C in a vacuum oven for 12 hours. Sepiolite(S), Nanofil®5 (N5) were also dried at 350 °C, 110 °C and 250 °C, respectively, to remove water.

In this study the experimental work is divided into three chapters viz., effect of compatibilisers types, effect of intumescent flame retardant and synergistic effects on sepiolite nanofillers, effect of glass fibre and sepiolite on flammability, mechanical and thermal properties. Tolsa

3.8 Formulation of Composites for effect of Compatibiliser Types

- Polypropylene (PP) (Icorene®4014) and polyamide 6 (PA 6) (Zytel® 7335F) were used as polymer blend components with the following. SEBS-g-MA (Kraton® FG 1901 -named as (S) and PP-g-MA (Polybond®3200, Addivant, USA) were used as blend compatibilisers named as (mpp). Pangel®-S9 sepiolite (named as SP.) from Tolsa (Spain)., An organomodified montmorillonite, modified with a quaternary ammonium (dimethyldihydrogenated tallow alkyl quaternary ammonium salt, named as (N5) was provided by Southern Clay Products (Nanofil®5). The following phosphorous flame retardants supplied by agent of clarinet in UK used as powders: an ammonium polyphosphate (APP® 423 named as FR) and short glass fibre (P355, Vetroxt, France). the material used are summarized in Table 3.10.

Table 3-10: Formulation of blend A PP/PA6 blend and their composites loading in weight percent (wt. %)

Sample code	PP:PA6:SEBS-g-MA(86:9:5)	Sp	N5	APP 423	GF
Blend A(S)	100				
FR0(S)	80				20
FR20(S)	60			20	20
FR15N5(S)	60		5	15	20
FR15SP5(S)	60	5		15	20
FR20 (mpp)	60			20	20
FR15N5(mpp)	60		5	15	20
FR15SP5(mpp)	60	5		15	20

Column 1: (S) and (mpp) respectively indicate compatibilisation with SEBS-g-MA and PP-g-MA.

Columns 2–6: Values respectively indicate the blend A, sepiolite clay (SP), Nanofil®5 (N5), APP® 423 FR, and glass fibre (GF) contents.

3.9 Formulation of Composites for Effect of Intumescent Flame Retardant and Sepiolite Nanofillers.

Polypropylene (PP) (Icorene®4014, ICO polymer, UK) , polyamide 6 (PA 6) (Zytel® 7335F, DuPont ,USA) and PP-g-MA (Polybond®3200, Addivant, USA) were used as blend compatibilisers named as (mpp) components with the following constant ratio PP/PA6/PP-g-MA 70:30:5 named as blend B. Sepiolite (Pangel® S9, Tolsa, Spain) used as nanofiller named as (SP). Phosphorous flame retardants supplied by agent of clarinet in uk used as powders: an ammonium polyphosphate (Exolit® AP 765 (TP), Clariant , Germany), named as (IFR) and chopped short glass fibre (P968,Vetrotex, France is modified with a silane coupling agent for better compatibility with PP and improve the mechanical properties ,the material used are summarized in Table 3-11.

Table 3-11: Formulation of blend B with glass fibre and sepiolite loading in weight percent (wt. %)

Sample code	PP:PA6:PP-g-MA(70:30:5)	IFR+SP=20 wt%		GF
		SP	IFR	
IFR15SP5	60	5	15	20
IFR17SP3	60	3	17	20
IFR18SP2	60	2	18	20
IFR20SP0	60	0	20	20

For all formulations, the glass fibre content is fixed at 20% and total intumescent flame retardant and sepiolite (IFR+SP) content is fixed at 20%.

Columns 2–5: Values respectively indicate blend B, sepiolite clay (SP), intumescent flame retardant (IFR), and glass fibre (GF) contents.

3.10 Formulation on Effect of Glass Fibre and Sepiolite on Properties

Polypropylene (PP) (Icorene 4014) and polyamide 6 (PA 6) (Zytel®7335F) were used as polymer blend components with the following constant ratio PP/PA 6 70:30, PP-g-MA (Polybond 3200, Addivant, USA) were used as blend compatibilisers named as (mpp). Pangel®S9 Sepiolite (named as SP) from Tolsa (Spain). The following phosphorous flame retardants supplied by agent of clarinet in UK used as powders: an ammonium polyphosphate (AP 765 named as IFR) and chopped short glass fibre (P968,Vetrotex, France) is modified with a silane coupling agent for better compatibility with PP and improve the mechanical properties named as(GF). the material used are summarised in the Table 3-12.

Table 3-12: Formulation of blend B with sepiolite and glass fibre loadings in weight percent (wt. %)

Sample code	PP:PA6:PP-g-MA(70:30:5)	IFR+SP=20 wt%		GF
		SP	F(APP 765)	
GF0IF15SP5	80	5	15	0
GF10 F15SP5	70	5	15	10
GF15 F15SP5	65	5	15	15
GF20S F15P5	60	5	15	20
GF10 F18SP2	70	2	18	10
GF15 F18SP2	65	2	18	15
GF20 F18SP2	60	2	18	20

For all formulations, the glass fibre content is varied from 0% to 20%, total intumescent flame retardant and sepiolite (IFR+SP) content is fixed at 20%, and compatibilisation is performed using PP-g-MA.

Columns 2–5: Values respectively indicate blend B, sepiolite clay (SP), intumescent flame retardant (IFR), and glass fibre (GF) contents.

3.11 Material Properties Characterization

For most the characterization studies, such as mechanical, thermal and morphological analyses, injection molded samples were used. For rheological analyses, compression molded samples were chosen. To be able to investigate the impact of the compatibilisers and additives on the final properties of polymer matrix morphological, chemical, thermal, mechanical and rheological analyses were conducted on the samples. Morphology of the nanocomposites was investigated by XRD, SEM analyses. To check into the reactive groups of polymer matrix and compatibilisers FTIR was done. Melting point and crystallinity of the nanocomposites were studied with DSC analysis. Thermal stability of the nanocomposites and degradation rate were studied by TGA/DTG.

Mechanical behaviour of the nanocomposites was assessed by measuring tensile properties (tensile strength, Young's modulus, elongation at break and flexural properties). Impact strength values of the samples were measured with the charpy impact test.

3.12 Mechanical Testing

3.12.1 Tensile test

Tensile test was carried out by Zwick Machine (SMART. PRO, Zwick Roell, UK) shown in Figure 3-8 according to BS EN ISO 527 with a crosshead speed of 5 mm/min and a 50mm gauge length. Five replicates were tested. The tensile strength elongation at break and elastic modulus were determined from tensile test according to BS EN ISO 527 and sample size shown in Figure 3-9. Two values are measured with this test method: the elongation-at-break and the tensile strength (TS).

Figure 3-8: Zwick universal test machine for tensile and flexural testing machine

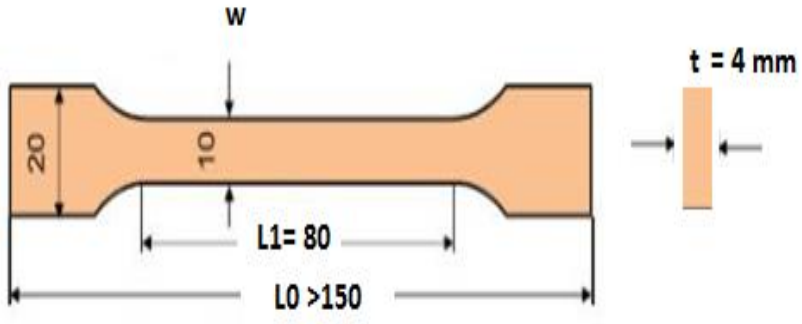

Figure 3-9: Tensile test specimen as per BS EN ISO 527

The $\varepsilon_{f\ is}$ the strain on the sample when it breaks and is expressed in percent. It is calculated using Equation (3-1). The TS is the stress which is needed to break the sample and is expressed in MPa.whereas l_0 is the origin length of the sample and l_f that obtained after test.

3.12.2Flexure Strength and modulus

Flexural properties of the nanocomposites were determined on the same tensile machine by three-point bending tests as per ISO 178 standard at a thickness to span length ratio of 1:16 and at cross head displacement rate of 2 mm/min as shown in Figure 3-10.

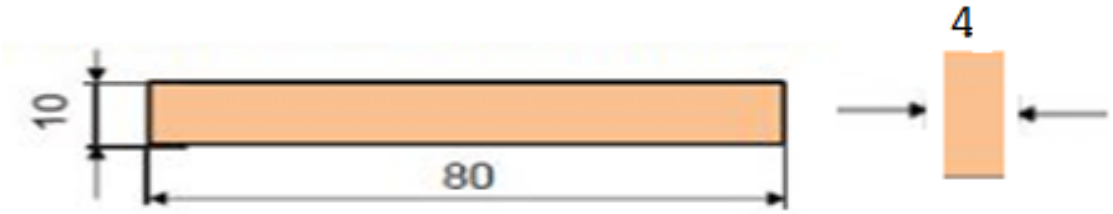

Figure 3-10: Flexural test specimen according to ISO 178 in mm and the dimension in mm

3.12.3Impact Strength

Charpy impact tests were performed by a pendulum CEAST Charpy machine shown in Figure 3-11, specimens according to the ISO 179 with a 4 J capacity was used to measure impact strength following ISO 179/1e shown in Figure 3-12 standard as it can be seen in All the above listed mechanical tests were performed at room temperature and at least five specimens were tested in all cases.

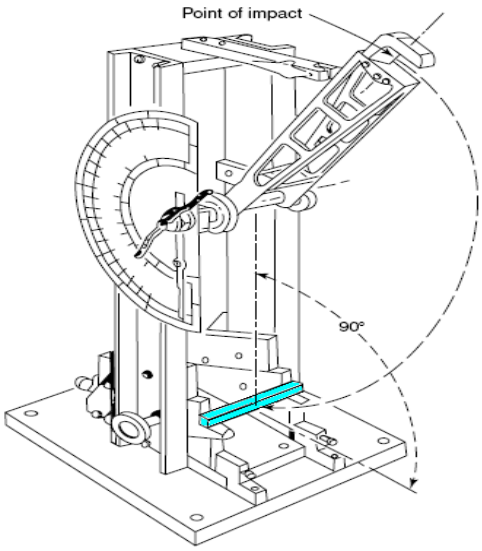

Figure 3-11 :The impact test machine

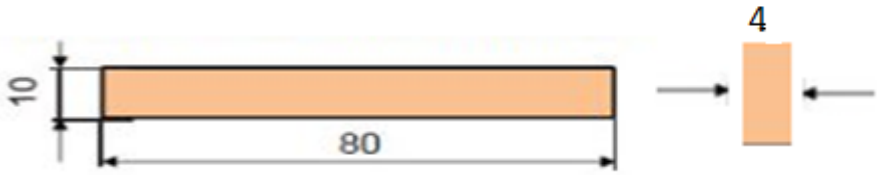

Figure 3-12: Charpy impact test on an unnotched specimen and the dimension in mm

Impact strength calculated from formula given in equation (3-2)

$$S_{uc} = \frac{E}{w \times t} \times 1000 \qquad (3\text{-}1)$$

Where

S_{uc} impact strength in (kJ/m^2)

E is an average absorbed energy (J)

w is sample width (mm)

and t is thickness of sample(mm)

3.13 Thermal Properties

3.13.1 Thermogravimetric analysis/differential thermogravimetric analysis (TGA/DTGA)

TGA has become a general method for comparing the thermal stability of polymers. TGA measures the amount and rate of change in the weight of a material as a function of temperature or time in a controlled atmosphere(Chartoff and Sircar, 2005). Measurements are used primarily to determine the composition of materials and to predict their thermal stability at temperatures up to around 700 °C. The procedure can characterize materials that exhibit weight loss or gain due to decomposition, oxidation, or dehydration. 5% and 50% weight loss with temperature. In comparing thermal stability, it should be remembered that TGA measurements only record the loss of volatile fragments of polymers, caused by decomposition.

In this study TGA was carried out in nitrogen at a heating rate of 10°C/min by using a thermo-gravimetric analysis (TGA Q500 series, TA Universal analysis, TA Instruments Inc., USA). A small amount of each sample (approximately 5-10mg) was examined under a nitrogen flow rate of 10 ml/min from 23 °C to 700 °C. The thermal degradation of PP/PA6 nanocomposites were investigated.

Details about the onset temperature of degradation, the maximum degradation rate temperature(s), the number of degradation steps, the residual weight at a certain temperature - usually when no more development is observed - can be obtained from the resulting weight/temperature curves and their derivatives. The temperatures at 95% and 50% of residual weight are also sometimes given. The mechanisms of degradation depend

not only on the material but also on the environment the test is performed in. In particular, it is classical to observe several degradation steps due to the active oxidative role of oxygen in air.

3.14 Flammability

Depending on the application of materials, different fire tests are used to evaluate their flammability. Some standardised tests are available for different heat and mass transport environments; however, all can acceptably assess the reaction of polymers in a real fire scenario. The flammability and fire behaviour of polymers are commonly characterised using three reliable laboratory measurement methods: limiting oxygen index (LOI) test, Underwriters Laboratories 94 (UL-94) test and cone calorimetry test (CCT).

3.14.1 Limiting oxygen index (LOI)

The limiting oxygen index (LOI) is a small heat source ignition test. With the LOI test (ISO 4589-2), the relative flammability of materials, their ignitability and inflammation can be described. The experimental set-up of the LOI device is shown in Figure 3-13. Limiting. LOI measurements are performed on a Fire Testing Technology device with barrels of 80 x 10 x 4 mm at room temperature. The specimen is clamped vertically into a glass cylinder in a controlled oxygen-nitrogen mixture atmosphere. The measured LOI value corresponds to the minimal oxygen concentration required to sustain the combustion of a material. It is expressed as the percentage of oxygen in an oxygen-nitrogen mixture Equation (3-3) whereas O_2 oxygen concentration and N_2 nitrogen concentration.

$$LOI = 100 \times \frac{[O_2]}{[O_2] + [N_2]} \quad (3\text{-}2)$$

Where:

LOI limited index in volume percent and

O and N stand for oxygen and nitrogen respectively

Limiting oxygen index(LOI) was preformed through the use of (stanton redcroft) oxygen index meter (Fire Testing Technology, UK) according to BS EN ISO 4589-2 (British Standards Institute, 1996), with 80x10x4 mm Sample size. The value of the LOI is defined as the minimal oxygen concentration [O_2] in the oxygen/nitrogen mixture [O_2/N_2] that either sustains flame combustion of the material for 3 minutes (180 seconds) or consumes a size of 5 cm (50 mm) of the sample, using the sample positioned in a vertical location as show in Figure 3-13 Vertical position (the top of the test sample is inflamed with a burner).

Materials having a LOI value under 21 vol% O2 are called combustible material, those with a LOI value over 21 vol% O2 are flame retarded. Thus, the greater the LOI value, the better the fire retardancy of the material. The materials introduced in this report should have a LOI value above 21 vol% O2 (Laoutid et al., 2009).

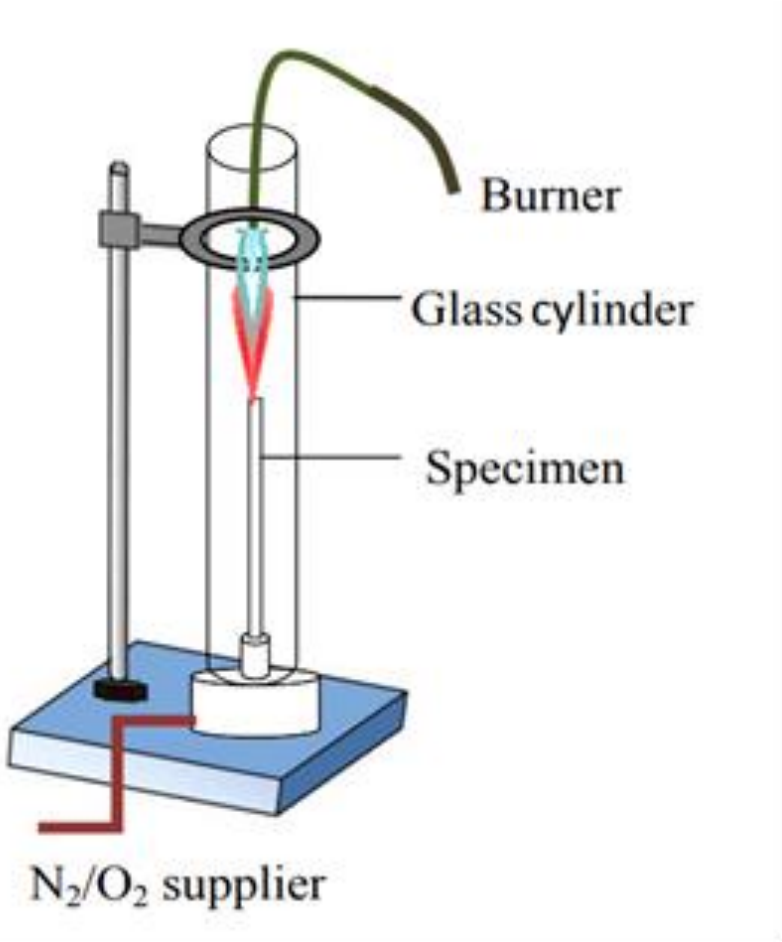

Figure 3-13: Limited Oxygen Index device

3.14.2 Underwriters Laboratories 94 (UL-94)

Like the LOI the UL-94 test, test of flammability of plastic materials is an example for small-scale ignition tests that is authorized by the Underwriters Laboratories Inc. The most frequent and widely used test is the UL-94 V (IEC 60695-11-10) that describes the tendency of a material to extinguish or to spread the flame after ignition of the material. A blue flame with a 20 mm high central cone is applied for 10 s to the bottom edge of the vertical specimen. After 10 s the flame is removed and the afterflame time required to extinguish the flame is recorded. The flame is reapplied for another 10 s and removed again. After the second burning, the time to extinguish and the afterglow time are

noted. possible that during the burning the barrels begin to drop and the burning drops inflame the piece of cotton that is below the specimen. For each material a set of 5 bars was tested. The specimens have a size of 127 x 13 x 3 mm³. It classifies specimens from NC (not classified), V-2, V-1 to V-0, whereas V-0 is the best rating. The different criteria for the classifications are presented in Table3-13: The experimental set-up for the UL-94 test can be seen in Figure 3-14.

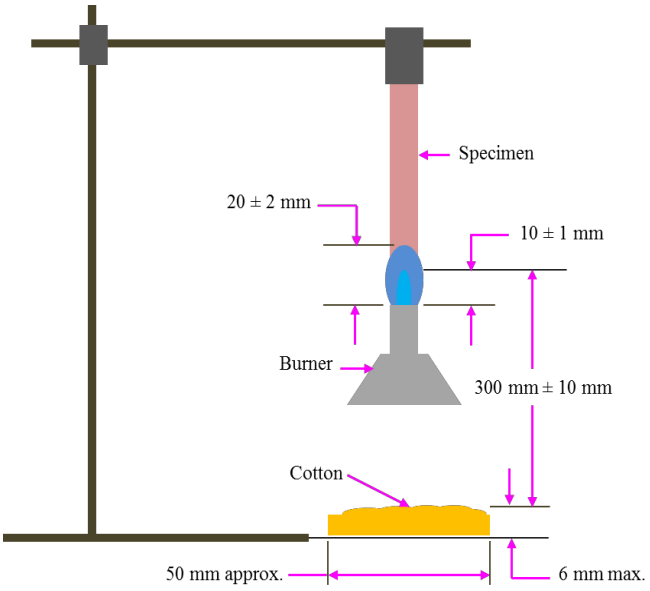

Figure 3-14: The UL94 V test setting up

Table 3-13: Requirements of vertical ratings of vertical ratings (V-0, V-1, V-2)

Criteria conditions	V-0	V-1	V-2
After flame time for each individual specimen t1 or t2	≤10 s	≤30 s	≤30 s
Total after flame time for any condition set (t1+t2 for 5 specimens)	≤50 s	≤250 s	≤250 s
After flame plus afterglow time for each individual specimen after the second flame application (t2+t3)	≤30 s	≤60 s	≤60 s
After flame or afterglow of any specimen up to the holding clamp	No	No	No
Cotton indicator ignited by flaming particles or drops	No	No	Yes

3.14.3Cone calorimeter test (CCT)

Samples were sent to Professor Jose-Marie director of Centre of Materials Engineering (C2MA), University of Ecole des Mines d'Alès (France). The Cone calorimeter devices manufactured by Fire Test Technology (FTT, UK). All samples (100×100×4 mm) at an incident heat flux of 50 kW/m^2 according to ISO 5660-1 standard see Figure 3-15.

In the CCT, experienced combustion occurs following ignition and flame spread supplying heat for the decomposition and pyrolysis of unburned fuel. The rate of which heat is produced is called as the heat release rate and is explained by the product of burning rate as well as heat of combustion. Apart from unambiguous effect of existence of flame retardant species, heat release rate from the exposed polymer includes complex benefits from external irradiation, sample positioning, radiative evaluations of flame towards the pyrolysing zone and completeness of combustion

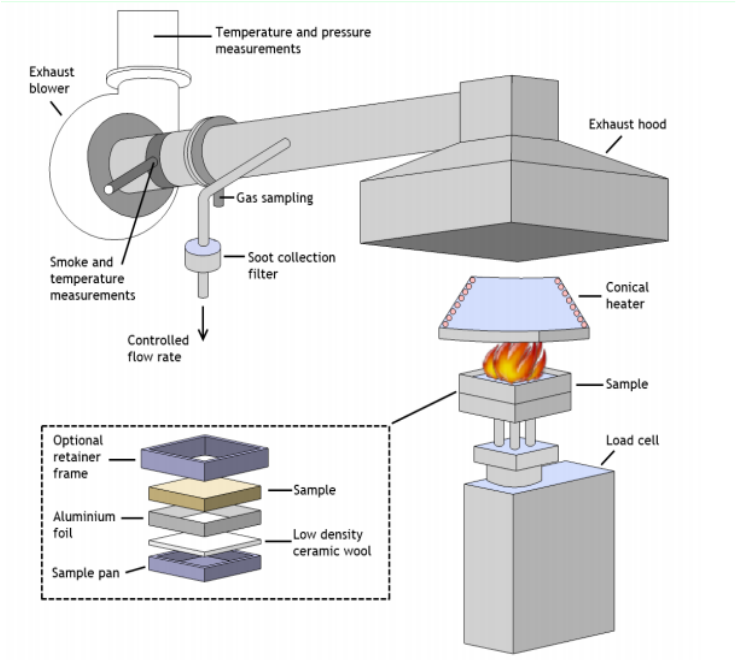

Figure 3-15: Cone calorimeter Test

The most important material properties that can be obtained by Cone calorimeter testing analysis are listed below and shown in Figure 3-16.

Peak heat release rate (PHRR): Considered as the most important parameter regarding a material's performance in a fire scenario and determines the contribution of the material to the severity of flashover of a fire. Standard unit of PHRR is kW/m^2.

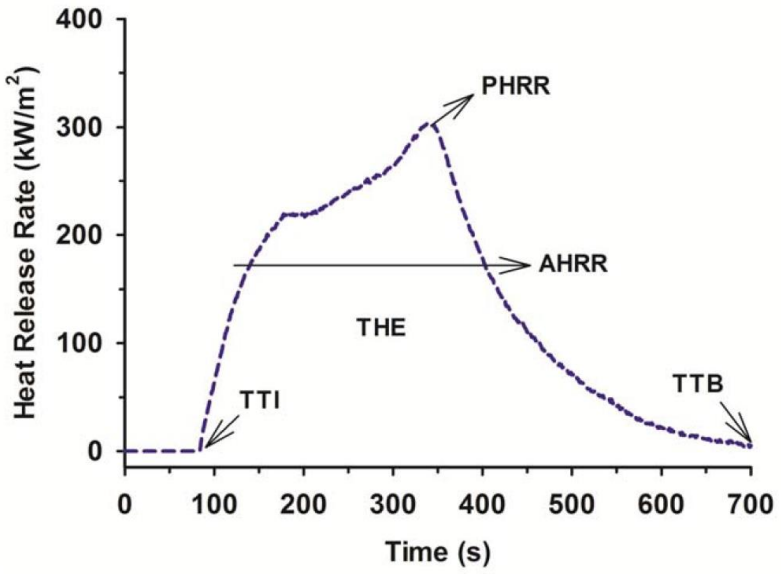

Figure 3-16: A typical mass loss calorimeter curve showing important fire parameters

- **Total heat released (THE)**: Area under the heat release rate versus time curve representing the total fire load of a material. Standard unit of THE is MJ/m^2 .

- **Time to ignition (TTI)**: Time elapsed before piloted ignition of a material under external irradiation. Standard unit of TTI is seconds.

- **Time to flameout (TTF)**: Time elapsed from the beginning of the test to flameout (extinguishment). Standard unit of TTF is seconds.

- **Total mass loss (TML)**: Change in sample mass upon combustion. Standard unit is grams. It is used to calculate percent fire residue by weight.
- **Fire growth index (FGI)**: Ratio of PHRR to TTI. It is an accurate way of describing flame spread rate. Reciprocal of fire growth index is defined as the fire performance index. Standard unit of FGI is kW/m^2 s.
- **Fire growth rate (FIGRA)**: Ratio of PHRR to time-to-PHRR. It is another accurate way of describing flame spread rate. Standard unit of FIGRA is kW/m^2.s.

3.14.4Raman spectroscopy

. The Raman spectra were obtained from a Renishaw inVia™ Raman microscope (inVia™, Renishaw, UK) equipped with a charge- coupled detector (CCD) camera and a Leica microscope. Excitation wavelengths were 514 nm using Argon (AR+) laser with a scanning range of 100-2000 cm–1. The laser was focused to a 2 μm diameter spot on the sample using a 50× objective lens. The spectral resolution was 1 cm–1. The data were collected and analysed with Renishaw Wire™ and Origin software.

Raman spectroscopy is a frequently used and highly effective tool for characterisation carbonaceous materials. Typically, the Raman spectra of a char display two prominent peaks at around 1590 cm^{-1} and 1360 cm^{-1}. The previous is called the G band, related to the stretching vibration mode of E2g symmetry in the aromatic layers of crystalline graphite, whereas the other is called the D band, arising from the disordered or amorphous carbon atoms The ratio of intensity of D peak (ID) to G peak (IG), defend as ID/IG, is inversely proportional to an in-plane microcrystalline size La. The higher the R, the smaller the microcrystalline size is. Thus the char formed in surface more compact and strong. Good char residues provide a protective shield resulting in better flame retardant properties.

3.15 Morphological Studies

To visualize the morphology of nanocomposites, two tools are commonly used: X-ray diffraction (XRD) and Scanning electron microscopy (SEM). They provide additional information on the dispersion of clays within the polymer matrix.

3.15.1 X-ray Powder diffraction (XRD)

Due to its ease of use and availability, DRX is the most commonly used to determine the structure of the nanocomposite. Kinetic studies of the melt intercalation of polymer are even carried out by this technique (Ray and Okamoto, 2003). This technique makes it possible to determine the spaces between the layers of the silicate using the Bragg law equation (3-4).

$$n\lambda = 2\, dSin(\theta) \qquad (3\text{-}3)$$

where λ corresponds to the wavelength of the x-ray radiation used in the diffraction experiment, d is the distance between the diffraction lattice planes and θ is the measured diffraction Bragg angle (Alexandre and Dubois, 2000;Porter et al., 2000). Position control , the shape and the intensity of the reflections peak of the nanoclay layers makes it possible to identify the structure of the nanocomposite (Ray and Okamoto, 2003).

Patterns were obtained either for the powder or for an oriented slide in for the analysis of clay mineral phases ($\varphi < 2$ μm). In the first case, reflection allows access, in the absence of any preferential orientation, to all lines (Hkl). In the second case, the powder is compacted on a flat surface, and platelets of clay minerals are deposited parallel to this surface (perpendicular to the structural axis c). Thus, a diffractogram of the oriented plate will show only the lines [001] corresponding to the structural planes perpendicular to the axis (Figure 3-17(C)).

The degree of clay dispersion and the crystal structure of the samples were characterized at ambient temperature by means of X-ray diffraction (XRD, Bruker D8 ADVANCE X-ray powder diffractometer) using CuKα radiation at a scan rate of 0.3°/min in a range of 2θ from 5° to 30°, and operated at 30 kV and 20 mA .

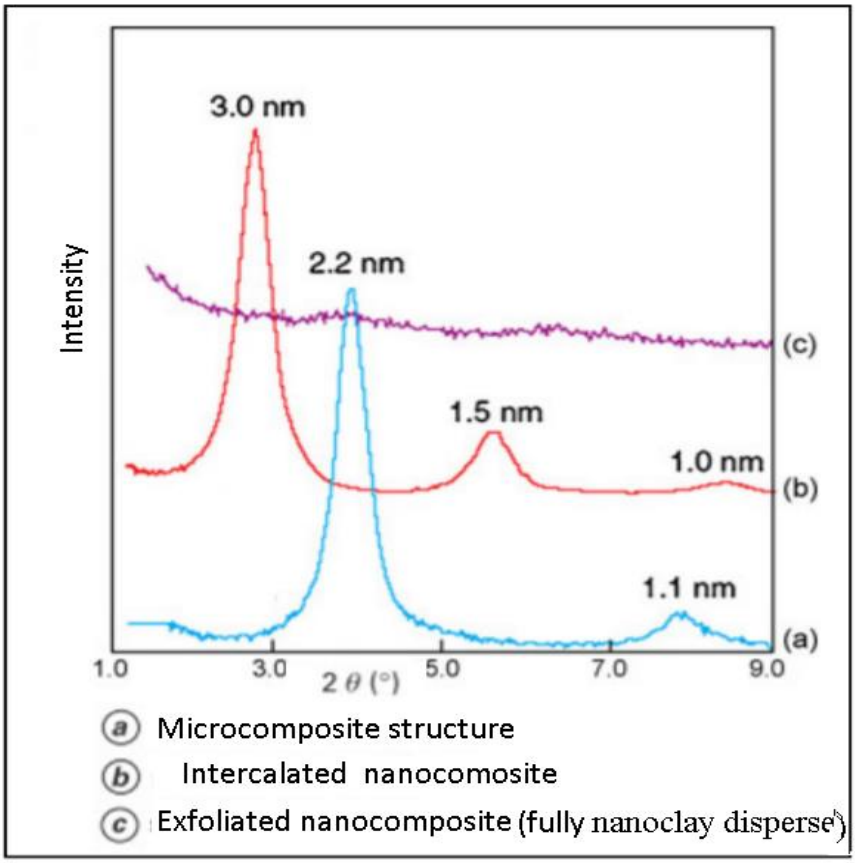

Figure 3-17: XRD morphologies for polymer–clay nanocomposite a)Microcomposites (b) intercalated nanocomposites (C) exfoliated nanocomposite(Alexandre and Dubois, 2000)

For intercalated nanocomposites, the XRD spectrum shows the diffraction peak of the basal plane [001] of stacking of the sheets which can be directly connected to the spacing between sheets d. The swelling of the clay by the polymer matrix then results in a displacement of the diffraction peak attributed to the [001] planes towards the small

angles. The change in the width of the peak at half height is moreover an indicator of the degree of disorder during the intercalation process. For the exfoliated systems, the diffraction peak [001] is no longer visible either because the distance between the sheets is too important, or because the ordered structure is no longer present.

However, this technique provides little information on the spatial distribution of the silicate layers or the structural heterogeneities in the nanocomposites. In addition, certain phyllosilicates do not exhibit well-defined basal reflections. Peak widening and intensity reduction are thus very difficult to study systematically. Therefore, this technique must be combined with transmission electron microscopy (TEM) (Alexandre and Dubois, 2000).

3.15.2 Scanning electron microscopy (SEM)

SEM was used to study the morphology of the prepared composites. The fractured specimen surface after Charpy impact tests was used to study the morphology of the blends. The samples were not polished or etched to avoid losing any surface features after the impact test. Each specimen from an impact test bar was mounted on an aluminium stub using carbon tape, and the fractured surface was coated with gold particles with a sputter coater (Polaron Desk Sputter Coater, Quorum Technologies, UK) for 2 min before observation. Samples were sputtered with gold to improve the quality of the micrographs. The stub with the coated specimen was then placed on the stage within the microscope by venting the machine. The door was closed and a vacuum was pumped. The microstructures of the blends were then observed by SEM (Zeiss Supra 35, Carl Zeiss AG, Oberkochen, Germany) with 15-kV accelerating voltage, as shown in Figure 3-18.

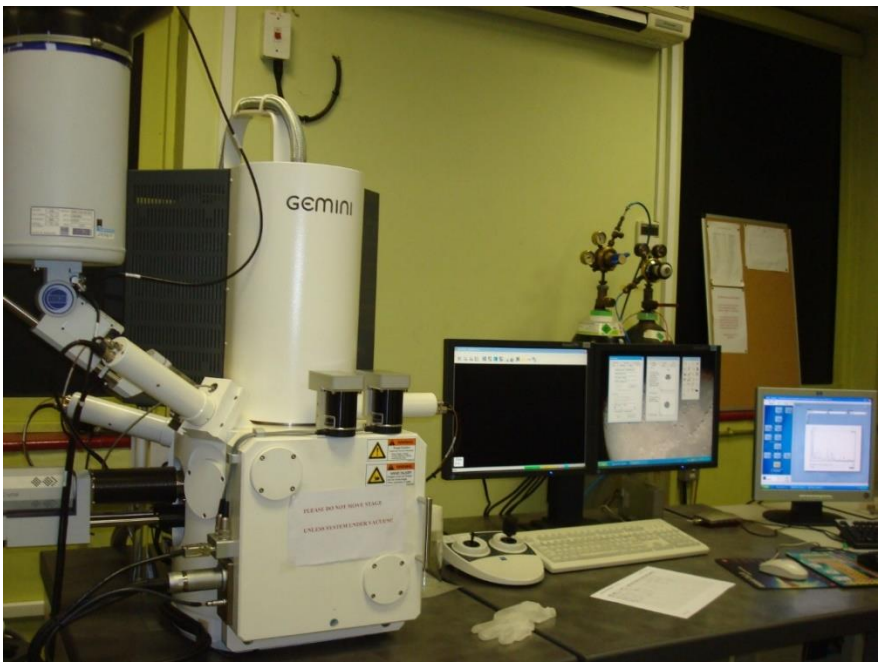

Figure 3-18: Zeiss Supra 35VP

3.16 Accuracy and limitation of equipment

Experimental errors can occur because of inherent limitations of the measuring equipment or measuring technique or possibly the practice and skill of the experimenter.

The accuracy, precision, limit of detection and selectivity of these results has been discussed with obtained results where necessary. Tables 3-14 and 3-15 summarise these factors.

Table 3-14:Instrumental errors and accuracies

Instrument	Error/Accuracy/Limitation
Extrusion	Temperature zones: ± 10°C, Screw speed: ± 40 rpm
Injection moulding	Temperature zones: ± 10°C, Mould temperature: ± 5°C, Injection pressure: ±15 bar, Cooling time: ± 10 sec
TGA	Temperature Range: ambient to 1200 °C. Temperature Accuracy: ± 1°C, Residue at 600°C: ± 0.1%, weight Precision ± 0.01% maximum sample weight 1000 mg
Universal tensile test	Tensile strength: ±3.5 MPa, elongation at break: ±4%, Elasticity Modulus: ±0.3 GPa, Flexural modulus: ± 0.5 GPa
SEM	10% error
XRD	Reproducibility 0.0001° ,Smallest angular step size 0.0001°

Table 3-15: :Flame retardancy equipment errors and accuracies

Instrument	Error/Accuracy/Limitation
Cone calorimeter	Heat flux ± 0.5 kW/m^2,Time measurements ± 1 second HRR Uncertainty: approx. 11%
UL94V	% O2 ± 0.5%, Time measurements ± 1 second Repeatability approx. 5% (based on gas flow and back-pressure accuracy)
LOI	0.1% of oxygen when using Dixons up and down method (see ISO 4589-2)

CHAPTER 4 : EFFECT OF COMPATIBILISERS TYPES ON PROPERTIES

This chapter discusses the preparation of GF-reinforced PP/PA6 blend composite using compatibilisers. Two types of compatibilisers were investigated: PP-g-MA and SEBS-g-MA. Further, two types of nanoclay were used in this study: N5 and SP. Composite samples were prepared by twin screw extrusion followed by an injection moulding machine. The flammability, thermal stability and mechanical properties of the composites were tested by CCT and by condensed phase analysis of the char residue from the cone calorimeter.

4.1 Introduction

In recent years, the use of nanoparticles in polymers for improving fire retardation has attracted much research interest. The performance is influenced by several parameters including chemical composition, microstructure, surface area, shape, particle size distribution, surface modification and dispersion state in the matrix.

(Jiang, 2009;Laoutid *et al.*, 2009) investigated nanoparticles, polymers and organo-modified silicates because of their presence, low price and flame resistance (Kiliaris and Papaspyrides, 2010;Laoutid *et al.*, 2009). Organo-modified montmorillonites (OMMT) have been combined with various FRs, especially phosphorous compounds (Laoutid and Lopez-Cuesta, 2009), to improve the fire performance of various polymers Tang *et al.* (2006) studied the flammability properties of PP/PA6/PP-g-MA/IFR with and without organophilic montmorillonite (OMT) along with the effect of PA6 and nano-PA6 (n-PA6) as a carbonisation agent for improving flame retardancy; the optimal n-PA6 content is 24%. Upon adding OMT to the composite, the HRR peak increases because the high loading of OMMT hinders NH3 from contributing to swelling because it acts as a gas barrier in the nanoclay. The formation of PP-g-PA6 compatibiliser improved the thermal stability and mechanical properties.

OMMTs and phosphorus compounds afford flame retardancy in IFR through several mechanisms (Isitman *et al.*, 2012;Tang *et al.*, 2005). These results could lead to investigations of new combinations of layered silicates with phosphorous compounds. This chapter assesses two types of layered silicates with different morphologies as well as their combinations with phosphorous compounds for enhancing the fire retardancy of PP/PA6 blends in which PP is dominant. PP/PA6 blends are prepared using two types of compatibilisers—SEBS-g-MA and PP-g-MA—for improving the thermal characteristics and mechanical properties. PP is used widely because it is cheap, and PA6 shows good mechanical, thermal and flammability properties along with char formation ability, making these materials suitable for use in this study.

Tang *et al.* (2006) studied the flammability properties of PP/PA6/PP-g-MA/IFR with and without organophilic montmorillonite (OMT) along with the effect of PA6 and nano-PA6 (n-PA6) as a carbonisation agent for improving flame retardancy; the optimal n-PA6 content is 24%. Upon adding OMT to the composite, the HRR peak increases because the high loading of OMMT hinders NH_3 from contributing to swelling because it acts as a gas barrier in the nanoclay. The formation of PP-g-PA6 compatibiliser improved the thermal stability and mechanical properties.

Vahabi *et al.* (2013) added SP and APP to PP/PA blends (PP:PA = 80:20). SEBS-g-MA enhanced the dispersion of SP. Synergistic effects contributed to the HRR for compositions containing 3 wt.% of SP.

4.2 Experimental Study

4.2.1 Materials and Sample Preparation

PP (Icorene® 4014, ICO Polymer, UK) and PA6 (Zytel® 7335F) were used as polymer blend components. SEBS-g-MA (Kraton® FG 1901; denoted as SGM) and PP-g-MA (Polybond® 3200, Addivant, USA) were used as blend compatibilisers. SP (Pangel® S9, Tolsa, Spain) and N5 were provided by Southern Clay Products. APP (Exolit® AP 423, Clarinet, UK) powder and short GFs (P355, Vetrotex, France) were

used as phosphorous FRs. The materials used are shown in Table 4-1. Flame retardants supplied by agent of clarinet in UK used as powders: an ammonium Polyphosphate (AP 423 named as APP) and short glass fibre (P355, Vetroxt,France). the material used are summarized in Table 4-1.

Table 4-1:Materials used in this study and their source

Materials	Commercial name	Source
Polypropylene (PP)	Incore®4014	ICO Polymer,Uk
Polyamide 6 (PA6)	Zytel® 733F	DuPut ,USA
Nanfil 5(N)	Nanofil®5	Sud Chemic,Germany
PP-g-MA(mpp)	Polybond3200	Addivant,USA
SEBS-g-MA (S)	FG®1901	Kraton FG, USA
Chopped short glass fibre	P355	Vetroxt,France
Ammonium polyphosphates (FR)	Exolite®APP 423	Klariant, Germany
Sepiolite (SP)	Pangal®S9	Tolsa ,Spain

4.2.2 Preparation of composites

GF-reinforced PP/PA6 blend composites were prepared by melt compounding using twin screw extrusion. Table 4.2 shows the formulations of different compositions. The PP/PA6 blend was melted and homogeneously mixed with an appropriate amount of SP and OMMT (Nanofil® 5). The processing temperature, rotor speed and blending time were set to 220°C, 100 rpm and 10 min, respectively, for melt compounding.

The total loading of both the nanoclay and IFR is always 20 wt% relative to the polymer and that of GF is 20%. The PP:PA6 ratio is 92:8 and the total amount of nanoclay and FR is fixed to 20%.

FR0(S) does not contain any flame retardant and nanoclay. FR20(S) contains 20% of FR without nanoclay. FR15N5(S) contains 5% of Nanofil (N5) with 15% of Exolit® AP 423. FR15SP5(S) contains 5% of SP with 15% of Exolit® AP 423. mpp denotes PP-g-MA compatibiliser.

Table 4-2 : Formulation of different compositions in wt. %

Sample code	PP:PA6 (92:8)	Compatibilisers		SP	N	FR	GF
		S	mpp				
FR0(S)	75	5				0	20
FR20(S)	55	5				20	20
FR15N5(S)	55	5			5	15	20
FR15SP5(S)	55	5		5		15	20
FR20 (mpp)	75		5			20	20
FR15N5 (mpp)	55		5		5	15	20
FR15SP5 (mpp)	55		5	5		15	20

4.2.3 Flame retardancy testing

Standard UL-94 flammability tests (Underwriters Laboratories, 2013) were conducted to classify the samples based on their flammability in vertical test setups. The sample had dimensions of 120 × 14 × 3.2 mm3. The UL-94 ratings used are V-2, V-1, V-0 and no rating, where V-0 is the best rating.

CCTs (FTT, UK) were conducted according to BS EN ISO 13927:2015 (British Standard Institution, 2015). Specimens (100 × 100 × 4 mm) were exposed to a constant heat flux of 50 kW/m2 and ignited. Heat release values and mass reduction were continuously recorded during burning.

4.2.4 Thermogravimetric analysis (TGA)

TGA was conducted in nitrogen at heating rate of 10°C/min (TGA Q500 series, TA Universal Analysis, TA Instruments Inc., USA). A small amount of each sample (~5–10 mg) was examined under a nitrogen flow rate of 10 ml/min from 23°C to 700°C. The thermal degradation of PP/PA6 nanocomposites was investigated.

4.2.5 Mechanical properties testing

Tensile tests were conducted using a Zwick universal testing machine (SMART PRO, Zwick Roell, UK), shown in Figure 3-6, according to BS EN ISO 527 with crosshead speed of 5 mm/min and gauge length of 50 mm. Five replicates were tested.

Charpy impact tests were performed using a pendulum CEAST Charpy machine according to ISO 179/1e with 4-J capacity to measure the impact strength.

The flexural properties of the nanocomposites were determined using the same tensile machine through three-point bending tests according to ISO 178 with thickness to span length ratio of 1:16 and crosshead displacement rate of 2 mm/min.

4.2.6 X-ray diffraction

XRD (Bruker D8 ADVANCE X-ray powder diffractometer) was performed using CuKα radiation at scan rate of 0.3□/min in a range of 5□–30□ and operated at 30 kV and 20 mA. It was used to assess the dispersion and to identify the type of nanocomposite formed—exfoliated, intercalated or conventional—and to determine its degree of crystallinity.

4.3 Results and Discussion

4.4 Influence of Compatibilisers and Nanoclay Types on Flame Retardancy

4.4.1 Cone calorimeter test (CCT)

A Cone calorimeter is considered to be the most powerful method for assessing the real life flammability The heat released rate and time to ignition is regarded as the most important factor . The flammability of nanocomposite gets improved by adding fillers such as nanoclay and flame retartant non helogned flame retardant . A cone calorimeter can be used to determine various combustion parameters including time to ignition (TTI), heat release rate (HRR), peak of heat release rate (PHRR), total heat release (THR), mass residue, mass loss rate (MLR), peak of mass loss rate (PMLR), total smoke production rate (SPR), peak smoke production rate (PSPR) and carbon monoxide production (COP). Table 4-3 shows the results obtained using a cone calorimeter under 50 kW/m^2 for different samples.

Table 4-3 presents a condensed review on the results of flammability by cone calorimeter test and showed that the peak heat realised rate drop by more than 85 % showing the synergetic effect of intumescent flame retardant and nanoclay. The highest value for nanocomposite contain only intumescent flame retardant and glass fibre FR20(S) followed by Nanofil (N5) in FR15N5(S) All composites show low time to ignition compared to pristine PP as APP423 decompose faster for forming char and viscous molten layer char to prevent dripping, Sepiolite flame retardant in FR15SP5(s)

has the higher ignition time contain 20% IFR and in case of FR15N5 and FR15SP5 only 15% APP and total weight of both nanoclay and flame retardant is fixed to 20%. The residue of nanocomposite without sepiolite is 34.4% flowed by glass fibre composite FR15SP5(33%) and FR15N5(33%). The ignition time decreases because of catalytic effect of ammonium polyphosphate in order to form char this in line with (Lim et al., 2016) and also can see that in TGA test. without SP is 34.4%, flowed by the GF composites FR15SP5 (33%) and FR15N5 (33%). The ignition time decreases because of the catalytic effect of APP to form char; this in line with (Lim *et al.*, 2016) and is supported by the TGA test.

Figure 4-1 shows the PHRR with different compatibilisers. It is the lowest when using SEBS-g-MA as a compatibiliser owing to its compatibility with GF (Lin et al., 2015) and the highest when no nanoclay is incorporated. PHRR of FR20(s) is 86% lower than that of PP. Nanofiller content of ≥5% tends to agglomerate, thereby preventing uniform dispersion. Figure 4-1 shows the HRR graph for two classes of composites.

PP shows a very sharp HRR curve (Table 4-1) with peak heat release of 1855 kW/m^2. For the PP/PA6/APP/GF composites FR20(S), FR15N5(S) and FR15SP5(S), PHRR decreased by 88.3%, 86% and 85%, respectively. For FR20(mpp), FR15N5(mpp) and FR5(mpp) with PP-g-MA as a compatibiliser, PHRR decreased by 86%, 84% and 84%, respectively.

Table 4-3 shows that the PHRR decreased by more than 85%, indicating the synergetic effect of the IFR and nanoclay. The nanocomposite containing only IFR and GF, FR20(S), showed the highest value followed by Nanofil (N5) in FR15N5(S). All composites show low TTI compared to pristine PP because AP 423 decomposes faster to form char and a viscous molten layer that prevents dripping. SP FR in FR15SP5(s) containing 20% of IFR has a higher ignition time. FR15N5 and FR15SP5 contain only 15% of APP and 20 wt% each of nanoclay and FR. The residue of the nanocomposite

without SP is 34.4%, flowed by the GF composites FR15SP5 (33%) and FR15N5 (33%). The ignition time decreases because of the catalytic effect of APP to form char; this in line with (Lim *et al.*, 2016) and is supported by the TGA test.

Table 4-3: summarises the results of flammability by cone calorimeter test with different compatibilisers and nanoclays

Sample	TTI (s)	PHRR (kW/m^2)	THE (kJ/m^2)	Mass residua (%)	PMLR	PSPR	PCOP
					(g/s)	(m^2/s)	(g/s)
FR20(S)	16	217	119	34	0.084	0.0408	0.0027
FR15N5(S)	14	264	124	31	0.126	0.0476	0.0028
FR15SP5(S)	17	270	120	33	0.096	0.0468	0.0027
PP(control)	35	1855	165	0	0.380	0.1406	0.0223
FR20(mpp)	18	257	116	30	0.073	0.0546	0.0031
FR15N5(mpp)	16	301	121	32	0.084	0.0573	0.0028
FR15SP15(mpp)	17	295	121	33	0.368	0.0518	0.0028

The combustion in cone calorimeter used to study flammability of PP and its composites to study the influence of nanoclays, compatibiliser on fire resistance and fire spared this called heat released rate and consider the most important parameter.

Figure 4-1 shows the PHRR with different compatibiliser and the Peak is the lowest when we use SEBS-g-MA as a compatibilisers it reduces due to the Compatibility between SEBS-g-MA and glass fibre as founded by (Lin et al., 2015) and it's the highest when no nanoclay is incorporated FR20(s) is dropped by 86% compared to

polypropylene .When Nano filler higher than or equal 5% it tend to nano- fillers when added in higher amount tend to agglomerate and uniform dispersion not achieved Also Figure 4-1shows the HRR graph two classes of composites. A very sharp HRR curve (in Table 4-1 shows for PP with a peak heat release of 1855kW/m^2. For PP/PA6/APP/GF composites, the PHRR declined by 88.3%, 86%, and 85% at FR20(S), FR15N5(S) and FR15SP5(S), respectively. Whereas when change compatibiliser to PP-g-MA it decreases by 86%,84% and 84% for FR20(mpp), FR15N5(mpp) and FR5(mpp) respectively.

All the composite show second peak this due to that the break of previous char productive and new one formed due to intumescent char and also because of glass fibre in presence of sepiolite clays.

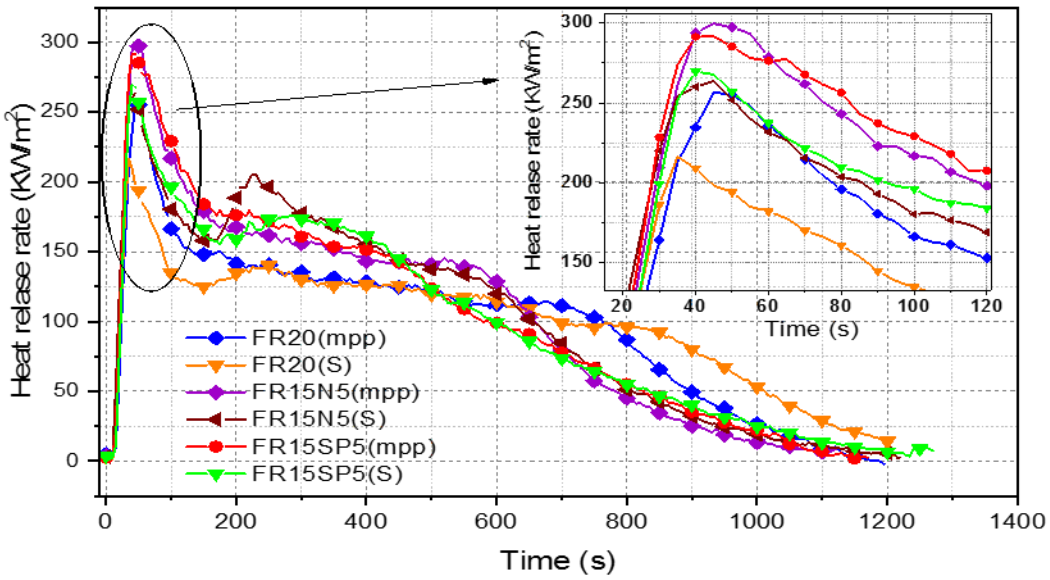

Figure 4-1: Influence of compatibilisers and nanoclays types on the heat release rate

Figure 4-2 shows the PHRR of the composites as a function of the nanoclay type and compatibiliser type. The graph clearly shows that no synergistic effect existed between the IFR and the nanoclay because agglomeration occurred, especially for

nanoclay content ≥5%. Further, there was no relation between both dripping and ignitibility and the HRR.

.

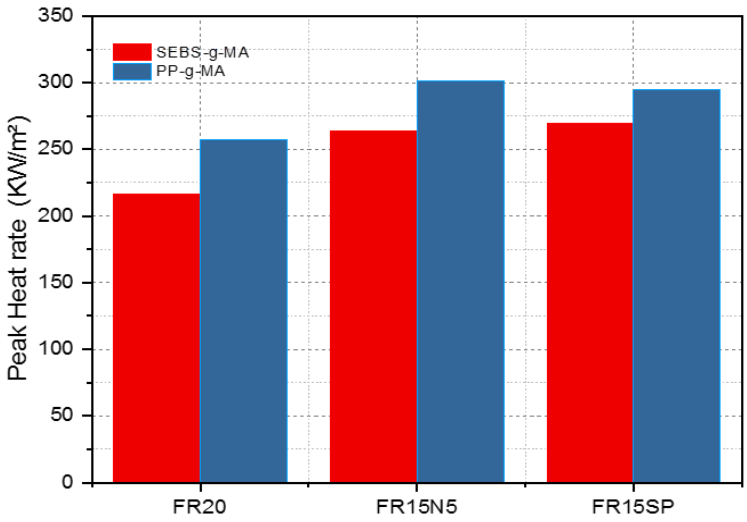

Figure 4-2: Effect of compatibilisers and nanoclays types on the PHRR

FR15N5 (mpp) shows the worst flammability when its PHRR reaches 300 kW/m^2; it is followed by FR5 (mpp). This may due to the breaking of the char layer because of higher heat and new char formation (Lim *et al.* (2016); Nie *et al.* (2008), as shown in Figure 4-1.

Figure 4-3 shows the mass residue of composites after the CCT as a function of time for different nanoclays (N5, SP) and compatibilisers. At the end of burning, composites compatibilised with SEBS-g-MA—pure PP, FR20(S), FR15N5(S) and FR15SP5(S)—showed 0%, 34%, 31% and 33% of char residue left, respectively. FR20(S) and FR15SP5(s) showed significantly higher mass residue, indicating that the formed char is stronger and more compact and thereby prevents both mass and heat

transfer. Further, SP addition results in the highest char residue and reduces the flame retardancy of IFR. Using PP-g-MA as a compatibiliser results in a slight difference in the presence of N5 and SP. The composite with only IFR showed 4% lower weight compared with FR20(S), possibly because the reaction of FR with PA6 formed PP-g-PA6

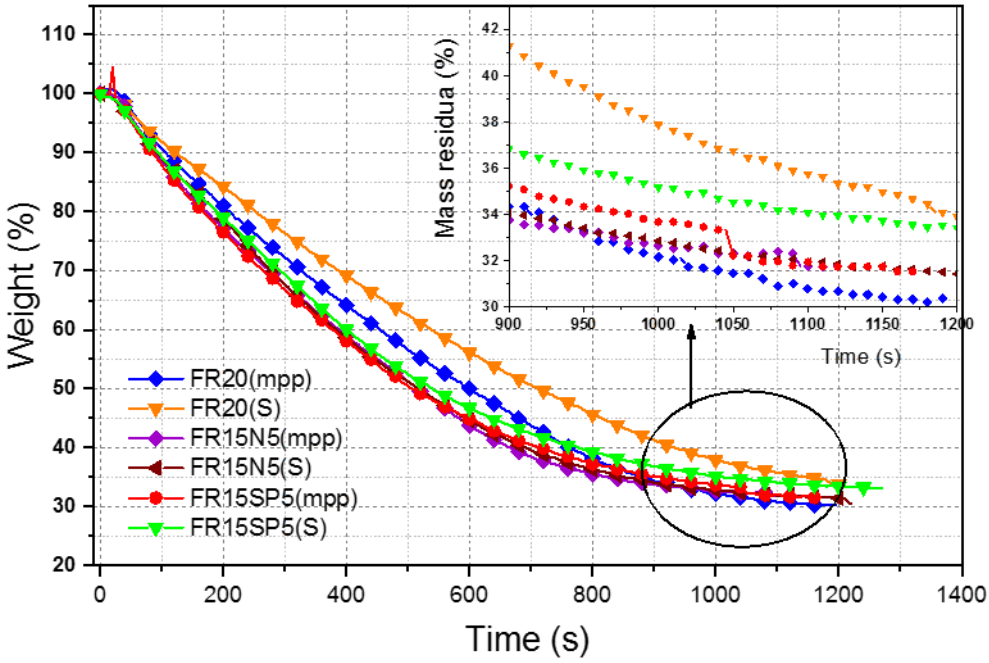

Figure 4-3 : Mass loss behaviour during combustion in the cone calorimeter test

The other important parameter related to flammability is the heat evolved after cone calorimeter testing The slope of THR representative of fire spread The PP-g-MA compatibilisers show slight reduction .Figure 4-4 shows the total heat released (THR) at the end of the CCT. The THR of all samples decreases. FRs with two different nanoclays and compatibilisers were incorporated in the composite. FR20 (mpp) sample shows the lowest THR, suggesting that the FR improves the flame retardancy of the composites. FR15SP5(S) shows intumescent properties when compatibilised with PP-g-MA because of char formation in the composite that prevents oxygen inflow into the composite and retards heat flow from the burned gas.

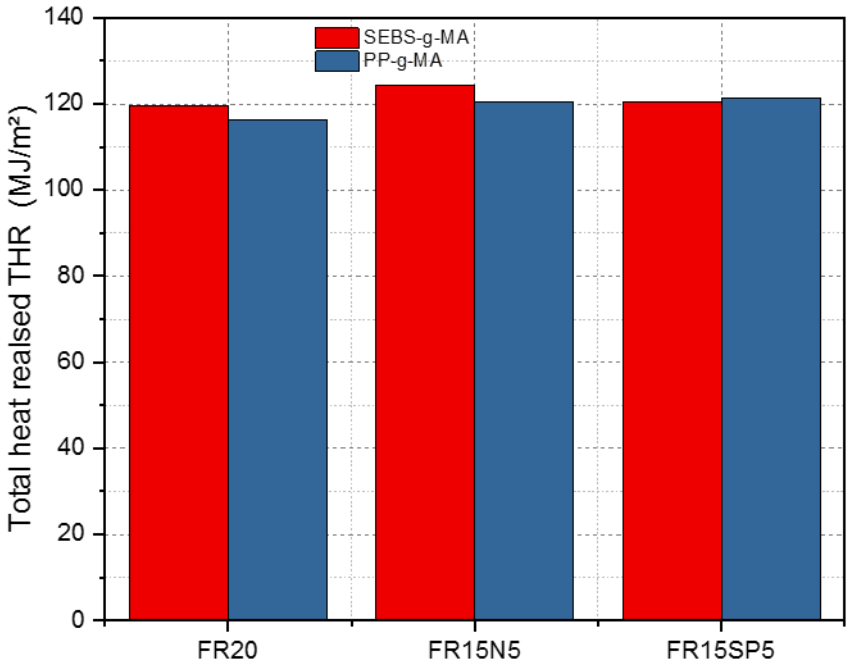

Figure 4-4:The total heat released at the end of cone calorimeter test

Figure 4-5 shows the mass loss rate (MLR) of PP composites with the two types of compatibilisers, namely, SEBS-g-MA and PP-g-MA. The PMLR of pristine PP is 0.38 g/s. By contrast, that of FR20(s), FR15N5(S) and FR15SP5(S) composites decreased by 78%, 67% and 74%, respectively, when compatibilised by SEBS-g-MA and decreased by 81%, 59% and 63%, respectively, when compatibilised by PP-g-MA.

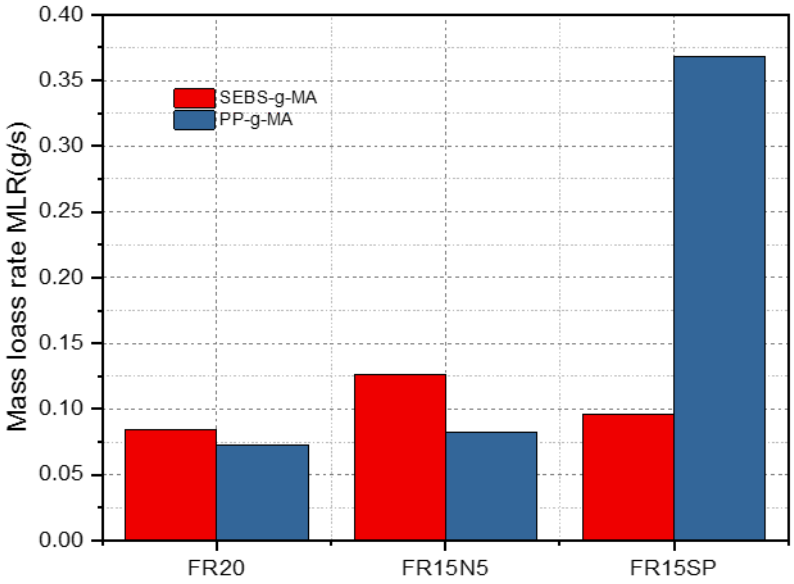

Figure 4-5 :The mass loss rate (MLR)for different composites and with SEBS-g-MA and PP-g-M A as compatibilisers

FR incorporation could greatly reduce the average MLR and result in increased residue. These results indicate that the intumescent system based on APP, SP and N5 can effectively improve the flame retardancy of PP as evidenced by the significantly reduced PHRR, THR and PMLR during combustion.

Figure 4-6 shows the SPR curves of PP composites. The SPR of pristine PP is 0.01406 m2/s and decreased by 71%, 66% and 67% with the incorporation of 20% of AP 423, FR20(S) and 5% of N5 + 15% of APP (FR15N5(S)), respectively. When using PP-g-Ma as a compatibiliser, SPR of FR20 (mpp), FR15N5 (mpp) and FR15SP5 (mpp) decreased by 61%, 59% and 63%, respectively. The SPR decrease of the composite compared with that of pristine PP may be due to accelerated char production because of the presence of AP 423, which can reduce the escape of volatiles.

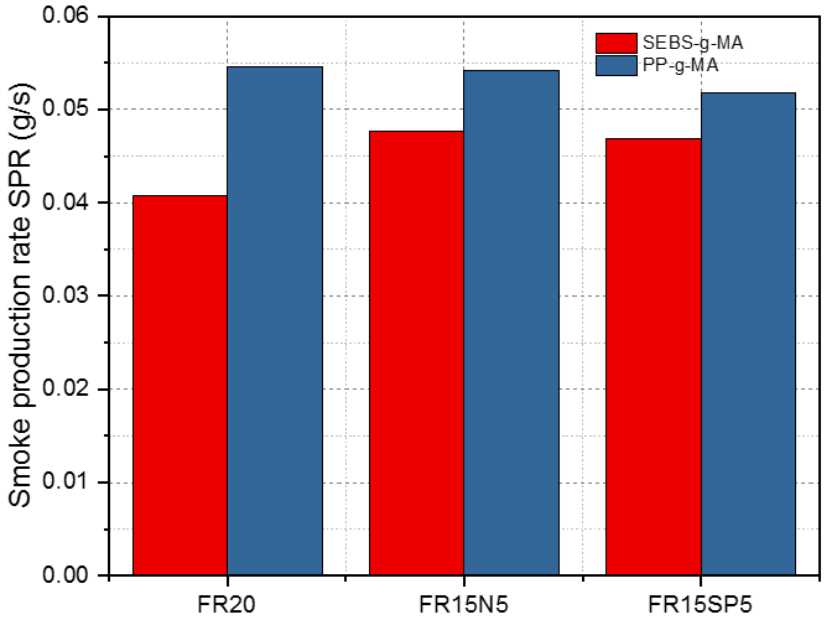

Figure 4-6: Smoke product rate (SPR) as function of two group of composites and with SEBS-g-MA and PP-g-M A as compatibilisers and with N5 and SP nanoclays

High SPR and COP can cause deaths in the early stage of a fire. Therefore, it is important to control these factors for increasing survival rates in a fire. Figure 4.7 shows that composites with MMT (N5) and SP nanoparticles produced the least amount of smoke. The amount produced for pristine PP is 0.0223 g/s. By contrast, the amount produced for FR20(s), FR15N5(S) and FR15SP5(S) compatibilised by PP-g-MA decreased by 88%, 87% and 88%, respectively. For the same composites compatibilised by SEBS-g-MA, all amounts decreased by 87%. In general, initially, the IFR greatly increases the carbon monoxide (CO) produced; the amount produced decreased with an increase in burning time (Figure 4-7). A well-controlled combination of IFR and nanoparticles in the system is another key factor for achieving better performance and realizing a safe environment.

.

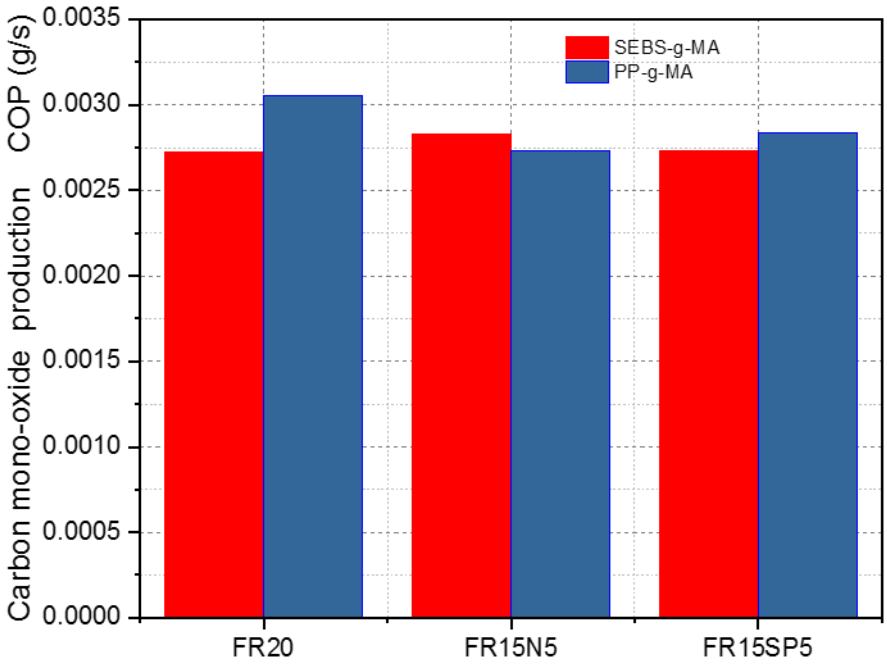

Figure 4-7: COP of the composite with two different compatibiliser and nanoclays

The amount of smoke release (SPR) and COP are cause death at early stage of fire during combustion processes are the two other important factors in fire atmosphere in order to increase the life survivability. Figure 4.7 shows that with the presence of MMT (N5) and sepiolite (SP) nanoparticles, the composites produce the least amount of smoke. In case PP it is 0.0223 g/s then it decreases by 88%,87% and 88% for FR20(s).FR15N5(S) and FR15SP5(S) respectively. When SEBS-g-MA all decrease by 87%. In general, the IFR systems increase the initial carbon monoxide(CO) considerably, even though it slows down with an increase in burning time (Figure 4(d)). The controlled combination of IFR and nanoparticles in the system is another key factor for achieving better performance under safe environment.

FPI, the ratio of TTI/PHRR, is independent of the tested sample thickness and is often used to predict whether a material can easily combust after ignition. The greater the FPI value, the better is the fire resistance. From graph 4-8, FR20(S) has the highest FPI this because the of loading is 20%; it is followed by FR15N5(s) which contains 5% of N5 and IFR of 15%. The loss rate decreases because of the formation of a physical barrier and because the IFR released H_2O and CO_2 which reduced the temperature below that for degradation.

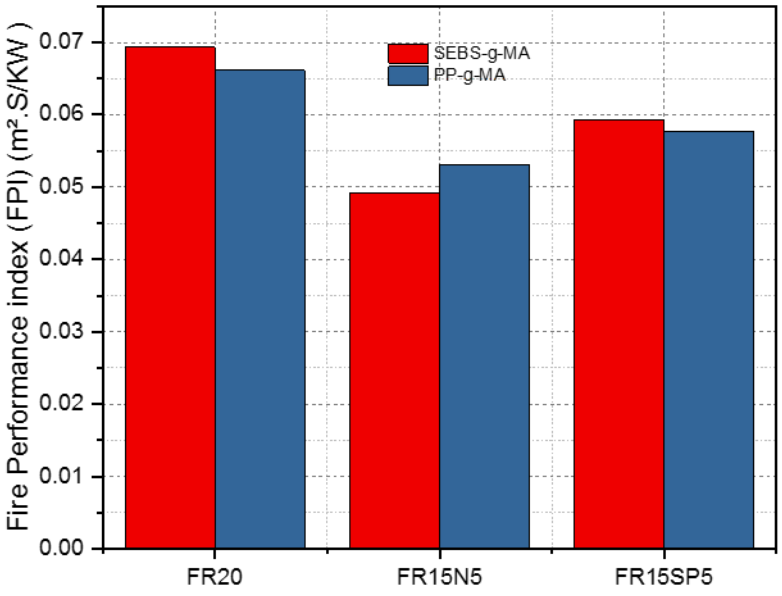

Figure 4-8:Fire performance index (FPI) for different composite

Figure 4-9 shows COP as function of time. The second peak breaks up because of char because the high heat and presence of GF and nanoclay break the continuity of char residue with the matrix.

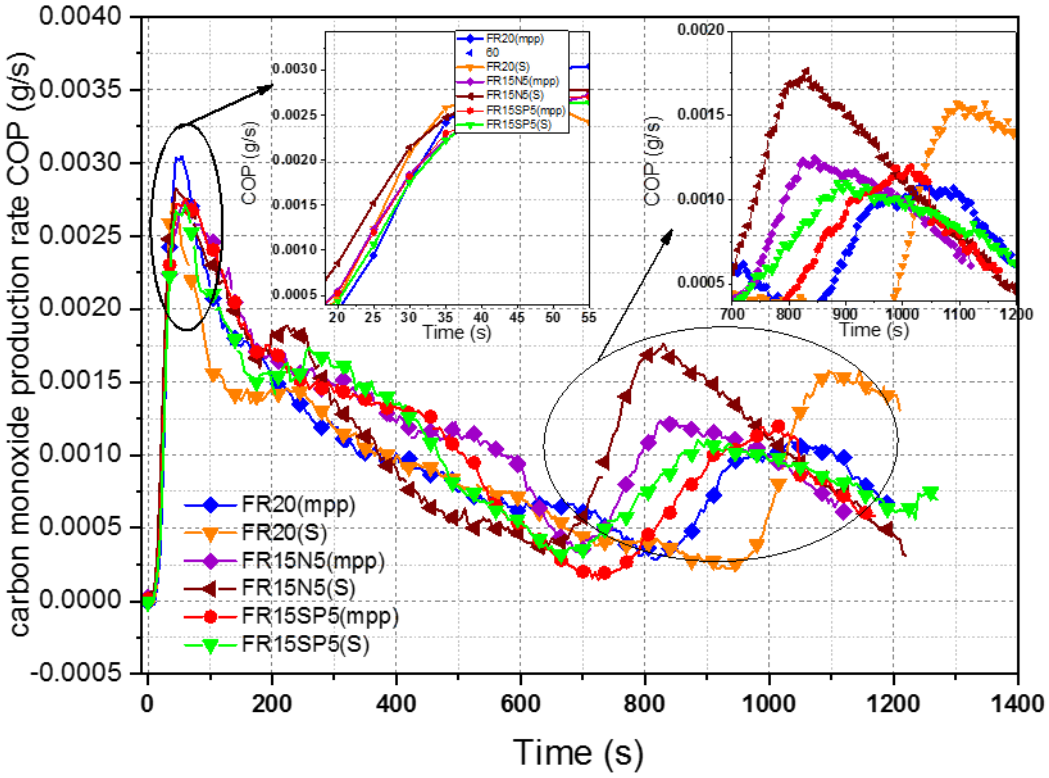

Figure 4-9: Effect of compatibilisers and nanoclays type on carbon monoxide production rate

4.4.2 LOI and UL-94 testing of PP/PA6 composites

The fire behaviour of the composites (PP/PA6/APP/GF (S) and PP/PA6/APP/GF (mpp) with two types of nanoclays, (SP) and (N5), was first evaluated by measuring the LOI and performing the UL-94 test. Table 4-4 shows the LOIs of the studied materials. Pristine PP had very low LOI of 16%, which was moderately enhanced These slight improvements were achieved via dripping, and material burning continues because no char is formed to stop combustion.

Char was developed in later stages of combustion during LOI tests of the PP/PA6 blend containing the AP 423 IFR. The char hindered heat transfer from the flame; this confirmed the increased oxygen demand to withstand flame combustion with the FR content, that is, 16%–22% of pristine PP (sample containing 20% of APP and 20% of GF)

for FR20(S). With the incorporation of even a small loading (5 wt%) of IFRs with the nanoclay, LOI increased by 18.5% for N5 and 19% for SP.

The LOI of FR PPs was enhanced more by nanoclays, from 21.5% for 5%SP/15%APP to 22% for 5%N5/15%APP, owing to the formation of thicker and stronger chars via clay nanolayer reinforcement without losing the char structure. Platelet N5 has a greater influence on LOI compared to SP. Consolidated, crack-free and thick protective barriers were formed at much earlier stages of combustion, and thus, N5 provides enhanced flame retardancy compared to SP in terms of LOI.

The UL-94V classification shows that incorporating GF and IFR prevented the material from dripping; 20%APP was classified as V2. PP-g-MA compatibiliser slightly reduced the LOI from 22% to 21% but did not change the classification (it remained V2) because it did not affect ignition or dripping.

Table 4-4 : Ul94V Classification and LOI for different compatibilisers and nanoclays

Sample	LOI	UL-94 rating
Pure PP	16	No rating
FR0(s)	19	No rating
FR20(s)	22.5	V2
FR15N5(s)	22	V2
FR15SP5(s)	21.5	V2
FR20(mpp)	21.5	V2
FR15N5(mpp)	21	V2
FR15SP5(mpp)	21	V2

4.4.3 Flame retardancy mechanism by residue analysis

Figure 4-10 (top view) and Figure 4-11 (front view) show photographs of samples with different nanoclays and compatibilisers subjected to heat flux of 50 kW/m2 for variable durations. The appearance of the residue changed with exposure time The structure evolution was visually the same for the other polymers irrespective of whether they were loaded with GF/APP alone or APP, N5 and SP with two different compatibilisers.

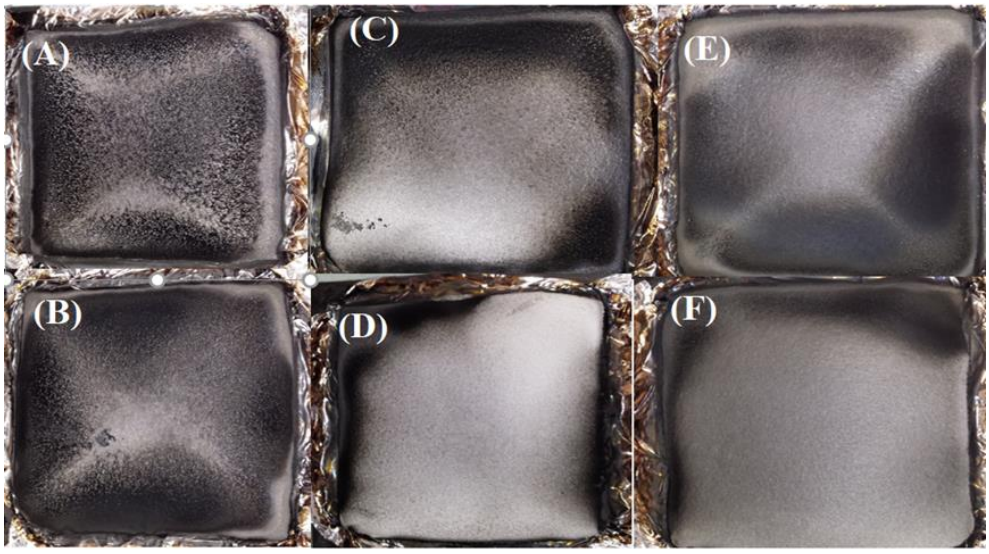

Figure 4-10 : Photographs of the residues after a calorimeter test (a) FR20(mpp) (b)FR20(S) (C) FR15N5(mpp) (D)FR15N5(s) (E) FR15SP5(mpp) and (F) FR15SP5(s)

A black carbon layer is observed on the surface after ignition, and smaller bubbles are observed in the material. A sample with 20% of IFR without any nanoclay shows the lowest PHRR of 217 kW/m^2 compared with 1855 kW/m^2 for pristine PP.

Figure 4-11 shows a front-view photographs of the char residue after CCT. Both FR20(s) FR15N5(s) show intumescent char and a compact surface that acts as a physical barrier, thereby supressing flammability and smoke by slowing down heat and mass transfer to the underlying polymer; this is in line with the results of Kaynak et al. (2017).

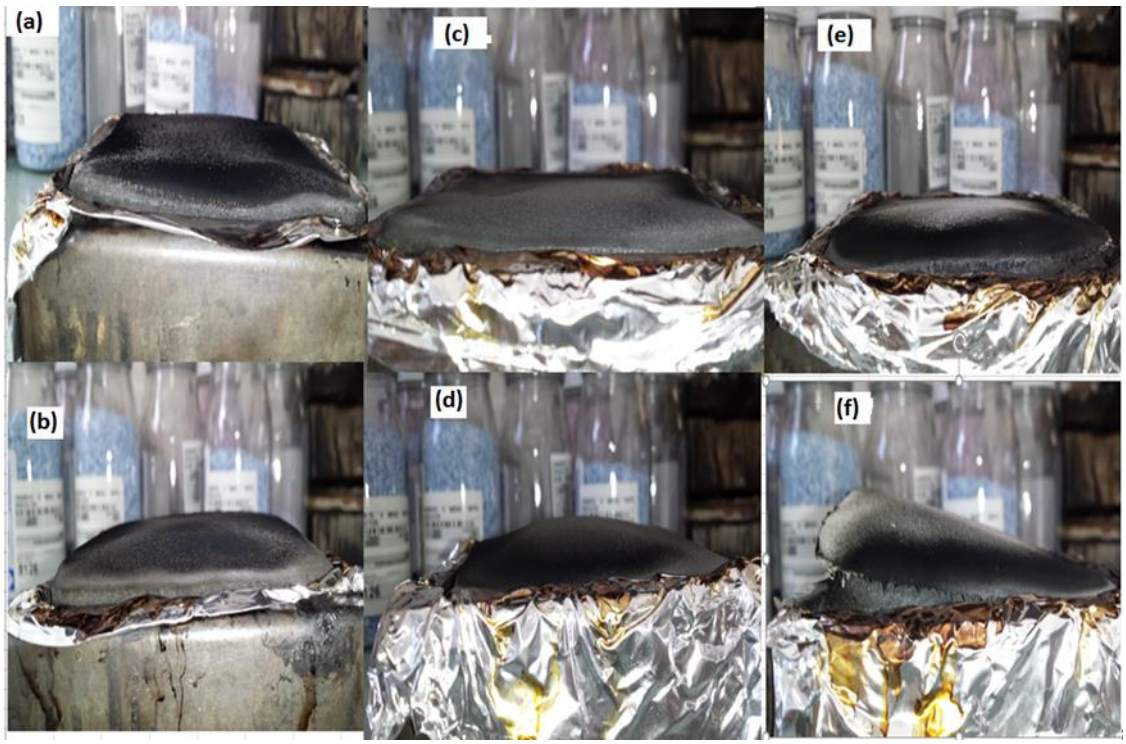

Figure 4-11 : Photographs (a) FR20(mpp) ,(b)FR20(S), (c) FR15SP5(mpp) ,(d)FR15SP(s), (e) FR15N5(mpp) and (f) FR15N5(s)

4.5 Influence of Compatibilisers and Nanoclay types on Thermal Stability and the Decomposition

This section evaluates the influence of the IFR, nanoclay and compatibiliser on the thermal stability of PP and its composites, PP/PA6/GF.

Table 4-4 shows quantitative values of the temperature to 5 wt% (T5%), 10 wt% and 50 wt% weight loss; maximum decomposition temperature (T_{max}) and residue char after the test under air and nitrogen.

The onset temperature for PP and the composite for 5% weight loss under nitrogen decreases from 359°C for PP by 3°C, 25°C and 40°C for FR20(S), FR15N5(S) and FR15SP5(S) composites, respectively, implying that the incorporation of both the IFR (AP 423) and nanoclays sped up degradation and therefore produced char. For SP, the drop in temperature and residual char is 36%. This char acts as a physical barrier to prevent the escape of flammable gas and the entry of oxygen into the polymer surface. Adding only GF to the blend increases the temperature by 30°C, implying that GF enhances the thermal stability. However, the char residue is only 18%, implying that the coefficient of heat transfer of the GF is higher than that of the polymer, and therefore, it burns faster and reduces the cohesion of the char residue (Liu *et al.*, 2011a).

When using PP-g-MA, the onset temperature for PP and composite for 5% weight loss under nitrogen decreases from 359°C for PP by 9°C, 43°C and 34°C for FR20(mpp), FR15N5(mpp) and FR15SP5(mpp) composites, respectively, implying that the incorporation of both IFR (AP 423) and nanoclay sped up degradation and produced char. For N5, the drop in temperature and residual char is 34%. Therefore, the presence of PP-g-MA promotes char more than does that of SEBS-g-MA in the early stage.

Table 4-5 summary of decomposition temperature of PP/PA6 and its composites

Sample code	Temperature at weight loss Air (° C)					Temperature at weight loss in Nitrogen (° C)				
	$T_{5\%}$	$T_{10\%}$	$T_{50\%}$	T_{max}	R%	$T_{5\%}$	$T_{10\%}$	$T_{50\%}$	T_{max}	R %
FR0(S)	308	329	373	380	21	410	425	462	460	21
FR20(S)	297	319	396	357	32	360	388	468	469	33
FR15N5(S)	308	332	443	446	34	337	379	466	462	34
FR15SP5(S)	297	323	402	400	34	342	390	472	471	36
FR20(mpp)						350	382	454	453	33
FR15N5(mpp)						316	368	455	456	34
FR15SP5(mpp)						325	361	446	446	34
PP	286	297	337	341	0	361	376	423	435	0.6

4.5.1 Thermogravimetric analysis (TGA)

The thermal stability of the nanocomposites was studied by TGA. Heating under inert N2 gas flow causes non-oxidative degradation occurs whereas heating under air or oxygen flow causes oxidative degradation of the samples (Hwang et al., 2008).

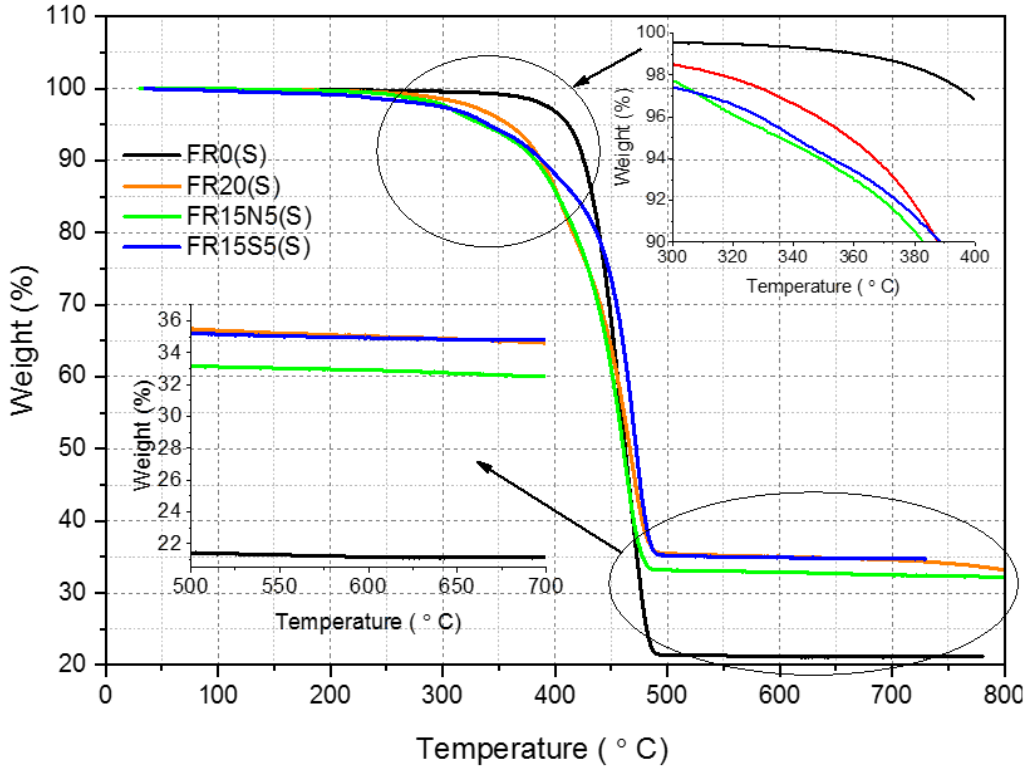

Figure 4-12: Inert thermal stability for different glass loading different clay loading

Under air (oxidative decomposition), the onset temperature for 5% weight loss for PP and composite under nitrogen increases from 261°C for PP by 1°C, 24°C and 19°C for FR20(S), FR15N5(S) and FR15SP5(S) composites, respectively, implying that the incorporation of both IFR (AP 423) and nanoclays accelerated degradation and produced char. For SP and N5, the residual char is 32 wt%, implying that the nanoclay strengthens

the char and prevents cracks from which volatiles can escape. As discussed in the previous section, char acts as a physical barrier to prevent the escape of flammable gas and entry of oxygen into the polymer surface. By contrast, adding only GF to the blend produces a 44°C temperature increase, implying that GF enhances thermal stability; the char residue is 21 wt%.

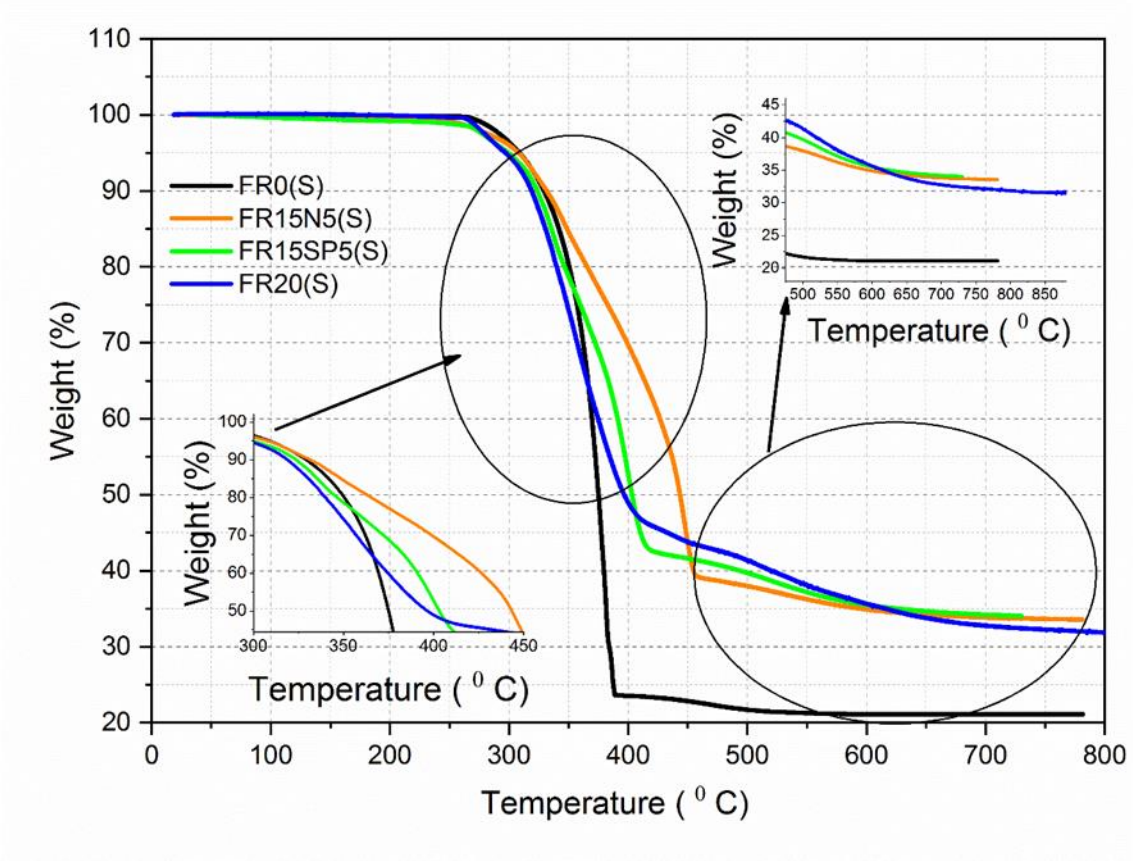

Figure 4-13: Oxidative thermal stability for different glass loading different clay loading

The decomposition temperature increase by incorporation both APP 423 and nanoclay fillers. In air the temperature increase from 341 °C by 105 °C in case of N5and in nitrogen the decomposition increase by 22 °C from 435 °C for PP. This prove the N5 is best thermal stability when we use glass fibre and the decomposition not influenced by compatibilisers.

Figure 4-14 shows the thermal stability of the composites under nitrogen the compatibiliser PP-g-MA show lower thermal stability at temperature between 350 ^{o}C to 450 ^{o}C whereas the composites with SEBS-g-MA are more stable and FR15SP5(S) has the highest temperature stability. The lower is FR15SP5(mpp) at same range above 500 °C the highest stability is found for FR20(S) with char residue 35 wt.% and the lowest is when FR15N5(S) with char residue about 33%. These results prove that SEBS-g-MA more stable in N_2 and more compatible with GFs.

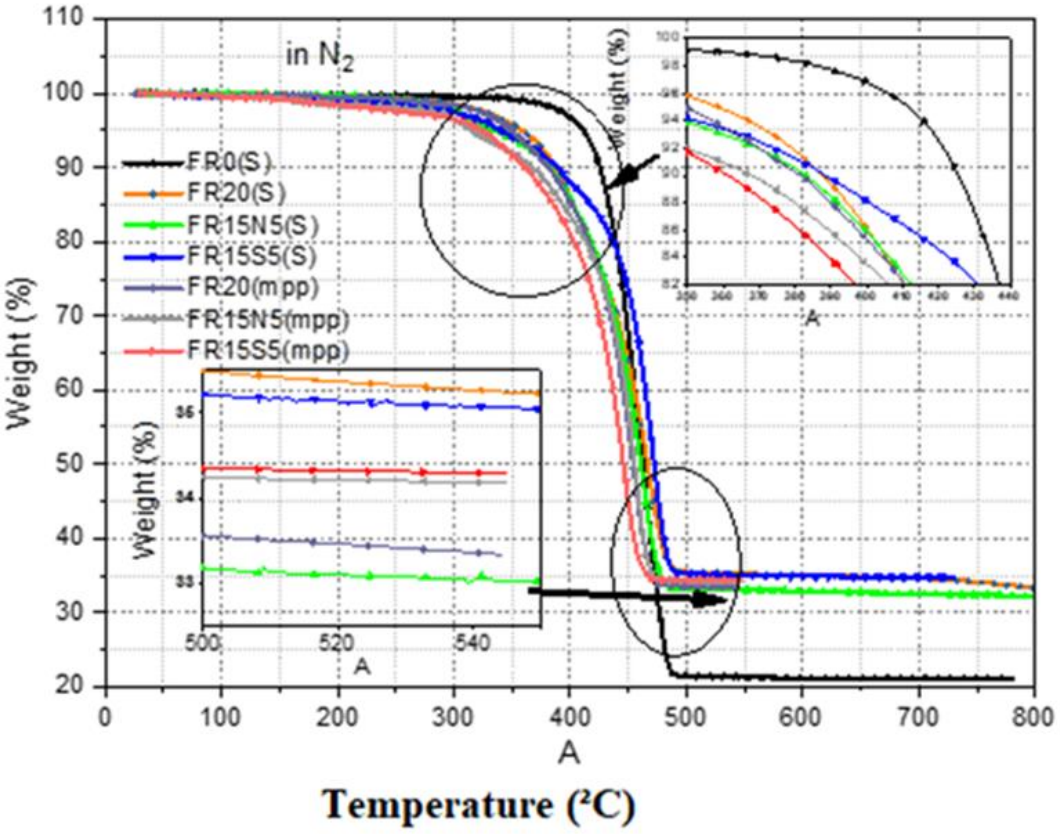

Figure 4-14: Inert thermal stability for different clay loading two different compatibilisers

4.5.2 Derivative weight change (DTG)

Figures 4-15 and 4-16 show the derivative weight change (DTG) versus temperature in nitrogen to show the decomposition temperature and weight loss per degree of temperature change.

Figure 4-15 shows nonoxidative thermal behaviours of FR0(S) without IFR and nanoclay; one-step decomposition occurs at 462°C with loss rate of 1.46 wt.%/°C. By comparison, PP at 440°C lost 1.94 wt.%/°C. The graph shows that the maximum temperature when using SEBS-g-MA is higher and lower decomposition values.

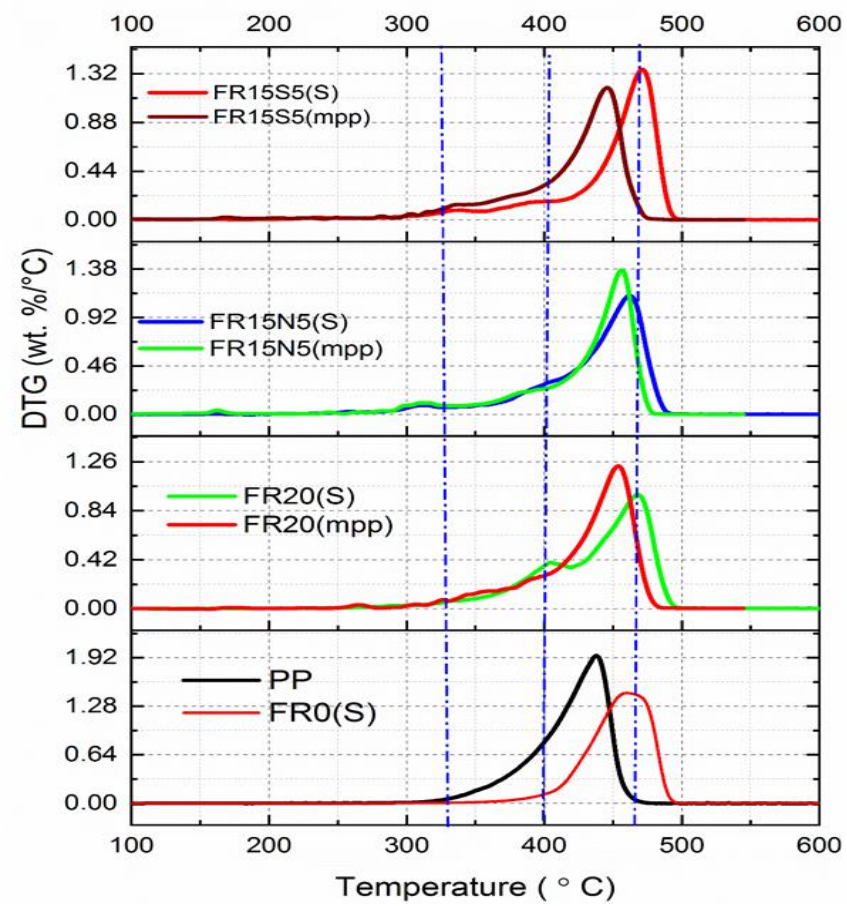

Figure 4-15: DTG results of composites with SEBS-g-MA and PP-g-MA compatibilisers under N_2

The graph also shows two peaks which are related to the decomposition of polymer and APP423 When the PP-g-MA is used there is no peak observed before 400°C, which means flame retardant improves the stability when compatibilised by PP-g-MA.

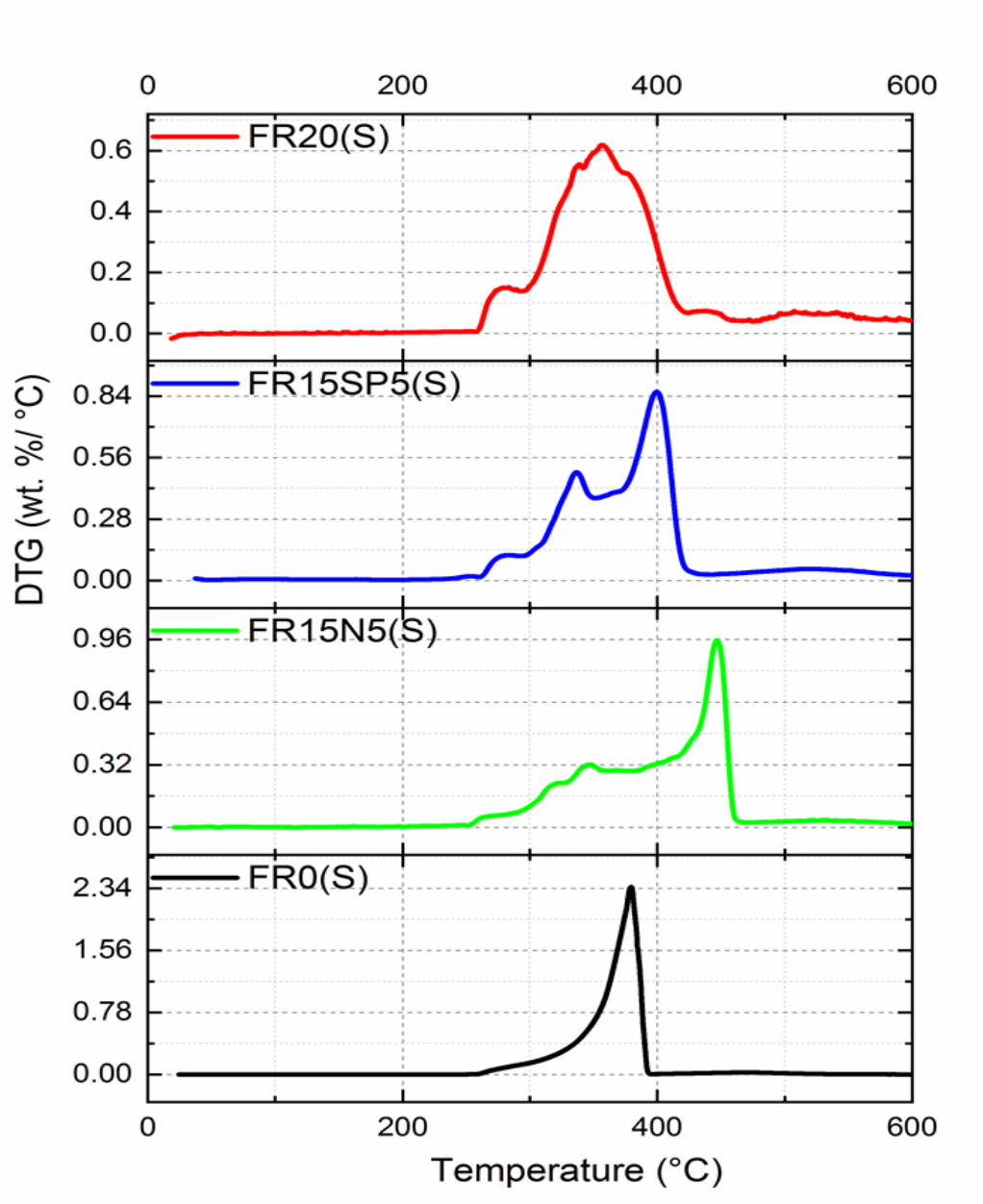

Figure 4-16: DTG results of composites with SEBS-g-MA compatibiliser under Air

4.6 Effect of Compatibilisers Type and Nanoclays on Mechanical Properties

Figure 4-17 shows a comparison between the tensile strength of the composites as function of compatibiliser type. The x-axis shows the difference in tensile strength between FR20, FR15N5 and FR15SP5 with SEBS-g-MA and PP-g-MA as compatibilisers.

FR20(mpp) shows higher tensile strength (>40 MPa) than SEBS-g-MA. FR15N5 with PP-g-MA shows higher tensile strength (>35 MPa) than SEBS-g-MA. FR15SP5 (mpp) shows tensile strength of ~35 MPa, which is higher than that of SEBS-g-MA. These results indicate that FR20(mpp) has the highest tensile strength among all composites.

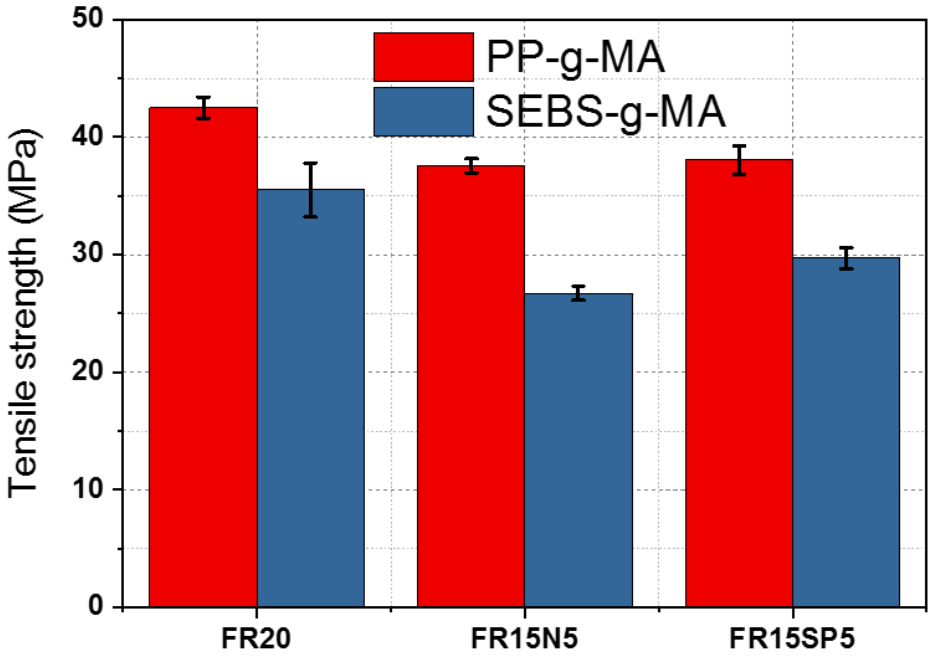

.

Figure 4-17 : Tensile strength of composites using SEBS-g-MA and PP-g-MA and using N5 and SP as nanoclays

FR20(mpp) shows a higher tensile strength value (more than 40 MPa) that is higher than SEBS-g-MA, FR15N5 of PP-g-MA shows higher tensile strength value more than 35 MPa which is higher than SEBS-g-MA and in FR15SP5 (mpp) the tensile strength is around 35 MPa which is more than SEBS-g-MA. This concludes that FR20(mpp) has the highest tensile strength among other composites.

Figure 4-18 shows a comparison between the tensile modulus of FRs. The x-axis shows the difference in tensile modulus between FR20, FR15N5 and FR15SP5 with SEBS-g-MA and PP-g-MA as compatibilisers.

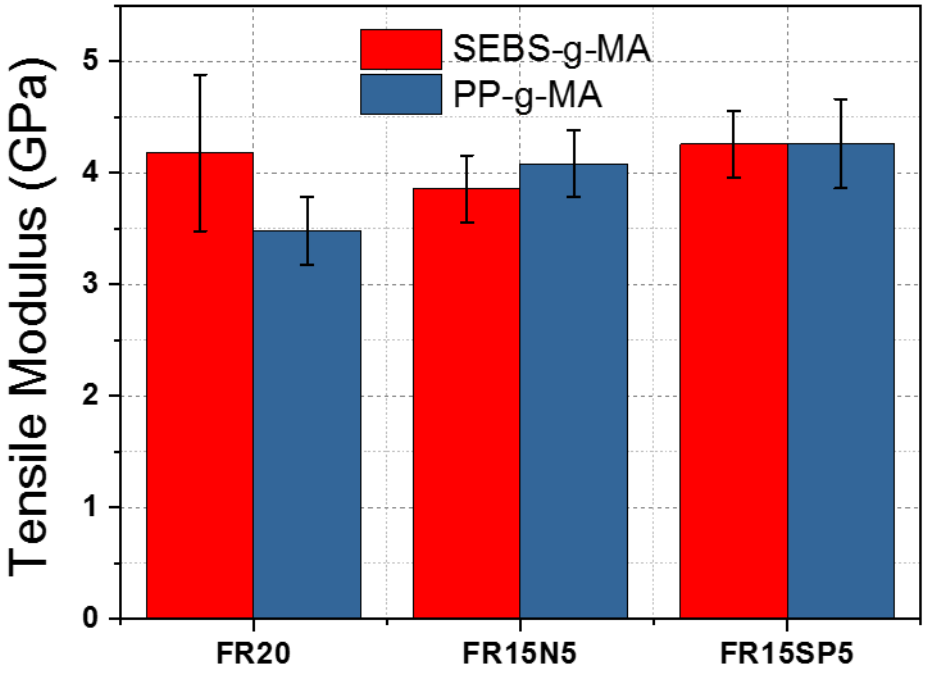

Figure 4-18 :Tensile modulus of composites using SEBS-g-MA and PP-g-MA and using N5 and SP as nanoclays

FR20 with SEBS-g-MA shows higher tensile modulus (>4 GPa) than PP-g-MA. FR15N5 shows higher tensile modulus (>4 GPa) than SEBS-g-MA. In FR15SP5, the

tensile modulus of SEBS-g-MA and PP-g-MA are both almost equal to 4.25 GPa, which is higher than that of SEBS-g-MA. These results indicate that FR15SP5 with SEBS-g-MA and PP-g-MA has almost equal tensile moduli, and these values are the highest among all FRs.

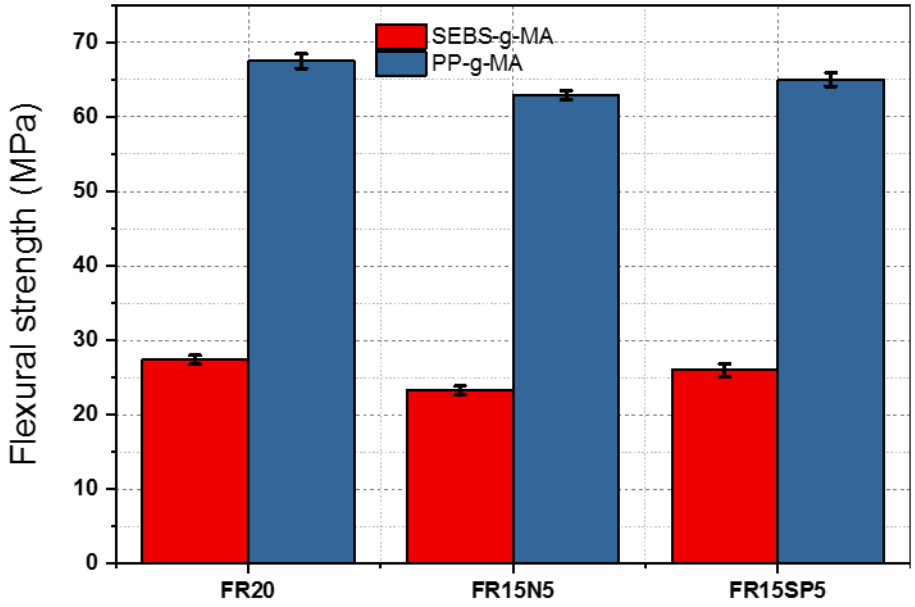

Figure 4-19 :Flexural Strength of composites using SEBS-g-Ma and PP-g-MA and using N5 and SP as nanoclays

Figure 4-19 shows the comparison between the Flexural strength of FRs. The X axis shows the difference in flexural strength between the FR20, FR15N5 and FR15SP5 of SEBS–g-MA and PP-g-MA.

FR20 with PP-g-MA shows higher flexural strength (>65 MPa) than SEBS-g-MA. FR15N5 with PP-g MA shows higher flexural strength (>60 MPa) than SEBS-g-MA. In FR15SP5, the flexural strength of PP-g-MA is ~65 MPa, which is higher than that of SEBS-g-MA. These results indicate that FR20 with PP-g-MA has the highest flexural strength among all FRs.

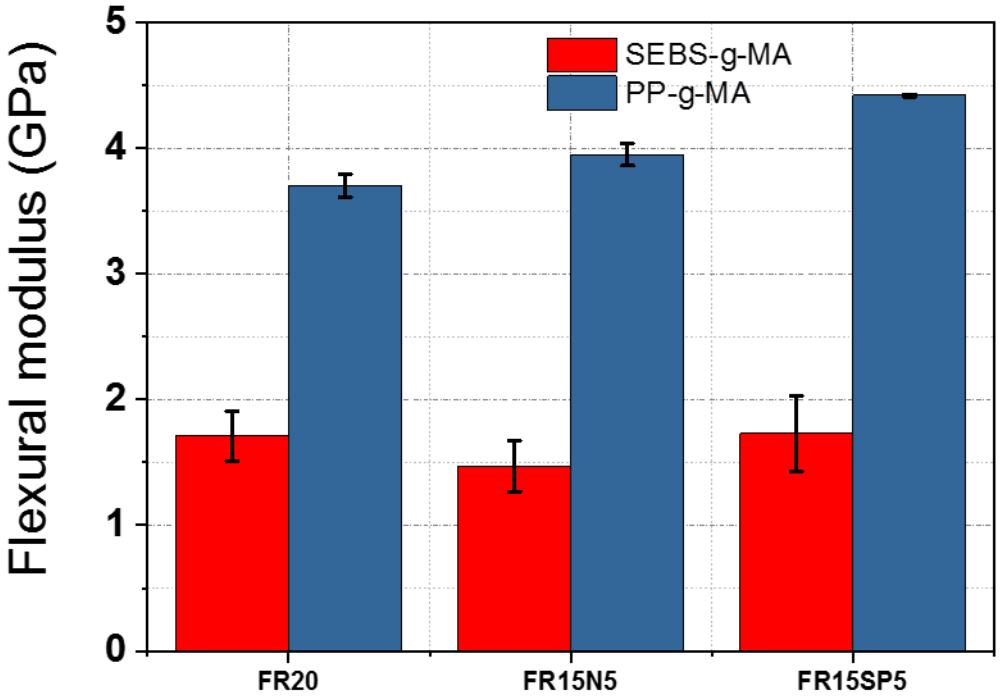

Figure 4-20: Flexural modulus of composites using SEBS-g-Ma and PP-g-MA and using N5 and SP as nanoclays

Figure 4-20 shows a comparison between the flexural modulus of FRs. The x-axis shows the difference in flexural modulus between FR20, FR15N5 and FR15SP5 with SEBS-g-MA and PP-g-MA as compatibilisers. Figure 4-19 shows the flexural moduli of samples with two different compatibilisers (PP-g MA and SEBS-g-MA). The results indicate that samples with PP-g-MA compatibiliser showed better results. FR15SP5 with PP-g-MA showed the highest flexural modulus of 4.42 GPa, and FR20 with SEBS-g-MA showed the lower modulus of 1.71 GPa. The percentage of improvement (PP-g-MA over SEBS-g-MA) was 53.78%, 62.78% and 60.85% for FR20, FR15N5 and FR15SP5, respectively.

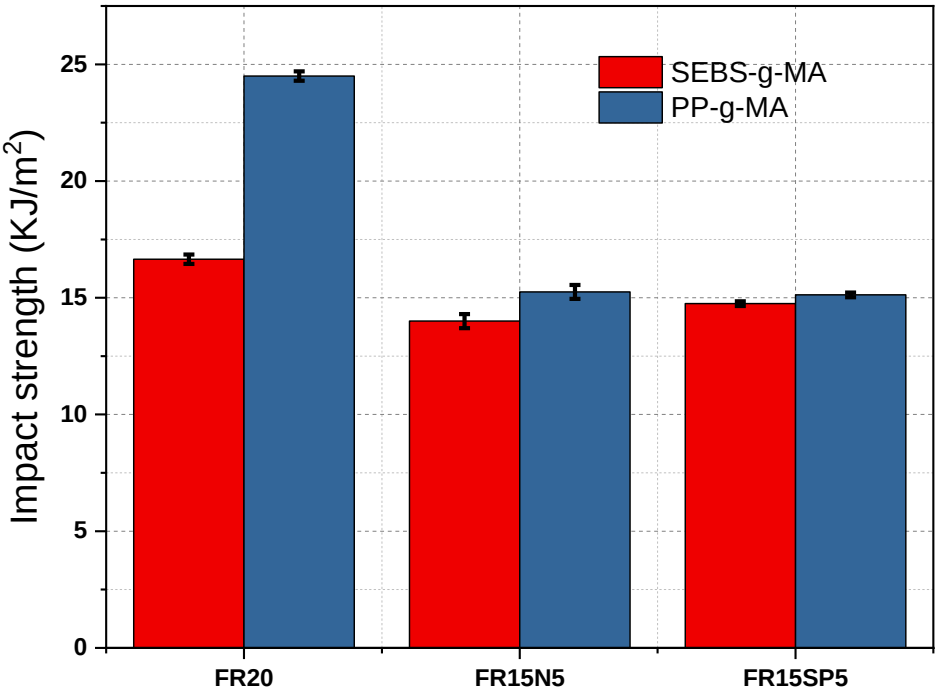

Figure 4-21:Impact strength of composites using SEBS-g-Ma and PP-g-MA and using N5 and SP as nanoclays

Figure 4-21 shows a comparison of the impact strength between FRs with SEBS-g-MA and PP-g-MA as compatibilisers. Considering the impact strength test results of FR20, FR15N5 and FR15SP5 with SEBS-g-MA and PP-g-MA, the results of FR15N5 and FR15SP5 are ~15 kJ/m^2; however, FR20 with PP-g-MA shows a significant result of ~25 kJ/m^2, which is the highest value. These results indicate that FR20 with PP-g-MA has the best impact strength.

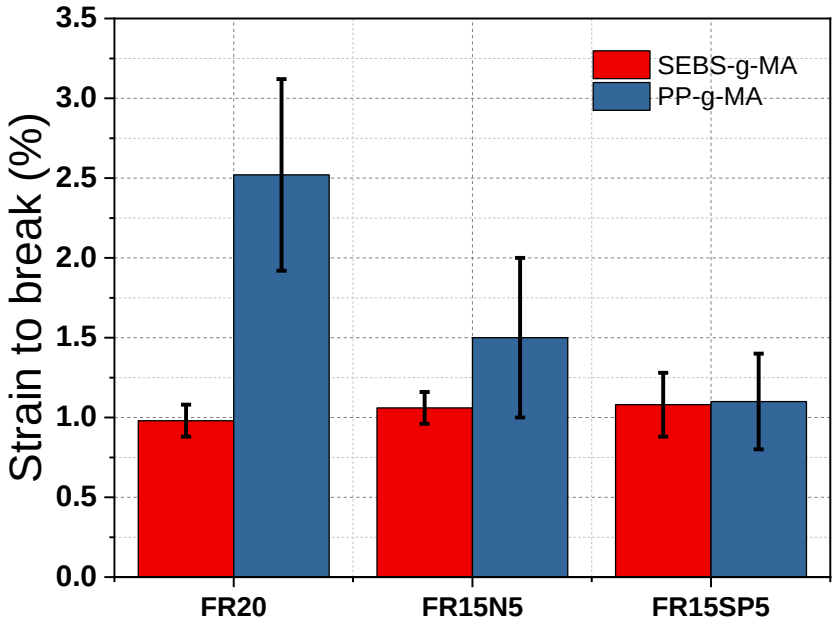

Figure 4-22: Strain to break composites using SEBS-g-Ma and PP-g-MA and using N5 and SP as nanoclays

Figure 4-22 shows a comparison between the percentage strain required to break the composite. The y-axis shows the difference in flexural modulus between FR20, FR15N5 and FR15SP5 with SEBS-g-MA and PP-g-MA as compatibilisers.

FR20 with PP-g MA shows higher percentage of strain to break (>2.5%) than SEBS-g-MA. FR15N5 with PP-g MA shows higher percentage of strain to break (~1.5%) than SEBS-g-MA. In FR15SP5, the percentage of strain to break of PP-g-MA is ~1%, which is higher than that of SEBS-g-MA. These results indicate that FR20 with PP-g-MA can withstand more elongation as it has the highest percentage of strain to break value among all FRs.

4.7 Summary

Table 4-4 shows the effect of the added compatibiliser and nanoclay on LOI. The LOI of FR20(S) with 20% of FR was the maximum, being 22.5. Further, LOI initially increases with increasing flame and then decreases with nanoclay inclusion. Nonetheless, LOI did not show a major change. Pure PP and FR0(S) samples compatibilised with SEBS-g-MA or PP-g-MA showed no rating in the UL-94 classification; all other samples had V2 rating for both compatibilisers. The effect of the compatibiliser and nanoclay on the combustion parameters—TTI, PHRR, THR, mass residue, MLR, SRP and COP—was determined using the CCT. These parameters had very high values for unblended samples [PP(control)]. The obtained results were compared for samples with and without nanoclays. Nanoclay addition and FR reduction enhances all combustion parameters except for mass residue and TTI for samples compatibilised by SEBS-g-MA (Table 4-3). The same trend was observed when the nanoclay was changed from N5 to SP. However, upon changing the compatibiliser from SEBS-g-MA to PP-g-MA, TTI, PMLR and PCOP decreased whereas other parameters increased with N5 addition. The parameters were compared between FR15N5(S) and FR15SP5(S) and between FR15N5(mpp) and FR15SP5(mpp). PHRR reduced greatly with the addition of FR and nanoclays. Compared with FR20(S) and FR20(mpp), PHRR increased by 88 and 86%, respectively. The onset temperature of the PP sample was 361°C; all other samples were compared to PP. FR0(S) showed the minimum onset temperature. FR15SP5(S) showed the highest thermal stability at 472°C. Table 4-5 shows that SEBS-g-MA-compatibilised samples showed better thermal stability than PP-g-MA-compatibilised samples.

PP-g-MA-compatibilised samples showed better performance than SEBS-g-MA-compatibilised ones. Tensile, flexural and impact tests were conducted. FR20(mpp) sample showed the highest tensile, flexural and impact strength of 40 MPa, 68 MPa and 24 kJ/m^2, respectively. The strength decreases with nanoclay addition. SEBS-g-MA-compatibilised samples showed similar trends. However, their tensile and flexural moduli increased with nanoclay addition.

CHAPTER 5 : EFFECT OF INTUMESCENT FLAME RETARDANT ON PROPERTIES

This chapter discusses the preparation of GF-reinforced PP/PA6 blend composites. The compatibility of hybrid composites was examined using APP (Exolit® AP 765 (TP); IFR) with PP-g-MA as a compatibiliser and SP nanoclay with loading of 0, 2, 3 and 5 wt.%. The amount of IFR and SP was limited to 20% (SP + APP = 20 wt.%). The composite samples were prepared using a twin extruder followed by an injection moulding machine. Composites were tested for flammability using CCTs as well as by condensed phase analysis of the char residue from the cone calorimeter to assess flammability. The carbonaceous char was evaluated using SEM, photographs and Raman spectroscopy. The thermal stability and mechanical properties were also measured.

5.1 Introduction

FRs are added to combustible materials (plastics, textiles, etc) for improving their FR properties. FRs can also reduce their combustion, thereby reducing the release of toxic chemicals and smoke. FRs are generally used in solid, liquid or gaseous phases. Metal hydroxides such as Aluminium hydroxide and magnesium hydroxide are commonly used as FRs. To achieve adequate flame retardancy, polymers need a large percentage (>60%) of these FR. However, such large percentages generally degrade the mechanical properties of filled polymer materials (Chen and Jiao, 2011). Therefore, in recent years, IFRs have attracted increased attention for improving FR properties. Intumescence means ‘swollen up’; in IFRs, heat exposure triggers a chain of physical and chemical reactions or processes that lead to a tumescent (swollen) condition (Camino et al., 1989). An IFR comprises three components: an acid source, a char forming agent and a blowing agent. Studies have extensively investigated the use of IFRs in polymers. APP (a conventional acid source) and melamine polyphosphate (MPyP), a reaction product of melamine and phosphoric acid (Chen and Jiao, 2011), are widely used as FRs in polyamides.(Chen and Jiao, 2011) .

CHAPTER 5 :EFFECT OF INTUMESCENT FLAME RETARDANT ON PROPERTIES

IFRs provide flame retardancy via their substantially high nitrogen and phosphorous contents. Nitrogen decomposes in the gas phase to create non-flammable fumes such as HNO_2 and HNO_3 and prevents the phosphorous components from pyrolyzing in the vapour phase. Further, phosphorous effectively dehydrates the polymer substances to form a layer of non-flammable phosphoric acid which forms char that often insulates the condensed phase.

IFRs offer good effectiveness at low loading. During combustion, they emit little toxic gas, show anti-dripping behaviour and are halogen free. The major disadvantages of IFRs compared to halogenated FRs are low thermal stability and low flame retardancy. To overcome these issues, synergistic agents have been incorporated to enhance the flame retardancy of IFRs based on PP, zeolites (Demir *et al.*, 2005), montmorillonite (Tang *et al.*, 2004), SP (Pappalardo *et al.*, 2016), silica (Wei *et al.*, 2003), alumina (Wei *et al.*, 2003), lanthanum oxide (Li *et al.*, 2008;Wu *et al.*, 2008), expandable graphite (Wei *et al.*, 2004), iron powder (Chen *et al.*, 2009), zinc borate (Fontaine *et al.*, 2008) and polysilsesquioxane (Vannier *et al.*, 2008).

AP 750, a commercial IFR, is more stable at higher temperatures between 250 and 800°C than modified APP with pentaerythritol (PER) and causes a sharp decrease in PHRR owing to the formation of a char layer which acts as a physical barrier and hinders heat transfer via the formation of ammonia and water (Bourbigot *et al.*, 2004b). Because it is used with low loading, it improves the mechanical properties.

In this study, a GF-reinforced PP/PA6 blend was modified by adding AP 765 (TP) as an IFR and SP nanoclay by melt compounding to study the influence of the combination of the IFR with SP on the flammability and fire retardancy of PP/PA6-based formulations.

5.2 Experimental study

5.3 Materials and Sample Preparation

5.3.1 Materials used

PP (Icorene® 4014, ICO Polymer, UK), polyamide 6 (PA6) (Zytel® 7335F, DuPont, USA) and PP-g-MA (Polybond® 3200, Addivant, USA) blend compatibiliser were used as polymer blend components with the constant ratio PP:PA6:PP-g-MA = 70:30:5. SP (Pangel® S9, Tolsa, Spain) was used as a nanofiller. APP (Exolit® AP 765 (TP), Clariant, Germany) and chopped short GFs (P968, Vetrotex, France) were used as FRs; they were modified with a silane-based coupling agent for better compatibility with PP and to improve the mechanical properties. The materials used are shown in Table 5-1.

Table 5-1 : Materials used in the study

Material	Commercial name	Source
Polypropylene (PP)	Icorene®4014	Ico polymer ,uk
Nylon6 (PA6)	Zytel®7335F	DuPont ,USA
Sepiolite (SP)	Pangel®S9	Tolsa, Spain
Ammonium Polyphosphate (IFR)	Exolite®APP765	Klariant,Germany
Chopped glass fibre (GF)	P968	Vetrotex , France
Polypropylene grafted maleic anhydride	Polybond®3200	Addivant,USA

5.3.2 Preparation of composites

PP/PA6/PP-g-MA was prepared in one step using a twin screw extruder with screw speed of 200 rpm and melt zone temperature of 180–240°C. Nanoparticles were introduced in the molten polymer blend. The pellets were injection-moulded at 220°C with mould temperature of 80°C to obtain square sheet specimens with dimensions of 100 × 100 × 4 mm3. Table 5-2 shows the sample names and compositions. Before processing, PA6 and SEBS-g-MA were dried at 80°C in a vacuum oven for 12 h. SP and N5 were also dried at 90°C overnight to remove water.

Table 5-2: formulation with intumcent loading in wt.%

Sample Code	C(70%PP+30%PA6+5%PP-g-MA)	GF (%)	IFR+SP=20 wt.%	
			IFR	SP(%)
IFR15SP5	60	20	15	5
IFR17SP3	60	20	17	3
IFR18SP2	60	20	18	2
IFR20SP0	60	20	20	0

5.4 Characterization

5.4.1 Flame retardancy

Standard UL-94 flammability tests (Underwriters Laboratories, 2013) were conducted to classify the samples based on their flammability in vertical test setups. The samples had dimensions of 120 × 14 × 3.2 mm3. The increasing values of UL-94 ratings are V-2, V-1, V-0 and no rating (NR).

CCTs (FTT, UK) were conducted according to BS EN ISO 13927:2015 (British Standard Institution, 2015). Specimens (dimensions: 100 × 100 × 4 mm3) were exposed to a constant heat flux of 50 kW/m2 and ignited. Heat release values and mass reduction were continuously recorded during burning.

5.4.2 Thermal gravimetric analysis

Thermal stability was evaluated in nitrogen and in air at heating rate of 10°C/min by TGA (Q500 series, TA Universal Analysis, TA Instruments Inc., USA). A small amount of each sample (~5–10 mg) was examined under a nitrogen flow rate of 10 ml/min from 23 to 600°C. The thermal degradation of PP/PA6 nanocomposites was investigated. Further, DTGA was conducted to determine the loss rate and decomposition temperature of the composite. Details about the onset temperature of degradation, maximum degradation rate temperature(s), number of degradation steps and residual weight at a certain temperature (usually when no more development is observed) can be obtained from the resulting weight/temperature curves and their derivatives. The temperatures at 95% and 50% of residual weight are also measured. The degradation mechanisms depend not only on the material but also on the testing environment. In particular, several degradation steps are typically seen owing to the active oxidative role of oxygen in air.

5.4.3 Thermal gravimetric analysis

Thermal stability was carried out in nitrogen and in air at a heating rate of 10°C/min by using a Thermo-gravimetric analysis (TGA Q500 series, TA Universal analysis, TA Instruments Inc., USA). A small amount of each sample (approximately 5-10mg) was examined under a nitrogen flow rate of 10 ml/min from 23 to 600 °C. The thermal degradation of PP/PA6 nanocomposites were investigated. As well as derivative thermal gravimetric analysis in order to show loss rate and decomposition temperature of the composite Details about the onset temperature of degradation, the maximum degradation rate temperature(s), the number of degradation steps, the residual weight at a certain temperature - usually when no

more development is observed - can be obtained from the resulting weight/temperature curves and their derivatives. The temperatures at 95% and 50% of residual weight are also sometimes given. The mechanisms of degradation depend not only on the material but also on the environment the test is performed in. In particular, it is classical to observe several degradation steps due to the active oxidative role of oxygen in air.

5.4.4 Mechanical testing

Tensile tests were conducted using a Zwick universal testing machine (SMART PRO, Zwick Roell, UK) according to BS EN ISO 527 with crosshead speed of 5 mm/min and gauge length of 50 mm. Five replicates were tested.

A Charpy impact test was performed using a pendulum CEAST Charpy machine according to ISO 179/1e with 4-J capacity to measure the impact strength.

The flexural properties of the nanocomposites were determined using the same tensile machine through three-point bending tests according to ISO 178 with thickness to span length ratio of 1:16 and cross head displacement rate of 2 mm/min.

5.5 Results and Discussion

5.6 Influence of Intumescent Loading on Flame Retardancy

5.6.1 Cone calorimeter test

Table 5-3 summarizes the results obtained from cone calorimeter The PHRR decrease from 346 kW/m2 in case of 5%SP+15% IFR to 167 kW/m2 0%SP+20% IFR this associate with low PSPR and COP which mean it suppress the heat and smoke and among all the formulation is the best flowed by Flame retardant with 18% IFR and 2%GF, since the mass loss rate is less compared to other IFR loading. So it is clear that by increasing the loading Intumescent on Flame Retardancy, increases the probability to be best flame retardant, but as

it is evident from the table that at 20%IFR and 0% SP, the flow actually changes. Since the mass loss increases abruptly and the total heat release is the highest than other loadings. Hence the best flame retardant as obtained from cone calorimeter results,is 18%IFR + 2%SP..

Table 5-3: Cone calormiter important pramater with difffrent IFR loading from 15-20 wt.%

Sample	TTI (s)	PHRR (kW/m^2)	THE (kJ/m^2)	Mass residua (%)	P_{MLR} (g/s)	P_{SPR} (m^2/s)	P_{COP} (g/s)
IFR15SP5	16	346	121.62	32.20201	0.113271	0.05971	0.003839
IFR17SP3	17.5	255	119.4	30.074	0.117433	0.05130	0.003867
IFR18SP2	16	188.5	120.11	31.1	0.100299	0.03856	0.002622
IFR20SP0	16.5	167.5	124.32	28.63	0.158237	0.03042	0.001683

Figure 5-1 shows HRR curves of the compositions loaded with IFR at rates between 15% and 20% by weight. Samples with 15% IFR (5% SP) and 10% GF release more heat and samples with 18% IFR (2% SP) and 10% GF release the least heat. The higher the GF content, the higher is the HRR in 18% IFR samples. By contrast, the lower the GF content, the higher is the HRR in 15% IFR samples. GFs cause the char to break and form a new peak due to heat transfer. The results show a decrease in PHRR of ~75% for 20 mass% of additive for all samples; this agrees with literature (Lim et al., 2016). It is evident that as IFR percentage increases, the Heat release rate (HRR) and mass loss rate decreases. But for 20%IFR+0%SP, there is a sudden and abrupt increase in mass loss rate. Hence this shows that SP plays a major role in controlling mass loss and the best fire retardant is 18%IFR+2%SP as obtained from Cone Calorimeter Observations.

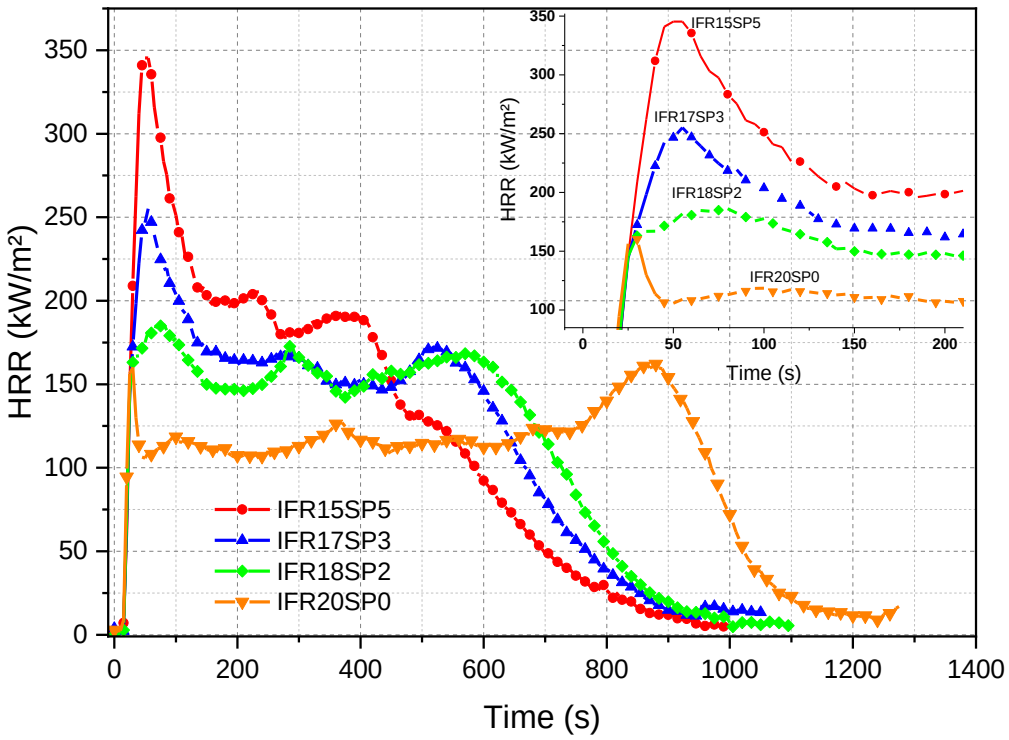

Figure 5-1: HRR curves of the composite with the intumescent flame retardant (IFR) at rates between 15 and 20

Similar behaviour was also observed with other IFR flame retardants. Depending on the polymer thermal stability, IFR in composites acts as a flame retardant in condensed phase, by creating less reactive radicals. Conversely, they also have the ability to create blanketing effect in the gas phase after the initial ignition. With different proportions of intumescent flame retardant in PP/PA6 composite indicates, gas phase blanketing effect has been dominant due to the presence of blowing agent, which is evident through flattening HRR curves with low pk-HRR, Figure 5-2.

The flame retardant scenario of IFR has led up to 91% reduction in overall pk-HRR compared to the pure PP, which is a significant improvement in developing flame retardant materials. Different flame retardants produce a different blanketing effect, which normally enhances with the amount of flame retardant present in a homogeneous blend and its blowing ability. The IFR used during this analysis further establish the difference in the effect of synergism with the presence of two peaks, as shown in Figure 5-2.

The first peak is quite distinguishable compared to the second one, which is attributed to ignition and flame spread on the surface of the material. The second peak is due to the effect of gaps in barrier (char) formation and its stability, which leads to release the volatiles to burning phase and thereby deepens the flame penetration into the material by increasing rate of combustion. When IFR to be more effective at an initial stage of burning compared to the second peak due to break of char formed.

From the observed results it was found that the final residue structure was thicker in IFR 20% compared to those in 15% and 18%, which proved that under oxidative atmosphere, formed more stable and dense char layer with the presence of hindering intumescent modifiers. However, the presence of cracks on the char surface increased the rate of volatile escape into combustion phase and thereby increased the HRR compared to those for other IFR, by diminishing the effectiveness of the char layer. Flame retardant composites ignite earlier than pure PP, but their pk-HRR is substantially low due to the formation of intumescent char barrier after the ignition caused by the presence of IFR. This increases their fire performance index (FPI) value, which is the best individual indicator of the size of fire hazard.

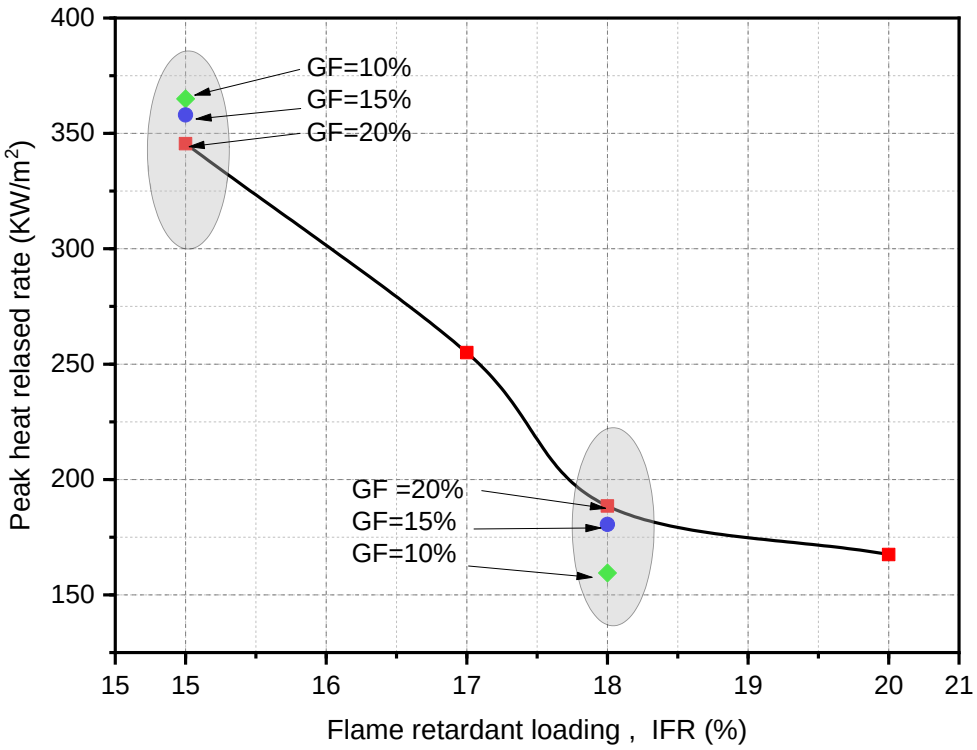

Figure 5-2: The peak rate of heat released against flame retardant loading

Figure 5-2 shows the PHRR versus IFR loading. Samples with 15% IFR (5% SP) and 10% GF release more heat, and samples with 18% IFR (2% SP) and 10% GF release the least heat. The higher the GF content, the higher is the HRR in 18% IFR samples. By contrast, the lower the GF content, the higher is the HRR in 15% IFR samples. When the GF is more than 10% the samples regularly makes the flame retardation of thermoplastics become a big challenge (candlewick effect). So in order to achieve UL-94 V-0, GF reinforced polymer need much more amount of IFR than neat polymers. Generally, about 30 wt.% flame retardants must be incorporated in order to achieve UL-94 V-0 rating (Zhao *et al.*, 2008b).

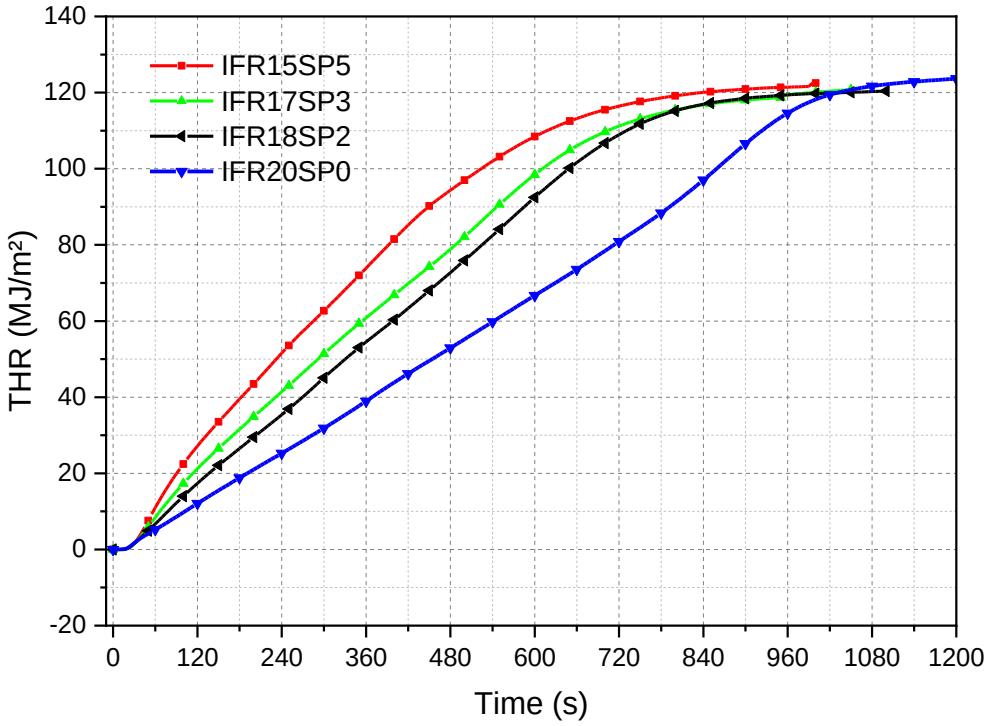

Figure 5-3: Total heat release(THR) rate versus time

This further enhances by reducing the total heat release (THR) compared to PP/PA6 composite when IFR increased, Figure 5-3. Literatures indicate that the lower the THR, the better is the sample under study. The figure shows that samples without SP (20% IFR) have lower THR than samples with SP (15%, 17%, or 18% IFR). Further, samples with lesser SP release lesser heat and those with more SP release more heat. Combustion characteristics of PP /PA6 blend is altered by the addition of IFR in a way that lower HRR and THE values are observed. The weight replacement of polymer (fuel) with IFR reduces the amount of fuel available, thus reducing the total heat evolved upon combustion (Hollingbery and Hull, 2012)

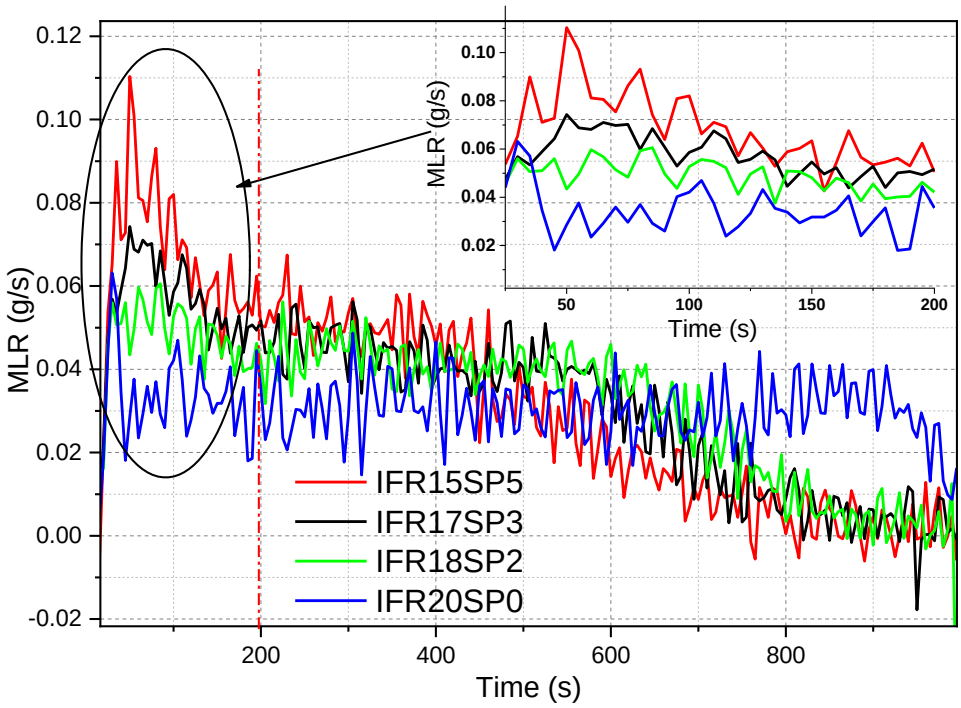

Figure 5-4 : Mass loss rate (MLR) with different loading of intumescent flame retardant

Figure 5-4 shows the MLR with different IFR loadings. Fire properties can well be followed through simultaneous evaluation of rates of heat release and mass loss from samples as a function of time . During combustion, an intumescent char may occur on the surface of the burning creating a physical protective barrier on the surface of material. The physical process of the char would act as a protective barrier in addition to the intumescent shield and can thus limit the oxygen diffusion to the substrate or give a less disturbing low volatilization rate. Higher content (20% IFR) results in MLR of ~0.06 g/s, and the highest MLR of >0.1 g/s is seen for 15% IFR. The lower the mass loss, the higher is the char formation; char forms owing to the swelling of AP 765 (TP) The mass loss rates are low in the presence of GFs. Therefore,

it can be concluded that the change in the combustion behavior with the incorporation of GFs is associated with a condensed phase physical process. It was described in the study of Casuet al, that, through the accumulation of GFs on the exposed surface of the specimen in the cone test, a protective layer is formed acting as a thermal insulator and a heat sink.. closely resemble the corresponding HRR curves in Figure 5-1.

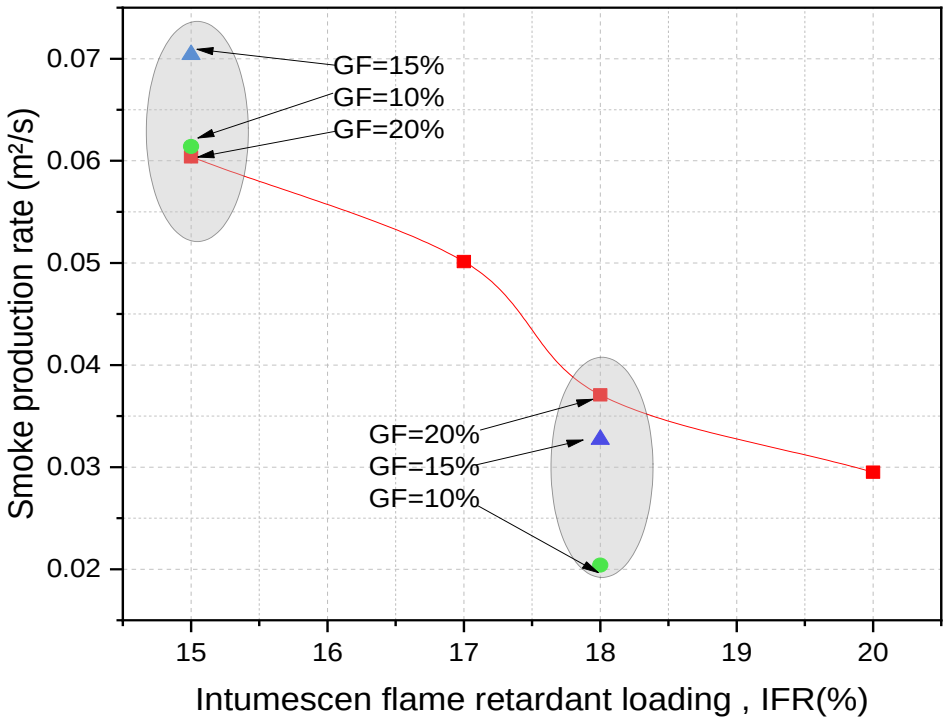

Figure 5-5 : Rate of smoke production rate of different intumescent flame retardants loading

Smoke production is one of the most important issues as smoke inhalation can cause death. . The amount of smoke production rate (SPR) and total smoke production (TSP) are the principal causes of death during fire. Thus, the determination of SPR and TSP for the various polymer compositions will be useful in indicating the relative hazard under well-ventilated

conditions presented by these materials. This section discusses the SPR of different samples. This closely resembles the Peak heat release rate curve..It is observed that samples with 18% IFR (2% SP) and 10% GF have lower SPR of 0.02 m/s^2 whereas samples with 15% IFR (5% SP) and 15% GF have higher SPR of 0.07 m/s^2, as shown in Figure 5-4. It is clear that the addition of sepiolite at a low additive amount appears to be an optimum blend ratio for the low heat release rate, total smoke, and CO2 production, as shown in Figure 5-5.

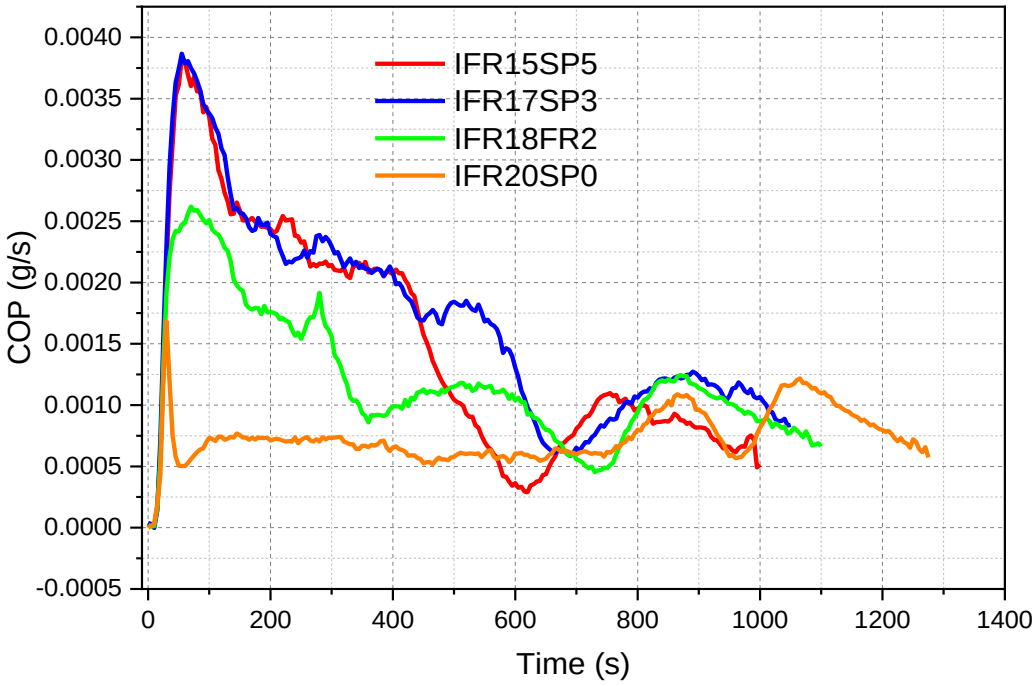

Figure 5-6: CO production rate as function of intumescent flame retardant (IFR)

CO is one of the dangerous gases released by a polymer, and therefore, it needs to be suppressed. 6 The formation of CO in fires takes place at low temperatures in the early stages of fire development primarily attributed to incomplete combustion of the pyrolyzed polymer volatile fuels. When the fire develops, the higher temperature favors the formation of CO2, which is particularly dependent on oxygen availability to the fire. The productions for CO are

presented in Figures 5-5. It can be seen that the CO productions of the flame-retardant of IFR 20% +SP 0%samples are much lower than that of other samples with more SP .. The peak COP value of IFR20%+SP 0% is the lowest, and that of IFR15% +SP 5% is the highest than all the flame-retardant composites. The addition of sepiolite accelerates the production of CO, which results from the incomplete combustion of the flame-retardant materials. At the same time, the incomplete combustion of the flame-retardant materials results in the decrease of the mass. This is the reason that the residual char left of IFR15%+SP5% is lower than that of IFR20%+SP0% at the end of the burning (shown in Figure 5-6 and Figure 5-7). By comparing the flame-retardant systems containing both AP and sepiolite with the system flame-retarded by AP alone, it can be seen that the former has lower COP value than the latter. In addition, the IFR composite flame-retarded with PP/PA6/GF could reduce the CO production during the combustion. Those results show that that COP is supressed by the FR owing to strong char formation and reduces heat by FR decomposition

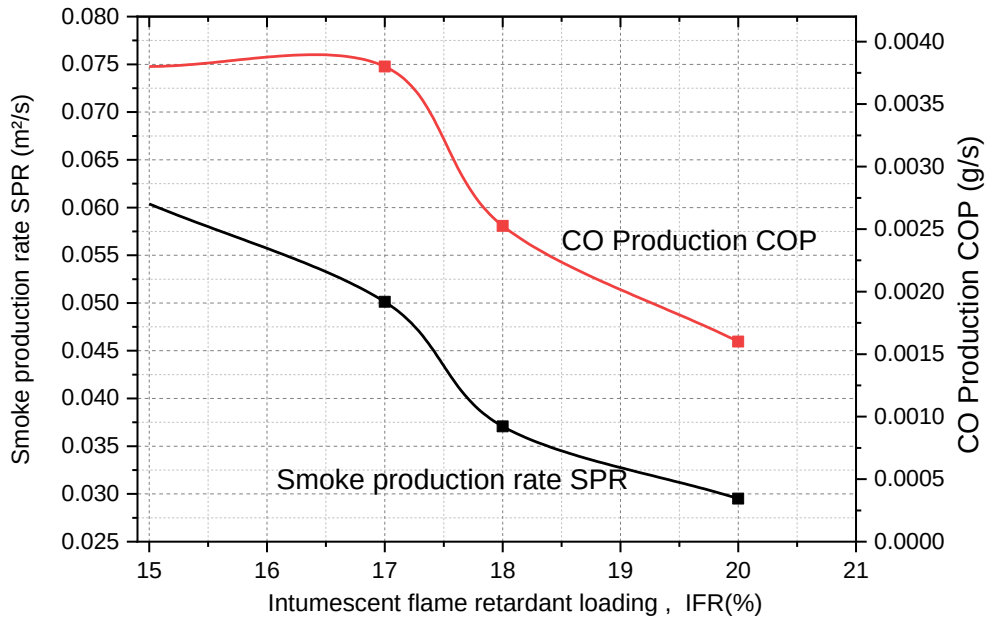

Figure 5-7: Smoke production rate and CO production with different intumescent flame retardant loading

The addition of the intumescent flame retardant and the low amount of sepiolite decrease the SPR of intumescent loaded flame-retardant. Similarly, the addition of sepiolite accelerates the production of CO, which results from the incomplete combustion of the flame-retardant materials. At the same time, the incomplete combustion of the flame-retardant materials results in the decrease of the mass. Hence the addition of sepiolite influences the smoke and CO production in Intumescent loaded flame retardant. Figure 5-6 shows the SPR with COP versus IFR loading. The SPR decreases with an increase in the IFR content. Similarly, the COP also decreases with an increase in the IFR content.

5.6.2 Synergic effect of glass fibre with Intumescent flame retardant

5.6.3 LOI and UL-94 testing of PP/PA6 composites

When IFR incorporated to the composite the LOI index increase from for PP 16 into 33 V% with classification Vo for the composite with loading of SP lower the 5%SP. The reason is that APP 765 is powerful and show high decrease of HRR from and glass increase melt viscosity of polymer.

Table 5-4 :The limited oxygen index and Ul94 classification

Sample	LOI	UL-94 rating
IFR15SP5	23	V2
IFR17SP3	30.5	V0
IFR18SP2	32	V0
IFR 20SP0	33	V0

5.6.4 Flame retardancy mechanism by residue analysis

During a fire, the complete protective mechanism of the specimen will exist with the formation of stable homogeneous char layer covering the entire sample surface. This further leads to the generation of a diffusion barrier and thereby improves the thermal shielding by reducing volatile escape and minimizing oxygen penetration. In the process of investigation, macroscale digital photos of the formed char residues were captured after the CC test this in line with (Subasinghe *et al.*, 2016).

When a specimen burns, a stable homogeneous char layer covering the entire sample surface is formed. This generates a diffusion barrier and thereby improves thermal shielding by reducing the escape of volatiles and minimizing oxygen penetration. In this study, macroscale digital photos of formed char residues were captured after the CCT in line with (Subasinghe *et al.*, 2016).

Figure 5-9 shows the representative fire residue morphology of composites with different IFR loadings. According to the FR mechanism, the char could form a barrier to both heat and mass transfer, making it more difficult for degrading material to escape to the vapour phase and preventing heat transfer back to the polymer. Char formation and the char structure are important for FR efficiency. Figures 5-9 and 5 -10 show photographs of the char after the CCT. The char residue of the composite with 15% IFR (with 5% SP) has a loose structure. The char residue of the composite with 17% IFR and 18% IFR shows small cracks; the sample with 18% IFR shows a swollen surface owing to intumescent openings in the surface and that with 17% IFR shows no swollen surface The sample surface of the composite with 20% IFR was more completely covered by char and more swollen than that of other samples, making it more flame resistant

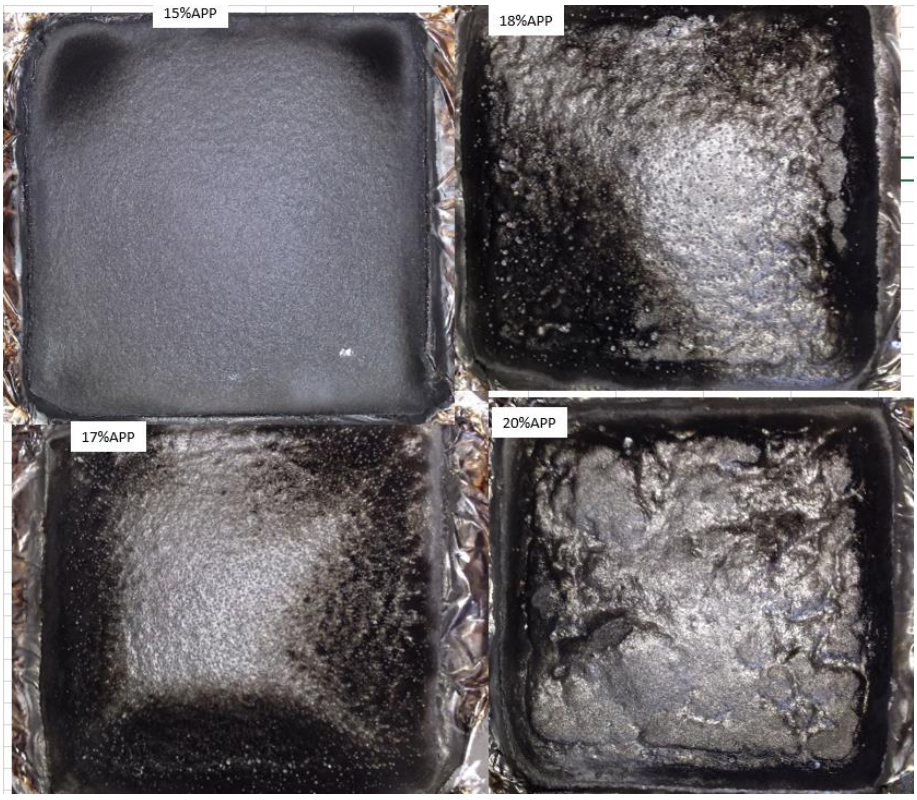

Figure 5-8: Top view The digital photographs of the residue char after cone calorimeter test of different intumescent flame retardant (a) 15% IFR (b)17% IFR, (c) 18% IFR.(d)20% IFR

Figure 5-9: Top view photographs of char residue after CCT with different IFR contents: (a) 15% IFR, (b)17% IFR, (c) 18% IFR and (d) 20% IFR

5.6.5 X-ray diffraction analysis (XRD)

XRD is frequently used to characterise the degree of dispersion of nanoparticles in a polymer. Figure 5-11 shows XRD plots of PP/PA6 nanocomposites. The peaks obtained correspond to the (110), (040) and (130) planes and represent the α form of similar peaks observed in XRD patterns of isotactic PP (Mani *et al.*, 2005). XRD patterns of nanocomposites show sharp and highly intense peaks. When the FR is incorporated in the composite and SP is increased from 2% to 5%, the peak shifts to a higher angle; by contrast, when SP is 2%–3%, the intensity is lower owing to dispersion. The intercalated nanocomposite and IFR do not

affect the crystallinity of the composite dispersion the is intercalated nanocomposite and intumescent flame retardant not effect on the crystallinity of the composite

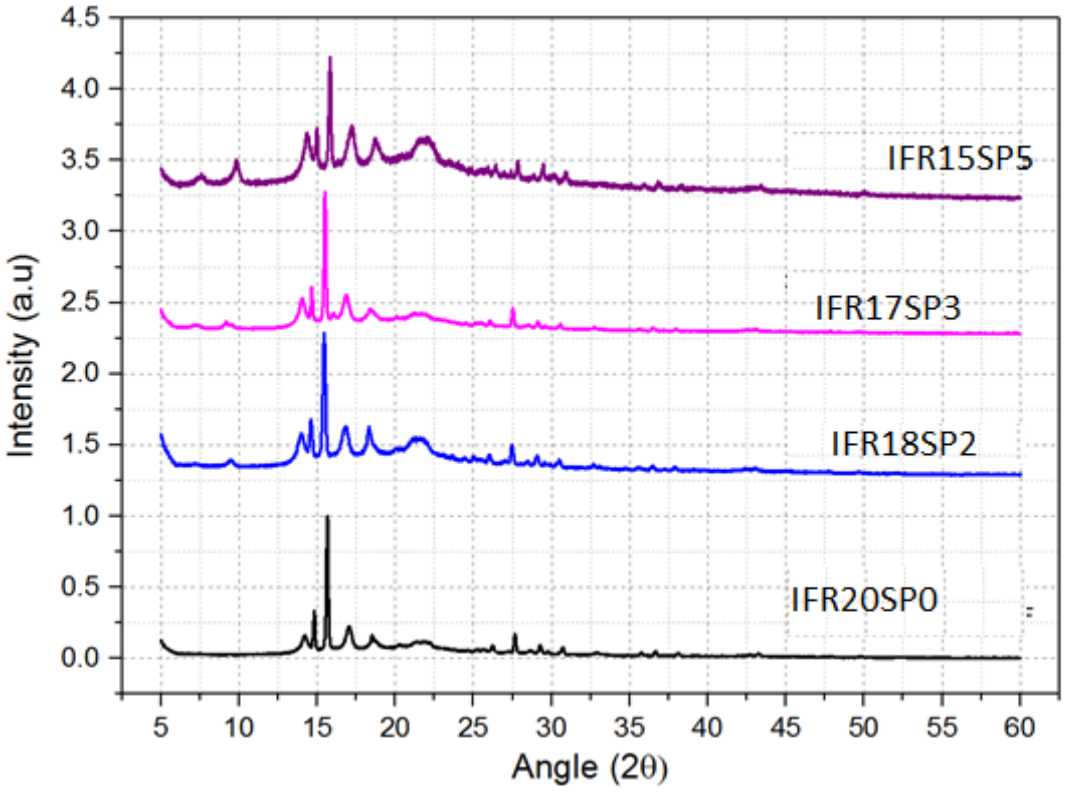

Figure 5-10: X-ray diffraction with different flame retardant loading

5.6.6 Raman spectra to assess the Char residue

Raman spectroscopy presents an appropriate method to illustrate the different types of carbonaceous materials, principally for the carbonaceous materials produced during combustion (Sadezky *et al.*, 2005).The residual chars composite with different intumescent loading from 15 to 20% after cone calorimetric were tested. As shown in Figure 15.8, the spectra for all testing samples showed two peaks with intensity maxima at about 1600 cm^{-1} and 1375 cm^{-1}, which represented graphitic structures. The first band (called the G band) associated to the stretching vibration mode with E2g symmetry in the sp2 hybridized carbon atoms in a

graphite layer, while the second one (called the D band) provides disordered graphite or glassy carbons (Yang *et al.*, 2011). According to Tuinstra and Koening, the ratio of the Area under intensities of D and G bands (ID/IG) was inversely proportional to an in-plane microcrystalline size, where ID and IG were the integrated intensities of D and G bands, respectively (Ferrari and Robertson, 2000;Tuinstra and Koenig, 1970). As shown in Figure 15.8, each spectrum was exposed to peak fitting using the curve fitting software Origin lab pro for peak fitting to resolve the curve into Gaussian fitting. Principally, the bigger the ratio of ID/IG is, the smaller size of carbonaceous microstructures is, which means better flame retardancy, as the described by other author (Zhao *et al.*, 2014). From Figure 5-12, the ratio ID/IG ratio followed the sequence of 15% IFR (2.339) < 17% IFR (2.398) < 18% IFR (2.492) < 20% IFR (2.77), representing the 20% IFR intumescent flame retardant with the highest cross-linked has the smallest carbonaceous microstructure, hence the best flame retardancy, and anti-dripping performance. The results of SEM and Raman is in agreement with the fire test results. The smaller the structure improve retardancy by means of heat and fuel transfer from to underlying material. From Figure 15-13, the ratio ID/IG ratio followed the sequence of 15% IFR (2.339) < 17% IFR (2.398) < 18% IFR (2.492) < 20% IFR (2.77), representing the 20% IFR intumescent flame retardant with the highest cross-linked has the smallest carbonaceous microstructure, hence the best flame retardance, and anti-dripping performance. The results of SEM and Raman is in agreement with the fire test results. The smaller the structure improve retardancy by means of heat and fuel transfer from to underlying material.

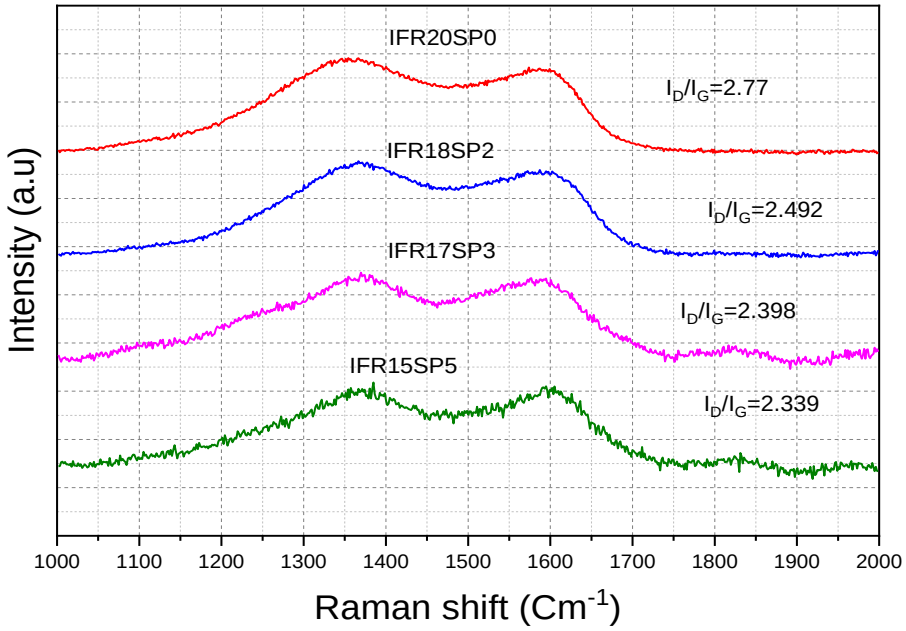

Figure 5-11 : Raman spectra of char residues for different IFR loading of PP/PA6 hybrid composites

5.7 Influence of Intumescent Loading on Thermal Stability and the Decomposition

Table 5-5 Summarizes the thermal stability of the composite under air and nitrogen with temperature at weight loss. The 5% weight loss temperatures (T5%) onset temperature for various IFR loading from 15%17% ,18% and 20% IFR it can be seen that at 2%SP and 18% is degrade at 289 °C in air which is the lost and this related to decomposition of IFR and work as char promoter and reduce temperature by release of water. In nitrogen the lowest at 5%SP and 15% IFR at 318 °C The 50% weight loss temperatures ($T_{50\%}$) onset temperature shows that the highest temperature at 471 °C at 5%SP and 15% IFR and at nitrogen is at 456 °C for the use 0 wt.% SP and 20wt. % IFR.

Figure 5-13 shows the effect of flame retardancy on thermal stability the thermal stability is reduced at early stage due to decomposition of IFR (AP765) and at higher temperature it stabilizes the composite and produce more char that is mechanism used in improve flame resistance.

Table 5-5 Effect of IFR on thermal degradation

Sample code	Weight loss under Air					Weight loss under Nitrogen				
	$T_{5\%}$	$T_{10\%}$	$T_{50\%}$	T_{max}	R%	$T_{5\%}$	$T_{10\%}$	$T_{50\%}$	T_{max}	R%
IFR15SP5	299	341	471	489	33	318	3469	452.1	453.5	35.49
IFR17SP3	303	330	421	426	30	332	352.0	449.3	451.6	31.1
IFR18SP2	289	316	418	442	29	319	347.6	449.8	452.2	32.19
IFR20SP0	347	365	453	451	28	333	355.0	456	460.8	30.1

When IFRs are added to the composites, the degradation behaviour of the flame-retardant composites changes significantly. Both the onset decomposition temperatures ($T_{5\%}$) (approximately 48 °C and 15°C below that of the IFR20SP0 under air and nitrogen respectively) and the maximum- decomposition-rate temperature (T_{max}) of the samples decrease when IFR alone is added, meaning that IFR can decrease the thermal stability of composite and increase when SP increase to 5%.The highest residue when IFR 15% and Sepiolite is 5% .

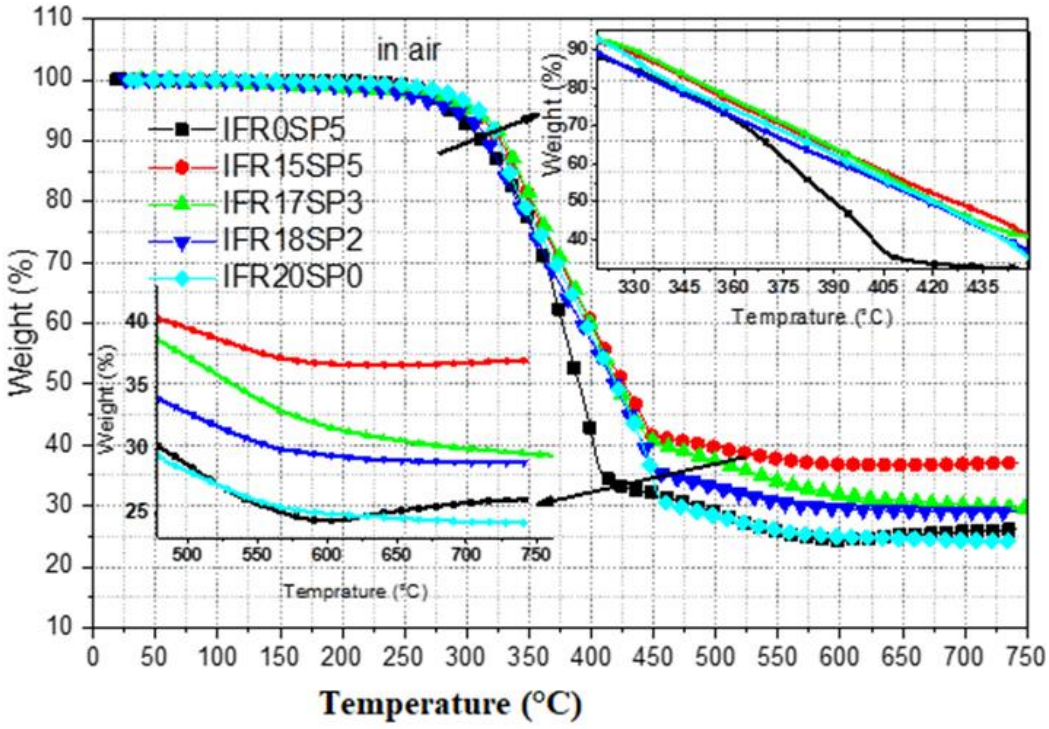

Figure 5-12 :Effect of IFR on thermal stability under air

The Figure 5-14 shows the relative thermal stability of composite under nitrogen was evaluated in the presence of different types of IFR (APP765). The 50% weight loss temperatures ($T_{50\%}$) measured for various samples from Figure 5.17. It can be that seen that composite degraded completely with $T_{50\%}$ at 455°C. The thermal decomposition temperature of composite containing different loading of IFR shifted to higher temperatures compared to composite with 0% IFR However, significant differences are seen in the thermal stability of nanocomposites containing different loading of IFR.

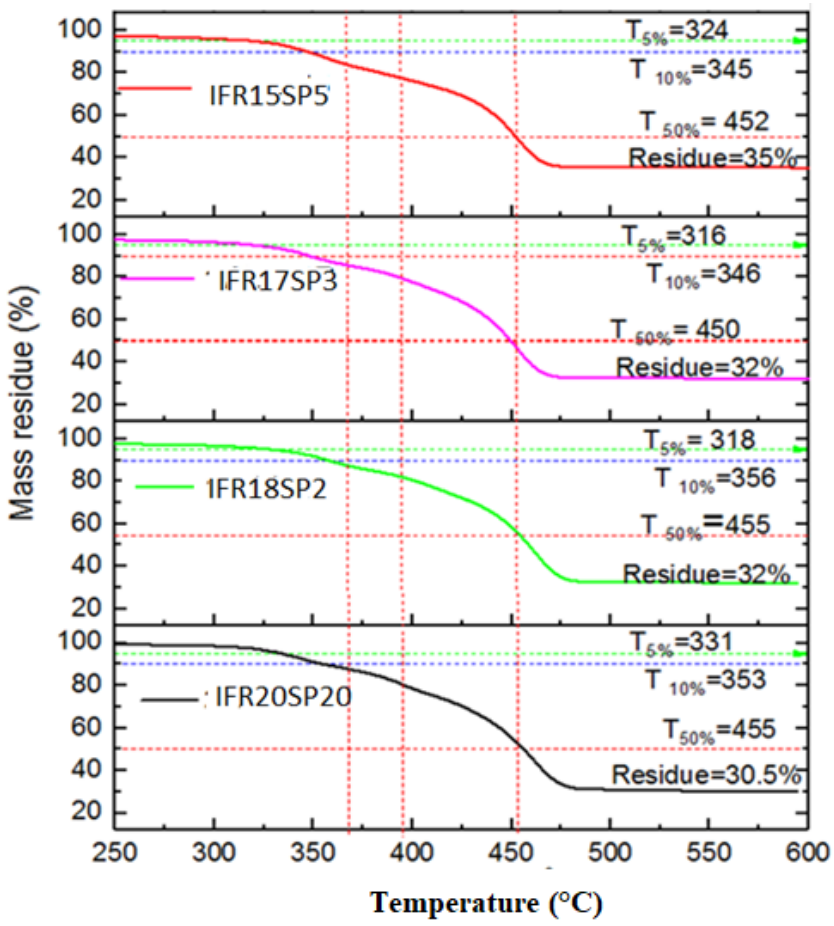

Figure 5-13: Thermal stability of composite with IFR loading under N_2

The char residue increase with increase IFR loading and it is 35 wt.% when 15%IFR is used with 5 wt. %SP compared to the composite with no flame retardant (0 wt. %IFR) is only 19% char residue. also this results shows that sepiolite synergistic of SP with IFR effect play role in thermal stability.

Figure 5-15 shows decomposition rate with different IFR loading the highest peak is decomposition of Polymer were 341 and 400 °C related to the flame retardant (AP®765) decomposition at low temperature about 300 °C is with low decomposition rate where at 460 ˚C the highest decomposition of all polymer blend which was 451°C. With increased in thermal stability in N_2.

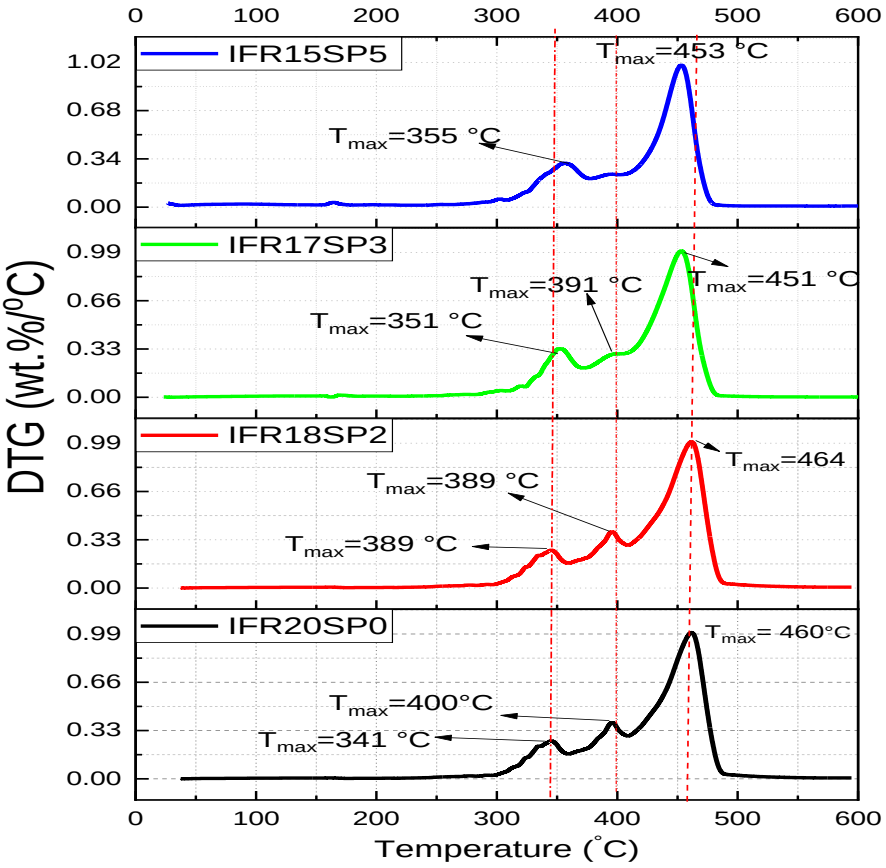

Figure 5-14: DTG of composite with different IFR loading under N_2

The decomposition of temperature in air shown in Figure 5-16. It degrades at lower temperature and show of two big peaks due to oxidation reaction at air. the maxim decomposition temperature is 448 °C when the loading is 20% IFR and is the lowest at 3%SP and 17% with temperature 396 °C may due to reaction between IFR and air

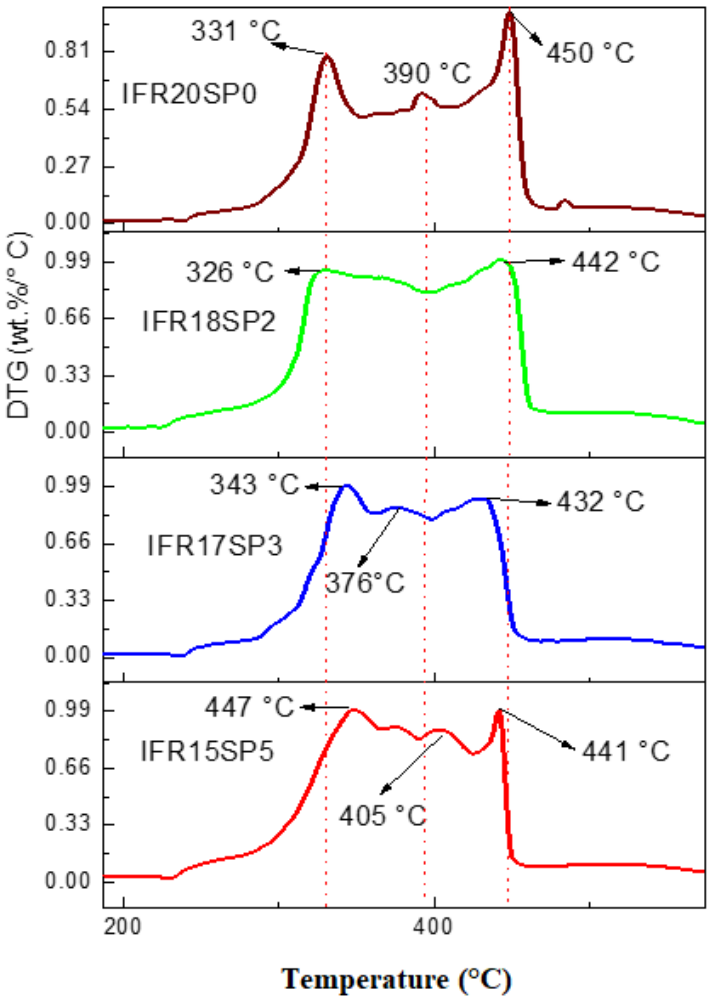

Figure 5-15 : DTG of composite with different IFR loading under air

5.8 Influence of Intumescent Loading on Mechanical Properties

Figure 5-17 shows the effect of IFR on tensile modulus. The modulus varies greatly with the amount of added AP 765 (TP). The tensile modulus is high for 18% AP 765 (TP). Beyond 18%, the modulus decreases. The tensile modulus is ~4.6 GPa for 18% AP 765 (TP) and 2% SP. The tensile modulus for 15% AP 765 (TP) and 5% SP is lower. Similar results are reported in Section 6 (Figure 6-18). The modulus may decrease owing to agglomeration with higher SP content. The modulus improves slightly for 17% APF and 3% SP, indicating that

agglomeration reduces with the SP content. For 20% APF with 0% SP, the modulus value decreases greatly

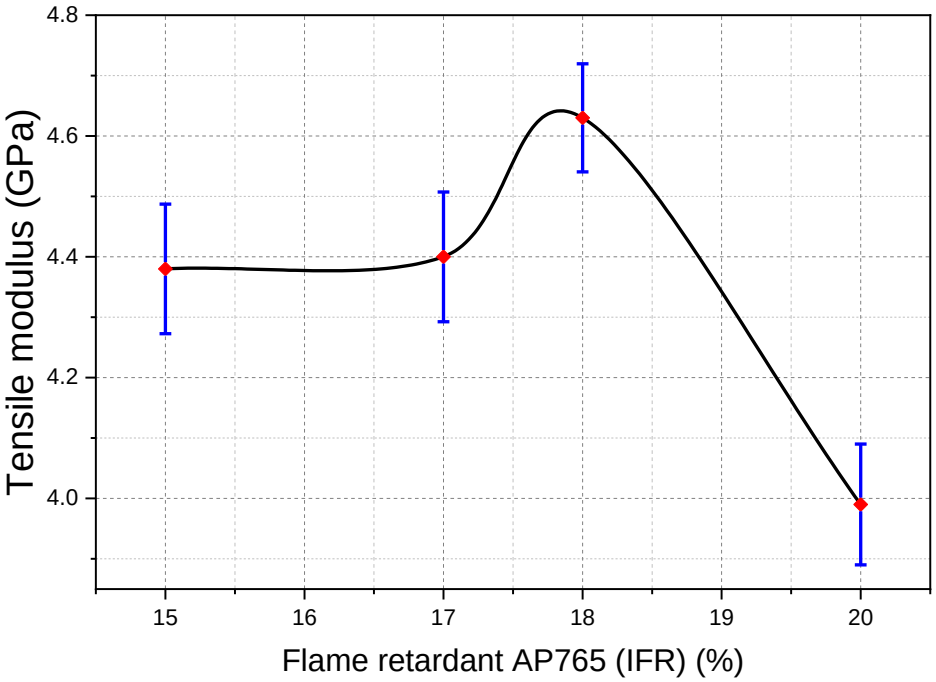

.

Figure 5-16 : Effect of IFR on tensile modulus

Figure 5-18 shows the effect of IFR on tensile strength. The test results indicate that the maximum tensile strength of 47 MPa is seen for 20% APF with 0% SP. The tensile strength is 45 MPa for 18% APF with 2% SP. With higher SP content, the tensile strength decreases. These results correspond to the values shown in Figure 6-17.

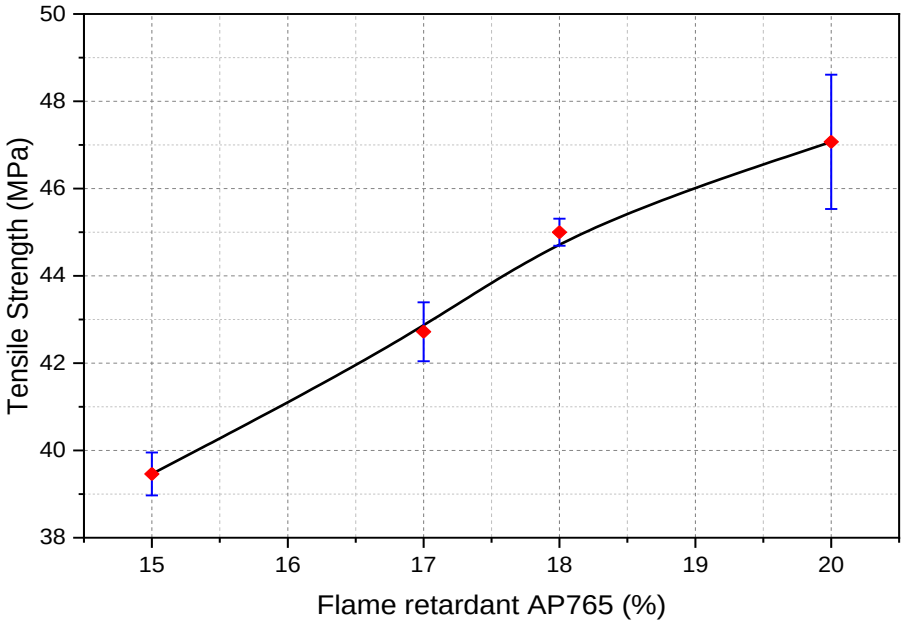

Figure 5-17 : Effect of IFR loading on Tensile Strength

Figure 5-19 shows the effect of IFR on flexural modulus. The flexural modulus increases with APF content. At higher APF content (20%), the flexural modulus has its maximum value of ~4.45 GPa. SP addition enhances the flexural modulus, as seen in Figure 5-20. These results correspond to the values shown in Figure 6-20. With higher SP content, the chances of agglomeration increase, and therefore, the flexural modulus decreases.

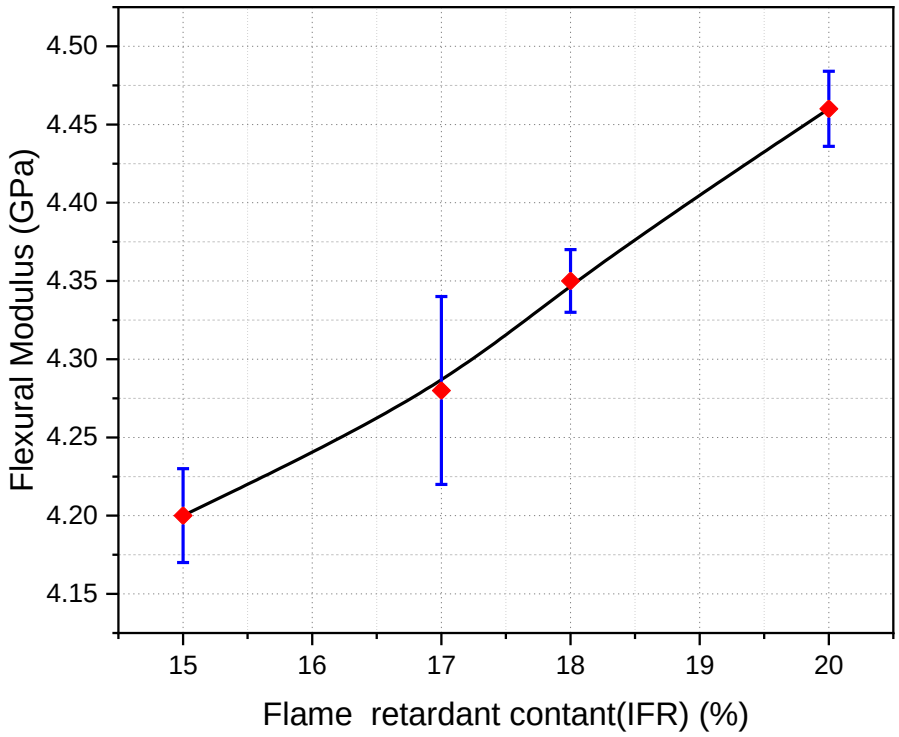

Figure 5-18 :Effect of IFR on flexural modulus

Figure 5-20 shows the flexural strength of composites with added AP 765 (TP). The addition of an FR along with SP enhances the flexural strength of the composites. Samples with lower SP content (18% APF) showed improved strength compared with 15% APF samples. Samples with lower SP content can better resist the applied load. Conversely, samples with higher SP content and GFs tend to agglomerate, thereby enhancing the stress concentration region and reducing the strength of the composite.

.

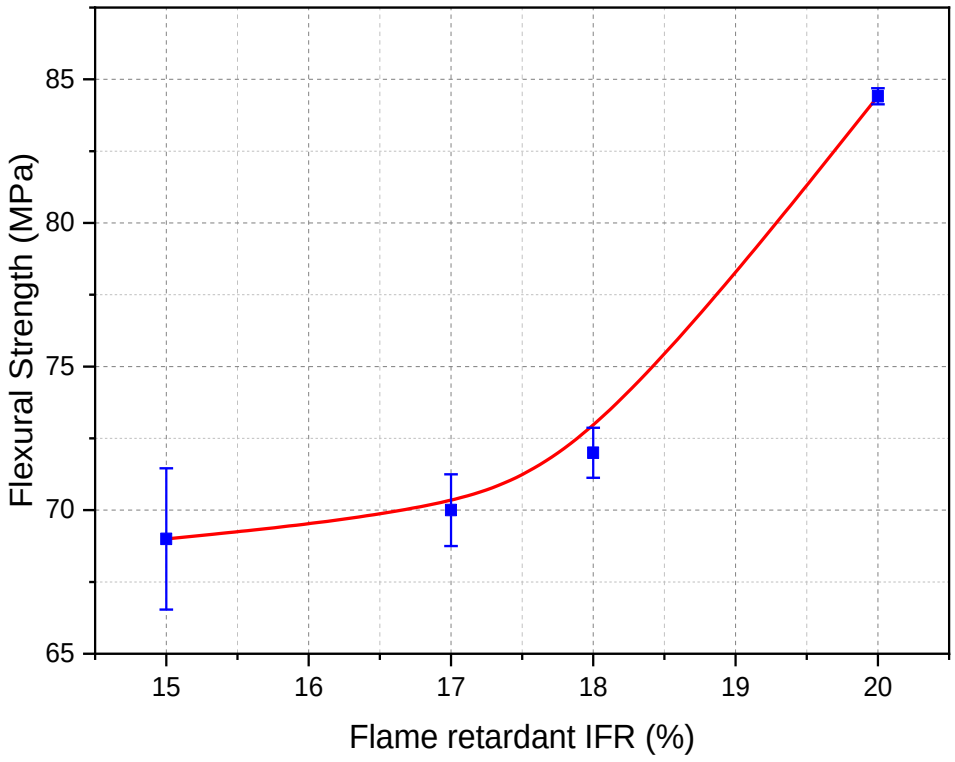

Figure 5-19 :Effect of IFR on Flexural strength

The impact strength of samples with and without sepiolite and with the addition of AP765 flame retardant has been studied in this section. Figure 5-21 shows that samples without sepiolite (20% APF) were able to absorb the maximum energy. 15% AP765 which contains 5% of SP shows a reduced impact strength. The energy absorbing capacity increases with the reduction in sepiolite content as observed with 18% AP765 samples. At higher content of sepiolite, the samples are susceptible to stress concentration and crack initiation. This reduces the impact strength of the composites.

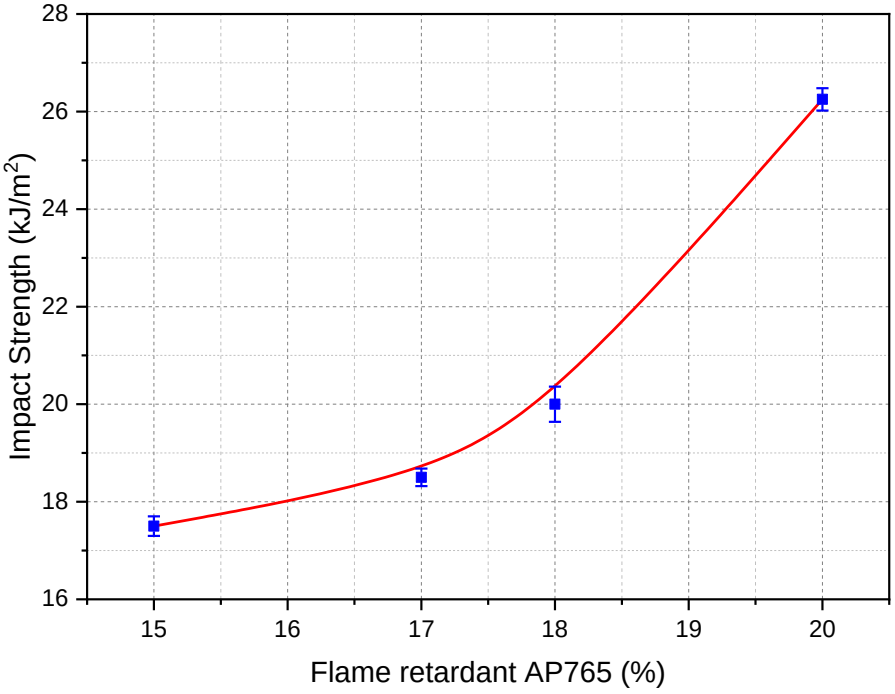

Figure 5-20 : Effect of IFR loading on impact strength

Figure 5-22 shows the effect of added FR on the strain. Samples with and without SP were studied. The sample with 17% AP 765 (TP) (3% SP) shows higher strain percentage than the samples with 18% AP 765 (TP) (2% SP) and 15% AP 765 (TP) (5% SP). Samples without SP showed much larger strain to break. The maximum strain to break observed was 1.5% for 17% AP 765 (TP) samples. However, the strain values decreased with SP content, as observed with 18% AP 765 (TP) samples.

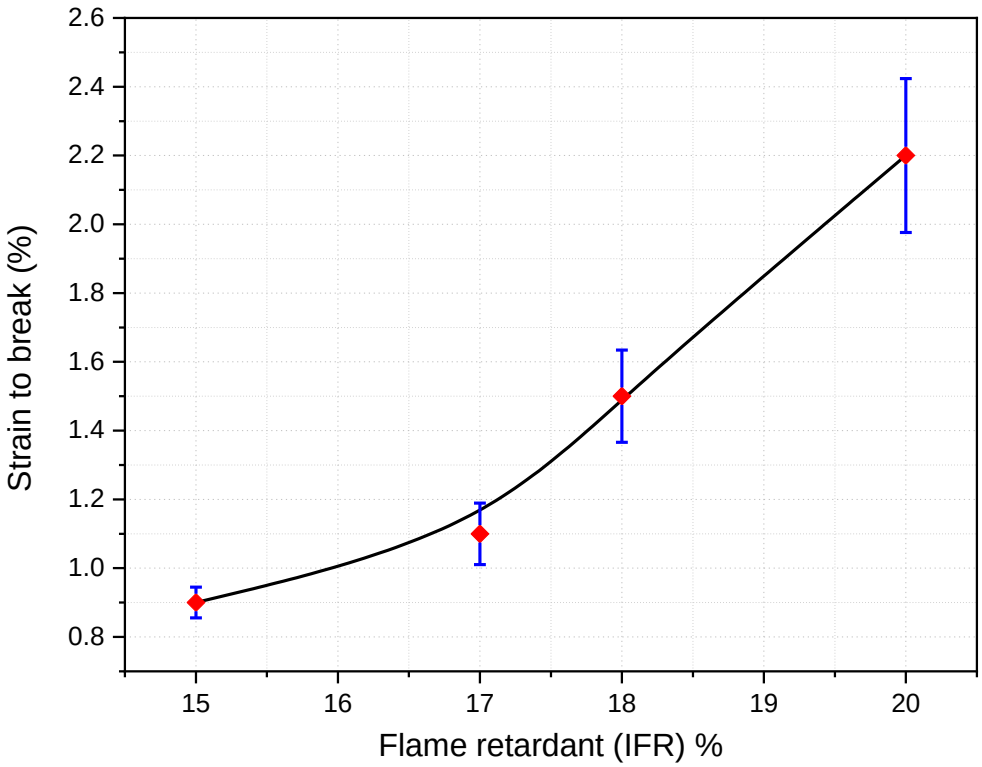

Figure 5-21: Effect of intumescent flame retardant on Strain to break

5.9 Summary

From the experimental work discussed in this chapter the following conclusions can be made:

The effect of the flame retardant (IFR) and nanoclay (SP) addition on LOI was studied and listed in Table 5-4. The LOI of IFR20SP0 sample reaches 33 and is the highest value among all the samples tested. It can be observed that with the decrease in the flame retardant and with the addition of sepiolite (nanoclay) the LOI reduces IFR15SP5 sample reaches an LOI of 23 IFR20SP0, IFR18SP2, IFR17SP3 have V0 rating in the UL-94 standard and IFR15SP5 sample was observed with V2 rating. Therefore, reduction in flame retardant below 17% may cause increased dripping.

The effect of the flame retardant (IFR) and nanoclay (SP) addition on different combustion parameters such as TTI, pHRR, THR, mass residue, MLR, SRP and COP obtained from the cone calorimetry studies is summarized here. The combustion parameters PHRR, THR, Mass residue and, SPR were the highest when the sepiolite content was 5%. For sample with 2% sepiolite (IFR18SP2) the TTI, PHRR, Mass residue, MLR, SPR and COP were very much less. and much nearer to the values of IFR20SP0 sample except the THR and MLR parameters. PHRR which is the most important parameter increased by 12.5 %, 52.23% and 106.56% for samples with 2%, 3% and 5% sepiolite as compared with IFR20SP0 sample. Inclusion of sepiolite above 2% does not add any value or advantage to the blends and samples show disturbing characteristics except for the mass residue. Because always the TTI, Mass residue should be on the higher side and PHRR, THR, MLR, SPR, COP should be minimized. But since the sepiolite content is more in IFR15SP5 the sample shows the opposite trend (maximum values as compared with IFR20SP0)

Summary of the thermal stability analysis on samples with different flame retardant and nanoclay is presented here. The onset temperature of IFR20SP0 sample was observed to 333 °C. and all other samples exhibited lesser onset temperature. The highest thermal stability was observed for IFR20SP0sample with temperature of 456 °C (see T50% in Table 5-5. The sepiolite content when high (IFR15SP5) the sample exhibit better thermal stability and is much closer to IFR20SP0 sample which has the highest flame retardant. But as the sepiolite content is reduced the stability reduces.

The effect of flame retardant and nanoclay on mechanical properties The IFR20SP0 sample exhibited the highest tensile strength of 47 MPa, but found a reduction in tensile modulus (4 GPa). Tensile modulus was highest for the sample IFR18SP2 with 4.6 GPa. If the sepiolite is greater than 2% then the sample loses its stiffness. This indicates that sepiolite content plays a major role in reducing and increasing the tensile modulus. Lesser the content higher is the modulus. Similarly, the flexural modulus reduced in samples with higher sepiolite. Maximum strength of 85 MPa was observed for sample with no sepiolite (IFR20SP0). For IFR18SP2, the flexural strength was around 72 MPa. The flexural modulus for IFR20SP0 and IFR18Sp2 were 4.45 GPa and 4.33 GPa respectively.

CHAPTER 6 : EFFECT OF GLASS FIBRE AND SEPIOLITE ON PROPERTIES

In this chapter, the hybrid composites were examined using glass fibre with PP grafted with maleic anhydride (PP-g-MA) and sepiolite by loading 2, and 5 wt.% respectively in order to study synergistic effect of sepiolite on flame retardancy of composites, mechanical and thermal stability. The composite samples were prepared on twin extruder followed by injection moulding machine. The results obtained were analysed on the basis of glass fibre loading and using two different

Sepiolite as synergy agents. Composites were tested for flammability by cone calorimeter testing as well as condensed phase of char residue from cone calorimeter to assess the flammability, thermal stability and mechanical properties techniques also used.

6.1 Introduction

In this chapter, the glass fibre reinforced retarded PP/PA6 was prepared using PPandPA6 blend and intumescent flame retardant (APP765). The compatibility of glass fibre incorporated PP/PA6 blend was studied using polypropylene grafted melic anhydride (PP-g-MA) as compatibiliser. The composite samples were melting, compounded in a twin-screw extruder followed by injection moulding machine. The results obtained were analysed based on glass fibre loading of and study the synergistic effect of sepiolite on the properties. Composites were tested for flammability, thermal stability and mechanical testing such as tensile strength, and morphology by SEM and photograph of char residue after cone calorimeter testing techniques.

6.2 Materials and Sample Preparation

6.2.1 Materials used

Polypropylene (PP) (Icorene 4014) and polyamide 6 (PA 6) (Zytel®7335F) were used as polymer blend components with the following constant ratio PP/PA 6 70:30, PP-g-MA (Polybond 3200, Addivant, USA) were used as blend compatibilisers. Pangel®S9 Sepiolite (named as SP) from Tolsa (Spain). The following phosphorous flame retardants supplied by agent of clarinet in UK used as powders: an ammonium polyphosphate (AP 765 named as IFR) and choppedshort glass fibre (P968,Vetrotex, France) is modified with a silane coupling agent for better compatibility with PP and improve the mechanical properties,the materials are summarised in the Table 6-1.

Table 6-1 : Materials used in the study

Material	Commercial name	Source
Polypropylene (PP)	Icorene® 4014	Ico polymer ,uk
Nylon6 (PA6)	Zytel® 7335F	DuPont ,USA
Sepiolite (SP)	Pangel®S9	Tolsa, Spain
Ammonium Polyphosphate (IFR)	Exolite® AP765	Klariant, Germany
Chopped glass fibre (GF)	P968	Vetrotex , France
Polypropylene grafted maleic anhydride	Polybond®3200	Addivant,USA

6.3 Preparation of Composites

The glass reinforced retarded PP/PA6 blend composites were prepared by melt compounding using twin screw extrusion. The formulations of different compositions are given in the Table 6.1 PP/PA6 blend was melted and homogeneously mixed with appropriate amount of Sepiolite. The processing temperature was maintained at 220 ˚C for melt compounding, while rotor speed and blending time were kept at 100 rpm and 10 minutes respectively

The formulations studied in this section are shown in Table 6-2. The total loading of both nanoclay and intumescent flame retardant rate was always 20% by weight relative to the polymer and glass fibre was 20%.

Table 6-2 : Formulation of glass fibre and sepiolite loadings in wt.%

Sample code	PP:PA6:PP-g-MA(70:30:5)	IFR+SP=20 wt%		GF(wt.%)
		SP	IFR(APP 765)	
GF0IF15SP5	80	5	15	0
GF10 F15SP5	70	5	15	10
GF15 F15SP5	65	5	15	15
GF20S F15P5	60	5	15	20
GF10 F18SP2	70	2	18	10
GF15 F18SP2	65	2	18	15
GF20 F18SP2	60	2	18	20

6.4 Characterization of Properties

6.5 Flame Retardancy Tests

6.5.1 Cone calorimeter fire testing (CCT)

Fire behaviour was assessed by means of a cone calorimeter (Fire Testing Technology, UK) according to the procedure described inBS 13927 (British standard institution, 2015). The heat flux of 50 kW/m2wasexposed on the samples andthe equipment was calibrated to correlate the measured thermopile temperatures to rates of heat released during combustion. Reference measurements on the samples indicate that the obtained heat release rates were repeated twice and the average is tabulated.

6.5.2 LOI and UL94 Flammability Testing

Limiting oxygen index (LOI) was assessed according to BS4589 (British standard institution, 1996) on an oxygen index apparatus (Fire Testing Technology, UK) having a paramagnetic oxygen analyser, so that precise adjustments of the oxygen concentration can be performed and repeatable results are obtained. Oxygen concentrations were varied according to up-and-down procedure explained in BS 4589. The method requires the usage of many specimens to measure oxygen index with a standard deviation of ~ 0.2% O2.

Samples were classified according to the standards of Underwriters Laboratories (Underwriters Laboratories, 2013)(UL94) for their flammability using vertical and horizontal burning tests on a custom flammability meter.

6.5.3 Thermal gravimetric analysis

Thermo-gravimetric analysis (TGA) was carried out in nitrogen at a heating rate of 10°C/min by using a thermo-gravimetric analysis (TGA Q500 series, TA Universal analysis,

TA Instruments Inc., USA). A small amount of each sample (approximately 5-10mg) was examined under a N2 flow rate of 10 ml/min from 23 to 700 °C. The thermal degradation of PP/PA6 nanocomposites was investigated.

6.5.4 Mechanical properties testing

Tensile test was carried out by Zwick Machine (SMART. PRO, Zwick Roell, UK) shown in Figure 3-6, according to BS EN ISO 527 with a crosshead speed of 5 mm/min and a 50mm gauge length. Five replicates were tested. The same equipment is used to measure flexural properties

Charpy impact tests were performed by a pendulum CEAST Charpy specimens according to the ISO 179 with a 4 J capacity to measure impact strength following ISO 179/1e (noticed edge) standard

Flexural properties of the nanocomposites were determined on the same tensile machine by three-point bending tests as per ISO 178 standard at a thickness to span length ratio of 1:16 and at cross head displacement rate of 2 mm/min.

6.6 Results and Discussion

6.7 Effect of Sepiolite with Glass fibre flame retardancy

6.7.1 Cone calorimeter test

The PHRR is the most important factor to prevent fire from the Figure 6-1 there is synergistic effect between flame retardant and nanoparticle and the best flame retardant when glass fibre is 10% GF with 2%Sp followed 2%SP and Glass fibre increased due to fact glass break the compact of char between matrix and flame retardant. So it is clear that by increasing the loading Intumescent on Flame Retardancy, increases the probability to be best flame retardant, but as it is evident from the table that at 20%IFR and 0% SP, the flow actually changes. Since the mass loss increases abruptly and the total heat release is the highest than other loadings. Hence the best flame retardant as obtained from cone calorimeter results, is

18%IFR + 2%SP. Hence by changing the composition of GF for particular IFR percentage, the burning behaviour can be changed. . It is clear that the addition of sepiolite at a low additive amount appears to be an optimum blend ratio for the low heat release rate, total smoke, and CO2 production

Table 6-3 summarizes the results obtained from cone calorimeter The PHRR decrease from 324 kW/m2 in case of 5%SP+15% GF to 160 kW/m2 2%SP+10% GF this associate with low PSPR and COP which mean it suppress the heat and smoke and among all the formulation is the best flowed by Flame retardant with 20% IFR and 20%GF.

Table 6-3: The results from CCT for different glass fibre load with 2%SP and 5%SP

Sample	**TTI**	**PHRR**	**THE**	**R**	**P_{MLR}**	**P_{SPR}**	**P_{COP}**
	(s)	(KW/m2)	(KJ/m2)	(%)	(g/s)	(m^2/s)	(g/s)
GF0F15SP5	15.5	324	134.17	11.86	0.1360	0.0595	0.0033
GF10 F15SP5	15.5	365.0	130.75	21.52	0.0577	0.0197	0.0016
GF15 F15SP5	16.5	358	123.63	27.50	0.1164	0.0648	0.0034
GF20 F15SP5	16.0	346	121.62	32.20	0.1133	0.0597	0.0038
GF10 F18SP2	14.5	160	130.46	25.33	0.0577	0.0197	0.0016
GF15 F18SP2	15.0	180.5	126.39	27.68	0.0762	0.0294	0.0017
GF20 F18SP2	16.0	189	120.11	31.10	0.1003	0.0386	0.0026

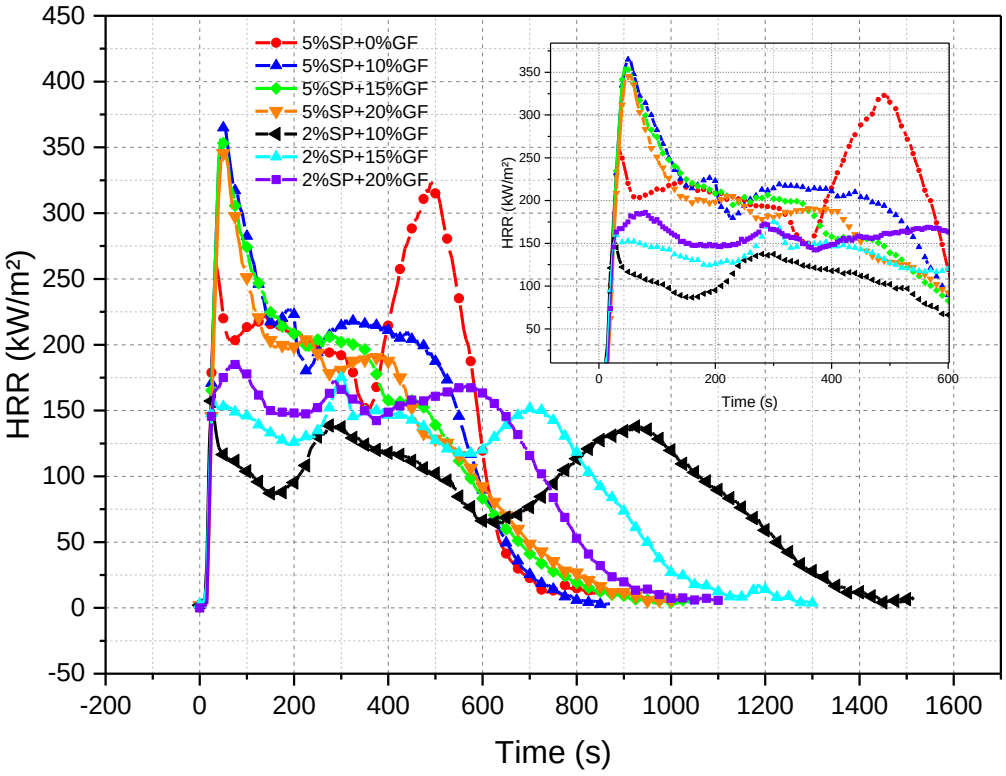

Figure 6-1: Influence of glass fibre and sepiolite on the heat release rate

The PHRR is the most important factor to prevent fire from the Figure 6-1 there is synergistic effect between flame retardant and nanoparticle and the best flame retardant when glass fibre is 10% GF with 2%Sp followed 2%SP and Glass fibre increased due to fact glass break the compact of char between matrix and flame retardant. In the Figure 6-1, the effect between flame retardant and nanoparticle and the best flame retardant is shown where the flame retardant works in the gas phase by the interference of the exothermic oxidation reaction in the flame through radical scavenging, thus decreasing the energy feedback to the polymer surface. A flame retardant also supports the development of a thermal barrier through the process of charring at the surface of the condensed phase which prevents the discharge of gaseous fuel and stops the transfer of heat back to the burning polymer. An increased char yield shows a decreased amount of combustible gases entering the flame, which in turn leads to destruction. Flame retardants working through the following mechanisms are identified as condensed phase active because they catalyse the development

of char. The purpose might be related to the growth of associated and thick intumescent char, which served as a barrier to restrict combustible gas from maintaining the flame and maintain the underlying matrix effectively from further burning. When incorporated in a polymer matrix, glass fibres cause a so-called “candlewick effect”, which generally means a big challenge for the flame retardation of thermoplastic composites. Due to the candlewick effect, glass fibres are able to transfer and feed the fuel from the pyrolysis zone of the polymer matrices to the flame by capillary action, speed the heat flowing back to polymers and thus

make the polymers decompose and burn faster. Thus, to achieve a UL-94 V-0 rating, the glass fibre-reinforced thermoplastics need a higher amount of flame retardants than neat polymers do. Cone calorimeter tests showed that long glass fibres damage the foaming ability of the intumescent flame retardants and the continuation of the residue char, which reduces the flame retardancy of IFR in long-glass-fibre-reinforced polypropylene composites. That is why glass breaks the compact of char between matrix and flame retardant for glass fibre with 10% GF with 2%Sp followed 2%SP and increased Glass fibre.

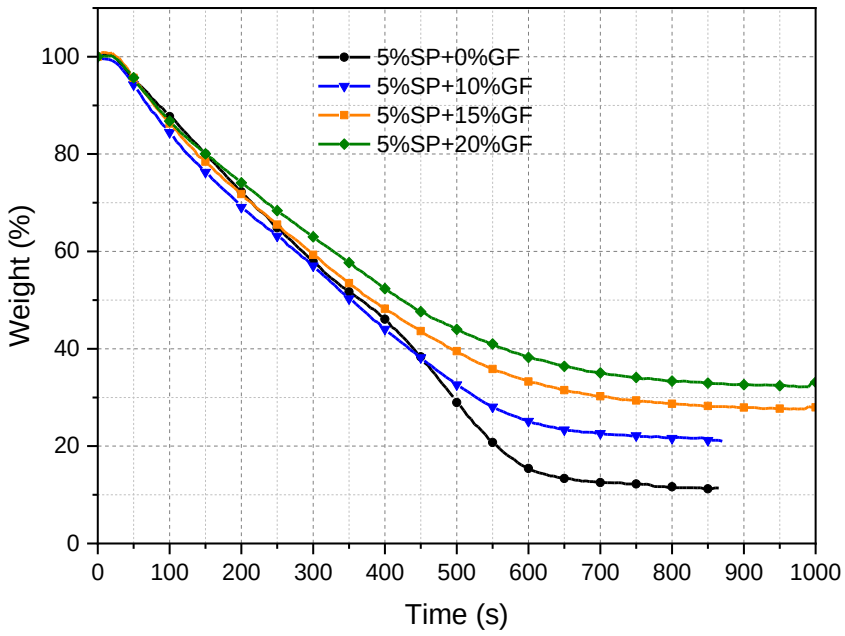

Figure 6-2 : Mass loss behaviour during combustion in the cone calorimeter test with different glass fibre loading

The mass loss over time developed with heat flux in conjunction with the heat release rate effects was obtained as assumed. We observe the identical trend as for the HRR data and the peaks on the MLR curve tend to concur with the peaks on the HRR curve. An introductory active peak for the mass loss rate, as estimated in the cone calorimeter, it can be a hurdle to represent the mass loss rate curve if the time response of the weight cell changes from the cone weight cell; as was in the above figure 6-2. The important parameter in char formation is the percent after cone calorimeter it can be seen in Figure 6.2 The mass residue is increased by increasing the glass fibre. It is increased by 12 %,22%,30% and 34% for 0%GF,10%GF,15% GF and 20 GF respectively. It is essential to define the sensitivity of the char reactivity to many conditions such as, atmosphere; particle size, etc., since it regulates the heat and mass transfer consequences during char formation. Char produced by rapid heating is almost twice as reactive as that produced by slow heating. Rapid heating yields higher volatile and more reactive char. Slower heating rate and longer residence time results in secondary char produced from reaction between primary char and volatiles.

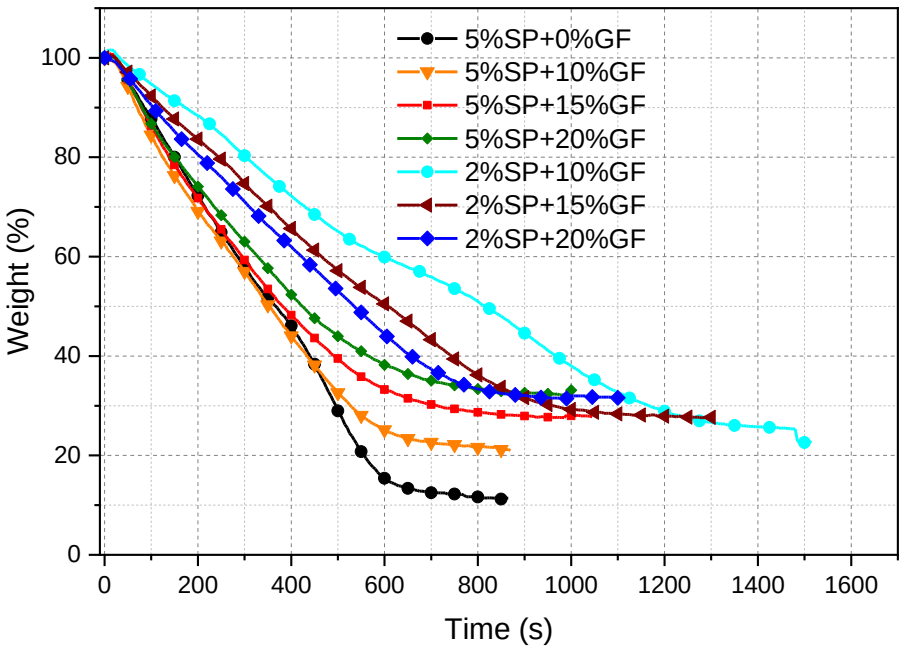

Figure 6-3 : Mass loss behaviour during combustion in the cone calorimeter test with different glass fibre loadings

Figure 6-3 shows the mass loss behaviour during combustion in cone for loading 2%SP and 5%SP rate and it shows the synergistic effect in loading 2%SP with increase in fibre loading, which showed the lower char residue when glass fibre is 0% and the highest at 2%SP +20% GF and mass residue is 33%. Intumescent flame retardant decomposes and produces a char layer. This char layer can partially hinder the decomposition of the material and reduces the heat release .It is evident that the nanoclay alone has little effect on the degradation of the polymer blend. It generally decrease the onset degradation temperature and also reduce the peak mass loss rate. It was found in the cone calorimeter that, though having negligible effect on ignition, the nanoclay reduces the heat release rate(HRR), and increases smoke and CO yields.

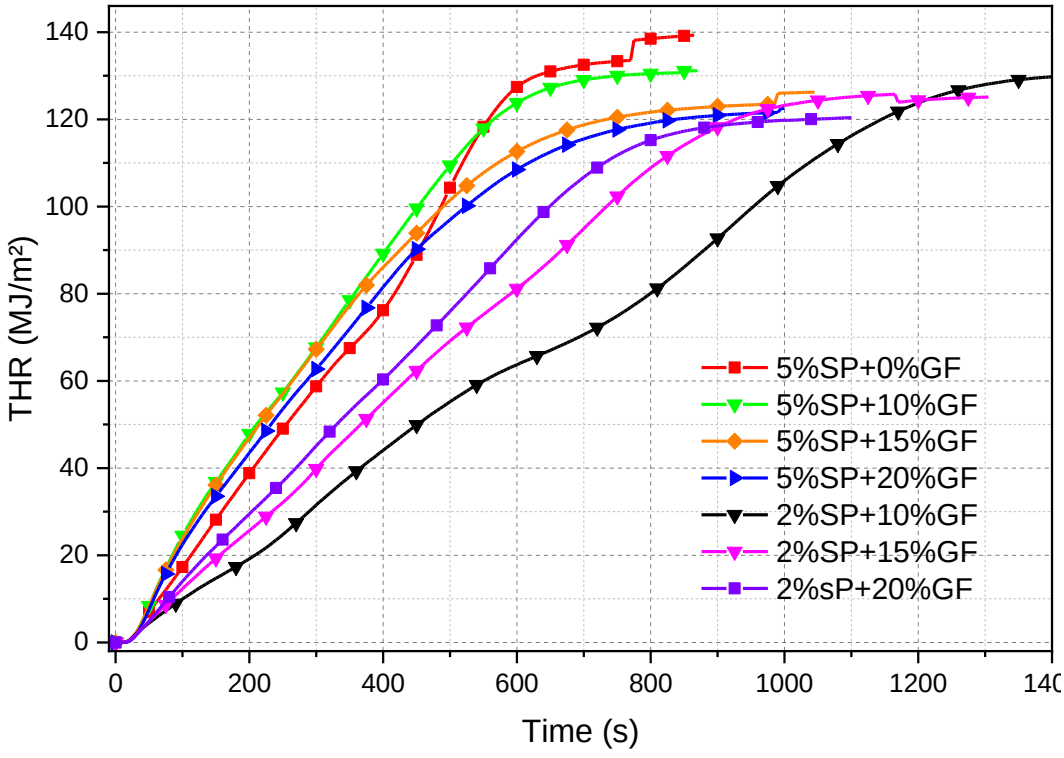

Figure 6-4 :Total heat released with different glass fibre loading

The total heat released is shown in Figure 6-4 and It show that lowering SP loading to 2% as well reduce glass fibre the reason is in shown in Heat released the higher the heat realised the higher the total heat and from the graph the best combination is 2%SP+10% GF which also have low PHRR. The total heat release (THR) curve in Figure 6-4 increases almost linearly. The complete heat release was associated with a total weight of specimens. Similar to the connection between the surface area and peak HRR, the simple regressions were calculated.

The total heat released is shown in Figure 6-4 and It show that lowering SP loading to 2% as well reduce glass fibre the reason is in shown in Heat released the higher the heat realised the higher the total heat and from the graph the best combination is 2%SP+10% GF which also have low PHRR.The total heat release (THR) curve in Figure 6-4 increases almost linearly. The complete heat release was associated with a total weight of specimens. Similar to the connection between the surface area and peak HRR, the simple regressions were calculated. THE is more or less independent of flame retardant content. Furthermore, regarding materials with same nominal filler content , increasing flame retardant loading leads to larger reductions in THE obtained by nanocomposite formulations.

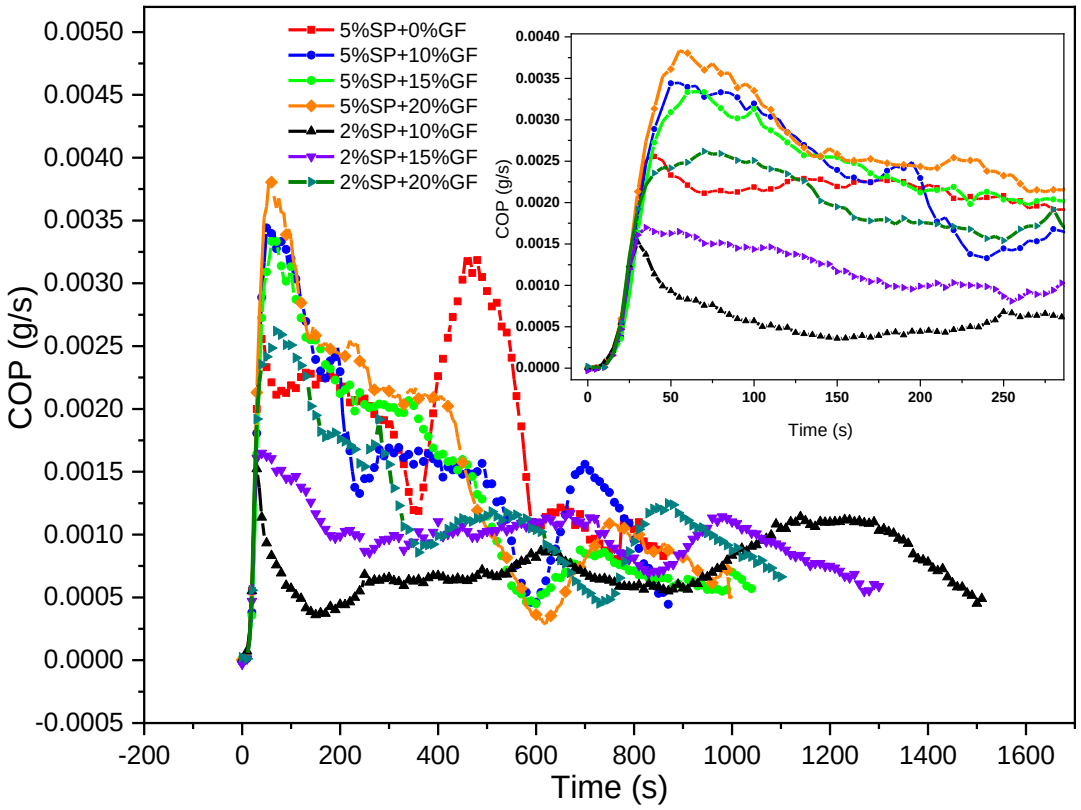

Figure 6-5 : Influence of different GF and SP loadings on Carbon monoxide production rate

The Figure 6-5 show the effect of glass fibre and synergistic effect of sepiolite from the material without glass fibre release more CO and it is optimal when use 20% IFR with 20%GF. The 2%SP+10% GF show also similar trend and it important to reduce flame retardant load in order not (damage or degrade) properties such as mechanical properties The graph showed the highest peak for the composites having 5% SP and 20% GF. The second highest peak is observed for 5 % SP and 0 % GF at another time period. The graph also shows second peak but at different time the second peak in 2wt.%SP+10 wt.% GF at around 900 second and the other is by 210 second. the char breaking and the intumescent material form new char.

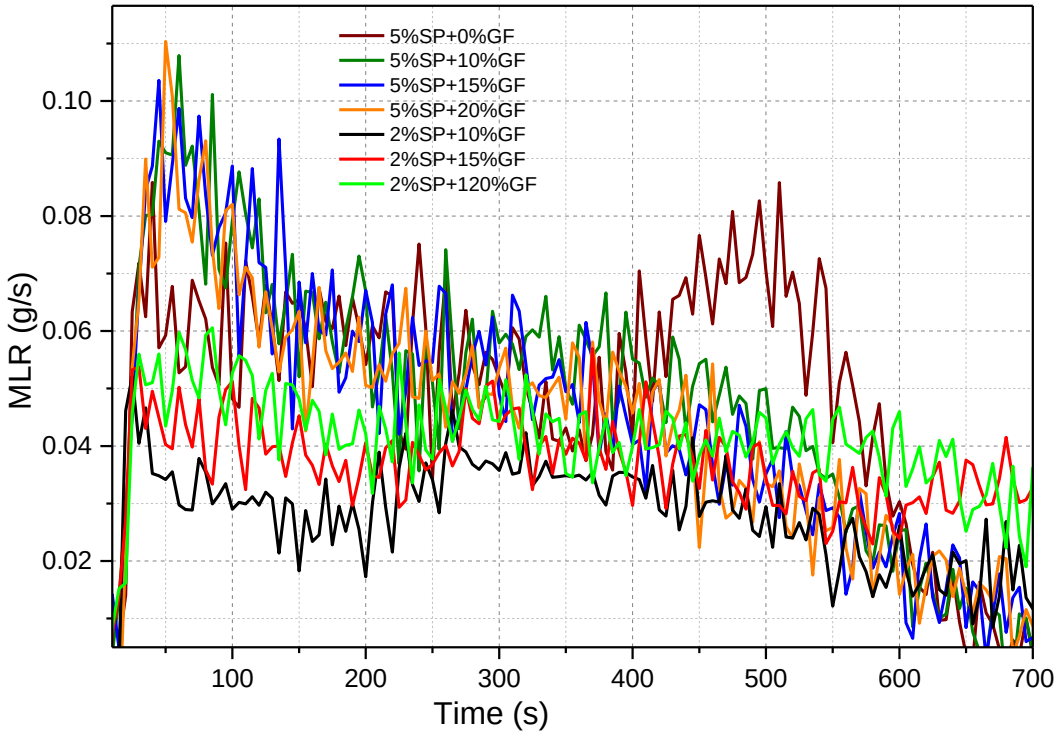

Figure 6-6 : Influence of different GF and SP loadings on MLR with time

Figure 6-6 shows the influence of glass fibre and sepiolite loading on the MLR. The measurements were made using cone calorimeter. Sample with 2% SP and 10% GF exhibits the least MLR. With the increase in GF content MLR increases. It is also observed that with the increase in SP content, there is an increase in MLR. Sample with 5% SP and 20% GF exhibits the highest MLR. But the sample with 0% GF initially exhibits lesser MLR and over the period of time losses more mass. The reason for this can be attributed to the formation of char that protects the PP. The results are in agreement with the work carried out by (Xu *et al.*, 2013)

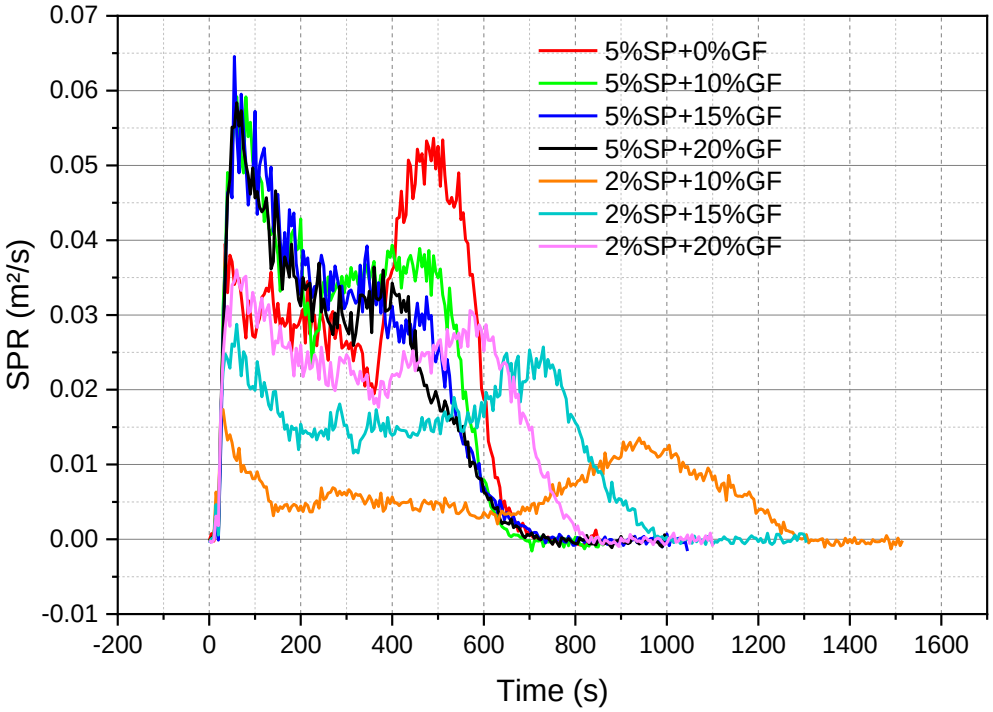

Figure6-7:Influence of glass fibre and nanoclays content and types on the smoke production rate (SPR)

Smoke production rate (SPR) is an important parameter for evaluating flame retardancy and flammability of polymeric materials. Smoke production is one of the most important issues as smoke inhalation can cause death. The amount of smoke production rate (SPR) and total smoke production (TSP) are the principal causes of death during fire. Thus, the determination of SPR and TSP for the various polymer compositions will be useful in indicating the relative hazard under well-ventilated conditions presented by these materials Shown in Figure 6-7 and Table 6-3 indicates that the smoke emission is retarded and delayed during the whole emission process and this is for the reason that the flame retardant and sepiolite inhibits the SPR by char formation released intumescent flame retardant. In case of 2% SP, the IFR is 18% and SPR is the least. Further, with the decrease in IFR percentage the SPR increases. The 5% SP and 15% IFR sample exhibits the highest SPR. The GF promotes more SPR initially and samples attain thermal stability over the period of time as observed from the

6.8 LOI and UL-94 testing of PP/PA6 composites

UL-94 vertical flammability tests were carried out using specimens of approximate dimensions of 127mm x 12.7mm x 3 mm. 5 specimens of each formulation were burnt in the test and the materials are classified according to the criteria given in the table shown in Table 6-1.

The Table 6-4 showed the ignitability (LOI) and anti-dripping value of UL94classification.It is increased from 22% with SP and with no flame retardancy. When the value of SP is 5%, the LOI decreases to about 22 V% mixture of minimum oxygen with classification V2 This results with agreement with CCT.

Table 6-4: Ul94V classification and LOI for different glass fibre loading

Sample	LOI	UL-94 rating
GF0IF15SP5	22	No rating
GF10 F15SP5	24	V2
GF15 F15SP5	23	V2
GF20S F15P5	23	V2
GF10 F18SP2	34.5	V0
GF15 F18SP2	32	V0
GF20 F18SP2	32	V0

6.9 Condensed Phase Char Assessment

6.9.1 Flame retardancy mechanism by residue analysis

Figure 6-8 and Figure 6-9 shows the photograph fire residue morphology of 2%SP, and 5%SP loading with glass fibre 10%, 15% and 20% by weight of composites. According to the barrier fire retardant mechanism, the char could form a barrier to both heat and mass transfer, which makes it more difficult for degrading material to leak the vapour phase and prevents heat transfer back to the polymer. Char formation and char structure are important for fire retardant efficiency. Photographs of the char after cone calorimetry are shown in Figure 6-9 front view. The char residue of sample contains compact structure. The char residues of 5%SP show a structure with large cracks and openings in the surface. The char residue of 2%Sp composite showed that the surface of the sample was more completely covered by the char than that in the other samples.

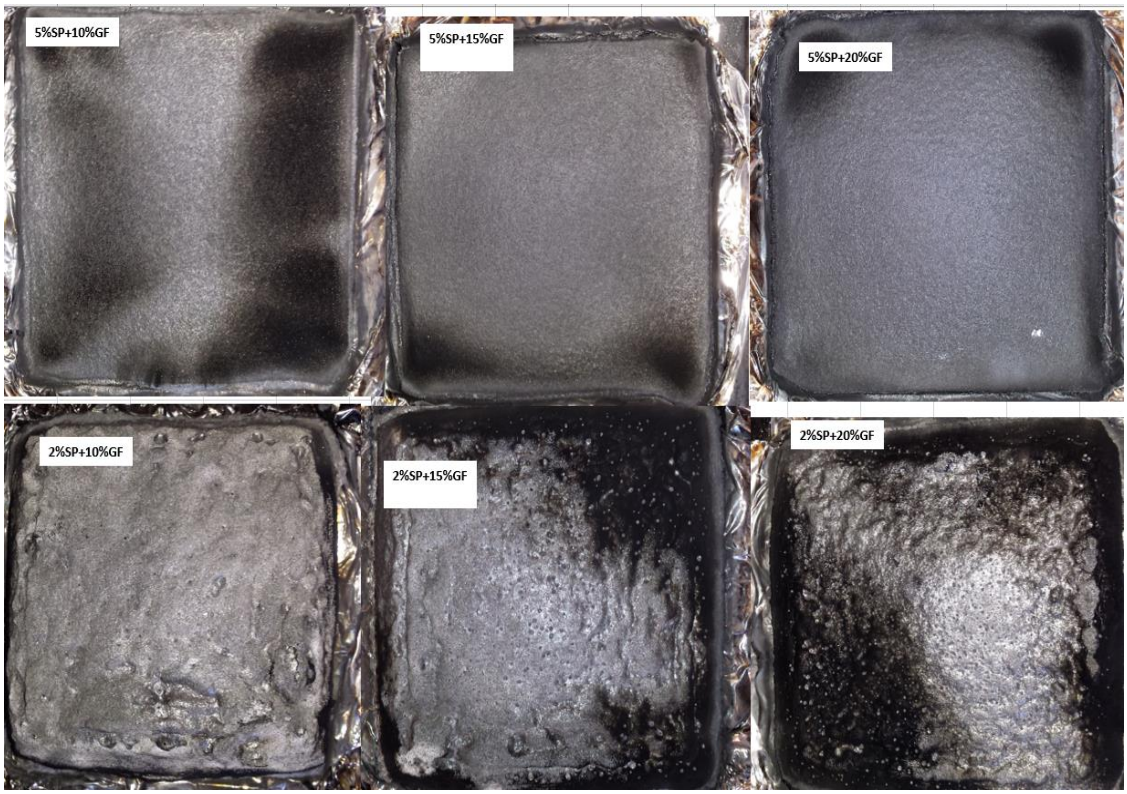

Figure6-8 :Photograph of char residue after CCT for low loading sepiolite 2%SP (top) and higher sepiolite 5%SP(bottom) with GF 10%,15%,20%

Figure 6-9 (c) shows a front view of the char residue and the intumescent char effect. In the case of 2% SP+10% GF with line of the residue whereas when sepiolite is 5% SP showed swelling. This result proves a synergism of sepiolite in which using lower amounts of intumescent and nan fillers.

Figure 6-9 : Photograph of char residue after CCT for low loading sepiolite 2%SP (left) and higher sepiolite 5%SP(right) with GF 10%,15%,20%

6.9.2 X-ray diffraction analysis of composites

XRD is a most frequently used method to characterize the degree of dispersion of nanoparticles in the polymer. XRD plots of PP/PA6n composites are given in Figure 6-10 and Figure 6-12. The peaks obtained were corresponding to the planes (110),(040),(130) represents α form of iPP. Mani *et al.* (2005) observed the similar peaks in the XRD pattern of isotactic PP.

X-ray diffraction pattern of nanocomposites show sharp and highly intense peaks whereas when glass fibre more than 20% the crystallinity decreases and shows less intensity peak. This may be due to the development of crystallinity in the polymer. When sepiolite is 2%, the angle

shifted to lower angle 7°compare with sepiolite at 7.3°, which proves the formation of intercalated nanocomposite. For the composite C14 (2%Sp+10%GF) supports the cone calorimeter, which show the best flame retardancy and with classification V0 the results were in line with most of authors.

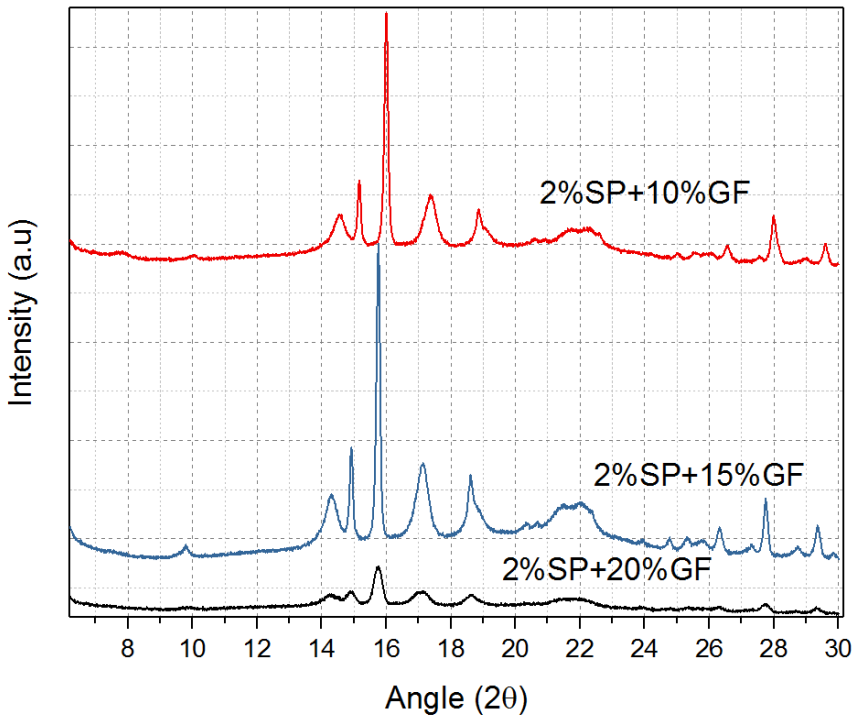

Figure 6-10:X-ray diffraction with low loading sepiolite loading (2%SP) and different glass fibre

When the sepiolite increased from 2 to 5% The angle shifted to higher angle with increase in intensity compare to the previous graph which doesn't show any peak. The composite formed in this case was conventional composite. This explained why the composite was more flammable than that with 2%Sp and provided synergistic effect to intumescent flame retardant was as shown in Figure 6-12.

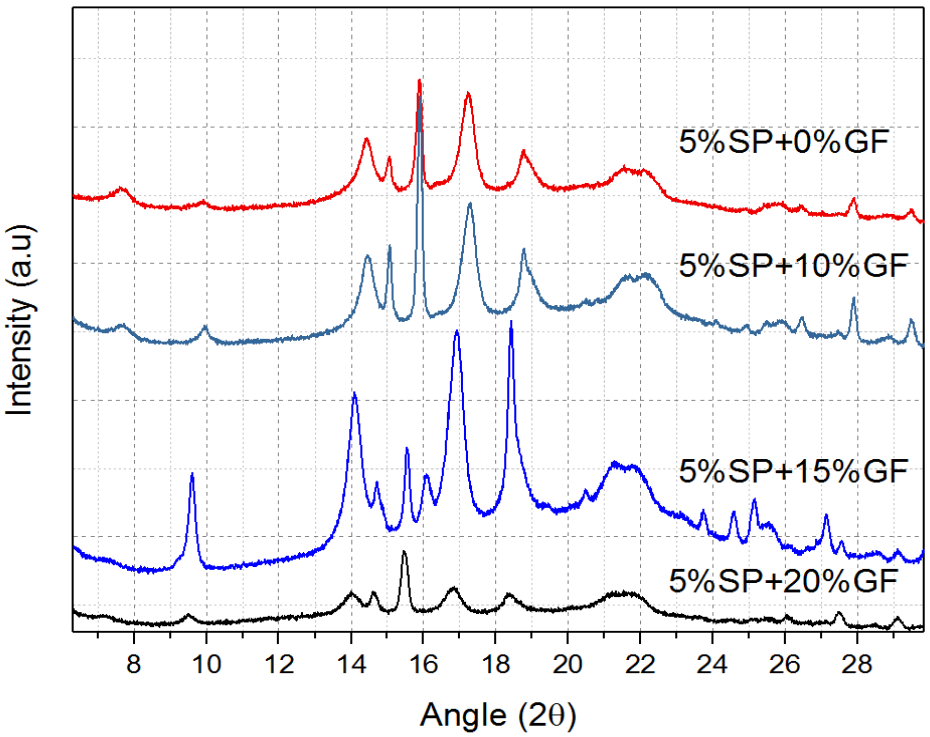

Figure6-11: X-ray diffraction with higher loading sepiolite (5%SP) loadings and different glass fibre contents

Software EVA is used with X-ray diffraction; the crystallinity was calculated. It decreases from 64% when no glass fibre is added and decreases further to 49% without incorporating sepiolite. All high sepiolite loading has slight decrease in crystallinity and become 54% when 2%SP is used.

6.9.3 Influence of glass fibre load and sepiolite on thermal stability and the decomposition

Table 6-5 shows the onset temperatures of degradation (T5%, T10% and T50%: temperature at 5%, 10% and 50% loss of mass, respectively) and the maximum degradation temperatures (T_{max}) of all formulations under nitrogen and air.

Table 6-5: Temperatures at 5% ,10% and 50% mass loss and maximum degradation temperatures (T_{max}), and R=residue for PP / PA6/ IFR systems under nitrogen and air

Sample code	Weight loss under Air					Weight loss under Nitrogen				
	$T_{5\%}$	$T_{10\%}$	$T_{50\%}$	T_{max}	R %	$T_{5\%}$	T_{10}%	$T_{50\%}$	$T_{max.}$	R %
GF0F15SP5	321	346	423	473	12	330	350	434	450	13
GF10 F15SP5	309	328	416	426	26.6	336	354	443	450	26
GF15 F15SP5	306	324	399	397	29.5	326	349	447	455	28
GF20S F15P5	299	341	471	472	33	318	347	452	454	35
GF10 F18SP2	308	330	400	410	21	336	351	446	455	24
GF15 F18SP2	307	326	406	411	27	339	355	451	458	27
GF20 F18SP2	289	316	418	442	29	319	348	450	452	32

Table 6-5 shows the temperatures of onset of degradation (T5% T10% and T50%: temperature at 5% ,10% and 50% of loss of mass respectively) and the maximum degradation temperatures (T_{max}) of all the formulations was studied under nitrogen and air. Therefore, the decreased thermal stability is likely essential rather than a drawback of the intumescent.

Table 6-5 shows the nanocomposite with 5% SP, 15% GF and 10% GF, the char residual (R)content at 700 ° C increased by 85% to 24% compared to sample without glass fibre (R=13%), which clearly indicates the formation of an intumescent char residue and it reach maximum temperature in air 472° C.

Incorporation of higher sepiolite 5% SP and IFR 15% significantly improves the thermal stability of the nanocomposite. The maximum char residue35% in nitrogen and maximum temperature is 454°C. Therefore, one can see that glass fibre with sepiolite helps in the formation of the char, which prevent the mass and heat transfer. Incorporation of 15% APP with or without glass reduces the overall thermal stability of composites.

Figure 6-12 shows the oxidative thermal degradation when the amount of SP and intumescent flame retardant is fixed to 5% and 15% respectively. The composite GF0F15SP5 without glass fibre is stable at temperature 340 to 460°C and it is stabilized when 15%GF is added. The samples tend to be more stable in the temperature range of 460 and 700°C. With the increase in the glass fibre content, the stability increases. But out of all samples, sample with 15% GF finds to be more suitable at every stage of temperature.

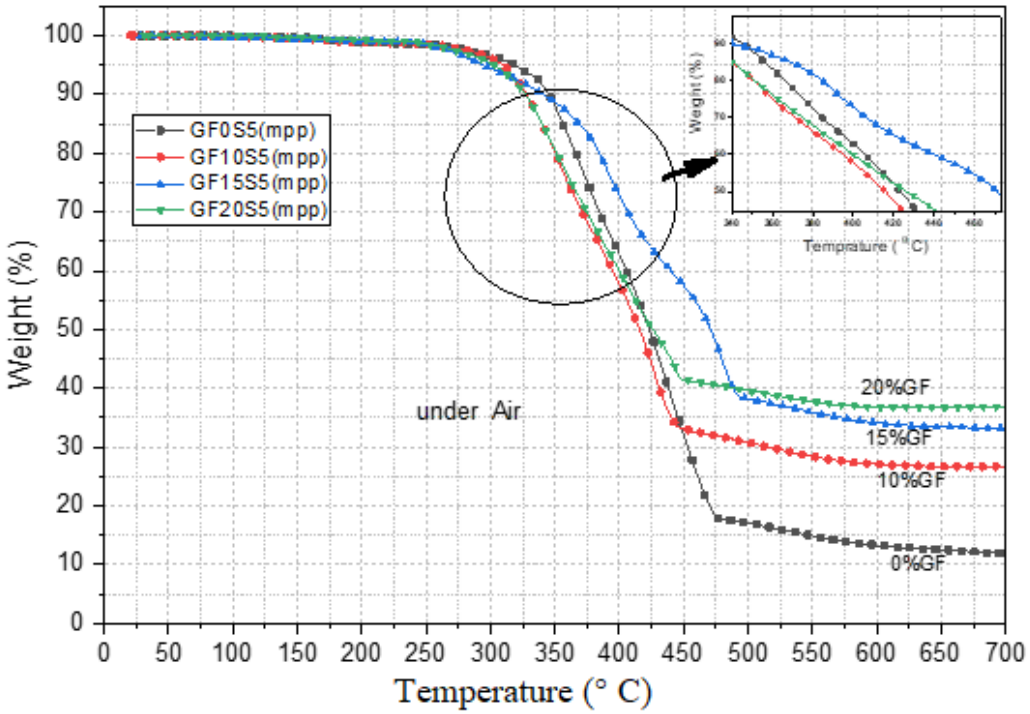

Figure 6-12 : Oxidative thermal degradation of samples with 5%SP and different GF loadings with temperature

The char residue at 700°C is increased with increase in the amount of glass fibre. It increases to 13%,27%,34% and 37% for Glass fibre load of 0% GF,10%GF,15% GF and 20% GF respectively. This means glass fibre improves the thermal stability and prompted the formation of char.

Figure 6-13 shows thermal stability of the composite with glass fibre loading in nitrogen with10%, 15% and 20% GF with loadings of 2%SP and 5%SP. The graph shows clearly the two trends- the first is noticed when the load of synergy agent is 2%SP at early stage. It is stable when glass fibre more than 15%. Higher the temperatures, the char residue is higher. When incorporate of 5%SP within creased glass fibre, increases the char to 23.6%. When 2%SP added into 10% GF, there is increase in the char residue of 36%.

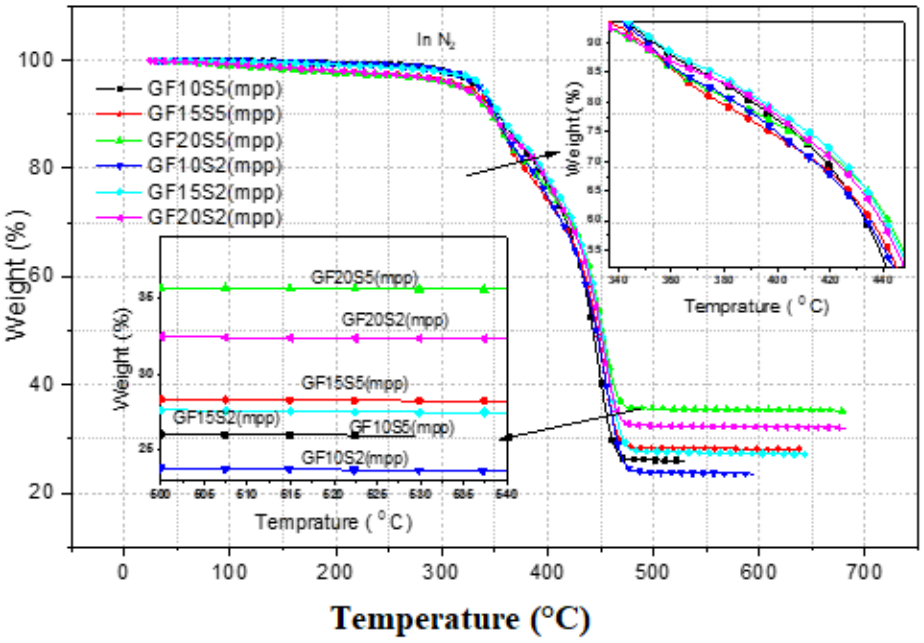

Figure 6-13 Thermal stability for different glass loading with 2%SP, 5%SP in inert N2

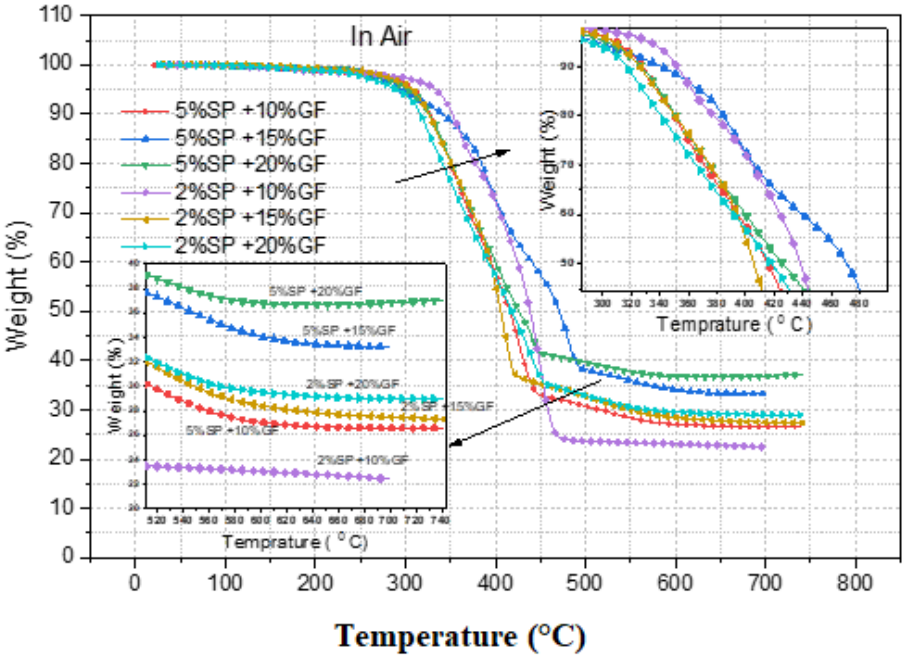

Figure 6-14:Oxidative thermal stability for different glass loading with 2%SP and 5%SP

Figure 6-14 shows the oxidative degradation at different temperatures up to 400 °C. It is stable at 15%GF with 5% SP and the less stable at 2%SP with 15%GF. At higher loading, chare residue increases from char 23% for composite with 2wt.%SP and 10wt.%GF and the higher residue is 37% at loading of 5%Sp and 20% GF. It is more stable in air than in nitrogen.

The maximum temperature is shown in Figure 6-15, which is the derivative of weights over temperature in air. Two peaks were observed, the first is the due to the degradation of APP765 and the second is at PP decomposition. It is quoted that the highest T_{max}(5wt.% SP and 15 wt.% GF) is 470 °C.

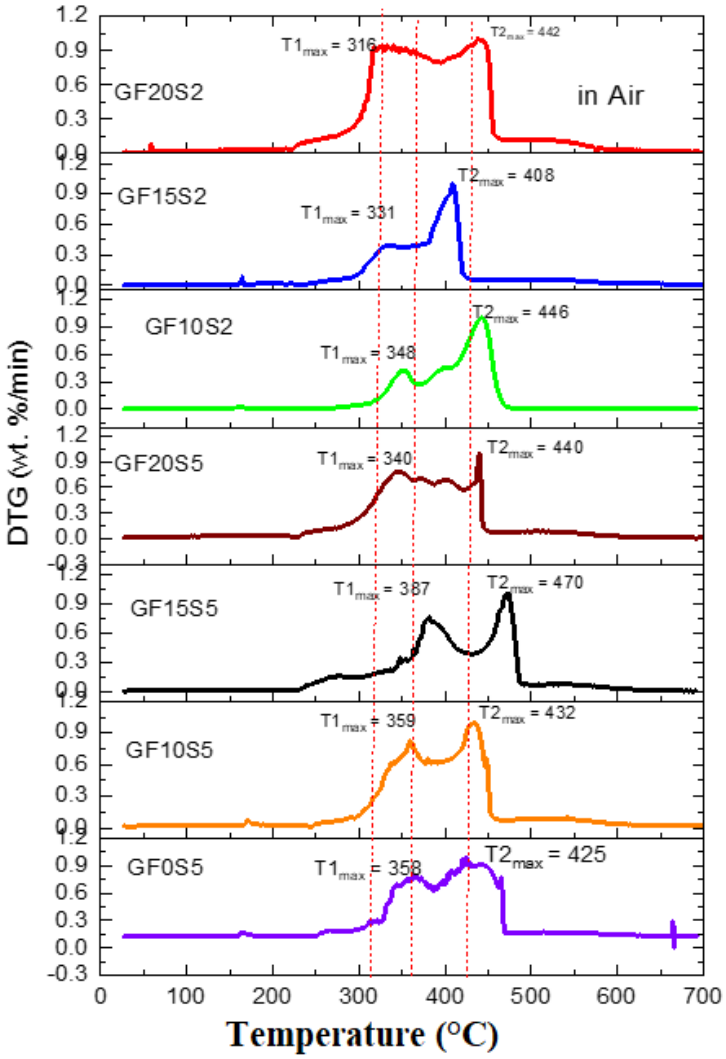

Figure6-15 :DTGA for the composite with different glass loading and 2%sSP and 5%SP in air

The DTG analysis for the composites with different glass fibre and sepiolite loadings was performed and is shown in the Figure 6-15. The results of the study indicate that the GF15S5 sample exhibits a maximum temperature of 470 °C and the two peaks were observed from the graphs. The first peak indicates the degradation of AP765 and the second peak

indicates the degradation of PP/PA6. In case of 2%SP and 20% GF, low decomposition of APP765 mean acceleration in retarding the polymer and form char.

Figure 6-16 is the derivative of weights over temperature in nitrogen. It has shown two peaks, the first is due to the degradation of APP765 and the second is for PP decomposition. The highest Tmax at 5%SP and 15wt.%GF is 454 ˚C and the 2wt.%SP and 10 wt.% GF shows low decomposition of APP765 at 320 ˚C that means the accelerated retardation of the polymer and form char.

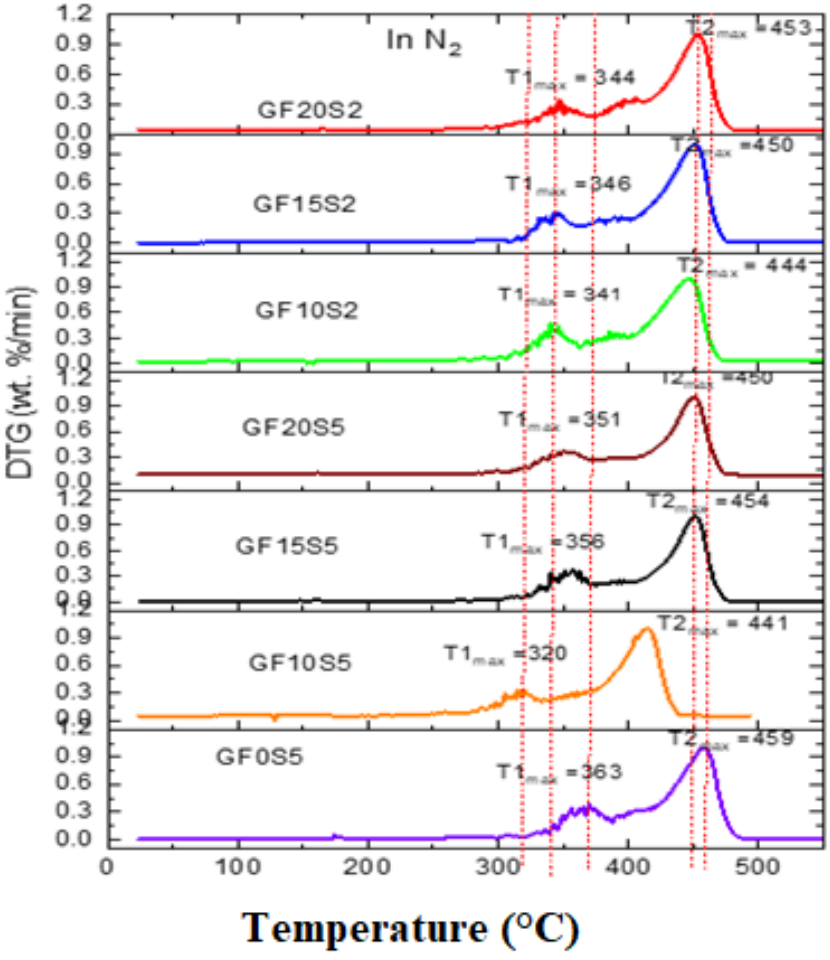

Figure 6-16 : DTGA for the composite with different glass loading and 2wt.% SP and 5wt.%SP in nitrogen

6.10 Effect of sepiolite and glass fibre on mechanical properties

The tensile strength was conducted on two types of samples viz., 2 wt.% SP and 5 wt.% SP as indicated in the Table 6-6. Glass fibre content was varied in both the samples. The GF content considered in the experiments were 10%, 15% and 20%. From the Table 6-6, it is understood that the samples with 2 wt. % SP exhibits a higher tensile strength as against 5 wt. % SP. The samples with 2 wt. % SP shows a linear increase in the strength with respect to the increase in glass fibre content. The maximum tensile strength attained was 45 MPa for 2 wt.% SP. Also, it can observe that with the increase in sepiolite from 2% to 5% the strength decreases.

Table 6-6: Effect of Sepiolite and Glass fibre addition on Tensile strength

Loading	Tensile strength (MPa)	
Sepiolite (%) / **Glass fibre loading(%)**	2 wt.% SP	5 wt.% SP
10	36 ±0.41	34.7 ±0.47
15	41 ±0.96	35.6 ±2.57
20	45±1.33	39.5 ±0.96

Tensile Modulus test was conducted on the 2 wt.% SP and 5 wt.% SP samples. The results of the test revealed that 2wt. % SP samples indicated a reduced modulus value at lower GF content and an enhanced modulus value at 20% GF content and on the other hand 5wt.% SP samples showed a higher modulus value at lower content of GF and a reduction in modulus value. at 20 wt.% GF The maximum value of GF as recorded from the experiments was 4.6 GPa for 2 wt.% SP it is understood that the samples with 2 wt. % SP and 5 wt. % SP has no effect on tensile modulus.

Table 6-7: Effect of Sepiolite and Glass fibre addition on Tensile Modulus

Loading	Tensile modulus (GPa)	
Sepiolite (%) / **Glass fibre loading (%)**	2 wt.% SP	5 wt.% SP
10	3.43 ± 0.16	3.5 ± 0.15
15	4 ± 0.13	4.3 ± 0.35
20	4.6 ± 0.21	4.4 ± 0.21

The flexural test was conducted on the samples with 2wt.% SP and 5wt.% SP with varying GF content. The results of the tests indicated that 2wt% SP samples exhibited better flexural strength value as compared with 5 wt.% samples. At lower content of GF, the load bearing capacity of samples is less and with the increase in GF content, the capacity increases. A steady increase in flexural strength is observed with 2wt.% SP samples. At 20 wt.% GF, wt.% SP and 5wt% SP samples exhibits almost a same value. The maximum flexural strength observed was 71 MPa. This value is much higher than the tensile strength value. for 2wt.% samples as observed from Table 6-8.

Table 6-8: Effect of Sepiolite and Glass fibre addition on flexural modulus

Loading	Flexural modulus (GPa)	
SP (%) / **GF(%)**	2 wt.% SP	5 wt.% SP
10	3.0±0.03	3.03 ± 0.04
15	3.62±0.02	3.7 ± 0.06
20	4.35±0.07	4.3 ± 0.08

The flexural modulus test was conducted on samples. The maximum value as observed from the Table 6-9 is 4.3 GPa for 2 wt.% SP The flexural modulus of 2 wt.% SP samples is a bit higher at 10% GF content but a higher modulus value can be observed at 20% GF. A contrasting result can be observed with 5 wt.% samples. The modulus value at 10% GF is lesser and increases thereafter. But at 20% GF, a reduction in modulus value is observed. The reason for this behaviour can be attributed towards good interfacial adhesion between the sepiolite and glass fibre at lower wt.% of SP and higher wt.% of GF.

Table 6-9: Effect of Sepiolite and Glass fibre addition on flexural Strength

Loading	Flexural strength (MPa)	
Sepiolite (%) / **Glass fibre loading(%)**	2 wt.% SP	5 wt.% SP
10	62 ±0.43	59 ± 0.41
15	67 ±1.4	62± 0.61
20	71 ±1.31	70.5 ± 2.46

The effect of sepiolite and Glass fibre addition on the impact strength can be observed from Table 6-10. The results of the tests indicate that samples with 2wt% SP shows a reduced strength as compared with 5wt.% samples. It is observed that at lower GF content samples tend to have higher impact. With the increase in GF content the samples tend to lose the strength. The reason for the decrement in strength could be attributed to the sepiolite and glass fibre aggregates that symbolise stress-concentration regions, which further acts as crack initiators. This results in the loss of toughness and drastic reduction in the energy absorption.

Table 6-10: Effect of Sepiolite and Glass fibre addition on impact strength

Loading	Impact strength (kJ/m^2)	
Sepiolite (%) / Glass fibre loading(%)	2 wt.% SP	5 wt.% SP
10	18±0.23	20±0.24
15	17.5±0.3	18±0.2
20	17±0.28	17.8 ±0.36

6.11 Summary

The following conclusions can be derived from the experiments:

The effect of the glass fibre(GF), flame retardant (IFR) and nanoclay (SP) addition on LOI was studied and is enlisted in the Table 6-4. The LOI of GF10SP2 sample reaches 34.5 and is the highest among all the samples tested. It can be observed that the samples with increased flame retardant and decreased sepiolite (nanoclay) content exhibits enhanced LOI with the increase in GF content. But for samples with increased sepiolite and reduced FR content, the LOI reduces. Interestingly, the GF has no or very minimal effect on samples(GF0SP5, GF10SP5, GF15SP5, GF20SP5) with 5% of sepiolite content. But samples with 5% sepiolite exhibits V2 rating in the UL-94 standard. This indicates that although these samples are considered as pass samples, yet they exhibit some dripping. But samples (GF10SP2, GF15SP2, GF20SP2) with 2% sepiolite content exhibits V0 rating and can be considered to be the best samples.

The effect of the glass fibre, flame retardant (IFR) and nanoclay (SP) addition on different combustion parameters such as TTI, PHRR, THR, mass residue, MLR, SPR and COP obtained from the cone calorimetry studies is summarized with respect to the increase in GF and sepiolite content. From Table 6-5 it is observed that, with the increase in GF, increases residue mass(R), MLR, SPR and COP; whereas it reduces THE. Also, increase in sepiolite content from 2% to 5% increases THE, PHRR, MLR, SPR and COP. A sample is always expected to have low THE, PHRR, MLR, COP, SPR and high residue mass. These expected vales can be observed in GF10SP2 sample when compared with GF0SP5. The GF10F15SP5 and GF10F18SP2 samples differ only with respect to PHRR and Residue values. The GF10SP2 samples exhibits 128.15% reduction in PHRR and 15% increased residue mass as compared with GF10SP5. Thus, this is one of the evidences of synergy effect when the sepiolite content is added in small quantity.

Summary of the thermal stability analysis on samples with glass fibre, flame retardant (IFR) and nanoclay (SP) addition indicates that with the increase in GF, the temperature required to completely burn off the material is more. This helps in formation of more char. The matrix burns off, whereas for the fibres, it takes more time and temperature to undergo degradation. GF20F15P5 and GF20F18P2 exhibits the lowest onset temperature of 299 °C and 289 °C and at T50% the values are 471 °C and 418 °C respectively. This indicates that the addition of GF plays an important role in the material. Observation also reveals that increase of sepiolite from 2% to 5% and reduction in flame retardant content from 15% to 18% reduces the degradation temperature in case of samples with 10 and 20% GF. But in case of samples with 15% GF the degradation temperature increases by about 7 °C. Therefore, to conclude GF20F15SP5 sample has a better thermal stability over the other samples.

The effect of the glass fibre, flame retardant (IFR) and nanoclay (SP) addition on the mechanical properties indicates that the addition of glass fibre and sepiolite enhances the tensile and flexural strength. The maximum tensile and flexural strength observed were 45 MPa and 71 MPa at 20% glass fibre and 2 wt. % of sepiolite content. The increase in tensile strength and flexural strength for 2 wt.% and 5wt.% samples with 10% and 20% Gf were 18.98% and 11.96% and 12.67% and 16.31% respectively. A good improvement in tensile and flexural modulus was also observed The maximum tensile and flexural modulus observed for 2 wt. %

samples were 4.4 GPa and 4.35 GPa. The increase in glass fibre content did not have much effect on the impact strength of the samples.

CHAPTER 7 : CONCLUSIONS AND RECOMMENDATIONS FOR FUTURE STUDY

This chapter presents the conclusions drawn from the investigations carried out in this thesis. It also gives some recommendations for future work in the area of development of flame retardancy, thermal stability, and mechanical properties of hybrid nanocomposite of PP/PA6 blends

7.1 Conclusions

The following conclusions can be drawn from the research carried out in this thesis:

- **Effect of compatibiliser types on the properties of flame retardancy, thermal stability, and mechanical properties:**
    - Flame retardancy: The compatibiliser type SEBS-g-MA shows better flame retardancy than PP-g-MA when it is added in hybrid nanocomposites PP/PA6/GF/APP, except for the total heat released rate.
    - Addition of Nanofil 5 to the compatibiliser type SEBS-g-MA shows better flame retardancy when glass fibre is incorporated.
    - Thermal stability: SEBS-g-MA shows better thermal stability and produces more char residue, and shows the best performance best when Nanofil5 is used—5 wt.% N5 with 15 wt.%FR.
    - Mechanical properties: PP/PA6 blends the compatibiliser with PP-g-MA to improve the mechanical properties such as tensile strength, tensile modulus, flexural modulus, and flexural strength, whereas

SEBS-g-MA improves the impact strength and elongation at break (strain to break).

- **Influence of intumescent flame retardant on properties of flame retardancy, thermal stability, and mechanical properties:**

  - Flame retardancy: The higher the flame retardant content IFR (20 wt.%), the better the flame retardancy. Sepiolite exhibits synergy at loadings between 2%SP and 3%Sp.

  - Thermal stability: The higher the IFR loading (20 wt.%) the better the thermal stability; sepiolite shows synergy at loadings below 5 wt.%SP.

  - Mechanical properties: Increasing the flame retardant contents increases the mechanical properties, except for the modulus of elasticity, with the highest modulus of elasticity at loading 18 wt.% IFR and 2 wt. %. SP .

- **The influence of glass fibre and sepiolite on properties of flame retardancy, thermal stability, and mechanical properties:**

  - Flame retardancy: Addition of glass fibre improves the flame retardancy of the composite. There is a synergistic effect at 2%SP, and the best retardancy is exhibited when the glass fibre is 10% GF. Samples with 10% GF and 2% SP exhibits 128.15% reduction in PHRR and 15% increased residue mass. This indicates that the composite suppresses the heat and smoke production.

- Thermal stability: Increase in the amount of glass fibre shows higher thermal stability, as the temperature required to completely burn off the material is more, i.e., temperature for degradation is more. But, the degradation temperature decreases with the increase in sepiolite (2% to 5%) and reduction in flame retardant (18% to 15%). Therefore, composite with 5% SP and 20% GF exhibits better thermal stability over other samples.

- Mechanical properties: The glass fibre improves the tensile and flexural strengths but has a negative effect on the impact strength and strain to break; it shows the synergistic effect at 2%SP.

The best flame retardancy (in terms of flammability and supressed smoke production) is at 2 wt.%SP+18 wt.% IFR+10 wt. % GF in the composite, measured by CCT. Digital photography shows swelling and more compact structures than when using a higher glass fibre loading because a higher glass fibre content destroys the intumescence of the intumescent flame retardants and the continuity of the residue char, which decrease the flame retardancy of IFR in the IFR-higher glass fibre content

7.2 Recommendations for Future Work

In the current study suggestions for suitable formulation of hybrid composite PP/PA6 with different loadings of intumescent flame retardant and sepiolite nanoclay were used. In order to further develop an understanding of flame retardancy and enhance its chances for large-scale industrial commercialization, the following future research recommendations are made:

- It was found that a higher loading of sepiolite (>3%) had a negative effect on flame retardancy and mechanical properties due to agglomeration that forms conventional composites and not nanocomposites. In order to avoid such agglomerations, it is recommended to use lower content of sepiolite

- Study the effect of organically modified sepiolite for different weight percentages, 0.5, 1, 1.5, and 2%, on flammability, thermal stability, and mechanical properties.

- Literatures reveal that studies on the use of nanoclay and its effects on flammability and other properties have been carried out. It is also understood that nanoclay helps in forming a strong and tough char structure that acts as a shield protecting the underneath polymer matrices from heat and mass transfer. However, studies related to the use of nanoclays in different combinations and reduced flame retardant content are very limited. Thus, the studies could help in identifying the best combination of nanoclays to achieve optimal thermal and mechanical properties with enhanced flame retardancy.

List of References

Alexandre, M. and Dubois, P. (2000) 'Polymer-layered silicate nanocomposites: preparation, properties and uses of a new class of materials'. Materials Science and Engineering: R: Reports, 28(1), PP 1-63.

Almeras, X., Dabrowski, F., Le Bras, M., Delobel, R., Bourbigot, S., Marosi, G. and Anna, P. (2002) 'Using polyamide 6 as charring agent in intumescent polypropylene formulations II. Thermal degradation'. Polymer degradation and stability, 77(2), PP 315-323.

Anna, P., Marosi, G., Bourbigot, S., Le Bras, M. and Delobel, R. (2002) 'Intumescent flame retardant systems of modified rheology'. Polymer degradation and stability, 77(2), PP 243-247.

Aseeva, R. M. and Zaikov, G. (1986) Combustion of polymer materials. Munich: Hanser publisher.

Bao, C. L., Song, L., Guo, Y. and Hu, Y. (2011) 'Preparation and characterization of flame-retardant polypropylene/α-titanium phosphate (nano) composites'. Polymers for Advanced Technologies, 22(7), PP 1156-1165.

Bartholmai, M. and Schartel, B. (2004) 'Layered silicate polymer nanocomposites: new approach or illusion for fire retardancy? Investigations of the potentials and the tasks using a model system'. Polymers for Advanced Technologies, 15(7), PP 355-364.

Beyler, C. L. and Hirschler, M. M. (2002) 'Thermal decomposition of polymers'. SFPE Handbook of Fire Protection Engineering, 2, PP 111-131.

List of References

Bocchini, S., Frache, A., Camino, G. and Claes, M. (2007) 'Polyethylene thermal oxidative stabilisation in carbon nanotubes based nanocomposites'. European Polymer Journal, 43(8), PP 3222-3235.

Borba, P. M., Tedesco, A. and Lenz, D. M. (2014) 'Effect of reinforcement nanoparticles addition on mechanical properties of SBS/Curauá fiber composites'. Materials Research, 17(2), PP 412-419.

Bourbigot, S. and Duquesne, S. (2007) 'Fire retardant polymers: recent developments and opportunities'. Journal of Materials Chemistry, 17(22), PP 2283-2300.

Bourbigot, S. and Flambard, X. (2002) 'Heat resistance and flammability of high performance fibres: A review'. Fire and materials, 26(4-5), PP 155-168.

Bourbigot, S., Gilman, J. W. and Wilkie, C. A. (2004a) 'Kinetic analysis of the thermal degradation of polystyrene–montmorillonite nanocomposite'. Polymer Degradation and Stability, 84(3), PP 483-492.

Bourbigot, S., Le Bras, M. and Delobel, R. (1993) 'Carbonization mechanisms resulting from intumescence association with the ammonium polyphosphate-pentaerythritol fire retardant system'. Carbon, 31(8), PP 1219-1230.

Bourbigot, S., Le Bras, M., Delobel, R., Decressain, R. and Amoureux, J.-P. (1996a) 'Synergistic effect of zeolite in an intumescence process: study of the carbonaceous structures using solid-state NMR'. Journal of the Chemical Society, Faraday Transactions, 92(1), PP 149-158.

Bourbigot, S., Le Bras, M., Delobel, R. and Tremillon, J.-M. (1996b) 'Synergistic effect of zeolite in an intumescence process. Study of the interactions between the polymer and the additives'. Journal of the Chemical Society, Faraday Transactions, 92(18), PP 3435-3444.

List of References

Bourbigot, S., Le Bras, M., Duquesne, S. and Rochery, M. (2004b) 'Recent advances for intumescent polymers'. Macromolecular Materials and Engineering, 289(6), PP 499-511.

Bourbigot, S., Siat, C. and Le Bras, M. (1998) 'Combustion behaviour of ethylene vinyl acetate copolymer-based intumescent formulations using oxygen consumption calorimetry'. Fire and materials, 22(3), PP 119-128.

Braun, U., Bahr, H., Sturm, H. and Schartel, B. (2008) 'Flame retardancy mechanisms of metal phosphinates and metal phosphinates in combination with melamine cyanurate in glass-fiber reinforced poly (1, 4-butylene terephthalate): the influence of metal cation'. Polymers for Advanced Technologies, 19(6), PP 680-692.

British standard institution (1996) BS EN ISO 4589-2:1999: Plastics. Determination of burning behaviour by oxygen index. Ambient-temperature test. London: British standard institution.

British standard institution (2015) BS EN ISO 13927:2015 : Plastics — Simple heat release test using a conical radiant heater and a thermopile detector. London: British standard institution.

British Standards Institution (2016) BS EN ISO 4589-1. Plastics. Determination of burning behaviour by oxygen index. Part 1. Guidance. London: British standard institution.

Burton, B. L. (1993) 'The thermooxidative stability of cured epoxy resins. I'. Journal of Applied Polymer Science, 47(10), PP 1821-1837.

Camino, G., Costa, L. and Martinasso, G. (1989) 'Intumescent fire-retardant systems'. Polymer Degradation and Stability, 23(4), PP 359-376.

Camino, G., Costa, L. and Trossarelli, L. (1984a) 'Study of the mechanism of intumescence in fire retardant polymers: Part I—Thermal degradation of ammonium polyphosphate-pentaerythritol mixtures'. Polymer Degradation and Stability, 6(4), PP 243-252.

Camino, G., Costa, L. and Trossarelli, L. (1984b) 'Study of the mechanism of intumescence in fire retardant polymers: Part II—Mechanism of action in polypropylene-ammonium polyphosphate-pentaerythritol mixtures'. Polymer Degradation and Stability, 7(1), PP 25-31.

Carpentier, F., Bourbigot, S., Le Bras, M. and Delobel, R. (2000) 'Rheological investigations in fire retardancy: application to ethylene–vinyl-acetate copolymer–magnesium hydroxide/zinc borate formulations'. Polymer international, 49(10), PP 1216-1221.

Casalini, R., Bogoslovov, R., Qadri, S. and Roland, C. (2012) 'Nanofiller reinforcement of elastomeric polyurea'. Polymer, 53(6), PP 1282-1287.

Chang, J.-H., An, Y. U., Kim, S. J. and Im, S. (2003) 'Poly (butylene terephthalate)/organoclay nanocomposites prepared by in situ interlayer polymerization and its fiber (II)'. Polymer, 44(19), PP 5655-5661.

Chartoff, R. and Sircar, A. (2005) Thermal analysis of polymers, encyclopedia of polymer science and technology. New Jersey: John Wiley & Sons.

Chen, H., Zheng, M., Sun, H. and Jia, Q. (2007) 'Characterization and properties of sepiolite/polyurethane nanocomposites'. Materials Science and Engineering: A, 445, PP 725-730.

Chen, X. and Jiao, C. (2011) 'Flame retardancy and thermal degradation of intumescent flame retardant polypropylene material'. Polymers for Advanced Technologies, 22(6), PP 817-821.

Chen, X., Jiao, C. and Wang, Y. (2009) 'Synergistic effects of iron powder on intumescent flame retardant polypropylene system'. Express Polymer Letters, 3(6), PP 359-365.

Chen, Y. and Wang, Q. (2006) 'Preparation, properties and characterizations of halogen-free nitrogen–phosphorous flame-retarded glass fiber reinforced polyamide 6 composite'. Polymer Degradation and Stability, 91(9), PP 2003-2013.

Chrissafis, K., Paraskevopoulos, K., Stavrev, S., Docoslis, A., Vassiliou, A. and Bikiaris, D. (2007) 'Characterization and thermal degradation mechanism of isotactic polypropylene/carbon black nanocomposites'. Thermochimica Acta, 465(1), PP 6-17.

Cinausero, N., Howell, B., Schmaucks, G., Marosi, G., Brzozwski, Z., Cuesta, J. L., Nelson, G., Camino, G., Wilkie, C. and Fina, A. (2008) Fire retardancy of polymers: new strategies and mechanisms. Royal Society of Chemistry.

Cipiriano, B. H., Kashiwagi, T., Raghavan, S. R., Yang, Y., Grulke, E. A., Yamamoto, K., Shields, J. R. and Douglas, J. F. (2007) 'Effects of aspect ratio of MWNT on the flammability properties of polymer nanocomposites'. Polymer, 48(20), PP 6086-6096.

Clerc, L., Ferry, L., Leroy, E. and Lopez-Cuesta, J.-M. (2005) 'Influence of talc physical properties on the fire retarding behaviour of (ethylene–vinyl acetate copolymer/magnesium hydroxide/talc) composites'. Polymer Degradation and Stability, 88(3), PP 504-511.

Coquelle, M., Duquesne, S., Casetta, M., Sun, J., Gu, X., Zhang, S. and Bourbigot, S. (2015) 'Flame retardancy of PA6 using a guanidine sulfamate/melamine polyphosphate mixture'. Polymers, 7(2), PP 316-332.

List of References

Cullis, C., Hirschler, M. and Tao, Q. (1991) 'Studies of the effects of phosphorus-nitrogen-bromine systems on the combustion of some thermoplastic polymers'. European polymer journal, 27(3), PP 281-289.

Davies, P. J., Horrocks, A. R. and Alderson, A. (2005) 'The sensitisation of thermal decomposition of ammonium polyphosphate by selected metal ions and their potential for improved cotton fabric flame retardancy'. Polymer degradation and stability, 88(1), PP 114-122.

Davis, R. D., Gilman, J. W. and VanderHart, D. L. (2003) 'Processing degradation of polyamide 6/montmorillonite clay nanocomposites and clay organic modifier'. Polymer Degradation and Stability, 79(1), PP 111-121.

Demir, H., Arkış, E., Balköse, D. and Ülkü, S. (2005) 'Synergistic effect of natural zeolites on flame retardant additives'. Polymer degradation and stability, 89(3), PP 478-483.

EFRA. (2007) Frequently Asked Questions on Flame Retardants. Available at: https://www.flameretardants-online.com/.../item_18192_pdf_1.pdf [Accessed 2015].

Ehrenstein, G. W. (2001) Polymeric Materials Structure : Structure, Properties, Applications. Munich: Carl Hanser

European Flame Retardants Association. (2006) How do flame retardants work Available at: http://flameretardants.eu [Accessed 10 July 2018].

European Flame Retardants Association. (2016) The Reality / Statistics. Available at: http://www.cefic-efra.com/index.php/en/fire-safety/reality-statistics [Accessed 17 October 2016 2016].

Ferrari, A. C. and Robertson, J. (2000) 'Interpretation of Raman spectra of disordered and amorphous carbon'. Physical review B, 61(20), PP 14095.

Ferry, L., Cuesta, J. L., Chivas, C., Hoy, G. M. W. and Dvir, H. (2001) 'Incorporation of a grafted brominated monomer in glass fiber reinforced polypropylene to improve the fire resistance'. Polymer degradation and stability, 74(3), PP 449-456.

Fontaine, G., Bourbigot, S. and Duquesne, S. (2008) 'Neutralized flame retardant phosphorus agent: facile synthesis, reaction to fire in PP and synergy with zinc borate'. Polymer Degradation and Stability, 93(1), PP 68-76.

Freedonia. (2015) World Flame Retardants (Study 3258) Available at: www.freedoniagroup.com [Accessed 2 October 2016].

Fu, M. and Qu, B. (2004) 'Synergistic flame retardant mechanism of fumed silica in ethylene-vinyl acetate/magnesium hydroxide blends'. Polymer Degradation and Stability, 85(1), PP 633-639.

Fujiwara, S. and Sakamoto, T. (1976) 'Falmmability properties of Nylon-6/mica nanocomposites'. Kokai patent application, no. SHO511976-109998, PP.

Galloway, J. A., Koester, K. J., Paasch, B. J. and Macosko, C. W. (2004) 'Effect of sample size on solvent extraction for detecting cocontinuity in polymer blends'. Polymer, 45(2), PP 423-428.

Gijsman, P., Hennekens, J. and Vincent, J. (1993) 'The mechanism of the low-temperature oxidation of polypropylene'. Polymer Degradation and Stability, 42(1), PP 95-105.

Gilman, J. W., Jackson, C. L., Morgan, A. B., Harris, R., Manias, E., Giannelis, E. P., Wuthenow, M., Hilton, D. and Phillips, S. H. (2000) 'Flammability properties of

polymer− layered-silicate nanocomposites. Polypropylene and polystyrene nanocomposites'. Chemistry of Materials, 12(7), PP 1866-1873.

Gilman, J. W., Kashiwagi, T. and Lichtenhan, J. D. (1997) 'Nanocomposites: a revolutionary new flame retardant approach'. Sampe Journal, 33, PP 40-46.

Grand, A. F. and Wilkie, C. A. (2000) Fire retardancy of polymeric materials. CRC Press.

Green, J. (1992) 'A review of phosphorus-containing flame retardants'. Journal of Fire & Flammability, 10(6), PP 470-487.

Gunduz, H. O., Isitman, N. A., Aykol, M. and Kaynak, C. (2009) 'Interfacial interactions and flammability of flame-retarded and short fiber-reinforced polyamides'. Polymer-Plastics Technology and Engineering, 48(10), PP 1046-1054.

Gururaja, M. and Rao, A. H. (2012) 'A review on recent applications and future prospectus of hybrid composites'. Int J Soft Comput Eng, 1(6), PP 352-5.

Gutiérrez, G., Fayolle, F., Régnier, G. and Medina, J. (2010) 'Thermal oxidation of clay-nanoreinforced polypropylene'. Polymer Degradation and Stability, 95(9), PP 1708-1715.

Hollingbery, L. A. and Hull, T. R. (2012) 'The fire retardant effects of huntite in natural mixtures with hydromagnesite'. Polymer Degradation and Stability, 97(4), PP 504-512.

Horacek, H. and Grabner, R. (1996) 'Advantages of flame retardants based on nitrogen compounds'. Polymer Degradation and Stability, 54(2), PP 205-215.

Horrocks, A. R. and Price, D. (2008) Advances in fire retardant materials. Cambridge: Woodhead Publishing.

Hossen, M. F., Hamdan, S., Rahman, M. R., Rahman, M. M., Liew, F. K. and Lai, J. C. (2015) 'Effect of fiber treatment and nanoclay on the tensile properties of jute fiber reinforced polyethylene/clay nanocomposites'. Fibers and Polymers, 16(2), PP 479-485.

Huang, N., Chen, Z., Wang, J. and Wei, P. (2010) 'Synergistic effects of sepiolite on intumescent flame retardant polypropylene'. Express Polymer Letters, 4(12), PP 743-752.

Iji, M. and Kiuchi, Y. (2001) 'Self-extinguishing epoxy molding compound with no flame-retarding additives for electronic components'. Journal of materials science: materials in Electronics, 12(12), PP 715-723.

IPCS. (1994) Flame Retardants: A General Introduction. Available at: http://www.inchem.org/documents/ehc/ehc/ehc192.htm [Accessed 20 October 2016].

Iring, M. and Tüdos, F. (1990) 'Thermal oxidation of polyethylene and polypropylene: effects of chemical structure and reaction conditions on the oxidation process'. Progress in Polymer Science, 15(2), PP 217-262.

Isitman, N. A., Dogan, M., Bayramli, E. and Kaynak, C. (2012) 'The role of nanoparticle geometry in flame retardancy of polylactide nanocomposites containing aluminium phosphinate'. Polymer Degradation and Stability, 97(8), PP 1285-1296.

Isitman, N. A., Gunduz, H. O. and Kaynak, C. (2009a) 'Halogen-free Flame Retardants that Outperform Halogenated Counterparts in Glass Fiber Reinforced Polyamides'. Journal of Fire Sciences, 28(1), PP 87-100.

Isitman, N. A., Gunduz, H. O. and Kaynak, C. (2009b) 'Nanoclay synergy in flame retarded/glass fibre reinforced polyamide 6'. Polymer Degradation and Stability, 94(12), PP 2241-2250.

Jang, B. N., Costache, M. and Wilkie, C. A. (2005) 'The relationship between thermal degradation behavior of polymer and the fire retardancy of polymer/clay nanocomposites'. Polymer, 46(24), PP 10678-10687.

Jarus, D., Hiltner, A. and Baer, E. (2002) 'Barrier properties of polypropylene/polyamide blends produced by microlayer coextrusion'. Polymer, 43(8), PP 2401-2408.

Jha, N., Misra, A. and Bajaj, P. (1984) 'Flame-retardant additives for polypropylene'. Journal of Macromolecular Science—Reviews in Macromolecular Chemistry and Physics, 24(1), PP 69-116.

Jiang, D. (2009) 'Chapter 11 : Polymer Nanocomposites', in Morgan, A. B. & Wilkie, C. A.(Eds.) Fire Retardancy of Polymeric Materials. New York: CRC press, PP 261-299.

Kashiwagi, T., Du, F., Winey, K. I., Groth, K. M., Shields, J. R., Bellayer, S. P., Kim, H. and Douglas, J. F. (2005) 'Flammability properties of polymer nanocomposites with single-walled carbon nanotubes: effects of nanotube dispersion and concentration'. Polymer, 46(2), PP 471-481.

Kashiwagi, T., Grulke, E., Hilding, J., Groth, K., Harris, R., Butler, K., Shields, J., Kharchenko, S. and Douglas, J. (2004) 'Thermal and flammability properties of polypropylene/carbon nanotube nanocomposites'. Polymer, 45(12), PP 4227-4239.

Kashiwagi, T., Grulke, E., Hilding, J., Harris, R., Awad, W. and Douglas, J. (2002) 'Thermal degradation and flammability properties of poly (propylene)/carbon nanotube composites'. Macromolecular Rapid Communications, 23(13), PP 761-765.

Kaynak, E., Ureyen, M. E. and Koparal, A. S. (2017) 'Thermal characterization and flammability of polypropylene containing sepiolite-APP combinations'. e-Polymers, 17(4), PP 341-348.

Kiang, J., Uden, P. and Chien, J. (1980) 'Polymer reactions—Part VII: Thermal pyrolysis of polypropylene'. Polymer Degradation and Stability, 2(2), PP 113-127.

Kiliaris, P. and Papaspyrides, C. (2010) 'Polymer/layered silicate (clay) nanocomposites: an overview of flame retardancy'. Progress in Polymer Science, 35(7), PP 902-958.

Kiuchi, Y., Iji, M., Nagashima, H. and Miwa, T. (2006) 'Increase in flame retardance of glass-epoxy laminates without halogen or phosphorous compounds by simultaneous use of incombustible-gas generator and charring promoter'. Journal of Applied Polymer Science, 101(5), PP 3367-3375.

Laoutid, F., Bonnaud, L., Alexandre, M., Lopez-Cuesta, J. M. and Dubois, P. (2009) 'New prospects in flame retardant polymer materials: From fundamentals to nanocomposites'. Materials Science & Engineering R, 63(3), PP 100-125.

Laoutid, F. and Lopez-Cuesta, J.-M. (2009) 'Chapter 12: Multi-components FR systems: polymer nanocomposites combined with additional materials', in Wilkie , C. & Morgan, A.(Eds.) Fire Retardancy of Polymeric Materials. New York: CRC Press, PP 301-328.

Laoutid, F., Persenaire, O., Bonnaud, L. and Dubois, P. (2013) 'Flame retardant polypropylene through the joint action of sepiolite and polyamide 6'. Polymer degradation and stability, 98(10), PP 1972-1980.

Le Bras, M., Wilkie, C. and Bourbigot, S. (2005) 'General Considerations on the Use of Fillers and Nanocomposites. An Introduction to the Use of Fillers and Nanocomposites in Fire Retardancy', in Le Bras, M., Bourbigot, S., Sophie, D., Charafedine , J. & Wilkie, C.(Eds.) Fire retardancy of polymers: new applications of mineral fillers. London: Royal Society of Chemistry, PP 1-14.

Lepoittevin, B., Devalckenaere, M., Pantoustier, N., Alexandre, M., Kubies, D., Calberg, C., Jérôme, R. and Dubois, P. (2002) 'Poly (ε-caprolactone)/clay nanocomposites prepared by melt intercalation: mechanical, thermal and rheological properties'. Polymer, 43(14), PP 4017-4023.

Levchik, S., Levchik, G., Balabanovich, A., Camino, G. and Costa, L. (1996) 'Mechanistic study of combustion performance and thermal decomposition behaviour of nylon 6 with added halogen-free fire retardants'. Polymer Degradation and Stability, 54(2-3), PP 217-222.

Levchik , S. and Wilkie, C. A. (2000) 'Chapter 6 : Char Formation', in Grand, A. F. & Wilkie, C. A.(Eds.) Fire Retardancy of Polymeric Materials New York: Marcel Dekker, PP 171-215.

Levchik, S. V. (2007) 'Introduction to flame retardancy and polymer flammability'. Flame Retardant Polymer Nanocomposites, PP 1-29.

Levchik, S. V. and Weil, E. D. (2004) 'Thermal decomposition, combustion and flame-retardancy of epoxy resins—a review of the recent literature'. Polymer International, 53(12), PP 1901-1929.

Levchik, S. V., Weil, E. D. and Lewin, M. (1999) 'Thermal decomposition of aliphatic nylons'. Polymer International, 48(7), PP 532-557.

Lewin, M. and Weil, E. (2001) 'Chapter 2 : Mechanisms and modes of action in flame retardancy of polymers', in Horrocks, A. R. & Price, D.(Eds.) Fire Retardant Materials. Cambridge: Woodhead Publishing, PP 31-68.

Li, C.-J., Yang, G.-J. and Wang, Z. (2003) 'Formation of nanostructured TiO_2 by flame spraying with liquid feedstock'. Materials Letters, 57(13), PP 2130-2134.

Li, J., Wei, P., Li, L., Qian, Y., Wang, C. and Huang, N. H. (2011) 'Synergistic effect of mesoporous silica SBA-15 on intumescent flame-retardant polypropylene'. Fire and Materials, 35(2), PP 83-91.

Li, Q., Jiang, P. and Wei, P. (2005) 'Thermal Degradation Behavior of Poly (propylene) with a Novel Silicon-Containing Intumescent Flame Retardant'. Macromolecular Materials and Engineering, 290(9), PP 912-919.

Li, Y., Li, B., Dai, J., Jia, H. and Gao, S. (2008) 'Synergistic effects of lanthanum oxide on a novel intumescent flame retardant polypropylene system'. Polymer Degradation and Stability, 93(1), PP 9-16.

Lim, K.-S., Bee, S.-T., Sin, L. T., Tee, T.-T., Ratnam, C., Hui, D. and Rahmat, A. (2016) 'A review of application of ammonium polyphosphate as intumescent flame retardant in thermoplastic composites'. Composites Part B: Engineering, 84, PP 155-174.

Lin, J.-H., Huang, C.-L., Liu, C.-F., Chen, C.-K., Lin, Z.-I. and Lou, C.-W. (2015) 'Polypropylene/short glass fibers composites: Effects of coupling agents on mechanical properties, thermal behaviors, and morphology'. Materials, 8(12), PP 8279-8291.

Liu, Y., Deng, C.-L., Zhao, J., Wang, J.-S., Chen, L. and Wang, Y.-Z. (2011a) 'An efficiently halogen-free flame-retardant long-glass-fiber-reinforced polypropylene system'. Polymer Degradation and Stability, 96(3), PP 363-370.

Liu, Y., Wang, Q., Fei, G. and Chen, Y. (2006) 'Preparation of polyamide resin-encapsulated melamine cyanurate/melamine phosphate composite flame retardants and the fire-resistance to glass fiber-reinforced polyamide 6'. Journal of Applied Polymer Science, 102(2), PP 1773-1779.

Liu, Y., Zhao, J., Deng, C.-L., Chen, L., Wang, D.-Y. and Wang, Y.-Z. (2011b) 'Flame-Retardant Effect of Sepiolite on an Intumescent Flame-Retardant Polypropylene System'. Industrial & Engineering Chemistry Research, 50(4), PP 2047-2054.

Lizymol, P. and Thomas, S. (1993) 'Thermal behaviour of polymer blends: a comparison of the thermal properties of miscible and immiscible systems'. Polymer degradation and stability, 41(1), PP 59-64.

Lizymol, P. and Thomas, S. (1997) 'Flame retardant properties of binary blends: a comparison of miscible and immiscible blends'. Polymer degradation and stability, 57(2), PP 187-189.

Lyons, J. (1976) 'Flame-retardant polymeric materials, M. Lewin, SM Atlas, and EM Pearce, Eds., Plenum Press, New York, 1975, 457 pp'. Journal of Polymer Science Part C: Polymer Letters, 14(9), PP 569-570.

Ma, J., Bilotti, E., Peijs, T. and Darr, J. (2007) 'Preparation of polypropylene/sepiolite nanocomposites using supercritical CO2 assisted mixing'. European Polymer Journal, 43(12), PP 4931-4939.

Maier, C. and Calafut, T. (1998) Polypropylene: The Definitive User's Guide and Databook. Norwich: William Andrew Publishing.

Mani, G., Fan, Q., Ugbolue, S. C. and Yang, Y. (2005) 'Morphological studies of polypropylene–nanoclay composites'. Journal of Applied Polymer Science, 97(1), PP 218-226.

Marosfoi, B., Garas, S., Bodzay, B., Zubonyai, F. and Marosi, G. (2008) 'Flame retardancy study on magnesium hydroxide associated with clays of different morphology in polypropylene matrix'. Polymers for Advanced Technologies, 19(6), PP 693-700.

Marquis, D. M., Guillaume, E. and Chivas-Joly, C. (2011) 'Properties of nanofillers in polymer', in Nanocomposites and polymers with analytical methods. InTech, PP.

Mngomezulu, M. E., John, M. J., Jacobs, V. and Luyt, A. S. (2014) 'Review on flammability of biofibres and biocomposites'. Carbohydrate Polymers, 111, PP 149-182.

Moniruzzaman, M. and Winey, K. I. (2006) 'Polymer nanocomposites containing carbon nanotubes'. Macromolecules, 39(16), PP 5194-5205.

Morgan, A. B. and Wilkie, C. A. (2007) Flame retardant polymer nanocomposites / Alexander B. Morgan, Charles A. Wilkie. Hoboken, NJ: Wiley.

Mouritz, A. P. and Gibson, A. G. (2006) 'Chapter 3 :Fire Reaction Properties of Composites', in Mouritz, A. P. & Gibson, A. G.(Eds.) Fire Properties of Polymer Composite Materials. Berlin,: Springer Science & Business Media, PP 59-101.

Nazare, S., Hull, T. R., Biswas, B., Samyn, F., Bourbigot, S., Jama, C., Castrovinci, A. and Camino, G. (2009) 'Chapter 12 : Study of the Relationship Between Flammability and Melt Rheological Properties of Flame-Retarded Poly (Butylene Terephthalate) Containing Nanoclays', in Hull, T. R. & Kandola, B. K.(Eds.) Fire Retardancy of Polymers New Strategies and Mechanisms. London: The Royal Society of Chemistry, PP.

Nehra, R., Maiti, S. and Jacob, J. (2018) 'Poly (lactic acid)/(styrene-ethylene-butylene-styrene)-g-maleic anhydride copolymer/sepiolite nanocomposites: I nvestigation of thermo-mechanical and morphological properties'. Polymers for Advanced Technologies, 29(1), PP 234-243.

Nie, S., Hu, Y., Song, L., He, Q., Yang, D. and Chen, H. (2008) 'Synergistic effect between a char forming agent (CFA) and microencapsulated ammonium polyphosphate on the thermal and flame retardant properties of polypropylene'. Polymers for Advanced Technologies, 19(8), PP 1077-1083.

Owen, S. and Harper, J. (1999) 'Mechanical, microscopical and fire retardant studies of ABS polymers'. Polymer Degradation and Stability, 64(3), PP 449-455.

Pal, G. and Macskasy, H. (1991) Plastics: their behavior in fires. New York: Elsevier

Palza, H., Vergara, R. and Zapata, P. (2010) 'Improving the thermal behavior of poly (propylene) by addition of spherical silica nanoparticles'. Macromolecular Materials and Engineering, 295(10), PP 899-905.

Pappalardo, S., Russo, P., Acierno, D., Rabe, S. and Schartel, B. (2016) 'The synergistic effect of organically modified sepiolite in intumescent flame retardant polypropylene'. European Polymer Journal, 76, PP 196-207.

Pearce, E. M. (1984) Contemporary topics in polymer science. New York: Plenum Press.

Pernot, H., Baumert, M. and Leibler, L. (2002) 'Design and properties of co-continuous nanostructured polymers by reactive blending'. Nature Materials, 1(1), PP 54.

Perret, B., Schartel, B., Stöß, K., Ciesielski, M., Diederichs, J., Döring, M., Krämer, J. and Altstädt, V. (2011) 'A New Halogen-Free Flame Retardant Based on 9, 10-Dihydro-9-oxa-10-phosphaphenanthrene-10-oxide for Epoxy Resins and their Carbon Fiber Composites for the Automotive and Aviation Industries'. Macromolecular Materials and Engineering, 296(1), PP 14-30.

Persenaire, O., Raquez, J. M., Bonnaud, L. and Dubois, P. (2010) 'Tailoring of Co-Continuous Polymer Blend Morphology: Joint Action of Nanoclays and Compatibilizers'. Macromolecular Chemistry and Physics, 211(13), PP 1433-1440.

Pitts, J. J. (1972) 'Antimony- Halogen synergistic reactions in fire retardants(Antimony-halogen synergistic reactions in fire retardants, noting antimony oxychloride role)'. Journal of Fire and Flammability, 3, PP 51-84.

Plastic Europe Association. (2016) Plastics - the Facts 2016. Available at: http://www.plasticseurope.org/cust/documentrequest.aspx?DocID=67651 [Accessed 10 October 2016].

Porter, D., Metcalfe, E. and Thomas, M. (2000) 'Nanocomposite fire retardants—a review'. Fire and Materials, 24(1), PP 45-52.

Price, D., Anthony, G. and Carty, P. (2001) 'Introduction: polymer combustion, condensed phase pyrolysis and smoke formation', in Horrocks, A. R. & Price, D.(Eds.) Fire retardant materials. Woodhead: Cambridge, PP 1-30.

Rahman, N. A., Hassan, A. and Heidarian, J. (2018) 'Effect of compatibiliser on the properties of polypropylene/glass fibre/nanoclay composites'. Polímeros, 28(2), PP 103-111.

Rautureau, M. and Tchoubar, C. (1976) 'Structural analysis of sepiolite by selected area electron difraction--relations with physico-chemical properties'. Clays and Clay Miner, PP.

Ray, S. S. and Okamoto, M. (2003) 'Polymer/layered silicate nanocomposites: a review from preparation to processing'. Progress in Polymer Science, 28(11), PP 1539-1641.

Reimschuessel, H., Shalaby, S. and Pearce, E. (1973) 'On the OxygenIndex of Nylon 6'. Journal of Fire and Flammability, 4(1), PP 299-308.

Robeson, L. M. (2002) 'Chapter 17 : Perspectives in polymer blend technology', in Utracki, L.(Ed.), Polymer Blend Handbook. London: Kluwer Academicl, PP 1167-1185.

Ruiz-Hitzky, E. (2001) 'Molecular access to intracrystalline tunnels of sepioliteBasis of a presentation given at Materials Discussion No. 3, 24–26 September 2000, University of Cambridge, UK'. Journal of Materials Chemistry, 11(1), PP 86-91.

Saba, N., Tahir, P. M. and Jawaid, M. (2014) 'A review on potentiality of nano filler/natural fiber filled polymer hybrid composites'. Polymers, 6(8), PP 2247-2273.

Sadezky, A., Muckenhuber, H., Grothe, H., Niessner, R. and Pöschl, U. (2005) 'Raman microspectroscopy of soot and related carbonaceous materials: spectral analysis and structural information'. Carbon, 43(8), PP 1731-1742.

Salaün, F., Lewandowski, M., Vroman, I., Bedek, G. and Bourbigot, S. (2011) 'Development and characterisation of flame-retardant fibres from isotactic polypropylene melt-compounded with melamine-formaldehyde microcapsules'. Polymer Degradation and Stability, 96(1), PP 131-143.

Schartel, B., Pötschke, P., Knoll, U. and Abdel-Goad, M. (2005) 'Fire behaviour of polyamide 6/multiwall carbon nanotube nanocomposites'. European Polymer Journal, 41(5), PP 1061-1070.

Shaw, S. (2010) 'Halogenated flame retardants: do the fire safety benefits justify the risks?'. Reviews on Environmental Health, 25(4), PP 261-306.

Song, R., Wang, Z., Meng, X., Zhang, B. and Tang, T. (2007) 'Influences of catalysis and dispersion of organically modified montmorillonite on flame retardancy of polypropylene nanocomposites'. Journal of applied polymer science, 106(5), PP 3488-3494.

Sonnier, R., Viretto, A., Taguet, A. and Lopez-Cuesta, J. M. (2012) 'Influence of the morphology on the fire behavior of a polycarbonate/poly (butylene terephthalate) blend'. Journal of Applied Polymer Science, 125(4), PP 3148-3158.

Sperling, L. H. (2005) Introduction to physical polymer science. New Jersey: John Wiley & Sons.

Statista. (2016) Global plastic production statistics. Available at: https://www.statista.com/statistics/282732/global-production-of-plastics-since-1950/ [Accessed 6 September 2018].

Stauffer, E. (2003) 'Concept of pyrolysis for fire debris analysts'. Science & justice, 43(1), PP 29-40.

Subasinghe, A., Das, R. and Bhattacharyya, D. (2016) 'Study of thermal, flammability and mechanical properties of intumescent flame retardant PP/kenaf nanocomposites'. International Journal of Smart and Nano Materials, 7(3), PP 202-220.

Šupová, M., Martynková, G. S. and Barabaszová, K. (2011) 'Effect of nanofillers dispersion in polymer matrices: a review'. Science of Advanced Materials, 3(1), PP 1-25.

Swoboda, B., Buonomo, S., Leroy, E. and Cuesta, J. L. (2007) 'Reaction to fire of recycled poly (ethylene terephthalate)/polycarbonate blends'. Polymer Degradation and Stability, 92(12), PP 2247-2256.

Szekely, T., Varhegyi, G., Till, F., Szabo, P. and Jakab, E. (1987) 'The effects of heat and mass transport on the results of thermal decomposition studies: part 2. Polystyrene, polytetrafluoroethylene and polypropylene'. Journal of Analytical and Applied Pyrolysis, 11, PP 83-92.

Talsness, C. E. (2008) 'Overview of toxicological aspects of polybrominated diphenyl ethers: a flame-retardant additive in several consumer products'. Environmental Research, 108(2), PP 158-167.

Tang, Y., Hu, Y., Li, B., Liu, L., Wang, Z., Chen, Z. and Fan, W. (2004) 'Polypropylene/montmorillonite nanocomposites and intumescent, flame-retardant montmorillonite synergism in polypropylene nanocomposites'. Journal of Polymer Science Part A: Polymer Chemistry, 42(23), PP 6163-6173.

Tang, Y., Hu, Y., Song, L., Zong, R., Gui, Z. and Fan, W. (2006) 'Preparation and combustion properties of flame retarded polypropylene–polyamide-6 alloys'. Polymer Degradation and Stability, 91(2), PP 234-241.

Tang, Y., Hu, Y., Xiao, J., Wang, J., Song, L. and Fan, W. (2005) 'PA-6 and EVA alloy/clay nanocomposites as char forming agents in poly (propylene) intumescent formulations'. Polymers for Advanced Technologies, 16(4), PP 338-343.

Tartaglione, G., Tabuani, D., Camino, G. and Moisio, M. (2008) 'PP and PBT composites filled with sepiolite: morphology and thermal behaviour'. Composites Science and Technology, 68(2), PP 451-460.

Times, T. (2017) Grenfell Tower: fire-resistant cladding is just £5,000 more expensive. Available at: https://www.thetimes.co.uk/article/grenfell-tower-fire-resistant-cladding-is-just-5-000-more-expensive-6gjqkg98g [Accessed 26 June 2018].

Troitzsch, J. (2004) Plastics flammability handbook. Munich: Carl Hanser Publ.

Troitzsch, J. r. (1990) International plastics flammability handbook : principles, regulations, testing and approval. Munich: Hanser.

Tsuchiya, Y. and Sumi, K. (1969) 'Thermal decomposition products of polypropylene'. Journal of Polymer Science Part A: Polymer Chemistry, 7(7), PP 1599-1607.

Tuinstra, F. and Koenig, J. L. (1970) 'Raman spectrum of graphite'. The Journal of Chemical Physics, 53(3), PP 1126-1130.

Tung, J., Gupta, R., Simon, G., Edward, G. and Bhattacharya, S. (2005) 'Rheological and mechanical comparative study of in situ polymerized and melt-blended nylon 6 nanocomposites'. Polymer, 46(23), PP 10405-10418.

Underwriters Laboratories (2013) UL 94, the Standard for Safety of Flammability of Plastic Materials for Parts in Devices and Appliances testing. United States: Underwriters Laboratories.

Vahabi, H., Sonnier, R., Otazaghine, B., Le Saout, G. and Lopez-Cuesta, J. (2013) 'Nanocomposites of polypropylene/polyamide 6 blends based on three different nanoclays: thermal stability and flame retardancy'. Polimery, 58(5), PP 350-360.

Vannier, A., Duquesne, S., Bourbigot, S., Castrovinci, A., Camino, G. and Delobel, R. (2008) 'The use of POSS as synergist in intumescent recycled poly (ethylene terephthalate)'. Polymer Degradation and Stability, 93(4), PP 818-826.

Visakh, P. and Yoshihiko, A. (2015) Flame retardants: Polymer blends, composites and nanocomposites. Berlin: Springer.

Volle, N., Challier, L., Burr, A., Giulieri, F., Pagnotta, S. and Chaze, A.-M. (2011) 'Maya Blue as natural coloring fillers in a multi-scale polymer-clay nanocomposite'. Composites Science and Technology, 71(15), PP 1685-1691.

Wakefield, J. (2010) A toxicological review of the products of combustion. Oxfordshire: Health Protection Agency, Centre for Radiation, Chemical and Environmental Hazards, Chemical Hazards and Poisons Division.

Wang, J. and Chow, W. (2005) 'A brief review on fire retardants for polymeric foams'. Journal of Applied Polymer Science, 97(1), PP 366-376.

Wang, S., Hu, Y., Lin, Z., Gui, Z., Wang, Z., Chen, Z. and Fan, W. (2003) 'Flammability and thermal stability studies of ABS/montmorillonite nanocomposite'. Polymer International, 52(6), PP 1045-1049.

Wei, P., Hao, J., Du, J., Han, Z. and Wang, J. (2003) 'An investigation on synergism of an intumescent flame retardant based on silica and alumina'. Journal of Fire Sciences, 21(1), PP 17-28.

Wei, P., Li, H., Jiang, P. and Yu, H. (2004) 'An investigation on the flammability of halogen-free fire retardant PP–APP–EG systems'. Journal of fire sciences, 22(5), PP 367-377.

Weiss, J., Takhistov, P. and McClements, D. J. (2006) 'Functional materials in food nanotechnology'. Journal of food science, 71(9), PP R107-R116.

Wilkie, C. A., Levchik, S. V. and Levchik, G. F. (2001) 'Is There a Correlation Between Crosslinking and Thermal Stability?', in Al-Malaika, S., Wilkie , C. & Golovoy , A.(Eds.) Specialty Polymer Additives: Principles and Application. Oxford, England: Blackwell Science, PP 359–374.

Wilkie, C. A., Morgan, A. B. and Nelson, G. L. (2009) Fire and polymers V : materials and concepts for fire retardancy. Washington: American Chemical Society

Wu, J., Hu, Y., Song, L. and Kang, W. (2008) 'Synergistic effect of lanthanum oxide on intumescent flame-retardant polypropylene-based formulations'. Journal of fire sciences, 26(5), PP 399-414.

Xanthos, M. (2005) 'Polymers and polymer composites'. Functional fillers for plastics, PP 1-16.

Xia, Y., Jin, F., Mao, Z., Guan, Y. and Zheng, A. (2014) 'Effects of ammonium polyphosphate to pentaerythritol ratio on composition and properties of carbonaceous foam deriving from intumescent flame-retardant polypropylene'. Polymer Degradation and Stability, 107, PP 64-73.

Xie, F., Wang, Y. Z., Yang, B. and Liu, Y. (2006) 'A Novel Intumescent Flame-Retardant Polyethylene System'. Macromolecular Materials and Engineering, 291(3), PP 247-253.

Xie, S., Zhang, S., Wang, F., Yang, M., Séguéla, R. and Lefebvre, J.-M. (2007) 'Preparation, structure and thermomechanical properties of nylon-6 nanocomposites with lamella-type and fiber-type sepiolite'. Composites Science and Technology, 67(11), PP 2334-2341.

Xu, Z.-Z., Huang, J.-Q., Chen, M.-J., Tan, Y. and Wang, Y.-Z. (2013) 'Flame retardant mechanism of an efficient flame-retardant polymeric synergist with ammonium polyphosphate for polypropylene'. Polymer Degradation and Stability, 98(10), PP 2011-2020.

Yang, C. P. and Lee, T. W. (1986) 'Synthesis and properties of 4-hydroxy-2, 3, 5, 6-tetrabromobenzyl phosphonates and effects of their flame retardance on impact polystyrene'. Journal of Applied Polymer Science, 32(1), PP 3005-3025.

Yang, W., Hu, Y., Tai, Q., Lu, H., Song, L. and Yuen, R. K. (2011) 'Fire and mechanical performance of nanoclay reinforced glass-fiber/PBT composites containing aluminum hypophosphite particles'. Composites Part A: Applied Science and Manufacturing, 42(7), PP 794-800.

Zanetti, M., Camino, G., Reichert, P. and Mülhaupt, R. (2001a) 'Thermal behaviour of poly (propylene) layered silicate nanocomposites'. Macromolecular Rapid Communications, 22(3), PP 176-180.

Zanetti, M., Camino, G., Thomann, R. and Mülhaupt, R. (2001b) 'Synthesis and thermal behaviour of layered silicate–EVA nanocomposites'. Polymer, 42(10), PP 4501-4507.

Zhang, K., Wu, K., Zhang, Y.-K., Liu, H.-F., Shen, M.-M. and Hu, W. (2013) 'Flammability characteristics and performance of flame-retarded epoxy composite based on melamine cyanurate and ammonium polyphosphate'. Polymer-Plastics Technology and Engineering, 52(5), PP 525-532.

Zhang, S. and Horrocks, A. R. (2003) 'A review of flame retardant polypropylene fibres'. Progress in Polymer Science, 28(11), PP 1517-1538.

Zhao, B., Hu, Z., Chen, L., Liu, Y., Liu, Y. and Wang, Y. Z. (2011) 'A phosphorus-containing inorganic compound as an effective flame retardant for glass-fiber-

reinforced polyamide 6'. Journal of Applied Polymer Science, 119(4), PP 2379-2385.

Zhao, C.-S., Huang, F.-L., Xiong, W.-C. and Wang, Y.-Z. (2008a) 'A novel halogen-free flame retardant for glass-fiber-reinforced poly (ethylene terephthalate)'. Polymer Degradation and Stability, 93(6), PP 1188-1193.

Zhao, C.-S., Huang, F.-L., Xiong, W.-C. and Wang, Y.-Z. (2008b) 'A novel halogen-free flame retardant for glass-fiber-reinforced poly(ethylene terephthalate)'. Polymer Degradation and Stability, 93(6), PP 1188-1193.

Zhao, H.-B., Liu, B.-W., Wang, X.-L., Chen, L., Wang, X.-L. and Wang, Y.-Z. (2014) 'A flame-retardant-free and thermo-cross-linkable copolyester: Flame-retardant and anti-dripping mode of action'. Polymer, 55(10), PP 2394-2403.

Zhao, X., Wei, P., Qian, Y., Yu, H. and Liu, J. (2012) 'Effect of talc on thermal stability and flame retardancy of polycarbonate/PSBPBP composite'. Journal of Applied Polymer Science, 125(4), PP 3167-3174.

Zheng, Y. and Zheng, Y. (2006) 'Study on sepiolite-reinforced polymeric nanocomposites'. Journal of Applied Polymer Science, 99(5), PP 2163-2166.

Zhong, H., Wei, P., Jiang, P. and Wang, G. (2007) 'Thermal degradation behaviors and flame retardancy of PC/ABS with novel silicon-containing flame retardant'. Fire and Materials, 31(6), PP 411-423.